

UNIVERSIDADE DE LISBOA
FACULDADE DE CIÊNCIAS
DEPARTAMENTO DE BIOLOGIA VEGETAL



**Ocean Colour off the Portuguese Coast: Chlorophyll a products
validation and applicability**

Carolina Garcia Vieira de Sá

DOUTORAMENTO EM CIÊNCIAS DO MAR

2013

UNIVERSIDADE DE LISBOA
FACULDADE DE CIÊNCIAS
DEPARTAMENTO DE BIOLOGIA VEGETAL



**Ocean Colour off the Portuguese coast: Chlorophyll a products
validation and applicability**

Carolina Garcia Vieira de Sá

Tese orientada pela Prof. Doutora Vanda Brotas e pelo Prof. Doutor José da Silva,
especialmente elaborada para a obtenção do grau de doutor em Ciências do Mar.

2013

Declaration

According to Chapter V, article 40, paragraph 1 of the Regulation concerning Post-Graduate Studies at the University of Lisbon, which was published in the Portuguese Republic's Official Journal (Series II, no153, of 5 July 2003), the PhD candidate hereby declares that she participated in the designing and carrying out the field work, as well as in interpreting the results, and drafting the manuscripts to be submitted for publication.

Carolina Sá

Lisboa, 19 October 2013

This study was performed in the framework of HabSpot FCT Project, PTDC/MAR/100348/2008 and European Space Agency projects DUE CoastColour (ESRIN/AO/1-6141/09/I-EC) and Climate Change Initiative – Ocean Colour (AO-1/6207/09/I-LG). The work has been also partially supported by the European Space Agency within the framework of the MERIS Validation Activities under contract n. 12595/09/I-OL, and sampling activities benefited from European projects HERMES (GOCE-CT-2005-511234) and Hermione (EC contract 226354) support. The candidate received a PhD grant from the Portuguese Science Foundation (FCT-SFRH/BD/24245/2005).

Parts of the work and dataset presented in this thesis have been considered and included in the following international publications:

1. **Sá, C.**, da Silva, J.C.B., Oliveira, P.B., Brotas, V. (2008). Comparison of MERIS (ALGAL_1 and ALGAL_2) and MODIS (OCM3) of chlorophyll products and validation with HPLC in situ data collected off the Western Iberian Peninsula. Proceeding of the 2nd MERIS/(A)ATSR Workshop. ESA, SP-666.
2. Ruddick, K., Brockmann, C., Doerffer, R., Lee, Z., Brotas, V., Fomferra, N., Groom, S., Krasemann, H., Martinez-Vicente, V., **Sá, C.**, Santer, R., Sathyendranath, S., Stelzer, K., Pinnock, S. (2010). The Coastcolour project regional algorithm round robin exercise. *Remote Sensing of the Coastal Ocean, Land, and Atmosphere Environment. Incheon, South Korea, October 13-14, 2010. Proceedings of SPIE, the International Society for Optical Engineering*, 7858: pp. DOI: 10.1117/12.869506.
3. Mendes, C.R., **Sá, C.**, Vitorino, J., Borges, C., Garcia, V.M.T., Brotas, V.(2011) Spatial distribution of phytoplankton communities in the Nazaré submarine canyon region (Portugal): HPLC-CHEMTAX approach. *Journal of Marine Systems* 89 (1):90-101.
4. Brotas, V., Brewin, R., **Sá, C.**, Brito, S., Silva, A., Mendes, R., Diniz, T., Kaufmann, M., Tarran, G., Groom, S., Platt, T., Sathyendranath, S. (2013). Approaches to derive phytoplankton functional types and size classes. Validation along a gradient of trophic status in Eastern Atlantic. *Remote Sensing of Environment*, 134, 66-77.
5. Brito, A., **Sá, C.**, Brotas, V., Vitorino, J., Platt, T., Sathyendranath, S. (under revision). Understanding bio-optical properties of phytoplankton in the western Iberian coast: application of theoretical models. *Remote Sensing of Environment*.
6. **Sá, C.**, D'Alimonte, Brito, A., Kajiyama, T., Zibordi, G., Mendes, C.R., Bherton, J-F., Canutti, E., Oliveira, P., da Silva, J., Brotas, V. (*in preparation*). Validation of satellite ocean colour chlorophyll products for the Western Iberia: comparison of algorithms.
7. **Sá, C.**, D'Alimonte, Brito, A., Kajiyama, T., Zibordi, G., Bherton, J-F., Canutti, E., da Silva, J., Brotas, V. (*in preparation*). Temporal and spatial variability of case I waters off the Western Iberia.

Acknowledgements

The decision to embrace a doctoral programme implies a commitment that is not possible just with the individual effort but needs the comprehension and support by colleagues and family. It is a long journey full of expectations, uncertainties and surprises. It is also a learning process in maturing to become a true scientist. In the next lines I would like to express my gratitude to all that to some extent contributed to the elaboration of this thesis.

I am thankful to my advisors, Prof. Vanda Brotas and Prof. José da Silva for their trust, scientific advisory and unconditional support. Thank you for giving me the opportunity to participate in multidisciplinary projects and never doubting my capabilities.

I am deeply grateful to Davide D'Alimonte whose expertise, and scientific discussions added considerably to my experience. Thank you so much for your kindness and for being an inspiration.

I express my most sincere gratitude to Ana Brito for her friendship and support throughout the writing process of this thesis. Thank you also for always challenging me into new projects.

To Ana Sousa and Rafael Mendes, who have been with me since the beginning of this scientific journey, I send a warm thank you for their friendship and encouragement. I also thank Tamito and his beautiful family for their support and happy times together.

I would like also to send a word of appreciation to all of those who have shared with me their laboratory experience and expertise, and to those who have spent with me hours of sampling, hours of joy and hard work while at sea. A thank you note to Alexandra Silva, Bruno Jesus, Carla Gameiro, Catarina Guerreiro, Inês Martins, Lourenço Ribeiro, Miguel Leal, Paulo Cartaxana, Sérgio Muacho, Teresa Silva and Vera Veloso.

A special thanks to Henko De Stigter, João Vitorino and Teresa Moita, for the opportunity to participate in their scientific cruises. Sampling would have not been possible without their support. Furthermore I would also like to acknowledge with much appreciation the crucial role of Jean-Paul Huot and Giuseppe Zibordi who made the optical sampling campaign possible.

Finally, a huge thanks to my dearest friends: Rita, Filomena, Ana Rita and Maria João, and to my big and lovely family, without whom this thesis would have not been possible. Life is so much funnier when you are around. Thank you for your daily support and encouragement.

Index

Resumo	23
Summary.....	27
Thesis motivation, objectives and outline.....	29
Chapter 1: Introduction	31
1.1 Ocean colour	33
1.1.1 Electromagnetic radiation and optical properties	33
1.1.2 Water types	38
1.1.3 Ocean colour algorithms	42
1.1.4 Ocean colour sensors	43
1.1.5 Ocean colour products validation	45
1.2 Phytoplankton	45
1.2.1 Phytoplankton: size classes and functional types	46
1.2.2 Phytoplankton Pigments	47
1.2.3 Phytoplankton from space	50
1.3 Study site	51
Chapter 2: Data and Methods	57
2.1 <i>In situ</i> data: sampling and processing	59
2.1.1 Phytoplankton pigments	59
2.1.2 Phytoplankton absorption spectra	64
2.1.3 Radiometric data	64
2.2 Satellite data.....	65
2.2.1 Standard algorithms	65
2.2.2 Novel algorithms	68
2.3 Data quality assurance for matchup analysis.....	70
2.3.1 <i>In situ</i> database	70
2.3.2 Satellite data.....	70
2.4 Match-up and comparison procedures	72
2.5 Statistics formulae	73
2.6 Water type index	74
2.7 1 st optical depth and euphotic depth	77

Chapter 3: Results	79
3.1 Dataset for the western Portuguese waters	81
3.2 Match-up analysis of Chlorophyll products	86
3.2.1 Standard Chlorophyll products	87
3.2.2 Novel Chlorophyll Products	91
3.2.2 Comparisons between MERIS and MODIS Standard products	98
3.3 Water typology: Case1 vs non-Case1 waters.....	100
3.3.1 Optical properties off the Portuguese coast using <i>in situ</i> data	100
3.3.2 Water typology using remote sensing data	101
3.3.3 Model constraints and applicability.....	109
3.3.4 Temporal and Spatial variability of Case 1 waters.....	114
3.4 Factors affecting satellite percentage error	117
Chapter 4: Discussion.....	121
4.1 <i>In situ</i> dataset.....	123
4.1.1 Chlorophyll <i>a</i> measurement uncertainties	123
4.1.2 Geographical and temporal coverage.....	125
4.1.3 Contribution to current knowledge	127
4.2 Match-ups	130
4.2.1 Analysis constraints.....	130
4.2.2 Assessment of algorithms effectiveness.....	132
4.2.3 Regional analysis	138
4.3 Assessment of water typology: Case 1 vs non-Case 1	142
4.3.1 Implications of water typology	143
4.3.2 Understanding regional optical properties.....	144
4.3.3 Water typology remote sensing model constraints: atmospheric correction....	148
4.3.4 Water type temporal and spatial distribution	150
4.4 Factors affecting chlorophyll product accuracy.....	153
4.4.1 Index water type	153
4.4.2 Phytoplankton size classes.....	154
4.4.3 Other parameters	155
Chapter 5: Final remarks.....	159
5.1 General considerations	161
5.2 Future perspectives	163

Chapter 6: References	165
Annex I: Dataset	185
Annex II: Case water-type maps	217

Thesis motivation, objectives and outline

This thesis was motivated by the need to better understand the performance of standard Chlorophyll a (Chl) satellite products. Phytoplankton represent the basis of oceanic food webs. Their dynamics may have significant implications in terms of fisheries and they can be considered as indicators of ecosystem quality. Therefore, they are key elements to evaluate and monitor, both in short and long-term perspectives. The aim of this thesis was to evaluate the standard MERIS and MODIS Chl products, to perform algorithm regional adjustments, and to identify the spatial and temporal variability of environmental parameters that influence their performance. The main objective was pursued by focusing on the following specific tasks:

- ①. To gather a phytoplankton pigment database for ocean colour product validation and application development;
- ②. To validate and compare MERIS and MODIS sensor Chl products for the Portuguese coast;
- ③. To perform regional adaptations to the algorithms;
- ④. To provide a classification of the waters off the Portuguese coast and a general seasonal and spatial analysis of its variability.

A schematic representation of the thesis organization is presented in Figure 1. The thesis is organized in 5 Chapters. Chapter 1 includes a general introduction to provide the reader the background and necessary context to understand the work described in the following chapters. Basis of ocean-colour and phytoplankton knowledge are provided, as well as a characterization of the study area. The data collected and methods applied are detailed in Chapter 2. Data collection and quality processing of both *in situ* and satellite datasets are described. Details on the comparison procedure and statistical analysis are also given. The complete *in situ* dataset is provided in Annex I. Results are presented in Chapter 3 and discussed in Chapter 4. Concluding remarks, as well as future perspectives are addressed in Chapter 5.

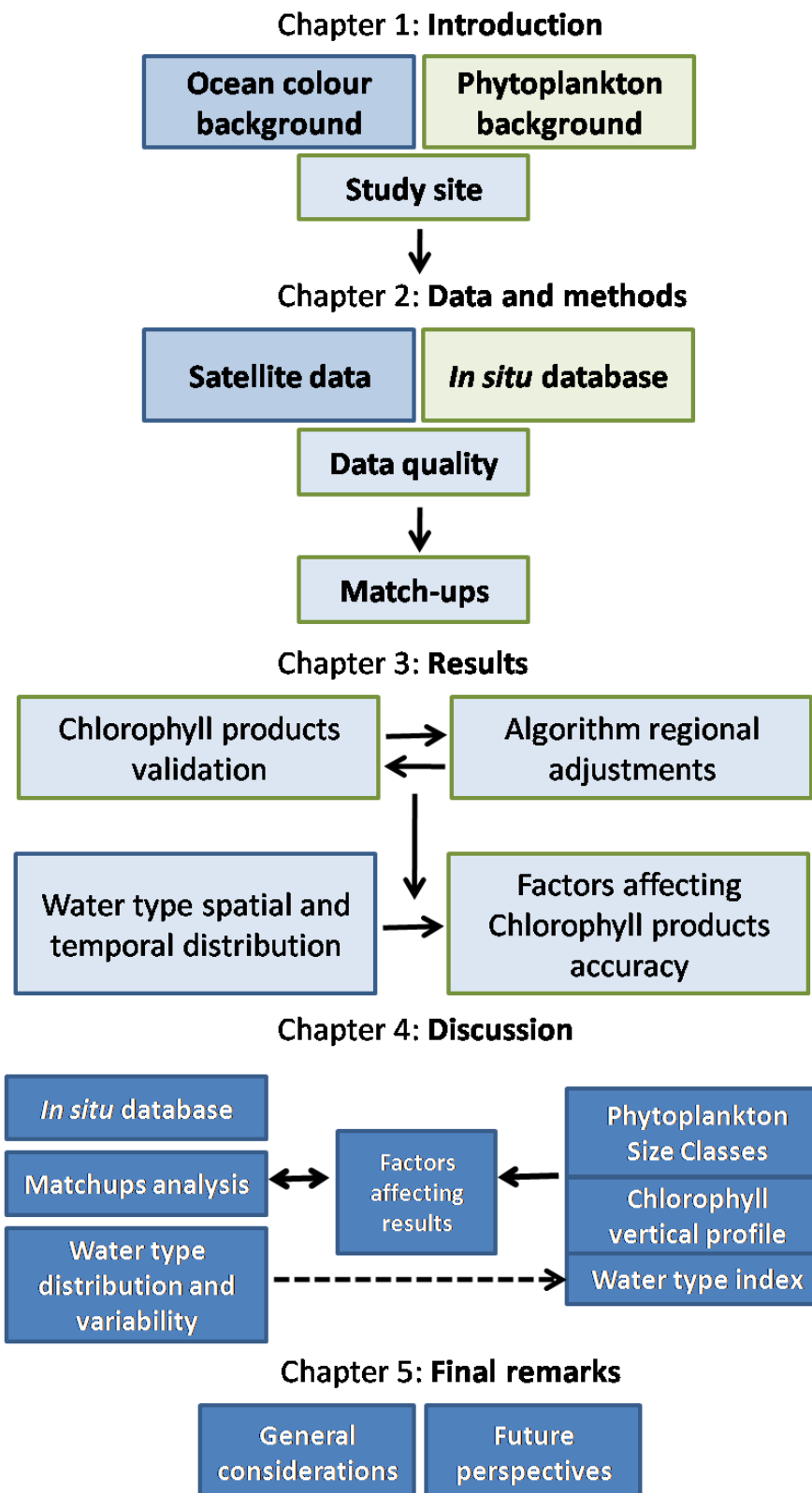


Figure 1 Schematics of thesis organization and investigated topics.

Tables Index

Table I List of ocean colour sensors (IOCCG, 2012).	44
Table II List of most relevant pigments and their correspondent occurrence in phytoplankton communities (Jeffrey et al., 1997).	48
Table III List of oceanographic cruises with respective sampling period, location, number of surface samples collected and Chlorophyll <i>a</i> (Chl) values range.	60
Table IV Summary of sampling and processing methods used in each cruise.	61
Table V List of flags used for processing the satellite data.	71
Table VI Summary statistics for linear regression analyses between TChl <i>a</i> and accessory pigments.	81
Table VII Statistical results obtained from the agreement between <i>in situ</i> field data and concomitant satellite data.	88
Table VIII Summary of the differences (diff) observed between the maps of SeaWiFS and MODIS classification for 2005. Results are presented for each season.	106
Table IX Statistics of MODIS radiometric data comparison with the <i>in situ</i> SeaBASS database.....	110
Table X Statistics of SeaWiFS radiometric data comparison with the <i>in situ</i> SeaBASS database	111
Table XI Statistics of MODIS radiometric data comparison with <i>in situ</i> data collected off the Portuguese coast (cruise GC11).	112
Table XII Correlation matrices for MODIS and MERIS standard products match-ups parameters. .	119

Figures Index

Figure 1 Schematics of thesis organization and investigated topics.....	30
Figure 2 Schematic representation of the atmospheric windows for remote sensing.....	34
Figure 3 Schematics of light pathways reaching a remote sensor.	35
Figure 4 Factors that influence the upwelling light leaving the sea surface.	39
Figure 5 Reflectance spectra of water masses dominated by different optical active components.	40
Figure 6 Water type classification scheme.	41
Figure 7 Chlorophyll <i>a</i> structure.....	47
Figure 8 Example of absorption spectra for a range of monospecific cultures.	50
Figure 9 The Western Iberia and Gulf of Cadiz regimes in a) spring and summer, and b) autumn and winter.	53
Figure 10 Schematics of a deep chlorophyll maximum (DCM).	54
Figure 11 Samples location taken on board RV Pelagia in 2005 (PG05) and 2006 (PG06); NI Noruega 2005 (NR05) and 2006 (NR06); NRP D.Carlos I in 2006 (DC06), 2007 (DC07) and 2008 (DC08); NRP Gago Coutinho in 2009 (GC09 and GC09M), 2010 (GC10) and 2011 (GC11); RV Mytilus in 2010 and 2011 under HABSpot project (HS10, HS11) and coastal monitoring stations in Cascais and Cascais, Sines and Algarve (CS and CSA, respectively).....	59
Figure 12 Lee and Hu 2006 model (result of equation 2.16 and 2.18)	75
Figure 13 Lee and Hu 2006 model (result of equation 2.17 and 2.19)	75
Figure 14 Pigment dataset after quality control: accessory pigments against total chlorophyll <i>a</i> (Tchl <i>a</i>).	82
Figure 15 Pigment dataset, after quality control, separated for size class dominance based on Uitz et al., 2006.	83
Figure 16 Distribution map of the different size dominant samples (a) and all dataset relation between accessory pigments (AP) and total chlorophyll <i>a</i> (Tchl <i>a</i>) (b).	84
Figure 17 Ternary plot showing the relative contributions (percent) of picoplankton, nanoplaknton, and microphytoplankton to total Chl, estimated from the relative contribution of some taxonomic pigments (Uitz et al., 2006).	85
Figure 18 Variations of size index (Bricaud <i>et al</i> 2004) as function of chlorophyll (TChla).	86
Figure 19 Match-up results obtained using the standard algorithms for MODIS (OC3M) and MERIS (algal 1 and algal 2). A 3h time difference was used in this analysis.	89
Figure 20 Match-up results obtained using the standard algorithms for MODIS (OC3M) and MERIS (algal 1 and algal 2). Two different time intervals are represented: 0 to 3h (black) and 3 to 6h (blue).	90

Figure 21 Regional adjustment of the equation 2.8 of the algal 2 Chl product, based on <i>in situ</i> absorption values at 442nm and Chl concentrations (a). Recalculation of match-up results using the regionally adjusted product, in black, and previous results of the standard product, in grey (b).	91
Figure 22 Match-up results obtained using the novel products developed in the CoastColour Project, using MERIS (CC_NN and CC_QAA). A 3h time difference was used in this analysis.	92
Figure 23 Match-up results obtained after regionally adjusting the novel products developed in the CoastColour Project, using MERIS (CC_NN and CC_QAA). A 3h time difference was used in this analysis.	93
Figure 24 Match-up results obtained using the novel algorithms developed for the regionally adjusted MLP-NN, using MERIS (MLP _{ME} _ATLP). A 3h time difference was used in this analysis.	94
Figure 25 Match-up results obtained using the novel algorithms developed for the regionally adjusted MLP-NN, using MERIS (MLP _{ME} _ATLP). Two different time intervals are represented: 0 to 3h (black) and 3 to 6h (blue).	95
Figure 26 Match-up results obtained using the novel algorithm developed for regional adjusted MLP-NN, using MODIS (MLP _{MO} _ATLP). A 3h time difference was used in this analysis.	96
Figure 27 Match-up results obtained using the novel algorithms developed the regionally adjusted MLP-NN, using MODIS (MLP _{MO} _ATLP). Two different time intervals are represented: 0 to 3h (black) and 3 to 6h (blue).	97
Figure 28 Match-up results obtained with the Chl CCI product. A 3h time difference was used in this analysis.	98
Figure 29 Location of common valid pixels using algal 1 and algal 2 MERIS algorithms (a); The comparison between the Chl product for these two algorithms is also presented (b).....	99
Figure 30 Location of common match-ups for MODIS and MERIS (algal 1) products, within a time window of 6h (a). The comparison between the Chl products for these two sensors is also presented (b).	99
Figure 31 Ternary plot of absorption at 442nm of CDOM, non-algal particles and phytoplankton measured during the GC11 cruise.	100
Figure 32 All <i>in situ</i> radiometric data collected during the GC11 cruise superimposed with Lee and Hu (2006) model: a) RR12_RR53 condition, b) Rrs555_RR53 condition.	101
Figure 33 Reflectance ratios applied to MODIS (in blue) and SeaWiFS (in black) data off the Portuguese coast with superimposed Lee and Hu (2006) model for Case 1-waters (lines). Data presented are averaged Rrs data for the Summer period of 2005.	102
Figure 34 Maps of percentage of pixel classification as Case 1 waters according to Lee and Hu (2006) model conditions for MODIS data, considering the four seasons of 2005.	103
Figure 35 Maps of percentage of pixel classification as Case 1 waters according to Lee and Hu (2006) model conditions for SeaWiFS data, considering the four seasons of 2005.	104
Figure 36 Maps of the difference between SeaWiFS and MODIS Case 1 waters percentage classification using only the RR12_RR53 condition for 2005: a) spring, b) summer, c) autumn and	

d) winter. Note that b) is the result of the difference between Figure 35 b) and Figure 34 b). Positive values result from higher percentage values for SeaWiFS classification and negative values from higher percentage values of MODIS classification.	107
Figure 37 Maps of the difference between SeaWiFS and MODIS Case 1 waters percentage classification using only the Rrs555_RR53 condition for 2005: a) spring, b) summer, c) autumn and d) winter.	108
Figure 38 Validation of radiometric MODIS data with SeaBaSS <i>in situ</i> database.	110
Figure 39 Validation of radiometric SeaWiFS data with SeaBaSS <i>in situ</i> database.	111
Figure 40 Validation of radiometric MODIS data with <i>in situ</i> data collected during the GC11 cruise.	112
Figure 41 RR12 ratio variation with distance from coast (km).	113
Figure 42 Radiometric MODIS match-ups with the CO database (n=75), for a 6h time window, plotted superimposed with the Lee and Hu 2006 model (lines).	114
Figure 43 Seasonal maps of percentage of pixel classification as Case 1 waters according to Lee and Hu (2006) model conditions for the MODIS data for a 7 years period, 2005-2011.	115
Figure 44 Maps of standard deviation of seasonal percentage of pixel classification as Case 1 waters according to Lee and Hu (2006) model (Rrs555_RR53 condition) for the MODIS data for a 7 years period, 2005-2011.	116
Figure 45 Mean percentage of total pixels between 2005 and 2011 for each season.	117
Figure 46 Target diagram for the relation of each Chl product with their correspondent <i>in situ</i> match-ups. URMS (Δ) is plotted in the x-axis, and bias (δ) in the y-axis. Dotted lines are isolines of RMS (Ψ), as according to equation $\Psi^2 = \Delta^2 + \delta^2$	134
Figure 47 Taylor diagram for the relation of each Chl product with their correspondent <i>in situ</i> match-ups. Normalized standard deviation is plotted in the x-axis, and the angle corresponds to the correlation coefficient. Dashed black lines are isolines of normalized standard deviation, dotted black lines are correlation coefficient isolines and dotted blue lines are isolines of URMS (Δ).	136
Figure 48 Target diagram for the relation of CoastColour QAA (a) and NN (b) Chl products with their correspondent <i>in situ</i> match-ups.	139
Figure 49 Target diagram for the relation of MODIS (a) and CCI (b) Chl products with their correspondent <i>in situ</i> match-ups.	140
Figure 50 Target diagram for the relation of MERIS algal1 (a) and algal2 (b) Chl products with their correspondent <i>in situ</i> match-ups.	141
Figure 51 Target diagram for the relation of MLP_ATLP MO (a) and ME (b) Chl products (novelty index < 3) with their correspondent <i>in situ</i> match-ups.	142
Figure 52 Morel and Belanger (2006) model superimposed (for sun-zenith angle of 45°) to satellite data and Lee and Hu (2006) second condition model. Data presented are averaged Rrs data for the summer period of 2005.	151

Figure 53 Variation of percentage error of MODIS matchups with Zeu.	157
Figure 54 Summary scheme of comparison between satellite Chl products and the <i>in situ</i> dataset. Absolute percentage of difference (APD) is presented for each of the standard (in blue) and novel (in green) products tested.....	163

Resumo

A detecção remota implica que a obtenção de informação sobre um objecto seja feita a distância. Nesse sentido, a informação que se pretende obter tem de estar directamente relacionada com algum parametro mensuravel a essa distância. A medição da “cor” do oceano permite recolher informação sobre as propriedades ópticas de uma determinada massa de agua, uma vez que se encontra directamente relacionada com essas propriedades. Preisendorfer (1961) definiu dois tipos de propriedades opticas para a coluna de agua: as propriedades opticas 1) aparentes e as 2) inerentes. As propriedades aparentes (AOPs), como sejam a reflectância ou a radiância, dependem não só da natureza e quantidade de substâncias presentes, mas são também influenciadas pela distribuicao angular do campo de luz. Ao contrario das propriedades inerentes (IOPs), a absorção, dispersão e atenuação, que são independentes das condições de iluminação e dependem somente do tipo e concentração das substâncias presentes na coluna de agua. As substâncias opticamente activas absorvem ou dispersam a luz, podendo as propriedades opticas inerentes serem descritas como a probabilidade de um fotão ser removido (absorvido) ou redireccionado (disperso) por unidade de medida. São estas propriedades que se relacionam directamente com a concentração das substâncias no meio. No entanto, são as propriedades aparentes que são mensuraveis por satellite.

A medição da “cor” é feita pela quantificacao da radiância/reflectância que é emitida pela coluna de agua nos comprimentos de onda do visivel. O sensor óptico, a cerca de 800km de altitude, recebe o sinal emitido. No entanto, 90% do sinal que é recebido provem da atmosfera ou de outras fontes que não da coluna de agua. Diferentes procedimentos foram desenvolvidos para efectuar a correcção atmosferica (ex. Gordon and Wang, 1994) e uma vez isolado o sinal proveniente da coluna de agua, este pode ser então interpretado e relacionado com as suas propriedade ópticas inerentes e consequentemente com as substâncias nela presentes.

Uma única expressão, a *radiative transfer equation* (RTE), relaciona as propriedades aparentes e inerentes entre si. Contudo, a sua resolução requer o uso de aproximações. Algoritmos empiricos, semi-empiricos e analiticos têm sido desenvolvidos de forma a determinar IOPs e concentrações de substâncias directamente a partir das AOPs medidas pelos sensores (ex.: Garver and Siegel, 1997, Lee et al., 2002, Maritorena et al., 2002, O’Reilly et al., 1998).

Os componentes opticamente activos são geralmente agrupados por semelhanca espectral, e podem ser de 3 tipos: 1) matéria orgânica dissolvida (CDOM), 2) fitoplâncton e 3) material inorgânico particulado (ou sedimentos em suspensão). De forma a simplificar o desenvolvimento

de algoritmos, as massas de água foram classificadas em dois tipos (Morel and Prieur, 1977). No caso das águas tipo-I, as suas propriedades ópticas co-variam com o fitoplâncton e material associado. Recorrendo à clorofila (Chl) como *proxy*, pode afirmar-se que a partir da concentração de Chl se conseguem determinar as propriedades ópticas da massa de água. Quando a presença de CDOM ou de sedimentos em suspensão ocorre simultaneamente e não co-varia com o fitoplâncton, as águas são ditas de tipo-II, e a interpretação das propriedades ópticas é mais complexa.

A clorofila absorve luz predominantemente na região azul e vermelha do espectro do visível e reflecte na região do verde. Um aumento de Chl conduz a uma diminuição na reflectância na zona do azul e apenas a um ligeiro aumento na região do verde. Estas diferenças de reflectância nos diferentes comprimentos de onda possibilitam o uso dos rácios de reflectância azul-verde para determinar a concentração de Chl através de relações empíricas. Estes algoritmos empíricos são operacionalmente usados pelas Agências Espaciais para gerar produtos de Chl, no entanto, são teoricamente apenas aplicáveis em águas tipo-I. Em águas tipo-II, a presença de CDOM ou de sedimentos em suspensão pode condicionar a relação dos rácios com a concentração de Chl e portanto, inviabilizar a operacionabilidade destes algoritmos. No entanto, algoritmos aplicáveis em águas tipo-II têm vindo a ser desenvolvidos (ex.: Doerffer and Schiller, 2007).

As especificidades dos algoritmos podem levar a diferenças nas incertezas dos produtos gerados, e a importância de validar os produtos de Chl com dados *in situ* de diferentes regiões tem sido reconhecida pelas Agências Espaciais. Estas agências promoveram a criação de bases de dados com o intuito de apoiar a actividade de validação dos seus produtos e de desenvolver novos algoritmos. Os resultados de validação têm revelado que a nível global os objectivos de exactidão de 5% para os dados radiométricos e de 35% para a concentração de Chl têm sido verificados (McClain, 2009), contudo, a nível regional, os erros associados podem ser superiores, tendo sido propostos ajustes regionais aos algoritmos (ex.: Garcia et al. 2005, Folkestad et al., 2007, Volpe et al., 2007). O uso dos produtos de Chl para monitorização ambiental, estudos de análise climatológica, ou cálculo de produção primária e análise de impacto dos ciclos biogeoquímicos a nível regional e global tornam prioritária a validação e análise de incertezas associadas a estes produtos.

O objectivo principal desta tese incluiu a avaliação dos produtos *standard* de clorofila dos sensors MERIS e MODIS, o ajuste regional de algoritmos usados para a determinação da concentração de Chl, bem como identificar a variabilidade espacial e temporal dos factores associados aos erros dos produtos de Chl. Os seguintes objectivos específicos foram

identificados e realizados: 1) Recolher dados de pigmentos fitoplanctónicos e organizar uma base de dados para a validação e desenvolvimento de aplicações de produtos de “cor” do oceano; 2) Validar e comparar os produtos de Chl dos sensores MERIS e MODIS para a costa portuguesa; 3) Proceder a ajustes regionais dos algoritmos; 4) Produzir mapas de classificação óptica das águas ao largo de Portugal de forma a possibilitar a análise da variabilidade sazonal e espacial da sua distribuição.

A validação dos produtos de Chl para a costa portuguesa foi feita através da análise estatística da comparação de produtos de diferentes sensores com dados *in situ* recolhidos durante dois programas de monitorização e a bordo de 13 cruzeiros de investigação. Os dados de pigmentos fitoplanctónicos foram colhidos ao longo dos anos, de 2005 a 2012, e foram processados por cromatografia líquida de alta precisão (HPLC). A concentração de Chl foi comparada com dados contemporâneos dos sensores MERIS e MODIS. Os produtos testados incluíram os produtos *standard* algal 1 e algal 2 do MERIS e o OC3M do MODIS, bem como novos produtos, recentemente desenvolvidos no âmbito de projectos da Agência Espacial Europeia (ESA), nomeadamente os produtos gerados pelo projecto CoastColour e pelo projecto *Climate Change Initiative* (CCI). O ajuste regional de um algoritmo baseado numa rede neuronal (MLP_ATLP) foi também testado.

De um modo geral, os produtos de satélite revelaram uma sobreestimação da concentração de Chl em comparação com os valores *in situ*. Os melhores resultados foram obtidos pelo algoritmo que foi especificamente ajustado para a região em estudo (MLP_ATLP). Dos produtos *standard* testados, os melhores resultados foram determinados com o OC3M do MODIS e o algal 2 do MERIS. O primeiro obteve menor dispersão dos dados ($<RMS$), o segundo revelou menor erro de exactidão ($<bias$) em relação aos dados *in situ*. A análise específica dos diferentes cruzeiros separadamente revelou diferenças estatísticas, tendo a região da Nazaré sido identificada como uma área de interesse para as actividades de validação. Esta região é oceanograficamente e bio-geoquimicamente muito dinâmica, possibilitando a avaliação da performance dos algoritmos em águas com diferentes propriedades ópticas numa reduzida área de amostragem. Dados ópticos *in situ* foram obtidos durante um cruzeiro nesta região e a análise dos dados revelou a presença de águas dominadas por CDOM. A informação recolhida neste cruzeiro (68 estações de óptica), durante a Primavera de 2011, permitiu uma caracterização da região amostrada, no entanto, não possibilita uma generalização, uma vez que a amostragem foi espacial e temporalmente restrita. De forma a obter um mapa da distribuição sazonal dos tipos de água ao longo e ao largo da costa portuguesa, usaram-se dados de detecção remota. O modelo descrito por Lee e Hu (2006)

foi testado, mas os resultados revelaram problemas de correcção atmosférica nas primeira bandas do visível (na região do azul). De qualquer forma, o esquema de classificação dos tipos de água foi aplicado parcialmente e permitiu mapear a distribuição das águas dominadas por sedimentos em suspensão. A distribuição destas águas revelou uma forte componente sazonal, sendo a sua presença mais predominante ao longo da costa norte, a norte do Cabo Espichel, durante o inverno.

O impacto de diversos parâmetros nos erros determinados para os produtos de Chl foi também avaliado. Apenas os produtos *standard* foram testados e os principais factores associados aos erros determinados variaram de acordo com o produto analisado. Os valores de clorofila, da primeira profundidade óptica e da radiância nos 555 nm foram parâmetros significativamente relacionados com a percentagem de erro encontrada entre o produto MODIS e os dados *in situ*. Para os produtos *standard* do MERIS, o erro associado ao produto algal 1 foi significativamente relacionado com o índice de tamanho das células da comunidade fitoplanctónica da amostra, com os valores de radiância na banda dos 555 nm e com o rácio das radiâncias nas bandas 412/443nm. Este rácio também esteve significativamente relacionado com o erro determinado para o produto algal 2. Os valores de clorofila e da primeira profundidade óptica estiveram também significativamente relacionados com o erro neste produto.

Todos os objectivos inicialmente propostos foram atingidos. Os resultados gerados são essenciais para aplicação em diversas áreas, não só de investigação, mas também como validação de ferramentas de monitorização ambiental. Um exemplo de investigação futura inclui a detecção de blooms de algas nocivas por satélite, o que envolve a análise de dados históricos de Chl, para estabelecer limites associados a variabilidade natural da biomassa fitoplanctónica e identificar anomalias. As contribuições desta tese, serão usadas durante o projecto Europeu EU FP7 AQUA_USERS, cujo objectivo será o de modelar e identificar precocemente o aparecimento deste tipo de blooms, e no qual a equipa do centro de oceanografia está envolvida. A base de dados recolhida durante este estudo pode ainda ser explorada a nível ecológico e contribuir para o conhecimento da dinâmica das comunidades de fitoplâncton em diferentes regiões da costa portuguesa (ex.: Mendes et al., 2011, Silva et al., 2008).

Palavras-chave: Clorofila, Cor do oceano, detecção remota, sensores MERIS e MODIS, validação, características ópticas das massas de água.

Summary

Ocean colour is an invaluable tool to monitor temporal and spatial distribution of phytoplankton biomass. Chlorophyll *a* (Chl) is the main biomass proxy for phytoplankton, and ocean colour sensors allow for a synoptic and quasi-permanent following of this pigment concentration in surface waters. However, algorithms that are designed for use at global scales may be less accurate at local and regional scales, namely in coastal areas. These optically complex areas are of utmost importance to monitor phytoplankton blooms as they are subject to major anthropogenic pressures. Therefore, regional evaluation of products accuracy is needed to ensure correct data analysis and interpretation. It is important to understand the limitations of the different products in reference to specific areas and to validate the ocean-colour standard products with *in situ* data, in order to satisfy the quality requirements for monitoring purposes. In this thesis, Chl product validation is undertaken by directly comparing remote sensing data with *in situ* surface data. Water samples collected during 2 monitoring programmes and on board 13 cruises off the Portuguese coast during the period 2005 – 2012 were processed by reversed phase High-Performance Liquid Chromatography (HPLC) for pigment determination, and the Chl concentration compared with coincident MERIS and MODIS sensors data. The performance of standard MERIS (algal1 and algal2) and OC3M MODIS products, as well as novel products generated by ESA projects (i.e., CoastColour and Climate Change Initiative, CCI, products) and a regionally adjusted algorithm were evaluated using match-up data sets. In general, satellite products were found to overestimate Chl concentrations in comparison to *in situ* values. Best results were determined for the regionalized algorithm (MLP_ATLP) and the standard products with best results were the MODIS OC3M and the algal 2 MERIS, the former having lower RMS, but the latter revealing lower bias. Statistical differences were verified for the various cruises, and Nazaré region was identified as an area of interest for validation activities due to its complex oceanographic dynamic. Optical *in situ* data collected in one cruise revealed the presence of CDOM dominated waters, however more comprehensive analysis is needed. The use of remote sensing data for water-type classification revealed the need for improved atmospheric correction in the blue part of the spectrum. Nonetheless, classification scheme applied revealed a strong seasonal component in the spatial distribution of non-case 1 water types, which were more relevant along the northern coast (i.e., north of Cape Espichel) during winter.

Factors influencing Chl products accuracy varied according to product under analysis. Biomass, first optical depth and water-leaving radiance at 555 nm were found to be significantly related to the percent error of MODIS Chl product. For MERIS standard products, algal 1 percent error was significantly related to the phytoplankton size index, to the water-leaving radiance at 555 nm and to the water-leaving radiance ratio 412/443 nm, which was also significantly related to the algal 2 product error. Biomass and the first optical depth were the other factors identified to be significantly related to algal 2 product percent error.

Keywords: Chlorophyll, Ocean colour, Meris and MODIS sensors, validation, water type

Thesis motivation, objectives and outline

This thesis was motivated by the need to better understand the performance of standard Chlorophyll a (Chl) satellite products. Phytoplankton represent the basis of oceanic food webs. Their dynamics may have significant implications in terms of fisheries and they can be considered as indicators of ecosystem quality. Therefore, they are key elements to evaluate and monitor, both in short and long-term perspectives. The aim of this thesis was to evaluate the standard MERIS and MODIS Chl products, to perform algorithm regional adjustments, and to identify the spatial and temporal variability of environmental parameters that influence their performance. The main objective was pursued by focusing on the following specific tasks:

- ①. To gather a phytoplankton pigment database for ocean colour product validation and application development;
- ②. To validate and compare MERIS and MODIS sensor Chl products for the Portuguese coast;
- ③. To perform regional adaptations to the algorithms;
- ④. To provide a classification of the waters off the Portuguese coast and a general seasonal and spatial analysis of its variability.

A schematic representation of the thesis organization is presented in Figure 1. The thesis is organized in 5 Chapters. Chapter 1 includes a general introduction to provide the reader the background and necessary context to understand the work described in the following chapters. Basis of ocean-colour and phytoplankton knowledge are provided, as well as a characterization of the study area. The data collected and methods applied are detailed in Chapter 2. Data collection and quality processing of both *in situ* and satellite datasets are described. Details on the comparison procedure and statistical analysis are also given. The complete *in situ* dataset is provided in Annex I. Results are presented in Chapter 3 and discussed in Chapter 4. Concluding remarks, as well as future perspectives are addressed in Chapter 5.

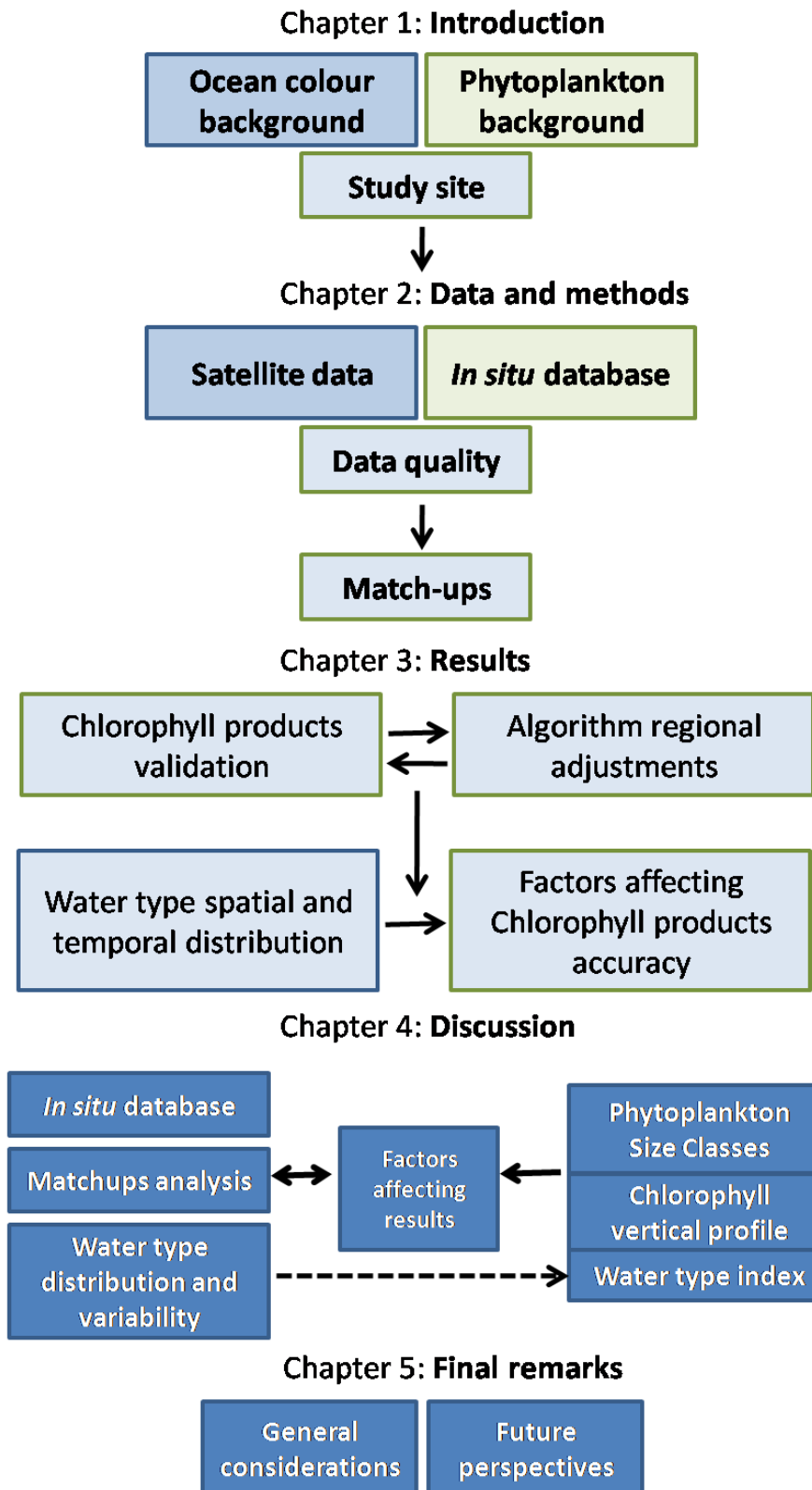


Figure 1 Schematics of thesis organization and investigated topics.

Chapter 1: Introduction

1.1 Ocean colour

Ocean colour has long been an invaluable tool for scientists to understand global and regional oceanographic events. In the 19th and early 20th centuries oceanographers were already using ocean colour as an indicator of water masses and, indirectly, ocean currents (Robinson, 2004). This was conducted through qualitative methods such as the Forel Scale (Forel, 1890), used to determine the colour of seawater, and the Secchi disk used to quantify the transparency of seawater (Secchi, 1866). In the 1960s and 1970s, the technological basis for marine applications of ocean-colour remote sensing began to emerge with airborne studies aimed at chlorophyll *a* (Chl) detection (Clarke et al., 1970). During that period the fundamental theoretical basis for marine radiative transfer (Preisendorfer, 1961) and the relationship between spectral radiance or reflectance at the sea surface and phytoplankton pigments (Morel and Prieur, 1977) also emerged, and the first satellite sensor to monitor ocean colour was launched in 1978, by the american space agency (National Aeronautics and Space Administration - NASA). The Coastal Zone Colour Scanner (CZCS) was a proof-of-concept mission which flew aboard the Nimbus-7 satellite for the period 1978-86. During this period, the feasibility of ocean-colour satellite remote sensing was finally established (e.g. Gordon et al., 1983, Smith and Wilson, 1981). It had been proven that the radiance leaving a water body could be detected and quantified by a sensor put into orbit, and further quantitatively related to its Chl content. The main concepts and processes involved in the quantification of substances present in a water body through ocean-colour will be introduced in the following sections.

1.1.1 Electromagnetic radiation and optical properties

Electromagnetic radiation is made up of a continuum of wavelengths ranging from very short (gamma rays, typically 0.1 nanometres) to very long (radio waves, typically in the order of meters). The sun emits all forms of radiation within the electromagnetic spectrum (EM), but the Earth's atmosphere blocks part of the radiation and passive remote sensing (RS) from space is only possible due to atmospheric windows in different parts of the EM (Figure 2). Atmospheric windows are parts of the EM where the atmosphere has a small influence on the transmission of light and determine which wavebands are available for oceanography. For instance, in the visible region (400-700 nm), atmospheric opacity is low allowing for the analysis of the “colour” of the targets observed. In fact, the visible portion of the EM accounts for approximately 45 % of total solar energy (Kirk, 1994) and, as a consequence, evolution has resulted in many organisms

utilising the visible portion of the EM whether for sight, as with the case of humans, or for energy, as in the case of photosynthetic organisms (Falkowski and Raven, 1997).

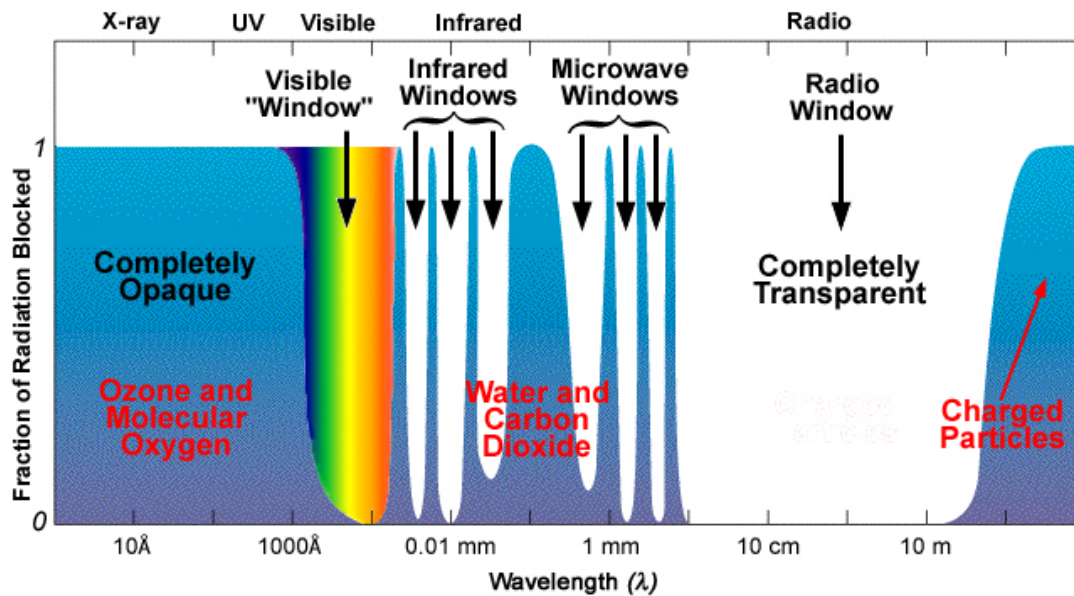


Figure 2 Schematic representation of the atmospheric windows for remote sensing.

Ocean colour satellites orbit the earth at around 700-800 km altitude. This means that the signal reaching the sensor needs to be corrected for the atmospheric component. More than 90 % of the signal reaching the sensor has an atmospheric origin, which needs to be subtracted from the total signal in order to get only the portion coming from the target of interest, in this case, the ocean. This means that only ~10 % of the signal reaching the sensor is relevant to retrieve the optically active sea-water components (Figure 3).

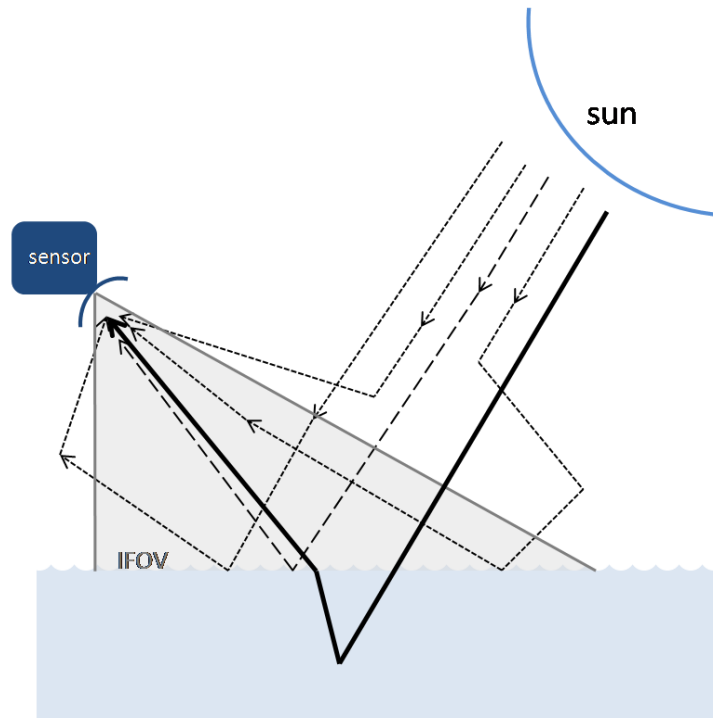


Figure 3 Schematics of light pathways reaching a remote sensor (adapted from IOCCG, 2000). IFOV refers to the instant field of view of the sensor.

Different atmospheric correction procedures have been developed to retrieve the ocean-colour signal (e.g. Gordon, 1997). The most simple correction relies on the fact that the water absorbs all radiance in the near infra-red (NIR) part of the spectrum (i.e., zero reflectance), which is also known as the “black pixel assumption” (Gordon and Wang 1994). The NIR bands are essentially used to identify the aerosol type and optical thickness in order to remove the contribution due to the atmosphere in the visible part of the spectrum (Antoine and Morel, 1999; Gordon and Wang, 1994; Siegel et al 2000). Once the upwelling radiance coming from the sea surface has been isolated, it can be used to infer on the water components. This involves the analysis of variations in magnitude and spectral quality of the water-leaving radiation to derive quantitative information on the type of substances present in the water and their concentrations. In other words, involves the analysis of the optical properties that characterize a water body, which contain latent information on its optically active constituents (OACs). Preisendorfer (1961) defines these optical properties according to their invariance under changes in the incident radiance distribution about the point at which the property is measured. According to this author, if the property is invariant with respect to changes in the radiance distribution, it is said

to be an inherent optical property, otherwise it is an apparent optical property. It should be noticed that all optical properties of ocean waters are wavelength (λ) dependent (IOCCG, 2000).

1.1.1.1 Apparent optical properties (AOPs)

Apparent optical properties (AOPs) are those optical properties that are influenced by the angular distribution of the light field, as well as by the nature and quantity of substances present in the medium (IOCCG, 2000). That is, properties which can be modified by the zenith-angular structure of the incident light field. Typically include the normalized water leaving radiance ($nL_w(\lambda)$), the remote sensing reflectance ($R_{rs}(\lambda)$) and the downwelling diffuse attenuation coefficient ($K_d(\lambda)$).

Radiance $L(\lambda)$ is defined as the measure of light energy leaving an extended source (Robinson, 2004) and depends on both the viewing and illumination geometry. It is a measure of radiant flux per unit area and per unit solid angle. Water leaving radiance ($L_w(\lambda)$) is the measure of the component of light energy leaving the water. The normalized water-leaving radiance ($nL_w(\lambda)$) is its normalization to a single sun-viewing geometry (Gordon, 2005): i.e., the radiance that would be measured leaving the flat surface of the ocean, with the atmosphere absent and the sun directly overhead (i.e. at zenith).

The ratio of upwelling and downwelling irradiances ($E_u(\lambda)$ and $E_d(\lambda)$, respectively) is defined as reflectance. Irradiance being the radiant flux per unit surface area in all directions. Reflectance is therefore a measure of how much of the downwelling light is reflected back up (Robinson, 2004). In ocean colour, remote sensing reflectance ($R_{rs}(\lambda)$) is commonly defined as the ratio of the upward normalized water leaving radiance ($nL_w(\lambda)$) and the downwelling irradiance ($E_d(\lambda)$).

The downwelling diffuse attenuation coefficient, $K_{Ed}(\lambda)$, defines the rate of decrease of downwelling irradiance with depth. That is, the variation of downwelling irradiance ($E_d(\lambda)$) in the water column per depth unit. It can be expressed according to $dE_d(\lambda, z)/E_d(\lambda, z) = -K_d(\lambda) dz$, where z is depth in metres. It is one of the geophysical variables that can be derived from ocean-colour data, and is often used as an index of water clarity.

These apparent optical properties are quantities measurable by remote sensing, but the ultimate goal is to derive, from them, quantitative information on the types of substances present in the water and on their concentrations. It is then necessary to relate the apparent optical properties to the substances in the water and its inherent optical properties.

1.1.1.2 Inherent optical properties (IOPs)

Inherent optical properties (IOPs) are independent of variations in the angular distribution of the incident light field, and are solely determined by the type and concentration of substances present in the medium (Preisendorfer, 1976 *in* IOCCG, 2000). This typically relates to how the water constituents present in the medium, absorb and scatter light. The IOPs can therefore be defined as those describing the probability of photon removal and photon redirection per unit length. The fundamental IOPs are the absorption, scattering and beam attenuation coefficients (a , b and c , respectively), where $c=a+b$, and the volume scattering function, which describes the scattering relative to the direction of light propagation and azimuth angle. Measurements of the volume scattering function are not commonly performed and restricted in the field to scattering coefficients.

An important characteristic of IOPs is that they are additive. This means that, for a seawater sample containing a mixture of constituents, the absorption and scattering coefficients of the various constituents are independent, and the total coefficient can be determined by summation. In an aquatic medium, the bulk IOPs are the sum of the IOPs for water itself and all the solutes and particles contained in it. Because of the impossibility of measuring the IOPs of each individual constituent, components are grouped operationally based on their spectral similarity or defined analytically. For total $a(\lambda)$, for example, Prieur and Sathyendranath 1981, suggested partitioning into contributions from: (1) water ($a_w(\lambda)$), (2) coloured dissolved organic matter, CDOM ($a_{\text{cdom}}(\lambda)$), (3) phytoplankton ($a_{\text{phy}}(\lambda)$) and (4) non-algal particles, NAP ($a_{\text{NAP}}(\lambda)$) (i.e. $a_{\text{total}}=a_w+a_{\text{CDOM}}+a_{\text{phy}}+a_{\text{NAP}}$). The same consideration can be applied to scattering (i.e. $b_{\text{total}}=b_w+b_{\text{NAP}}+b_{\text{phy}}$), but note that there is no scattering by CDOM. All these coefficients are bulk inherent optical properties, whereby each constituent in the water column is considered as a composite entity with no regard as to specific component contributions. The contributions of each component can be expressed as the product of the concentration of that substance and a corresponding specific absorption coefficient. The specific coefficient is the absorption normalized by the concentration of the constituent of interest (e.g. $a^*_{\text{phy}}(\lambda)=a_{\text{phy}}(\lambda)/\text{Chl}$). The absorption coefficients superscripted by an asterisk indicate the absorption components of each constituent per unit concentration. Analog for scattering.

Other IOPs can be derived given the mentioned basic set. For example, back-scattering coefficient (b_b) is defined as the integral of the volume scattering function ($\beta(\chi)$) over all

backward directions $\chi > 90^\circ$. From an Earth observation perspective, the bulk backscattering coefficient (b_b) from the ocean may be attributed mainly to bubbles, submicron particles and viruses (Stramski and Kiefer, 1991; Zhang et al., 1998), and some larger particles. Phytoplankton groups such as Coccolithophores and *Trichodesmium* can also have a particularly strong influence on backscattering of light (Balch et al, 1996; Subramaniam et al., 2002). Absorption, however, has been found to be the main optical property that can be used to identify phytoplankton (Ciotti et al., 2002), as phytoplankton absorb light for photosynthesis.

1.1.2 Water types

Based on their optical properties, water types/classes have been defined to simplify algorithm development. Case 1 waters were identified by Morel and Prieur (1977) and Gordon and Morel (1983) as waters for which phytoplankton and their associated materials (such as debris, heterotrophic organisms and bacteria, excreted organic matter) control the optical properties. Using Chl as a proxy for phytoplankton, it can be said that the Chl concentration defines the optical properties of Case 1 waters, which denotes not only Chl *a* pigment *per se* but also includes divinyl Chl *a* and chlorophyllide *a*, when the pigments are determined via high performance liquid chromatography (HPLC) technique (Morel and Antoine, 2011). However, this dependence of optical properties on Chl is not linear, the main reasons being: (1) the varying detritus-to-Chl ratio; (2) the varying pigments-to-Chl ratio in algal cells; (3) the packaging effect, which is an internal “shadowing” effect of the pigment that occurs in bigger cells with high pigment content; (4) the relative proportions of algae and of endogenous “yellow substance” which are not regularly varying along with Chl; to name a few (Morel and Antoine, 2011). Despite the non-linearity, optical properties follow closely the optical properties of phytoplankton. However, in regions influenced by land drainage or by sediment resuspension, the optical properties depart from those in Case 1 waters because of the presence of at least two additional components, already mentioned in the previous section, which can occur separately or simultaneously and are not generally correlated with Chl, namely: (1) the coloured dissolved organic matters, collectively named “yellow substance”, or CDOM; and (2) the mineral particles and various suspended sediments also referred to as non-algal particles (NAP). Generically, the optical properties of a “natural” water body are dependent on the presence/variability of these three OACs (phytoplankton, CDOM and suspended sediments) Figure 4. In other words, the presence and varying proportion of these components strongly change the optical properties of a water body.

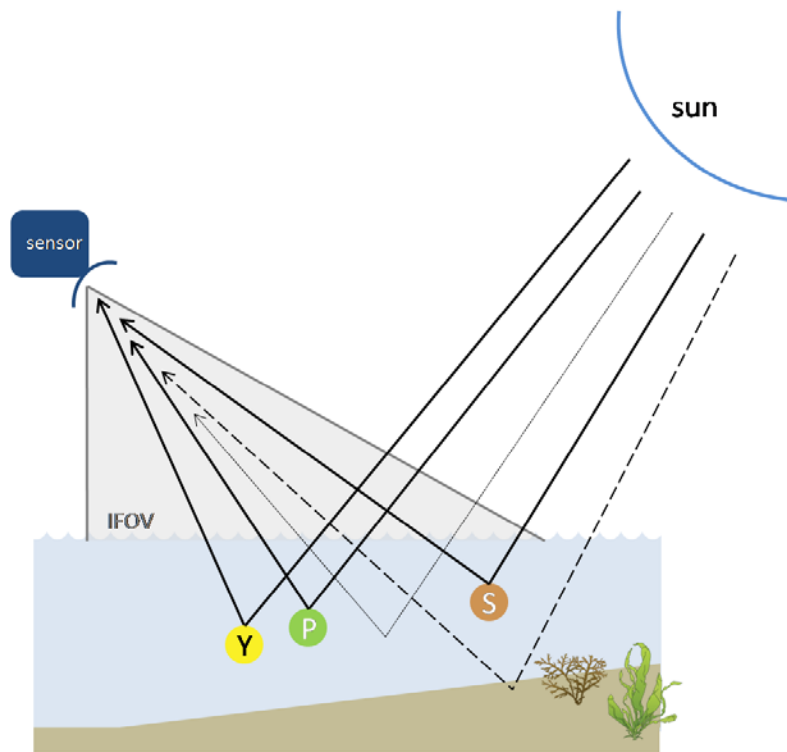


Figure 4 Factors that influence the upwelling light leaving the sea surface (adapted from IOCCG, 2000). Y - yellow substance (or CDOM); S – suspended sediment (or NAP); P – phytoplankton. IFOV refers to the sensors instant field of view.

For instance, the yellow substance-dominated waters are essentially absorbing (thus with extremely low reflectances), whereas the sediment-dominated waters are strongly scattering, with high reflectances (Figure 5).

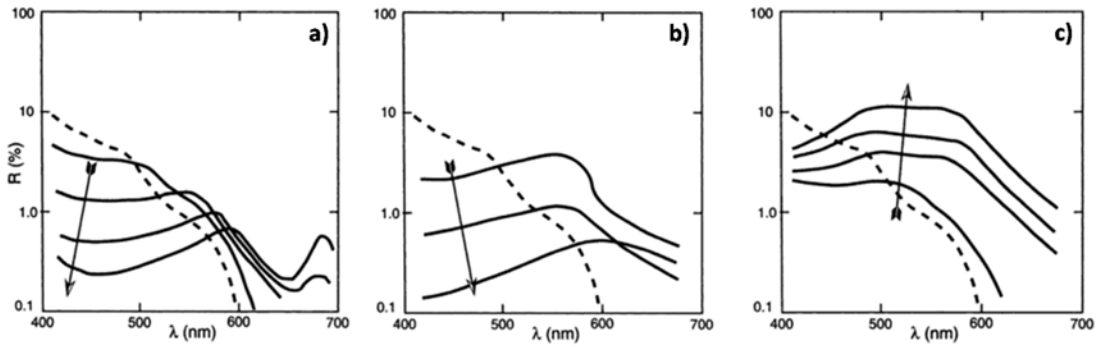


Figure 5 Reflectance spectra of water masses dominated by different optical active components. Chlorophyll (a), Yellow substance (b), and Inorganic sediments (c). Arrows indicate increasing concentration. (Image taken from Robinson, 2004)

It is generally recognized that Case 2 waters are more complex than Case 1 waters in their composition and optical properties. Interpretation of an optical signal from Case 2 waters can therefore be rather difficult. The "natural" waters have been conceptually organized by Prieur and Sathyendranath (1981) in Case 1 and Case 2 according to the triangular diagram in Figure 6. The 3 tips (denoted Chl, Y and S) represent the Chl-dominated waters, (i.e. the "true Case 1 waters"), the yellow substance-dominated Case 2 waters, and the sediment dominated Case 2 waters, respectively. The central part of the triangle represents Case 2 waters with various mixtures of OACs.

In Case 1 waters, and depending on the trophic regime, the Chl concentration can vary over about 3 orders of magnitude, starting from very low values ($\sim 0.02 \text{ mg m}^{-3}$) in vast oligotrophic zones (as subtropical gyres) up to high values, $5\text{-}30 \text{ mg m}^{-3}$, in more restricted upwelling areas (e.g. off Peru, Mauritania or Benguela), or during the short blooming period in moderate and high latitude ocean, as observed off the coast of Portugal.

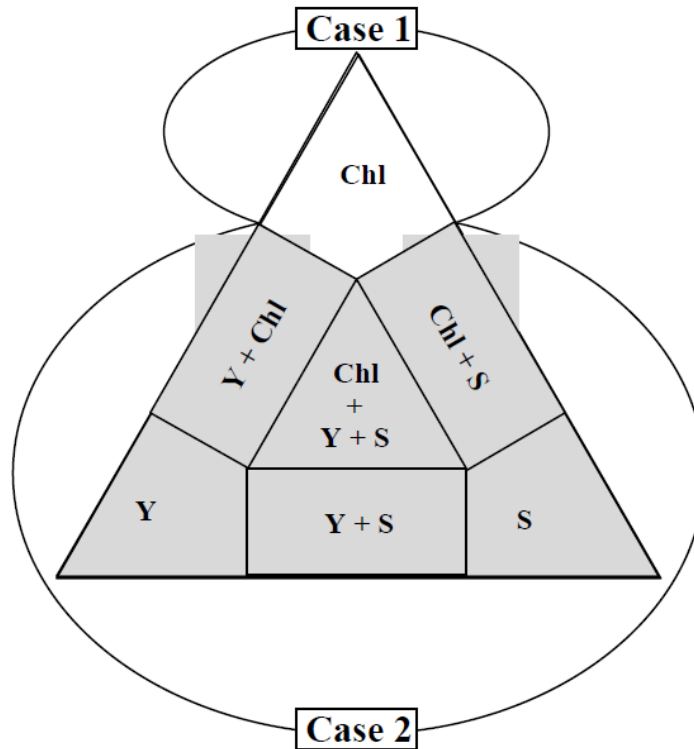


Figure 6 Water type classification scheme (in Morel and Antoine, 2011) Y - yellow substance; S – suspended sediment; Chl - phytoplankton

Geographically, Case 2 waters are usually associated to coastal zones, where the presence of rivers and dynamic processes like waves and tides promote introduction and resuspension of sediments. Contrastingly, Case 1 waters are typically associated to the open ocean, which does not mean that such waters are uniform. Peculiar situations are to be expected in the open ocean like the occurrence of monospecific blooms such as coccolithophorids blooms (Brown and Podestá, 1997), *Trichodesmium* blooms (Subramanian et al., 1999), *Phaeocystis*, or *Synechococcus* blooms (Morel, 1997), which lead to strong deviations from the Case 1 typical properties. In fact, the association of coastal and open ocean waters to Case 2 and Case 1 waters, respectively, can be misleading as waters can be differently classified depending on criterion applied (Mobley et al., 2004) and non-Case 1 waters can be found offshore (Lee and Hu, 2006).

1.1.3 Ocean colour algorithms

Satellite sensors cannot measure IOPs of the sea directly, instead they measure AOPs. In order to determine IOPs they must be estimated from AOPs, which implies assumptions on the distribution of the underwater light field. A unique expression, namely the radiative transfer equation (RTE), establishes the exact relationship that links the two classes of properties. Deriving the AOPs from the knowledge of IOPs combined with boundary conditions (e.g. the incident solar radiation) is generally called the forward problem; the inverse problem consisting of retrieval of the IOPs from measured AOPs under known illumination conditions. However, both problems require the manipulation of the RTE, which are integral equations that do not permit an easy solution. This has resulted in the development of a variety of numerical and analytical techniques involving approximations in order to produce a solution (Robinson, 2004). Empirical, semi-empirical and analytical techniques have arisen that directly estimate IOPs and/or water substances concentrations from AOPs using satellite data (see Carder et al., 1999; Garver and Siegel, 1997; Lee et al., 2002; Maritorena et al., 2002; O'Reilly et al., 1998; Smyth et al., 2005).

Empirical approaches rely on a specific spectral feature, such as a spectral ratio modelled to biophysical measurements using statistical regression, whereas semi-analytical algorithms rely on greater knowledge of optical properties of the water column and dealing to isolate the spectral influence of several optical variables (IOCCG, 2006). The empirical algorithms are derived from regression of coincident ship and satellite observations of $L_w(\lambda)$ against shipboard observations of Chl. The inputs to these algorithms are satellite observations of L_w or equivalently R_{rs} at several wavelengths; the output is Chl concentration.

Chlorophyll *a* absorbs light in the blue and red portions of the visible spectrum and reflects light at green wavelengths (Figure 5-a). As the Chl concentration increases, light is absorbed more strongly in the blue and red portions of the spectrum and reflects more strongly in the green. Therefore, as Chl increases, the reflectance in the blue regions decreases and in the green it increases slightly. Thus a ratio of blue to green water reflectance can be used to derive quantitative estimates of the satellite-derived Chl concentration. However, one has to be cautious when using band-ratio algorithms to derive the Chl concentration as they will only function in waters whose variations in optical properties are mainly driven by the abundance of phytoplankton, i.e. Case 1 waters. In more optically complex waters (Case 2 waters), where $R_{rs}(\lambda)$ is more heavily influenced by CDOM and suspended sediments, band ratio algorithms are likely to break down. Various authors have attempted to use semi-analytical models to derive

the Chl concentration in more optically complex waters (e.g. Morel and Maritorena 2001; Maritorena et al., 2002).

Operational algorithms in use by Space Agencies for Chl products retrieval are generally band-ratio algorithms derived and applicable to Case 1-waters, although specific algorithms have been also developed for application in Case 2-waters (e.g. Algal 2 MERIS product, Doerffer and Schiller, 2007). Chlorophyll is typically the main variable derived from ocean colour imagery and its synoptic estimates have allowed to greatly increase the knowledge about spatial, seasonal and inter-annual variability of phytoplankton biomass as indexed by Chl, at regional and global scales (e.g. Behrenfeld et al., 2006; Dandonneau et al., 2004; Kahru and Mitchell, 1999; Kahru et al., 2012; Werdell et al., 2009; Yoder et al., 2010).

1.1.4 Ocean colour sensors

The first ocean colour dedicated mission was the NASA's proof-of-concept sensor, Coastal Zone Color Scanner (CZCS), which exceeded all expectations and end up operating from 1978 until 1986. CZCS was aboard satellite Nimbus 7 which was launched into a 995 km near polar sun-synchronous orbit in 1972 (Gibson et al., 2000). The CZCS obtained reflected radiation in five bands in the 433-800 nm range and had a spatial resolution of 825 m for a 1,556 km wide swath (Gibson et al., 2000). With the goal of measuring water-leaving radiance, at a limited number of wavebands in the visible domain, and to use the signal to infer concentrations of phytoplankton pigments in the near-surface layers of the ocean, CZCS demonstrated, for the first time, the feasibility of retrieving Chl from RS data on a synoptic and global scale. The next satellite instruments were the Japanese Ocean Colour and Temperature Sensor (OCTS) on the ADEOS-1 satellite that operated from August 1996 to June 1997, and the German Modular Optical Scanner (MOS) launched in 1996 on the Indian Remote Sensing Satellite IRS-P3 (Martin, 2004). The Sea-viewing Wide Field-of-view Sensor (SeaWiFS) was launched on the ORBVIEW-2 satellite in August 1997, and operated between the 412-865 nm range since September 1997 until December 2010. The Moderate Resolution Imaging Spectrometer (MODIS) was launched on the TERRA satellite in December 1999 and on AQUA satellite in May 2002 (Martin, 2004). MODIS sensors have a spatial resolution of 250 m in the UV band, 500 m in the visible waveband in the red, and 1 km in the ocean-colour wavebands (Robinson, 2004). In March 2002, the European Space Agency (ESA) launched its first ocean colour sensor, the Medium Resolution Imaging Spectrometer (MERIS), onboard the ENVISAT platform, where MERIS is in a descending sun-

synchronous orbit with 15 observing bands between 400 and 900 nm (Martin, 2004). Its primary goal was to monitor ocean colour. However, it was also designed to determine atmospheric and land surface information. MERIS had five parallel arrays to gain a swath width of 1150 m, offering ocean colour and geophysical products at a reduced resolution of 1200 m (RR) and full resolution (FR) capability of 300 m (Robinson, 2004). MERIS operationally ceased in April 2013. More recently (March 2011), NASA launched the Visible Infrared Imaging Spectro-Radiometer Suite (VIIRS), under the National Polar-orbiting Operational Environment Satellite System (NPOESS). ESAs next ocean colour mission is expected to be launched in 2014, Ocean and Land Colour Instrument sensor (OLCI) on Sentinel-3 satellite, within the European Union-ESA Global Monitoring for Environment and Security (GMES) programme.

Table I List of ocean colour sensors (IOCCG, 2012)

Sensor (Satellite)	Mission Developer	Launch year	Spatial Resolution (m)
CZCS (NIMBUS-7)	NASA (USA)	1978	825
POLDER (ADEOS)	CNES (FRANCE)	1996	6000
OCTS (ADEOS)	JAXA (JAPAN)	1996	700
SeaWiFS (SeaStar)	NASA (USA)	1997	1100
OCI (ROCSAT)	NSPO (TAIWAN)	1999	800
OCM (IRS-P4)	ISRO (INDIA)	1999	350
MODIS (Terra/Aqua)	NASA (USA)	1999	1000
MERIS (ENVISAT)	ESA (EU)	2002	300 & 1200
GLI (ADEOS-II)	JAXA (JAPAN)	2002	1000
COCTS (HY-1B)	CAST (CHINA)	2007	1100
GOCI-I (COMS)	KIOST (KOREA)	2010	500
VIIRS (Suomi NPP)	NOAA (USA)	2011	750
OLCI (SENTINEL 3)	ESA (EU)	2014	300
SGLI (GCOM-C1)	JAXA (JAPAN)	2015	250 & 1000
GOCI-II (GeoKOMPSAT-2B)	KIOST (KOREA)	201	250 & 1000

1.1.5 Ocean colour products validation

Ocean-colour missions have revealed the importance of validating satellite products. NASA (e.g. SeaWiFS, MODIS) and ESA (e.g. MERIS) sensors have been validated with both geographically distributed field measurements and radiometric data collected by moored systems. The space agencies defined as goals for accuracy 5% for radiometry and 35% for Chl concentration (e.g. McClain, 2009) supporting large datasets programs for algorithm development and validation (e.g. NASAs SeaBASS database and ESAs MERMAID matchup database). Although global results are within the error expectations, satellite validation with *in situ* data has revealed the need for specific algorithm adjustments at regional levels (e.g. Folkestad et al., 2007; Garcia et al., 2005; Komich et al., 2009; Ohde et al., 2007; Sorensen et al., 2007; Volpe et al., 2007).

The need for validation of ocean-colour products is also emphasized by the necessity of merging satellite ocean colour observations. Different projects have focused on data merging to provide continuous global products, including the GlobColour project (<http://www.globcolour.info>), the NASA SIMBIOS Program (McClain et al., 2002; Maritorena and Siegel, 2005), and the recent OC-CCI ESA project (Ocean Colour Climate Change Initiative). Such projects aim to improve the consistency of ocean colour time-series, spatial and temporal coverages, and produce the necessary requirements to use ocean colour as an Essential Climate Variable (EVC). This thesis uses the MODIS and MERIS datasets for ocean colour product validation off the Portuguese coast.

1.2 Phytoplankton

The term *plankton* was introduced by Viktor Hensen in 1887, and originally described “everything that drifts in the water, whether shallow or deep, living or dead” (from Taylor 1980 in Hoppenrath, 2009). The term evolved to include only living organisms caused probably by the “Plankton-Studien” of Ernst Haeckel published in 1890 (Taylor 1980 in Hoppenrath, 2009). Phytoplankton refers to the *phyto*, “plants” in greek, component of plankton. The small “plants”/ “algae” / photosynthetic protists that drift in the water column. A broad variety of taxa are represented in the marine phytoplankton, including cyanobacteria, Prochlorophyta, Chlorophyta, Euglenophyta, Dinophyta, Cryptophyta and Chromophyta (Bacillariophyta, Chrysophyceae, Rapidophyceae and Prymnesiophyceae). These phytoplankton communities are essential to the majority of ecological processes and affect the structure of food webs (e.g., primary production), nutrient cycling and the flux of particles to deep waters. Primary production is one of the most important ecological aspects of the phytoplankton as the biomass

built through photosynthesis is the nutritional basis for all higher trophic levels (e.g. zooplankton). Relevance of phytoplankton role not only in the oceans but also in the global ecosystem has been emphasized by Field et al (1998) remote sensing study, where, for the first time, estimates of phytoplankton production were shown to account for 50 % of the world's primary production.

Phytoplankton distribution changes both horizontally and vertically (Barlow et al., 2007; Brunet and Lizon, 2003; Leal et al., 2009). Locally, temperature, salinity and currents, along with other factors, determine the horizontal distribution, while vertical distribution is primarily determined by irradiance, nutrients and water column stability. The effect of these factors on phytoplankton abundance and community structure is known to vary among worldwide regions, from tropical to temperate ecosystems (Longhurst, 1998).

1.2.1 Phytoplankton: size classes and functional types

Phytoplankton cover a wide spectrum of biological diversity (Bowler et al., 2009), encompassing taxonomic groups with distinct sizes, life cycles, turn-over rates, nutrient stoichiometry, biochemical composition and ecological requirements, performing therefore an array of diverse functions in the marine ecosystem. In this context, phytoplankton functional types (PFTs) have been defined to link certain phytoplankton groups (which can be polyphyletic) with specific biogeochemical functions (Nair et al., 2008). The number of defined PFTs can vary according to the scientific question being addressed (Le Quéré et al., 2005), but calcifiers (coccolithophores), silicifiers (diatoms), nitrogen fixers (Trichodesmium and N_2 fixing prokaryotes), pico-autotrophs (pico-eukaryotes, and cyanobacteria such as *Prochlorococcus* and *Synechococcus*) and DMS producers (e.g., autotrophic flagellates) are commonly considered.

Concerning size, phytoplankton have been categorized in: (1) picoplankton (<2 μm in diameter), comprising pro-prokaryotes (cyanobacteria, prochlorophytes and other bacteria) and pico-eukaryotes; (2) nanoplankton (2-20 μm), eukaryotic flagellates (cryptophytes, chrysophytes, prymnesiophytes and chlorophytes); (3) microplankton (20-200 μm), diatoms and dinoflagellates (Sieburth et al., 1978). This size-based approach to phytoplankton functionality is not always fully satisfactory from a biogeochemical perspective (Nair et al., 2008). For example, diatoms are silicifiers and typically categorised as micro-phytoplankton, yet some diatoms fall into the nano-size range. Although these smaller diatoms have the same biogeochemical function, they are likely to respond differently with respect to size-based functionality (e.g., export production).

There are also some examples of nano-phytoplankton of a similar size having a contrasting biogeochemical function (e.g., calcifiers and DMS producers). Despite this, many functions of phytoplankton, such as nutrient uptake, light absorption, metabolic rates and sinking are strongly related to size.

1.2.2 Phytoplankton Pigments

Phytoplankton contain three types of pigments involved in light harvesting and photoprotection: chlorophylls, carotenoids and biliproteins (Wright and Jeffrey 2006). All photosynthetic phytoplankton contain one or more types of chlorophylls as part of the light-harvesting complexes in their chloroplasts. Chlorophyll *a* (Chl) is ubiquitous to phytoplankton and the reason why it is used as a biomass proxy. Chlorophyll *a* are magnesium coordination complexes of conjugated cyclic tetrapyrroles with a fifth isocyclic ring and often esterified long-chain alcohol (Figure 7). Other chlorophylls differ according to the oxidation state of the macrocycle, the type of side-chains, and the type of esterifying alcohol, if present. For instance, Divinyl form of Chl, which can be found in prochlorophytes, results from a substitution of an ethyl group into a second vinyl one.

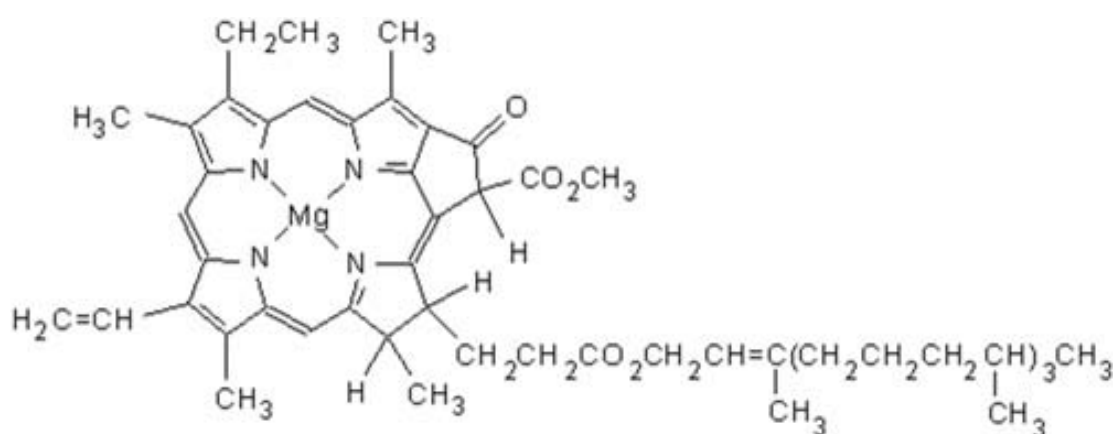


Figure 7 Chlorophyll *a* structure

Many Chl derivatives can be found both naturally and as artefacts of sample extraction. They may lose only the magnesium atom (pheophytins) or the phytol chain (chlorophyllides), or lose both the magnesium atom and phytol (pheophorbides). They may also spontaneously rearrange (epimers) or oxidize (allomers). Significant peaks of chlorophyllide *a* (Chlide *a*) are often seen in chromatograms because chlorophyllase enzymes can be activated when a cell is damaged (e.g., during filtration, storage or extraction). Significant degradation of Chl may occur if the cells are left too long on the filter, frozen too slowly or not cold enough, or extracted in a solvent that does not inactivate the chlorophyllase. Chlide *a* concentration is generally included in the total Chl fraction for biomass estimation. For satellite validation purposes, in this thesis, Chl is determined as the sum of chlorophyll *a* (including epimers and allomers), Chlorophyllide *a* and Divinyl form of chlorophyll *a*.

Table II List of most relevant pigments and their correspondent occurrence in phytoplankton communities (Jeffrey et al., 1997)

Pigment	Abbreviation	Occurrence
Chlorophyll <i>a</i>	Chl <i>a</i>	A proxy of algae biomass
Divinyl chlorophyll <i>a</i>	DvChl <i>a</i>	<i>Prochlorococcus</i> sp.
Total Chlorophyll <i>a</i> (Chl <i>a</i> + DvChl <i>a</i>)	TChl <i>a</i>	A proxy of total algae biomass
Chlorophyll <i>b</i>	Chl <i>b</i>	Chlorophytes, euglenophytes, and prasinophytes
Chlorophyll <i>c</i> 3	Chl <i>c</i> 3	Crysophytes and prymnesiophytes
Chlorophyll <i>c</i> 1+c2	Chl <i>c</i> 1,c2	Diatoms, prymnesiophytes, crysophytes, and dinoflagellates
Fucoxanthin	Fuco	Diatoms, prymnesiophytes, and crysophytes
19' Hexanoyloxyfucoxanthin	Hexa	Prymnesiophytes
19' Butanoyloxyfucoxanthin	Buta	Crysophytes and prymnesiophytes
Alloxanthin	Allo	Cryptophytes
Zeaxanthin	Zea	Cyanobacteria and chlorophytes
β,β-carotene	β-car	

Phycobiliproteins, which can be of three subtypes: phycoerythrobilins, phycocyanobilins and phycourobilins, are generally the third type of light harvesting pigment found in cyanobacteria, rhodophytes and cryptophytes. However, biliproteins are water soluble and not extractable by organic solvents used in the analysis of chlorophylls and carotenoids. Carotenoids are a diverse family of yellow, orange or red isoprenoid, polyene pigments, which are involved in light-harvesting or involved in photoprotection. These pigments have the ability to absorb light of blue and green wavelengths (420-550 nm) and, although quantitatively variable in response to

irradiance, are qualitatively very useful taxonomically as some carotenoids can be exclusive of some taxa. In fact, phytoplankton community structure can be assessed at some level (e.g. Class) through pigment analysis, and this method is widely used in oceanographic studies and has been widely applied (e.g., Barlow et al., 2008; Kyewalyanga et al., 2007; Leal et al., 2009; Mendes et al., 2007; Sá et al., 2013; Silva et al., 2008). A summary table of major taxonomical pigments and its meaning are presented in Table II (Jeffrey et al., 1997).

Concerning size-class, Vidussi et al. (2001) used diagnostic pigments as markers to derive pico-plankton, nano-plankton and micro-plankton components of phytoplankton in the Mediterranean. In this implementation, micro-plankton included diatoms and dinoflagellates, nano-plankton comprise haptophytes, cryptophytes, chrysophytes, prasinophytes and chlorophytes, whereas pico-plankton, included the cyanobacteria *Prochlorococcus* and *Synechococcus*, as well as several other classes, designated under the general term of pico-eukaryotes, whose composition and diversity are poorly known (Worden and Not, 2008). Later, using a large *in situ* database of vertical pigment profiles, Uitz et al. (2006) performed an empirical parameterisation for inferring the vertical structure in phytoplankton size classes from surface Chl. On account of its simplicity, the use of diagnostic pigments to derive algal size-class groups gained a wide acceptance in the marine community (e.g. Barlow et al., 2007; Bouman et al., 2005; Brewin et al., 2011; Bricaud et al., 2004; Dandonneau et al., 2004; Sá et al., 2013, Taylor et al., 2011, amongst others).

Pigments suffer several disadvantages as markers. Special conditions must be employed to preserve them, as they are sensitive to light, heat, oxygen, acids and alkalis, as well as spontaneous forming families of isomers in solution. Their distribution is complex, with few unambiguous markers and its expression variable, even within a particular class. Its content per cell can also vary with environmental factors such as irradiance and nutrients (e.g. Ruivo et al., 2011). However, pigment analysis is presently the best cost-effective technique for mapping phytoplankton populations and monitor their abundance and composition. Quantifying the pigment composition with techniques like HPLC allows for identifying phytoplankton communities, as well as to study the impact of pigments variation in the final Chl satellite products accuracy.

1.2.3 Phytoplankton from space

Chlorophyll *a*, as already mentioned, is an ubiquitous pigment. Some pigments, however, which are associated to specific groups, can change in type and amount relative to Chl concentration and affect substantially the phytoplankton absorption spectra (Hoepffner and Sathyendranath, 1992), Figure 8. Therefore, phytoplankton groups can have an influence on Chl product accuracy as algorithms may fail at local and regional scales due to their sensitivity to changes in composition of phytoplankton species present in the water (Sathyendranath et al., 2004).

The detection of PFTs and/or PSCs from space has been the subject of ocean-colour research in recent years (e.g. Brotas et al., 2013; Hirata et al., 2011; Nair et al., 2008) with the aim of supplementing our understanding of biogeochemical cycles on a global scale (e.g. Blackford et al., 2004; Le Quéré et al., 2005).

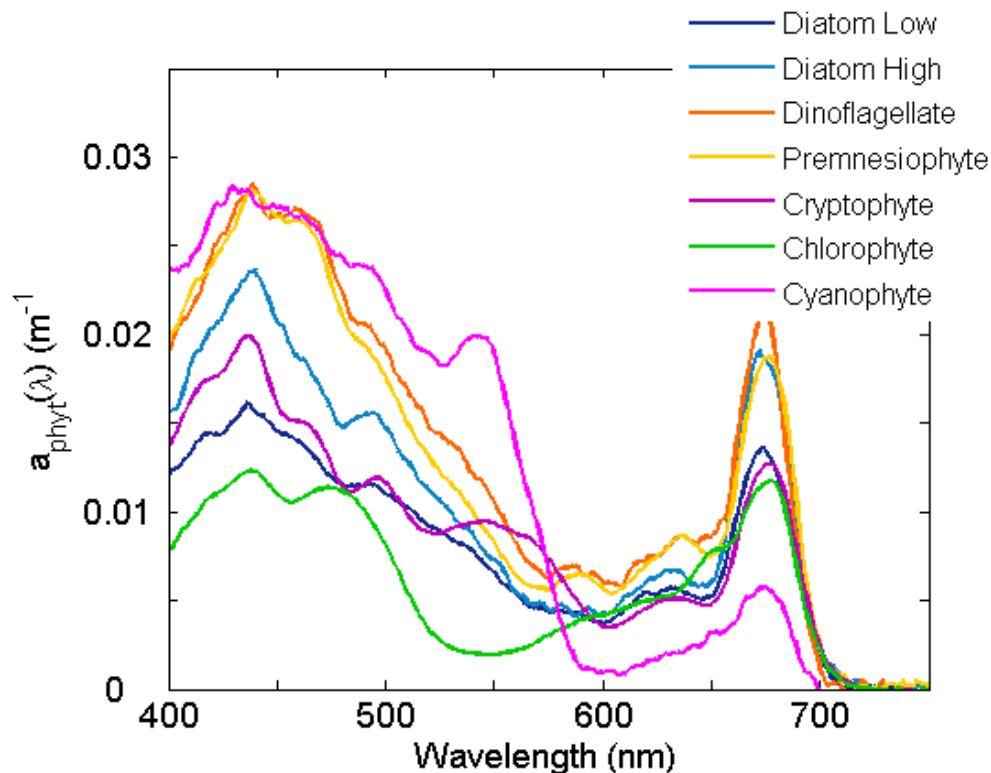


Figure 8 Example of absorption spectra for a range of monospecific cultures. Note the difference in the absorption coefficients of diatoms grown in high light compared to those grown in low light. (source: <http://www.oceanopticsbook.info>)

Two major bio-optical methods have been established: (1) those based on distinctive spectral-characteristics of each group (e.g. Alvain et al., 2005; Ciotti & Bricaud, 2006; Devred et al., 2011;

Kostadinov et al., 2009; Sathyendranath et al., 2004); and (2) those based on the well established relationships between cell-size and phytoplankton abundance (i.e. Chl concentration) (Brewin et al., 2010; Hirata et al., 2008, 2011; Uitz et al., 2006). This latter approach emphasizes the need for accurate Chl products. Such bio-optical methods have relied upon a combination of remote sensing and *in situ* data, namely, the analysis of phytoplankton pigments by HPLC. For instance, Brewin et al. (2010) developed a model to derive PSC from remotely-sensed Chl concentration. In their approach, Atlantic Meridional Transect (AMT) data and the Uitz et al. (2006) diagnostic pigment approach, adjusted to account for pico-eukaryotes in oligotrophic waters, were used to parameterise a conceptual model (Sathyendranath et al., 2001) and produce maps of pico-, nano- and micro-plankton at a global scale. Brotas et al. (2013), using regional pigment information, adjusted Brewin et al. (2010) method for application to the Eastern Atlantic and further developed the method to provide number of size-class cells. In another study, the relationship between Chl, PSC and seven PFT was statistically analysed from a large pigment database by Hirata et al. (2011), who determined, using SeaWiFS imagery, the relative abundance of PSC and PFT at the global scale.

Despite collection of *in situ* data being expensive and time consuming, the need to acquire more information on phytoplankton community structure, ecophysiological parameters or bio-optical properties, is identified by most authors as a major requirement to the further development of both remote sensing of PFT and ocean-biogeochemistry models (Brewin et al., 2011; Hirata et al., 2012; Le Quéré et al., 2005; Raitsos et al., 2008).

1.3 Study site

The coast of Portugal, between 37° and 42°N, is included in the North Atlantic Upwelling Region, which extends from the northern Iberian Peninsula at 43°N to the south of Senegal at approximately 10°N (Relvas et al., 2007). The major characteristics of this current system are comparable to the other Eastern Boundary Currents, as Benguela, Humbolt or California. They are characterized off-shore by slow broad equatorward gyre recirculation, a meridional alignment of coastlines and predominant equatorward wind direction during a substantial part of the year (Relvas et al., 2007). These equatorward winds promote upwelling events. They force an offshore Ekman transport in the upper layer and the consequent decline of the sea level towards the coast. As a result of the geostrophic adjustment of the coastal ocean, an alongshore equatorward jet is formed, transporting cold and nutrient rich upwelled water. The occurrence

of these upwelled waters is therefore dependent on the wind regime, which has a sharp seasonality in the western Iberia system mainly due to the annual cycle of the atmospheric systems. Between April and October, the Azores high pressure cell is strengthened and displaced northward, while the Iceland low pressure cell is weakened. These promote the set up of upwelling favourable winds (northerlies) (Fiuza et al., 1982). In the winter months, the dominant wind direction changes (mainly Westerlies and Southerlies) and a poleward flow of relatively warm and saline water propagate along the coast (Relvas et al., 2007).

Satellite derived sea surface temperature (SST) maps have been used in the past decades to describe the upwelling patterns in the region. There is a clear contrast between the cold, vertically mixed upwelled waters found typically over the shelf, and the oceanic thermally stratified waters. This pattern is observed throughout the west coast, however, SST anomaly maps reveal three main upwelling centres, where upwelled water filaments can be seen and extend more than 200 km off the coast: (1) between Capes Sao Vicente and Sines (37°-38°N), (2) between Capes Espichel and Carvoeiro (38.5°-39.5°N), (3) and between the mouth of Douro and Minho rivers (41°-42°N) (Relvas et al., 2007). Localized and/or intensified coastal upwelling is often associated with the presence of capes or promontories (Manson et al., 2005), Figure 9.

Coastal upwelling, water column stratification and nutrient availability were identified as the major sources of seasonal and spatial variability of phytoplankton abundance and assemblage composition (Moita, 2001). A band of high Chl concentration values (proxy of phytoplankton biomass) can be found in summer near the coast associated with cold upwelled waters, with a strong cross-shelf gradient characterizing the separation between upwelled and oceanic waters. Assemblages associated with upwelling are mainly composed of chain-forming diatoms (microplankton) and dominant through spring and summer, extending its distribution to a distance offshore dependent on the intensity of the upwelling. Coccolithophores (nanoplankton) dominate in oligotrophic oceanic areas, outside the areas influenced by the upwelling. Dinoflagellates (microplankton) in general are indicative of stratification conditions (Moita, 2001).

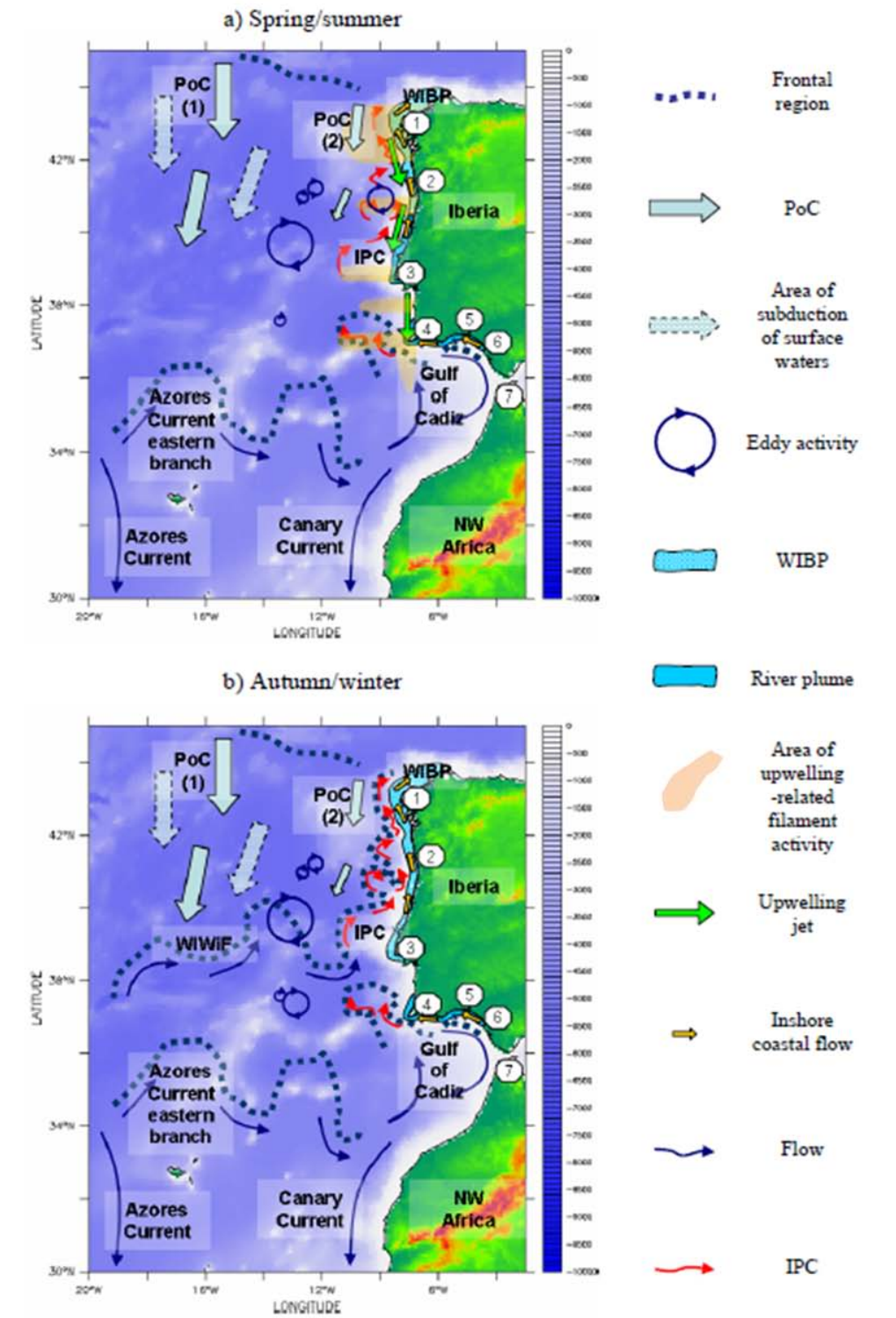


Figure 9 The Western Iberia and Gulf of Cadiz regimes in a) spring and summer, and b) autumn and winter (in Manson et al., 2005). PoC: Portuguese current; IPC: Iberian Poleward Current; WIWIF: Western Iberian Winter Front; WIBP: Western Iberian Buoyant Plume. 1) Cape Finisterre; 2) River Douro; 3) Roca Cape; 4) Cape S.Vicente; 5) Guadiana river; 6)Guadalquivir river; 7) Strait of Gibraltar.

Coastal Chl maximum values measured by Moita (2001) were recorded subsuperficially, while, offshore, these extended along the pycnocline and nutricline. In autumn, Chl maxima were recorded at the surface, with values of only one fourth of those recorded during summer. In winter, Chl maxima remained low and were recorded also at the surface. In spring, Chl maxima sank at the slope, after being advected by upwelled waters. A subsurface Chl maximum is a common feature of middle latitude oceanic waters, where after spring blooms the near-surface layers become depleted of nutrients and a subsurface Deep Chlorophyll Maximum (DCM) develops (Figure 10). Such layers can cause a significant increase in the satellite measured Chl (e.g. Da Silva et al. 2002; Stramska and Stramski 2005; Muacho et al. 2013).

Riverine input can also have a significant influence on the water column stratification and nutrient availability. Most of river outflow of the Iberian Peninsula occurs in the northern segment of the western Iberia. Several rivers drain between the latitudes of Lisbon and Cape Finisterre, namely the Tagus, Mondego, Douro and Minho. The river runoff in this area can result in buoyant plumes, The Western Iberia Buoyant Plume (WIBP), that develops into an inshore current (Peliz et al., 2003).

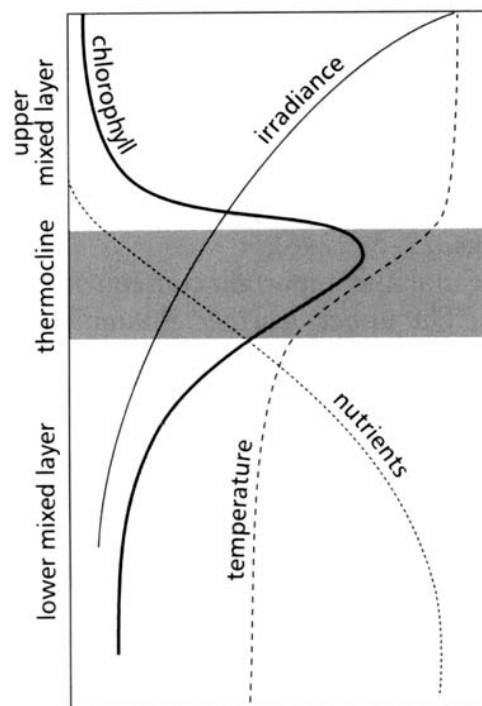


Figure 10 Schematics of a deep chlorophyll maximum (DCM). Source:

http://www.jochemnet.de/fiu/bot4404/BOT4404_9.html

A few studies in different areas of research (e.g., Peliz et al., 2005, Valente and Da Silva, 2009; Muacho et al., 2013, Mendonca et al., 2010) have been conducted in the region using ocean

colour data. Valente and Da Silva, (2009) by analysing the nLw at the 553 nm MODIS band, studied the variability of Tagus river outflow. Oliveira et al. (2009a) analysed circulation patterns for specific bloom events. Peliz et al. (2005) documented biomass variability along the coast. However, ground truth was only considered later for specific front detection by comparing SeaWiFS data to *in situ* fluorometer data by Ribeiro et al. (2005). Sá et al. (2008) reported a first preliminary match-up exercise with MODIS and MERIS data for the Portuguese coast. Mendonca et al. (2010) made a first attempt to evaluate the performance of SeaWiFS and MODIS over Sedlo and Seine seamount regions, located in the NorthEast Atlantic. Results revealed SeaWiFS overestimation of *in situ* measured values at more oligotrophic areas such as Seine, while MODIS slightly underestimated. Despite the differences observed between the two sensors, the authors concluded that the same tendency was found between Chl satellite estimations and Chl *in situ* measurements and the same patterns were detected by both satellites, making them both suitable for variability and large temporal scales studies.

Besides the insight into the bio-physical processes occurring in the study site, the high biomass variability and harmful algae blooms (HABs) occurrences in the area (Amorim et al., 2001, Amorim et al., 2004, Ribeiro and Amorim, 2008) highlight the importance of ocean-colour sensors as a consistent observational platform for monitoring purposes in comply with the Marine Strategy Framework Directive (MSFD) of European Union (EU). Portugal has the third largest Exclusive Economic Zone (EEZ) in EU, and such an extended area can only be properly monitored relying on RS tools. Goela et al. (2013) very recently reported absorption phytoplankton data measured from samples collected at the Southern Portuguese coast, as a contribution to ocean colour algorithm development in the region and Brotas et al. (2013) reported maps of class-size phytoplankton cell counts for the North Eastern Atlantic.

Chapter 2: Data and Methods

2.1 *In situ* data: sampling and processing

2.1.1 Phytoplankton pigments

Surface water samples were taken during two monitoring programmes and on board 13 opportunity cruises off the Portuguese coast (Figure 11) on a total of 820 water samples (Table III).

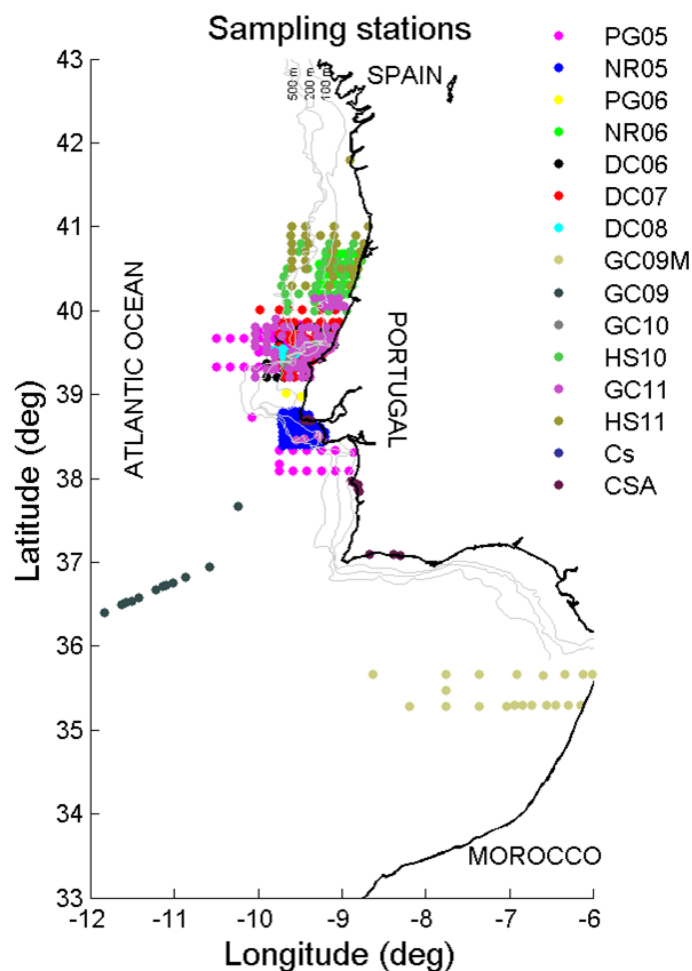


Figure 11 Samples location taken on board RV Pelagia in 2005 (PG05) and 2006 (PG06); NI Noruega 2005 (NR05) and 2006 (NR06); NRP D.Carlos I in 2006 (DC06), 2007 (DC07) and 2008 (DC08); NRP Gago Coutinho in 2009 (GC09 and GC09M), 2010 (GC10) and 2011 (GC11); RV Mytilus in 2010 and 2011 under HABSpot project (HS10, HS11) and coastal monitoring stations in Cascais and Cascais, Sines and Algarve (CS and CSA, respectively).

Samples were collected using Niskin bottles, with the exception of Pelagia 2005 cruise, where samples were collected through an Aquaflow pumping system. All water samples were filtered onto Whatman GF/F filters and immediately deep frozen. In the laboratory, samples were analysed for pigments identified with reversed phase HPLC. Sampling and pigment analysis methods applied were optimized throughout the years and are summarized in Table IV, where methodology differences can be easily identified.

Table III List of oceanographic cruises with respective sampling period, location, number of surface samples collected and Chlorophyll *a* (Chl *a*) values range.

CRUISE	DATE	LOCATION	NR of surface samples	Chl <i>a</i> range [mg/m3]
PG05	28.04.05-17.05.05	Nazaré, Lisbon	66	0.01-2.72
NR05	30.08.05-02.09.05	Lisbon bay	80	0.08-2.77
PG06	05.09.06-11.09.06	Nazaré	9	0.15-2.67
NR06	14.09.06-16.09.06	Aveiro	45	0.16-2.83
DC06	23.06.06-06.07.06	Nazaré	93	0.03-4.25
DC07	13.06.07-06.07.07	Nazaré	129	0.06-5.09
DC08	02.03.08-07.03.08	Nazaré	61	0.21-2.02
GC09_M	15.06.09-19.06.09	Morocco	21	0.01-1.70
GC09	02.06.09-05.06.09	Gorringe seamount	15	0.03-0.25
GC10	06.03.11-18.03.11	Nazaré	74	0.09-10.15
HS10	30.08.10-05.09.10	Aveiro	44	0.07-4.05
GC11	30.03.11-12.04.11	Nazaré, Lisbon, Figueira	85	0.07-1.74
HS11	09.09.11-15.09.11	Aveiro	35	0.02-2.34
Cascais	03.2011-02.2012	Cascais monitoring station	45	0.13-2.74
CSA	08.2010 & 09.2011	Cascais, Sines, Algarve	18	0.26-3.57
All cruises	2005-2012	Portuguese coast; Gorringe Seamount and Morocco	820	0.01-10.15

Water samples were filtered onto Whatman GF/F filters (nominal pore size 0.7 µm). The filters were deep-frozen immediately and stored at -80°C. For the earlier cruises, phytoplanktonic pigments were extracted with 95% cold-buffered methanol (2% ammonium acetate) for 30min at -20°C, in the dark. Previously sonicated (Bransonic, model 1210, w: 80, Hz: 47) for 1 min and, after extraction period, centrifuged at 1100 g for 15 min, at 4°C. The samples from later cruises were extracted with 95% cold-buffered methanol (2% ammonium acetate) enriched with a known concentration of trans-beta-apo-8'-carotenal (used as internal standard) for 1h at -20°C, in the dark. At half-time period of extraction, samples were sonicated for 5 min and after

extraction period centrifuged for 5 min. All extracts were filtered (Fluoropore PTFE filter membranes, 0.2 μm pore size) and immediately injected in the HPLC. Pigment extracts were analyzed using a Shimadzu HPLC comprised of a solvent delivery module (LC-10ADVP) with system controller (SCL-10AVP), a photodiode array (SPD-M10ADVP), and a fluorescence detector (RF-10AXL).

Table IV Summary of sampling and processing methods used in each cruise.

CRUISE	Sampling	Filter (type, diameter)	Filtration vol. (L)	Extraction volume (mL)	HPLC method
PG05	aquaflow pump	GF/F, 47mm	5	5-6	C18*
NR05	Niskin bottle	GF/F, 47mm	5	5-6	C18*
PG06	Niskin bottle	GF/F, 47mm	5	5-6	C18*
NR06	Niskin bottle	GF/F, 47mm	5	5-6	C18*
DC06	Niskin bottle	GF/F, 47mm	5	5-6	C18*
DC07	Niskin bottle	GF/F, 47mm	5	5-6	C18*
DC08	Niskin bottle	GF/F, 47mm	5	5-6	C18*
GC09_M	Niskin bottle	GF/F, 25mm	2	2-3	C8**
GC09	Niskin bottle	GF/F, 25mm	2	2-3	C8**
GC10	Niskin bottle	GF/F, 25mm	2	2-3 ¹	C8**
HS10	Niskin bottle	GF/F, 25mm	2	2-3 ¹	C8**
GC11	Niskin bottle	GF/F, 25mm	2	2-3 ¹	C8**
HS11	Niskin bottle	GF/F, 25mm	2	2-3 ¹	C8**
Cascais	Niskin bottle	GF/F, 25mm	1	2-3 ¹	C8**
CSA	Niskin bottle	GF/F, 25mm	1	2-3 ¹	C8**

* Kraay *et al.* (1992) adapted by Brotas and Plante-Cuny (1996); **Zapata *et al.* 2000; ¹with internal standard

Chromatographic separation in earlier cruises was carried on using a C18 column for reverse phase chromatography (Supelcosil; 25 cm long; 4.6 mm in diameter; 5 mm particles) and a 35 min elution program. The solvent gradient followed Kraay *et al.* (1992) adapted by Brotas and Plante-Cuny (1996) with a flow rate of 0.6 mL min⁻¹ and an injection volume of 100 μL . For later cruises, chromatographic separation was achieved using a C8 column for reverse phase chromatography (Symmetry C8, 15 cm long, 4.6 mm in diameter, and 3.5 μm particle size) and a 40 min elution program. The solvent gradient followed Zapata *et al.* (2000) with a flow rate of 1 mL min⁻¹ and an injection volume of 100 μL . For all samples, pigments were identified from both absorbance spectra and retention times and concentrations calculated from the signals in

the photodiode array detector. The HPLC system was previously calibrated with pigment standards from DHI. For validation purposes, and according to ESAs protocols recommendations (Doerffer, 2002), Chl was calculated as the sum of Chl *a*, epimers and allomers, Chlorophyllide *a* and DvChl *a* (if C8 method was used).

The protocol using the C18 column was developed mostly to analyse estuarine and coastal samples. It has significantly lower detection and quantification limits than the protocol using the C8 column, and is also cheaper and faster to run as it uses a shorter elution program and a lower solvent flow rate. The protocol using the C8 column however, allows for discriminating more pigments, namely, it separates Chlorophyll *c*1 from *c*2, and monovinyl Chl *a* from divinyl Chl *a* (further details of both methods can be found in Mendes et al., 2007 and Hooker et al. 2012). Quality assurance of data is described in section 2.3.

As mentioned in section 1.2.2, pigment information can be used to calculate phytoplankton size class dominance. Conventionally, marine biologists have categorized phytoplankton types by size: 1) picoplankton (<2 µm in diameter); 2) nanoplankton (2-20 µm) and 3) microplankton (20-200 µm) (Sieburth et al., 1978). To calculate the abundance of each size class in the analysed samples the method proposed by Vidussi et al. (2001) was used. With this method the fraction of each size class is given by the ratio of diagnostic pigments characteristic of the algal groups contributing to that size class versus the total of selected diagnostic pigments (see also section 1.2.2). For this analysis Vidussi's method was used with the coefficients proposed by Uitz et al. (2006). Accordingly, the total Chl can be recreated from the expression $C = \sum DP_w$, where $\sum DP_w$ is the sum of the seven selected diagnostic pigments, weighted with respect to the total Chl concentration and is described as following:

$$\begin{aligned} \sum DP_w = & 1.41[Fuco] + 1.41[Perid] + 1.27[Hexa] + 0.35[Buta] + 0.6[Allo] + \\ & 1.01[TChlb] + 0.86[Zea] \end{aligned} \quad (2.1)$$

After $\sum DP_w$ calculations, the fractions (f) of each size class are then calculated by applying the following expressions:

$$f_{micro} = \frac{(1.41[Fuco] + 1.41[Perid])}{\sum DP_w} \quad (2.2)$$

$$f_{nano} = \frac{(1.27[Hexa] + 0.35[Buta] + 0.6[Allo])}{\sum DP_w} \quad (2.3)$$

$$f_{pico} = \frac{(1.01[TChlb] + 0.86[Zea])}{\sum DP_w} \quad (2.4)$$

In order to synthesize the above information, a “size index” , as proposed by Bricaud et al. (2004), was derived from these proportions. Size index is calculated by attributing a central size to each class (1 µm, 5 µm and 50 µm to picophytoplankton, nanophytoplankton, and microphytoplankton, respectively) and weighting this value by the biomass proportion of the corresponding class:

$$SI (\mu m) = [1 * (\% \text{ picoplankton}) + 5 * (\% \text{ nanoplankton}) + 50 * (\% \text{ microplankton})] / 100 \quad (2.5)$$

This index is only a rough approximation of average sample cell size but as the advantage of providing a single continuous parameter to characterize the samples (Bricaud et al., 2004).

2.1.2 Phytoplankton absorption spectra

Additionally to filtration for phytoplankton pigments, water samples from GC11 cruise were also collected for determination of phytoplankton absorption spectra. One liter per selected station was filtered and absorption spectrum determined using the Quantitative Filter Technique (Mitchell et al., 2000). The phytoplankton absorption spectra analysis was carried out in a spectrophotometer. The frozen filters containing the phytoplankton sample were placed in a petri dish on sea-filtered water in order to hydrate and thaw, for at least 5 min, and then measured. Measurements were done from 400 to 800nm with 1nm resolution. After measuring the sample, filters were placed in a filtration rack and bleached using approximately 5ml of 0.1 % NaClO solution for 10 min (Sodium hypochlorite oxidation method). Method is fully described in Mitchell et al. (2000). This procedure is carried out to remove the phytoplanktonic fraction (particulate organic material) of the sample. The filters were then rinsed with 0.2 μ m filtered seawater, to remove any residual NaClO, and measured against a bleached blank. Phytoplankton absorption data were then corrected for differential scattering, volume filtered, area of the filter and pathlength amplification (Mitchell et al., 2000). The differential scattering was carried out by subtracting the mean absorption between 730 and 750 nm from the initial absorption data (see also Tassan et al., 2000). The theoretical pathlength amplification correction (beta) of Roesler (1998) was then applied. Phytoplankton absorption was finally computed as the difference between scans, after corrections described above, before (total particulate) and after (organic material) extraction.

2.1.3 Radiometric data

Water samples and data collection during the GC11 cruise were conducted in co-operation with a Joint Research Centre (JRC) team. This team has been collecting optical data in the European Seas under the projects CoASTS (Coastal Atmosphere and Sea Time Series, 1998-2009, Zibordi et al 2004) and BiOMaP (Bio-Optical mapping of Marine Properties, 2000-2010, Zibordi et al. 2011). The participation in this cruise allowed for the collection of a small dataset of IOPs and AOPs in the Atlantic off Portugal. Measurements were collected with: microPRO free-fall optical profilers manufactured by Satlantic Inc. (Halifax, Canada); AC-9 absorption and beam-attenuation meters manufactured by WET Labs (Philomat, USA); and Hydroscat-6 backscattering meters manufactured by HoboLab (Bellevue, USA). Additional laboratory analysis of water samples were

undertaken for the determination of pigments concentration, absorption coefficients by pigmented and non-pigmented particles (see previous section: 2.1.1), absorption coefficient by CDOM and concentration of total suspended matter. Protocols of measurements are fully described in Zibordi et al. (2002) and Zibordi et al. (2011).

2.2 Satellite data

Data from the ocean colour sensors MODIS Aqua and MERIS were acquired for the sampling area during the period of the cruises. Reprocessing of data by Agencies is expected along the space mission duration for calibration adjustments (*vicarious* calibration). The data used in this analysis are from the latest reprocessing available at the time of this study: MODIS 2012 reprocessing and MERIS 3rd reprocessing. Reprocessing information details can be found in <http://oceancolor.gsfc.nasa.gov/WIKI/OCReproc20120MA.html> for MODIS and in http://earth.eo.esa.int/pcs/envisat/meris/documentation/meris_3rd_reproc/ for MERIS.

2.2.1 Standard algorithms

2.2.1.1 MODIS AQUA OC3M algorithm

MODIS/Aqua L2 data processed by NASAs Ocean Biology Processing Group (OBPG) were downloaded from the Ocean Color Website (<http://oceancolor.gsfc.nasa.gov/>). MODIS is a 36-band sensor that spans the spectral range from 0.4–14.4 μm and OC3M is the NASA standard Chl algorithm for MODIS. The empirical OC3M algorithm was extended from the OC4 and OC2 algorithms developed for the SeaWiFS sensor and adapted to the spectral bands of MODIS (O'Reilly et al., 2000). In essence, these algorithms are obtained as being the best fit when relating the log-transform of the observed *in situ* Chl concentrations and the log-transform of the remote sensing reflectance ratios. These quantities (also called blue-to-green ratios) are the ratios of observed Rrs at two wavelengths, namely at a wavelength in the green domain of the spectrum ($\lambda \sim 550\text{--}560\text{ nm}$), and at one of three available λ , in the blue and blue–green domain (namely $\lambda \sim 443, \sim 490$ and $\sim 510\text{ nm}$). The OC2 algorithm uses only the single Rrs(490)/Rrs(555) ratio. The OC3 algorithm, uses the largest of the Rrs(443)/Rrs(551), and Rrs(488)/Rrs(551) ratios,

while OC4 (SeaWiFS) uses in the same way the largest of the three, $Rrs(443)/Rrs(555)$, $Rrs(490)/Rrs(555)$, and $Rrs(510)/Rrs(555)$ ratios.

Standard Chl concentration images produced by NASA OBPG group using MODIS imagery are based on the OC3 algorithm:

$$\text{Chl } a = 10^{(0.283 - 2.753R + 1.457R^2 - 0.659R^3 - 1.403R^4)} \text{ (mg m}^{-3}\text{)} \quad (2.6)$$

where $R = \log_{10}((Rrs(443) > Rrs(488))/Rrs(550))$. This algorithm was statistically derived based on Chl concentrations ranging from 0.0008 to 90 mg m^{-3} . However, most of the measurements have concentrations between 0.08 and 3 mg m^{-3} (O'Reilly *et al.*, 2000), which is generally within the range that has been observed along the Portuguese coast for this study (Table I).

2.2.1.2 MERIS standard algorithms

For the present study, processed MERIS Full Resolution (FR) Level 2 (L2) data were provided by the ESA ground segment processor – 3rd reprocessing, which was recently completed using the MERIS Ground Segment (MEGS) Processor Version 8.0 (see Bourg *et al.* 2011).

2.2.1.2.1 MERIS algal 1

Meris algal 1 product results of a four-band polynomial algorithm but relates the log-transformed ratio of irradiance reflectance (R) to the Chl concentration. This fit differs from the MODIS OC3M as it is semi-analytical. It is parameterised using a theoretical model of ocean colour (Morel and Maritorena, 2001) tuned using data gathered by the Laboratoire d'Océanographie de Villefranche on K_d and Chl (see Morel and Antoine, 2011, for details, https://earth.esa.int/instruments/meris/atbd/atbd_2.9.pdf). The $R(\lambda)$ values, as well as any $R(\lambda_1)/R(\lambda_2)$ ratio are related to Chl and only applicable in Case 1 waters. The polynomial fits inverting these R -to-Chl relationships provide the semi-analytical algorithm OC4Me developed for MERIS:

$$\text{Chl } a = 10^{(0.450 - 3.259R + 3.523R^2 - 3.359R^3 - 0.949R^4)} \text{ (mgm}^{-3}\text{)}, \quad (2.7)$$

where $R = \log_{10}((R(443) > R(490) > R(510))/R(560))$.

2.2.1.2.2 MERIS algal 2

A shortcoming of the Case 1 water algorithms for Chl retrievals is the uncertainty to fully distinguish the contribution to R_{rs} by Chl and other optically active components (OACs) in the water column, such as inorganic particulate matter and CDOM (see section 1.1.3). To overcome this problem, new methods for retrieving Chl and other OACs have been developed. In the 3rd reprocessing, a NN dedicated to Case 2 water atmospheric correction and data products generation has been included. The MERIS Case 2 water Chl product (algal 2) estimates Chl also in waters where Chl is not the only OAC present, being independently generated from the algal1 product. In this study, this product's performance is compared to the sensors' standard Case 1 water Chl products, as well as to *in situ* Chl measurements. This algorithm is based on a neural network, which takes the log of the above-surface remote-sensing reflectance (R_{rs} – directional water leaving radiance divided by the downwelling irradiance) of MERIS bands 1-7 and 9 and 3 angles (solar zenith, viewing angle and azimuth difference) and gives as output the log of 3 optical coefficients at 442 nm: (1) the scattering coefficient for all particles, (2) the sum of the absorption by CDOM and by the bleached particulate matter, and (3) the absorption by phytoplankton pigments, which is the difference between the absorption by the total and the bleached particulate matter (IOCCG, 2006). These outputs are then converted into total suspended matter dry weight (TSM), CDOM absorption at 442 nm, and into Chl, respectively, using empirical relationships.

According to the MERIS Product Handbook the algal 2 product is given as:

$$\text{Chl } a = k_1 [a_{\text{phy}}(442)]^{k_2} \quad (\text{mgm}^{-3}), \quad (2.8)$$

where $a_{\text{phy}}(442)$ (m^{-1}) is the pigment absorption at wavelength 442 nm, and k_1 and k_2 are the parameters, 21 and 1.04, respectively, that can be adjusted to regional conditions.

Further details of the algorithms for atmospheric correction and the retrieval of the algal 1 and algal 2 products can be found in Aiken and Moore (2000), Antoine and Morel (1999), Doerffer and Schiller (2007), Moore et al. (2001), Morel and Antoine (2011).

2.2.2 Novel algorithms

2.2.2.1 CoastColour

For coastal applications, ESA has funded an ocean colour project to specifically develop products that could account for the coastal waters constraints. The CoastColour project developed, among other products, a Chl product based on an updated version of the NN algorithm firstly developed for algal 2 product. The CoastColour products benefit of a newly atmospheric correction specifically developed for application in coastal areas, also based on a NN algorithm. All details on the CoastColour processing of MERIS data are available at <http://www.coastcolour.org/documents/Coastcolour-PUG-v2.1.pdf>. Besides the updated NN algorithm, CoastColour also provides a product based on the Quasi-analytical algorithm (QAA) developed by Lee et al. (2002). Further details on the QAA inversion method can be also found in IOCCG, (2006). Both CoastColour Chl products have the same atmospheric correction, but use different inversion schemes (NN and QAA) to retrieve the IOPs from the radiances (AOP) measured by the MERIS sensor. The same parameters applied in algal 2 product (equation 2.8) are then applied to convert the retrieved IOPs (i.e, $a_{\text{phy}} 442\text{nm}$) into concentrations (Chl).

2.2.2.2 CCI

The Climate Change Initiative (CCI) Chl product is a ~4km resolution product which results from the merging of SeaWiFS, MODIS and MERIS data. The merging procedures are done at the radiometric data level and require band-shift correction. Processing details can be found in the Algorithm Theoretical Baseline Documents (ATBD) in the project web site <http://www.esa-cci.org/>. Once the radiometry of the three sensors are combined, algorithms are applied for retrieval of geophysical parameters. The version 6 of the OC4 algorithm is used to compute the Chl product. This algorithm is an updated version of the polynomial band-ratio chlorophyll algorithm developed for SeaWiFS (O'Reilly 2000), and was selected due to its historical and heritage value for climate studies. The OC4v6 uses a four-band blue-green reflectance ratio, following a reprocessing of the algorithm in 2009. See <http://oceancolor.gsfc.nasa.gov/REPROCESSING/R2009/ocv6/> for reprocessing details.

2.2.2.3 MLP-ATLP

Multi Layer Perceptron (MLP) neural networks (NN) have been developed to derive Chl concentration, absorption of yellow substance at 412nm and concentration of total suspended matter (TSM) from Rrs values (D'Alimonte and Zibordi 2003; D'Alimonte et al 2004). Using the CoASTS and BiOMaP datasets, different MLPs were trained for the European seas, namely, the Eastern Mediterranean Sea, the Ligurian Sea, the Northern Adriatic Sea, the Western Black Sea, the English Channel and the Baltic Sea (D'Alimonte et al 2011). *In situ* training data were band-shift corrected to match SeaWiFS, MODIS and MERIS bands, in order to retrieve data products using sensor specific radiometric center wavelengths as input. Field measurements collected during the GC11 cruise by the JRC team were used to train a regional MLP for the Atlantic off Portugal (ATLP). This single-cruise dataset includes a limited number of samples (i.e., 68 stations) with Chl concentrations ranging between 0.2-2 mg.m⁻³, which might impose some constraint on the application of the ATLP regional MLP. However, this regional inversion model is also featured with a novelty detection scheme that allows for defining its applicability range based on the novelty index of input Rrs spectral values. Higher novelty index values indicate that: 1) radiometric spectral patterns are significantly different from the *in situ* data used for the algorithm development (D'Alimonte et al., 2003, D'Alimonte et al., 2014); and 2) corresponding MLP output values have hence large uncertainties. For this reason, in this thesis work, the use of the ATLP regional algorithms have been also tested by restricting the input Rrs data with a novelty index less than 3, defined based on the scale parameter of log-transformed ATLP radiometric data.

2.3 Data quality assurance for matchup analysis

2.3.1 *In situ* database

HPLC protocols changed along the years due to laboratory procedures optimization. To guarantee consistency of *in situ* data, a quality control filter was applied to all pigment data, following Aiken et al. (2009), which uses the relationship of accessory pigments, (i.e, all carotenoids plus chlorophylls *b* and *c*) and TChl *a* (the sum of Chl *a*, DvChl *a* and Chlorophyllide *a*) to accept or eliminate specific samples or entire cruises. This quality control is based on results of Trees et al. (2000) who reported that Chl *a* is highly correlated to accessory pigments (AP) . In this study, only the main pigments used for the size class retrieval (Fucoxanthin, Peridinin, 19'Hexanoyloxy-fucoxanthin, 19'Butanoyloxy-fucoxanthin, Alloxanthin, Chlorophyll *b* and Zeaxanthin) were used for the AP calculation.

Quality control was firstly applied by calculating the difference of TChl *a* and AP. This should be less than 30% of the total pigments, TPig, (TChl *a* + AP) concentration, and all samples with higher percentage differences were eliminated from the dataset. Regression analysis statistics were then applied to each cruise to give a quality rating (QR) for each parameter analysed. Data with a $r^2 > 0.94$, was given a QR = 1, else 2; RMS error > 0.08 , QR = 1, else 2; slope = 1 ± 0.1 , QR = 1, else 2. Overall quality rating (OQR) was set as A* if QR= 1 for all three criteria, A if QR= 2 for any criterion, B if QR= 2 for any 2 criteria and C if QR= 2 for all criteria. These criteria were adapted from Aiken et al. (2009).

2.3.2 Satellite data

In a validation exercise, not only the *in situ* data need to be of best quality, but we must also guarantee that these are only compared to high quality satellite data. Agencies supply specific flags with their products to characterize the conditions in which the data were acquired.

Table V List of flags used for processing the satellite data.

MODIS	
Flag name	Description
ATMFAIL	Atmospheric correction failure
LAND	Pixel is over land
HIGLINT	High sun glint
HILT	Observed radiance very high or saturated
HISATZEN	High sensor view zenith angle
STRAYLIGHT	Straylight contamination is likely
CLDICE	Probable cloud or ice contamination
HISOLZEN	High solar zenith
LOWLW	Very low water-leaving radiance (cloud shadow)
CHLFAIL	Derived product algorithm failure
NAVWARN	Navigation quality is reduced
MAXAERITER	Aerosol iterations exceed maximum
CHLWARN	Derived product quality is reduced
ATMWARN	Atmospheric correction is suspect
NAVFAIL	Bad navigation
MERIS	
Flag name	Description
LAND	Pixel classified as Land in L1B, adjusted radiometrically during L2 pixel classification to allow for geocorrection errors and tidal changes.
CLOUD	Pixel classified as cloud by the L2 cloud screening algorithm (Sub-pixel, scattered cloud not included.)
PCD_1_13	Confidence flag for 1 to 13 (reflectances). Raised at low sun angles, when atmospheric correction fails or there are difficulties with aerosol correction. Also for pixels with whitecaps or uncorrected glint, when reflectances in any band are negative, or when reflectance at 510nm exceeds a threshold without the turbidity flag having been raised.
PCD_15	Confidence flag for algal_1. Raised when atmospheric correction fails or there are difficulties with aerosol correction. Also for pixels with uncorrected glint or whitecaps, and for pixels with high turbidity.
PCD_17	Confidence flag for algal_2. Raised when PCD_13 is raised, or when the algorithm input or output is outside the expected range.

For the present study, MODIS data was masked with the following L2_flags: Land, cloud or ice, straylight, sun glint, high TOA radiance, low nLw(551) - a flag used to identify cloud-shadowed pixels, or atmospheric correction failure, and specific product warning flags. MERIS algal 1 and algal 2 products were masked with land, cloud and with confidence flags PCD_15 and PCD_17, respectively. Flags used are summarily described in Table V.

Data from images where the viewing angle and solar zenith angles exceeded 60° and 75°, respectively, were also excluded due to limitations on reliability of atmospheric correction

algorithms at extreme viewing and solar geometries (Bailey and Werdell, 2006). Same quality criteria were applied to the CoastColour and CCI products.

2.4 Match-up and comparison procedures

The time and spatial differences between the collection of the *in situ* sample and the satellite overpass need to be taken in consideration for match-up retrieval. The time and spatial windows need to be loose enough to maximize the number of match-ups, however, cannot compromise contemporaneity of *in situ* and satellite data. A trade-off is therefore necessary. Time window is here defined to be small enough to reduce the effects of temporal variability in the *in situ* data, yet sufficiently large to allow for statistical validity of match-up results. Two time windows were considered for this analysis: ± 3 h and within 3 to 6h).

The spatial resolution of the ocean-colour sensors used in this study fall in the range of 300m to 1 km (at nadir view). As small scale spatial variability can be expected, instead of a single validation pixel, a multi-pixel box is recommended as to allow for the generation of simple statistics to assist in the evaluation of spatial stability, or homogeneity at the validation point. Further, the use of a multi-pixel box increases the possibility of a measurement being available for validation by increasing the chance that the satellite retrieval will have sufficient cloud free pixels to be useful.

A Matlab routine was implemented for match-up identification. In summary, satellite images, properly masked (see section 2.3), of same day of *in situ* sampling were automatically selected and mean satellite Chl concentration was calculated for space windows of 300 m (MERIS only) and 1 km within station location. For CoastColour and CCI products equivalent 3x3 pixel boxes were used. Time differences between satellite overpass and *in situ* sampling were then calculated and match-ups organized per time intervals (less than 3h and within 3-6h).

2.5 Statistics formulae

Several parameters were calculated in order to evaluate algorithm performance and uncertainty in comparison to *in situ* data. Linear regression parameters: coefficient of determination (r^2), slope, and intercept. Also, error estimate parameters: root mean square error (RMS, Ψ), bias error (δ), and unbiased root mean square error (URMS, Δ), were computed as following:

$$\Psi = \left(\frac{1}{N} \sum_{i=1}^N [\log(\text{Sat}_i) - \log(\text{In situ}_i)]^2 \right)^{\frac{1}{2}} \quad (2.9)$$

$$\delta = \frac{1}{N} \sum_{i=1}^N [\log(\text{Sat}_i) - \log(\text{In situ}_i)] \quad (2.10)$$

$$\Delta = \left(\frac{1}{N} \sum_{i=1}^N [(\log(\text{Sat}_i) - \overline{(\log(\text{Sat}_i))}_{i=1,N}) - (\log(\text{In situ}_i) - \overline{(\log(\text{In situ}_i))}_{i=1,N})]^2 \right)^{\frac{1}{2}} \quad (2.11)$$

where N is the total number of samples, and i is the sample index. All statistical analysis are performed and presented in log scale given that bio-optical data tend to be log-normally distributed (Campbel, 1995).

For more intuitive analysis the mean Relative Percentage Difference (RPD) and the mean Absolute Percentage Difference (APD) were also calculated without log-transforming the data:

$$\text{RPD} = \frac{1}{N} \sum_{i=1}^N \frac{[\text{Sat}]_i - [\text{In situ}]_i}{[\text{In situ}]_i} \times 100 \quad (2.12)$$

$$\text{APD} = \frac{1}{N} \sum_{i=1}^N \frac{|[\text{Sat}]_i - [\text{In situ}]_i|}{[\text{In situ}]_i} \times 100 \quad (2.13)$$

2.6 Water type index

Since Case 1 waters are those whose IOPs can be determined solely by Chl (Gordon and Morel, 1983; Loisel and Morel, 1998; Morel, 1988), for optically deep waters, a unique relationship exists between Chl and Case 1 $Rrs(\lambda)$ (Haltrin, 1999; Morel, 1988; Morel and Maritorena, 2001). Lee and Hu (2006) proposed an inclusive remote-sensing criterion to map Case 1 waters using $Rrs(\lambda)$ based on bio-optical models developed from extensive measurements (Morel and Maritorena, 2001).

Considering RR12 and RR53 defined as:

$$RR12 = \frac{Rrs(412)}{Rrs(443)} , \quad (2.14)$$

$$RR53 = \frac{Rrs(555)}{Rrs(490)} , \quad (2.15)$$

where RR12 represents the relative abundance of CDOM per Chl (Carder et al., 1999) and RR53 is a measure of Chl (e.g., Aiken et al., 1995; O'Reilly et al., 1998), a monotonic line exists between the calculated RR12 and RR53 values, because by definition optical properties of Case 1 waters are determined by Chl alone. According to Lee and Hu (2006) this monotonic line can be represented accurately (less than 1% error) by the following empirical polynomial function (RR53 in a range of ~0.2 to ~2.0):

$$RR12^{[CS1]} = 0.9351 + \frac{0.113}{RR53} - \frac{0.0217}{RR53^2} + \frac{0.003}{RR53^3} , \quad (2.16)$$

where the superscript [CS1] refers to Case 1 waters (blue line in Figure 12). Similarly, a monotonic line exists between $Rrs(555)$ and RR53 for Case 1 waters (blue line in Figure 13), where $Rrs(555)$ is a measure of particle backscattering (Carder et al., 1999):

$$Rrs(555)^{[CS1]} = 0.0006 + 0.0027RR53 - 0.0004(RR53)^2 - 0.0002(RR53)^3 \quad (2.17)$$

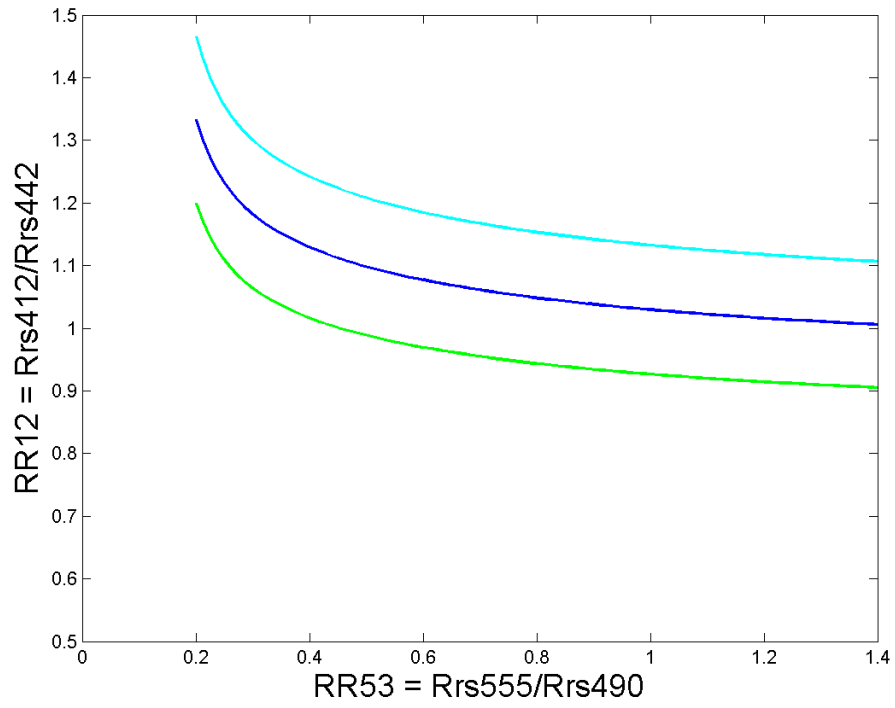


Figure 12 Lee and Hu 2006 model (result of equation 2.16 and 2.18)

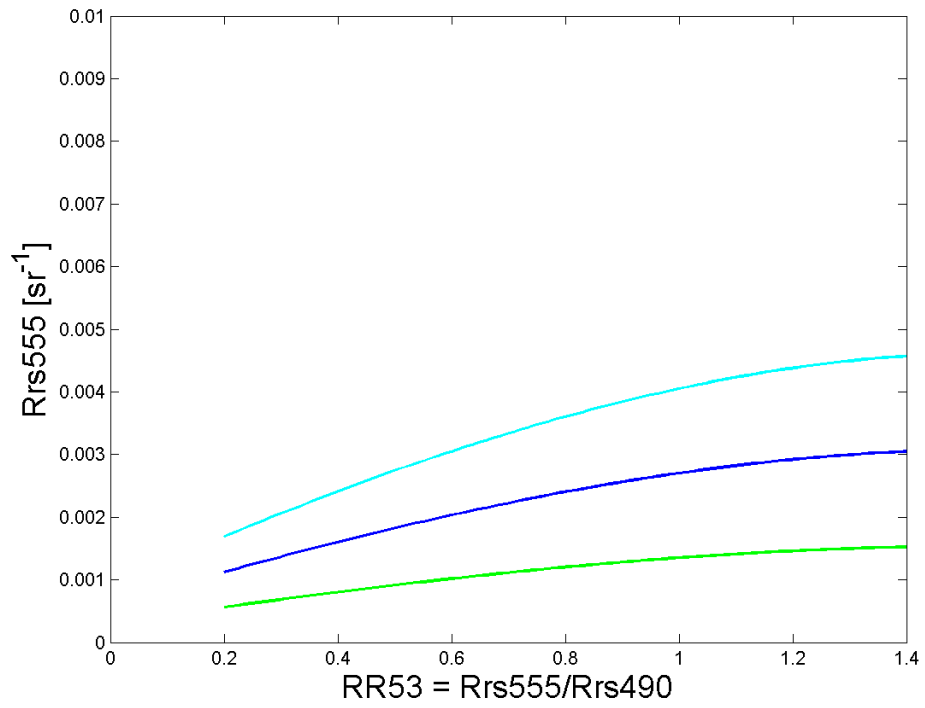


Figure 13 Lee and Hu 2006 model (result of equation 2.17 and 2.19)

These equations provide guidance on the CDOM absorption (RR12) and particle backscattering (Rrs555) per Chl (RR53) for theoretical Case 1 waters. However, for natural waters, CDOM and particles do not necessarily co-vary with Chl and will show deviations around these theoretical values. Therefore, to be classified as a Case 1-water type, both these equations need to apply. To be inclusive, both equations need also to be relaxed. As described in Lee and Hu (2006), a water pixel is considered as Case 1 if the following two conditions are met simultaneously:

$$(1 - \gamma) RR12^{[CS1]} \leq RR12 \leq (1 + \gamma) RR12^{[CS1]} \quad (2.18)$$

$$(1 - \nu) Rrs(555)^{[CS1]} \leq Rrs(555) \leq (1 + \nu) Rrs(555)^{[CS1]} \quad (2.19)$$

To be inclusive and account for natural variability, as well as approximations of models and measurements, γ and ν were set to 0.1 and 0.5, respectively, allowing a $\pm 10\%$ deviation of RR12 and at the same time a $\pm 50\%$ deviation of Rrs(555) around their exact Case 1 values (Lee and Hu, 2006). These deviations are represented in Figure 12 and Figure 13 by the green and cyan lines. In a practical point of view, if the values obtained, after applying the conditions (2.17) and (2.18) to the Rrs values of a pixel, fall within the green and cyan lines in both Figures 12 and 13, the pixel is considered a Case 1 water pixel.

This method allows for the direct use of Rrs to classify Case 1 waters and was applied in this study to satellite images off Portugal to calculate seasonal Case 1 water percentage and spatial distribution. For influence of water type on the match-up analysis, three indices of water type were also calculated as the difference between the obtained points for each sample point and the theoretical Case 1 equivalent. As higher the index, the further away from the Case 1 water properties it is. Indices were calculated as follows:

$$\text{Index 1} = d1 \cdot d2, \quad (2.20)$$

$$\text{Index 2} = d1, \quad (2.21)$$

$$\text{Index 3} = d2, \quad (2.22)$$

where $d1 = |RR12^{[CS1]} - RR12|$ and $d2 = |Rrs555^{[CS1]} - Rrs555|$.

2.7 1st optical depth and euphotic depth

The information obtained by means of RS is the pigment concentration within the penetration depth (Z_{90}), defined by Gordon and McCluney (1975) as the layer of water column from which 90% of the total water leaving radiance originates. This is generally also referred as the first optical depth (Z_1^{st}), and for a homogenous ocean, can be approximated with the inverse of the diffuse attenuation coefficient ($Z_1^{st}=Z_{90}\approx k^{-1}$). When comparing to an *in situ* discrete sample, if a Chl maximum (DCM) or optically active substances are present above or below the sample depth and within the layer “seen” by the remote sensor, significant errors can be introduced, reducing the algorithm performance. Consequently, details on the vertical structure of the Chl are necessary to calculate the weighted mean pigment concentration within the layer “seen” by the satellite (Gordon & Clark, 1980). This calculation was not feasible in the present study given the lack of information on the vertical structure of the water column, however, euphotic depth was estimated using the surface Chl concentration following Morel et al. 2007:

$$\log_{10}(Z_{eu}) = 1.524 + 0.436X - 0.0145X^2 + 0.0186X^3, \quad (2.23)$$

where $X = \log_{10} [\text{Chl}]_{surf}$. The euphotic depth is defined as the depth where the downwelling PAR is reduced to 1% of its value at the surface. Maximum of Chl values and/or DCM occur within the euphotic zone (Figure 10). The euphotic depth can then be related by empirical equation to the first optical depth, Z_1^{st} :

$$Z_1^{st} = \frac{Z_{eu}}{4.6} \quad (2.24)$$

Both depths were calculated to infer on the impact of a non-uniform vertical profile in the match-up analysis.

Chapter 3: Results

3.1 Dataset for the western Portuguese waters

Sampling took place from 2005 to 2012, mostly in early-Spring to late-Summer months, covering mainly the North West coast of Portugal (Figure 11), and including a few samples from the Southern coast, the Gorringe bank region and the Moroccan coast. Total Chl *a* ranged from 0.01 to ~10 µg L⁻¹, with the lower maximum values found for the Gorringe area and the highest values registered in the Nazaré region in 2007 and 2010 (Table III). HPLC methods used for analysis of the samples changed throughout the years, as mentioned previously (Table IV) and a quality control procedure was applied to guarantee uniformity and comparability of results (see section 2.3 for details on method used). Results of the application of the quality control criteria are summarized in Table VI.

Table VI Summary statistics for linear regression analyses between TChl*a* and accessory pigments

Cruise	N	X	Slope	QR	Offset	r ²	QR	RMS	QR	OQR
PG05	49	17	0.69	2	0.058	0.969	1	0.187	2	B
NR05	76	4	0.61	2	0.063	0.965	1	0.312	2	B
PG06	8	1	0.91	1	0.039	0.999	1	0.08	1	A*
NR06	45	-	1.05	1	-	0.949	1	0.161	2	A
DC06	91	2	0.87	1	-	0.963	1	0.189	2	A
DC07	129	-	0.70	2	0.046	0.988	1	0.232	2	B
DC08	59	2	0.60	2	0.072	0.94	1	0.247	2	B
GC09_M	19	2	0.93	1	0.012	0.998	1	0.034	2	A
GC09	15	-	0.90	1	-	0.972	1	0.018	1	A*
GC10	69	5	0.67	2	0.114	0.989	1	1.002	2	B
HS10	44	-	1.15	2	0.063	0.963	1	0.354	2	B
GC11	84	1	0.94	1	0.066	0.95	1	0.101	2	A
HS11	27	8	0.65	2	0.101	0.97	1	0.454	2	B
Cs	37	8	0.84	2	0.063	0.79	2	0.308	2	C
CSA	18	-	1.18	2	-	0.90	1	0.544	2	B

A total of 50 samples were discarded and linear regression analyses were applied to the remaining data, for each cruise. Following the method for quality control proposed by Aiken et al. (2009), only one set of data was classified as C (i.e. Cs), and two cruises had maximum classification, A* (i.e. PG06 and GC09). NR06, DC06, GC09_M, GC11 cruises were classified as A and the others as B. None of the datasets was eliminated as differences may arise from photophysiology of samples or other factors, but these results have to be considered in the

match-up analysis. Poor statistical results between satellite data and low quality *in situ* data are expected. In Figure 12-a, total Chl data are represented against accessory pigments, considering all cruises. Statistics are also presented in Figure 12-a, as a whole, and separated per trophic status (Figure 12 b-d). Trophic status was considered based only on Chl concentration and following Aiken et al. 2009 (for the Atlantic Meridional Transect, AMT). Dataset spreads throughout all the considered status: oligotrophic ($\text{Chl } a < 0.25 \mu\text{g.L}^{-1}$), mesotrophic ($0.25 < \text{Chl } a < 1.2 \mu\text{g.L}^{-1}$) and eutrophic ($\text{Chl } a > 1.2 \mu\text{g.L}^{-1}$), but was verified to be more dispersed (higher RMS) at higher Chl concentration values (Figure 12).

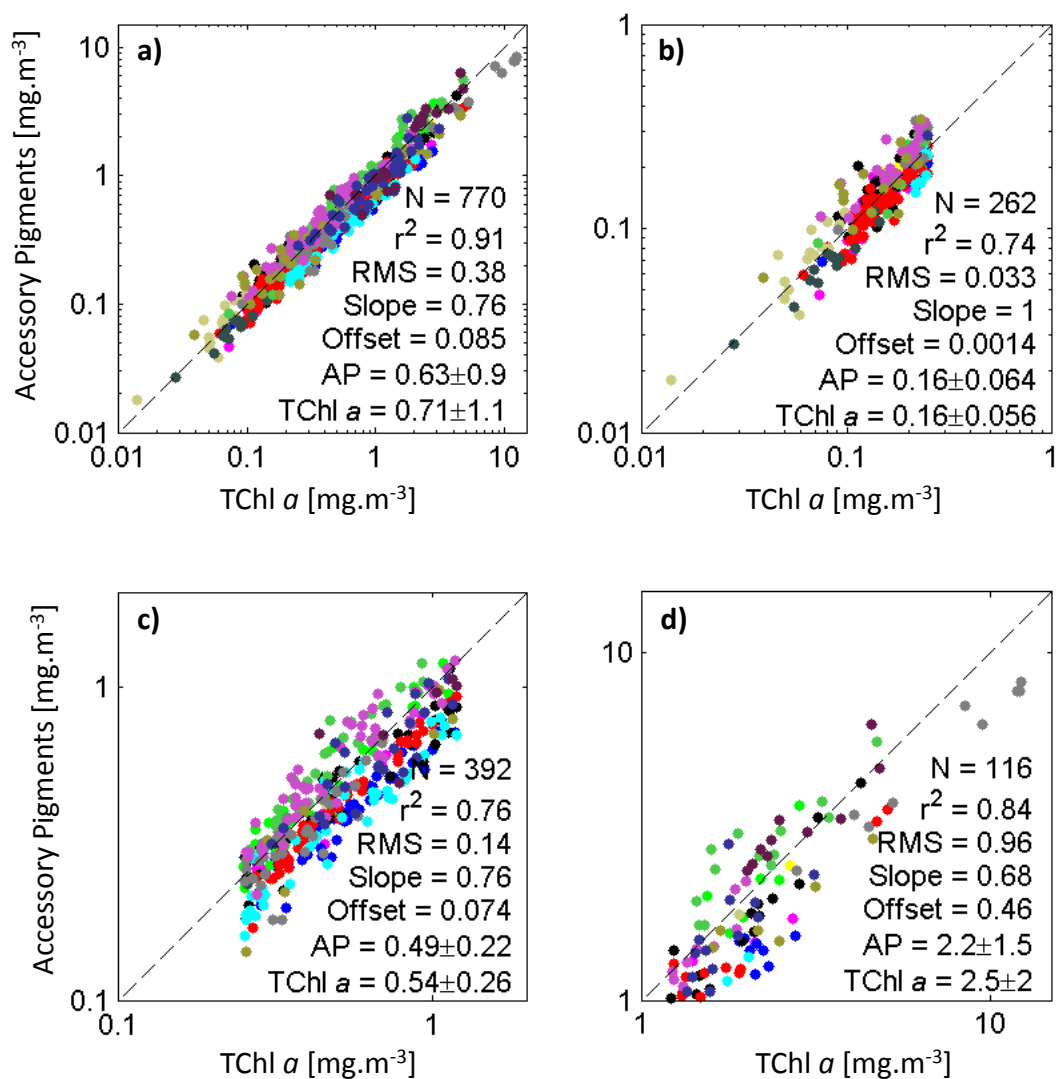


Figure 14 Pigment dataset after quality control: accessory pigments against total chlorophyll *a* (Tchl *a*). Statistics are presented for all dataset **(a)**, for oligotrophic conditions: Tchl *a* < 0.25 $\mu\text{g.L}^{-1}$ **(b)**, mesotrophic conditions: 0.25 < Tchl *a* < 1.2 $\mu\text{g.L}^{-1}$ **(c)**, and eutrophic conditions: Tchl *a* > 1.2 $\mu\text{g.L}^{-1}$ **(d)**. Colours refer to each cruise and are in accordance with Figure 11.

Trophic status are generally associated with the presence and dominance of specific phytoplankton size-classes: oligotrophic with presence of picoplankton, mesotrophic associated with the presence of nanoplankton and eutrophic with the presence of microplankton size-class (e.g., Siokou-Frangou et al., 2009, Šolić et al., 2010). Dataset was also analysed per size-class dominance following the method proposed by Uitz et al. (2006) (Figure 15). For each sample, dominance was attributed to a size-class whenever its fraction was >50%. If none of the classes was >50%, the sample was classified as mixed. Results revealed only a few samples dominated by pico-sized plankton and majority of samples either dominated by the presence of microphytoplankton, or with no clear dominance of a size-class.

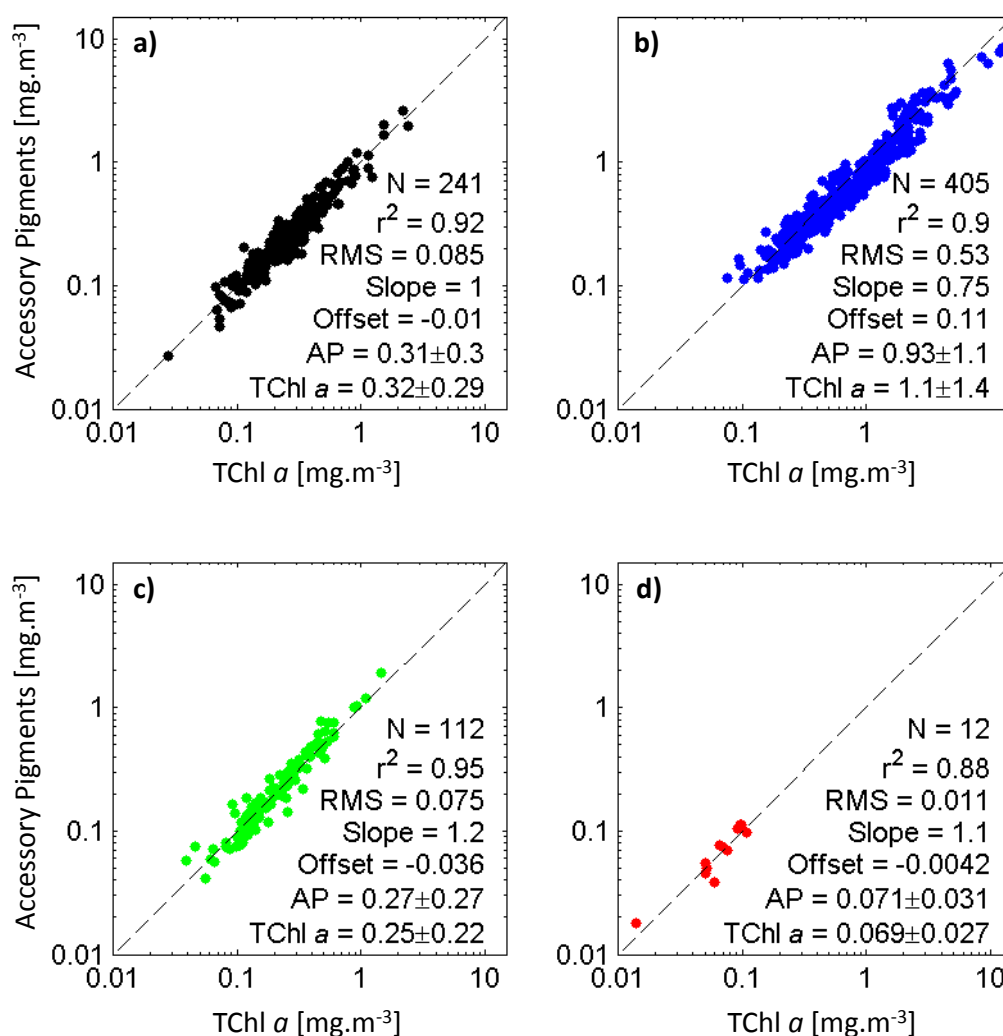


Figure 15 Pigment dataset, after quality control, separated for size class dominance based on Uitz et al., 2006. Statistics are shown for mixed samples (a), Microphytoplankton dominated samples (b), Nanophytoplankton dominated samples (c) and picophytoplankton dominated samples (d).

Results showed that microphytoplankton dominated most samples near the coast (Figure 16-a), although this size-class could be dominant in a few more offshore stations. Nevertheless, generally, off-shore samples were dominated by nano- or pico-sized phytoplankton (Figure 16-a). Higher Chl concentrations ($>0.5 \mu\text{g.L}^{-1}$) were associated to micro-sized plankton, nano dominated in Chl ranges between 0.1 and $0.5 \mu\text{g.L}^{-1}$ and pico-sized plankton were dominant at Chl values below $0.1 \mu\text{g.L}^{-1}$ (Figure 16-b).

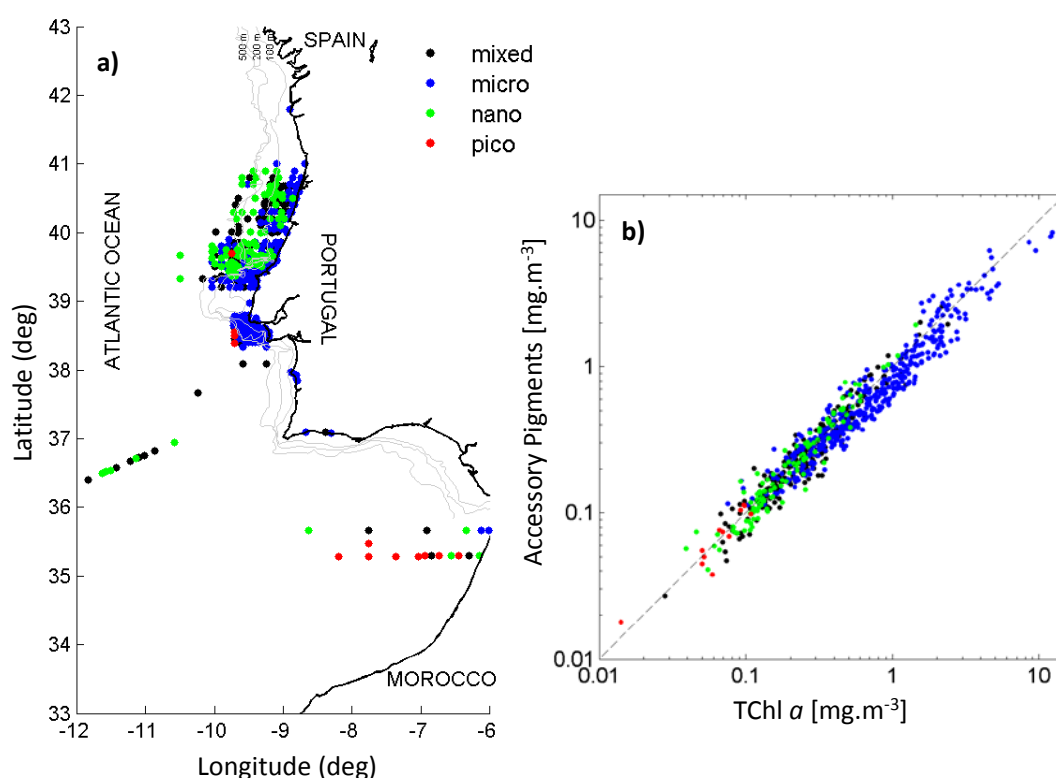


Figure 16 Distribution map of the different size dominant samples **(a)** and all dataset relation between accessory pigments (AP) and total chlorophyll a (TChl a) **(b)**. Mixed dominated stations in black, micro-dominated stations in blue, nano-dominated samples in green and pico-dominated samples in red.

Analysing the phytoplankton size distribution per cruise (Figures 17 and 18) differences are visibly marked. Samples with more than 40% of pico-sized plankton are mostly from 3 cruises (PG06, DC06 and GC09M). The first two cruises (PG06 and DC06) were both in the Nazaré region during 2006 and the third, GC09M, are samples collected off the Moroccan coast in 2009. Samples with more than 80% micro-sized dominance are from a cruise in the Nazaré region during the spring of 2011 (GC11) and very coastal monitoring stations (Cs and CSA). High dominance of micro-sized phytoplankton is also verified for some samples of the DC08 cruise, in

the Nazaré region. A second cluster of samples of this cruise can be seen in the graph, where samples are nano-sized dominated. This cruise was conducted in two phases with distinct wind-regimes with visible impact on the size of phytoplankton community. Large part of the samples exhibit co-dominance of nano and micro-sized phytoplankton, mostly in cruises (DC07, GC10, NR06, HS10). All in the Nazaré (DC07 and GC10) and Aveiro (NR06 and HS10) area.

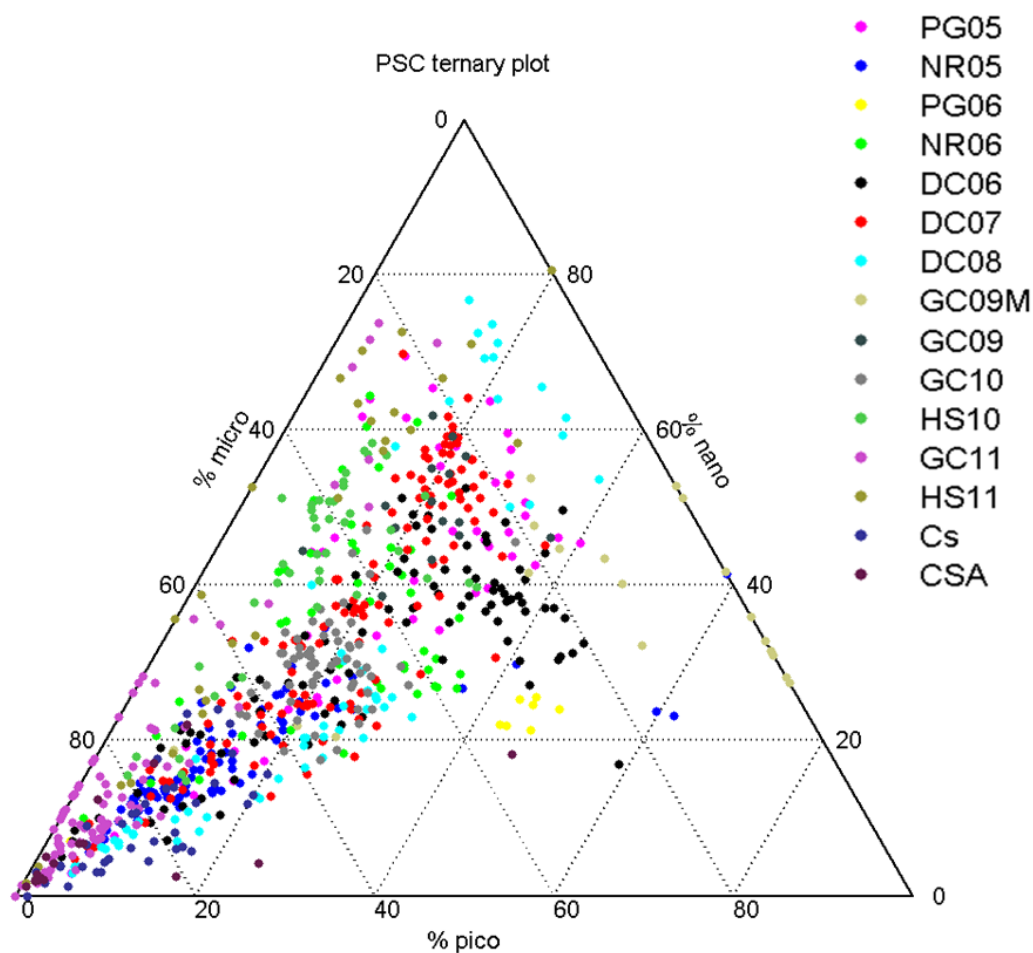


Figure 17 Ternary plot showing the relative contributions (percent) of picoplankton, nanoplankton, and microphytoplankton to total Chl, estimated from the relative contribution of some taxonomic pigments (Uitz et al., 2006) Colours refer to each cruise and are in accordance with Figure 11.

Attributing an average size to each class (equation 2.5) it is possible to observe the size distribution variation with the total Chl for each sample (Figure 18). Maximum size possible is 50 μm as this is the average size attributed to the micro-sized class. This maximum size is observed in most samples of GC11 (Nazaré) throughout a large range of Chl. However, general observed tendency of size is to decrease with decreasing of Chl. Exceptions are observed for a set of data of cruise DC08, where relatively high values of Chl are associated to small size particles. Smaller samples are verified for the Moroccan cruise.

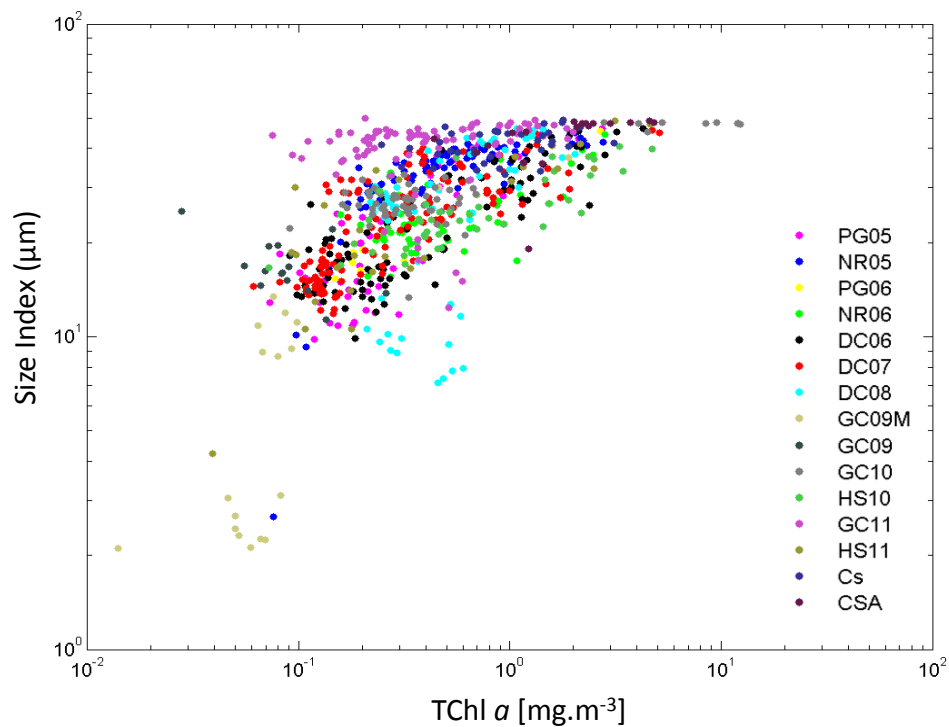


Figure 18 Variations of size index (Bricaud et al., 2004) as function of chlorophyll (TChl_a). Colours refer to each cruise and are in accordance with Figure 11.

3.2 Match-up analysis of Chlorophyll products

For the match-up analysis, eleven different Chl products were tested, i.e. different algorithms. Most products were developed for satellite data from MODIS and/or MERIS. One Chl product (CCI) was developed using satellite data from MODIS, MERIS and SeaWiFS (Table VII). As explained in methods (section 2.4), match-ups were evaluated considering two time-windows between satellite passage and sample collection: 3h and 6h (Figure 19, 20 and Table VII). The total number of samples used in each analysis was variable, even when using data from the same sensor, due to the use of different flags (see Table V in Methods), which should be specific for each algorithm. For MODIS, considering a time interval of 3h, 26 match-ups were found, almost tripling for a 6h time window. For MERIS, the number of match-ups ranged from 19 to 35, for a 3h time interval, and from 35 to 73, for a 6h time interval, for algal 1 and algal 2 product, respectively.

3.2 1 Standard Chlorophyll products

Considering only the standard Chl products, the OC3M algorithm using MODIS data yielded the best agreement with *in situ* HPLC data (i.e. bias (δ)=0.153; r^2 =0.74, for 3h interval; Figure 15-a,b). The comparison between *in situ* data and the output of algal 1 algorithm yielded an important positive bias of 0.290 for the 3h time difference, indicating an overestimation of Chl concentrations (Figure 15-c,d). This algorithm also yielded relative percentage differences (RPD) higher than 100% (Table VII), approximately the double of what was found for OC3M and algal 2. Data dispersion for algal 2 algorithm was high (URMS(Δ)=0.313 for 3h time difference; Figure 15-e,f), compared to what was found for OC3M (URMS(Δ)=0.218).

In terms of statistics, the results obtained using a 6h time difference were relatively similar with the ones obtained using only a 3h time difference (Figure 19, 20 and Table VII). The number of samples used for these analyses increased considerably, by a factor of 3 for MODIS and a factor of ~ 2 for MERIS. The URMS obtained for MODIS was smaller than for a 3h time difference. The same decrease was reported for algal 2. The coefficient of determination was similar or higher for all three products (Figure 19, 20 and Table VII).

Table VII Statistical results obtained from the agreement between *in situ* field data and concomitant satellite data. This match-ups analysis was performed for different Chlorophyll a products, i.e. different algorithms (standard and novel), using satellite data from MODIS, MERIS and SeaWIFS. Regional algorithms are indicated as 'reg'. The novelty < 3 for MLP_ATLP algorithm indicates a threshold for the degree of novelty of the input data (D'Alimonte et al., 2014).

Product	Satellite	Algorithm	Tdiff (h)	N	δ	Ψ	Δ	Slope	Offset	r^2	RPD*(%)	APD*(%)
Standard	MODIS	OC3M	< 3	26	0.153	0.267	0.218	0.78	0.03	0.74	57	68
			< 6	75	0.196	0.26	0.170	0.89	0.15	0.75	67	73
Standard	MERIS	Algal_1	< 3	19	0.290	0.343	0.183	0.97	0.28	0.73	111	116
			< 6	35	0.279	0.34	0.194	0.98	0.27	0.73	109	111
Standard	MERIS	Algal_2	< 3	35	0.07	0.321	0.313	0.87	0.03	0.42	42	62
			< 6	73	0.08	0.309	0.299	1.02	0.08	0.52	49	72
Novel	MERIS	Algal_2 _{reg}	< 3	35	0.108	0.359	0.343	1.31	0.16	0.42	64	82
			< 6	73	0.122	0.359	0.338	1.31	0.22	0.52	79	101
Novel	MERIS	CC_NN	< 3	35	0.189	0.498	0.460	1.27	0.24	0.43	533	551
Novel	MERIS	CC_NN _{reg}	< 3	35	0.277	0.602	0.534	1.65	0.40	0.43	1185	1203
Novel	MERIS	CC_QAA	< 3	31	-0.03	0.466	0.465	1.35	0.03	0.48	73	121
Novel	MERIS	CC_QAA _{reg}	< 3	31	0.027	0.551	0.551	1.74	0.14	0.48	138	7
Novel	MERIS	MLP _{ME} _ATLP	< 3	19	0.111	0.228	0.199	0.67	-0.02	0.68	41	55
		(novelty < 3)	< 3	12	0.182	0.209	0.103	0.81	0.07	0.84	56	56
		MLP _{ME} _ATLP	< 6	35	0.093	0.243	0.224	0.6	-0.07	0.63	39	57
		(novelty < 3)	< 6	20	0.167	0.216	0.136	0.69	-0.00	0.82	22	56
Novel	MODIS	MLP _{MO} _ATLP	< 3	26	0.105	0.261	0.239	0.62	-0.1	0.71	46	61
		(novelty < 3)	< 3	11	-0.02	0.23	0.23	0.73	-0.07	0.52	6	32
		MLP _{MO} _ATLP	< 6	75	0.075	0.226	0.214	0.87	0.018	0.62	33	51
		(novelty < 3)	< 6	46	0.05	0.189	0.182	1.18	0.1	0.61	21	38
Novel	MODIS, MERIS & SeaWIFS	CCI	< 3	139	0.245	0.331	0.222	0.75	0.12	0.74	97	105

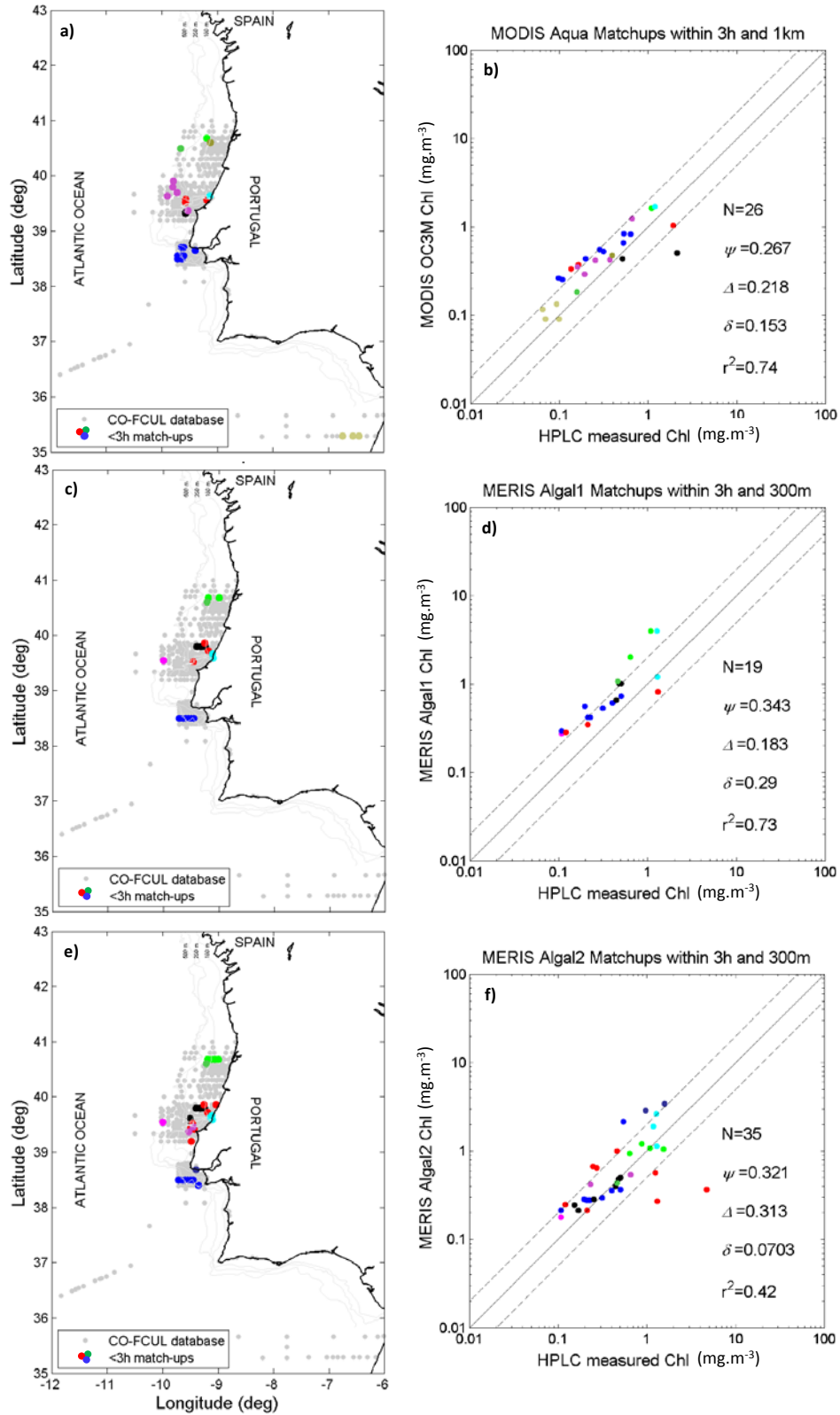


Figure 19 Match-up results obtained using the standard algorithms for MODIS (OC3M) and MERIS (algal 1 and algal 2). A 3h time difference was used in this analysis. **a)**, **c)** and **e)** indicate the location of each sample considered for each analysis. **b)**, **d)** and **f)** show the comparison between each standard product and the *in situ* HPLC data. Colours refer to each cruise and are in accordance with Figure 11.

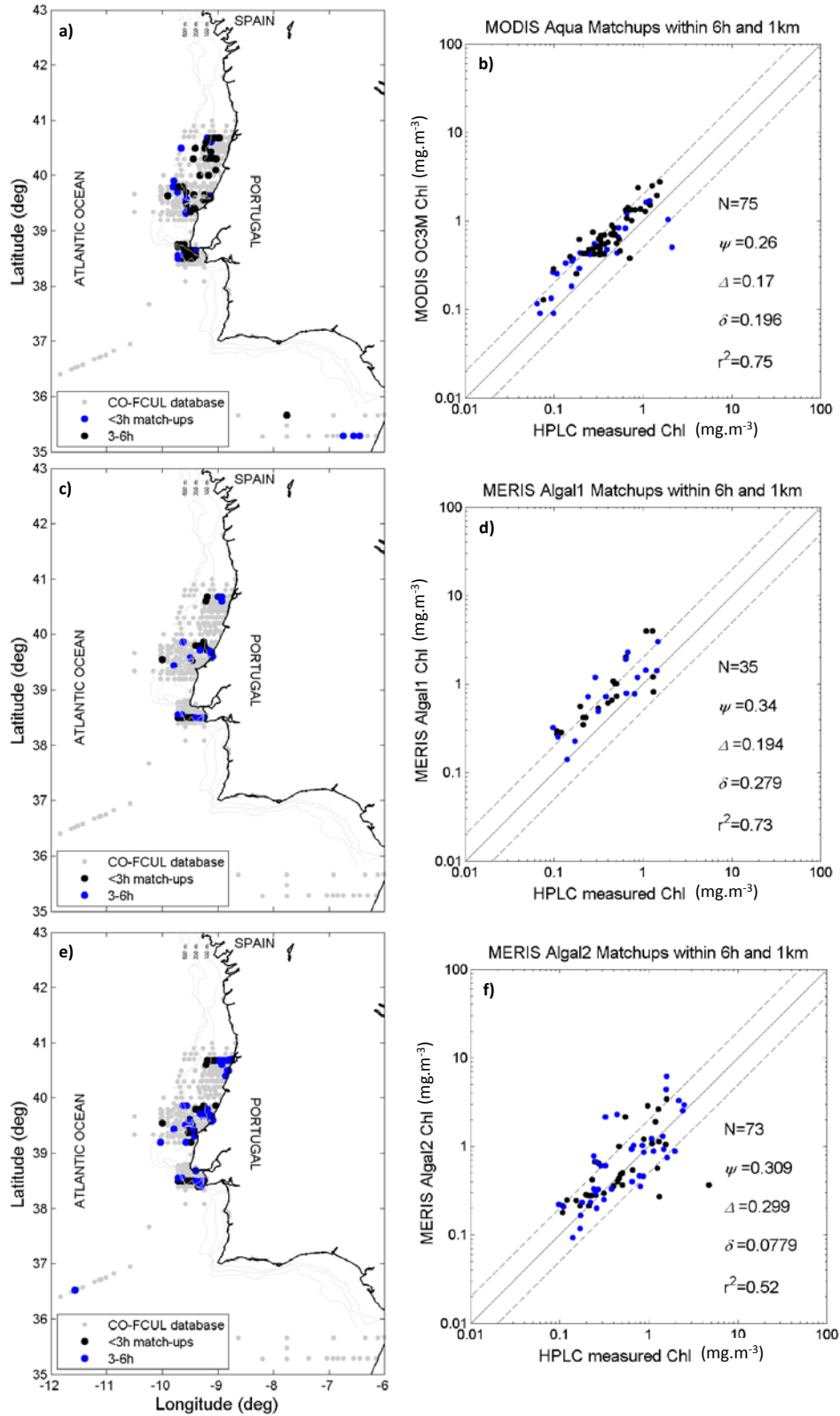


Figure 20 Match-up results obtained using the standard algorithms for MODIS (OC3M) and MERIS (algal 1 and algal 2). Two different time intervals are represented: 0 to 3h (black) and 3 to 6h (blue). **a)**, **c)** and **e)** indicate the location of each sample considered for each analysis. **b)**, **d)** and **f)** present the comparison between each standard product and the *in situ* HPLC data.

3.2.2 Novel Chlorophyll Products

In situ data of Chl concentrations and absorption at 442nm were used to derive an adjusted curve, i.e. a regional adaptation of the algal 2 algorithm (Figure 21-a). The coefficient of determination for this adjustment was 0.86. This adjustment was done using concomitant measurements taken during the GC11 cruise (at Nazaré and Bay of Lisbon during Spring 2011, Figure 11). Chlorophyll product was re-calculated from the satellite retrieved absorption at 442nm, using the standard (equation 2.8) and the regionally adjusted models (red equation in Figure 21-a). It is important to note that the dataset used for this regional adjustment is temporal and spatially very restricted. Results of the match-ups between *in situ* and derived Chl concentrations are presented in Figure 21-b. Both standard product results (in grey, same as Figure 20-f) and regionally adjusted product (in black) are presented for comparison. Higher values of bias (δ), RMS (Ψ), URMS (Δ), RPD and APD were obtained using the regional adjustment of algal 2 algorithm (see also Table VII). Thus, this adjustment failed to provide a better regional output using MERIS satellite data.

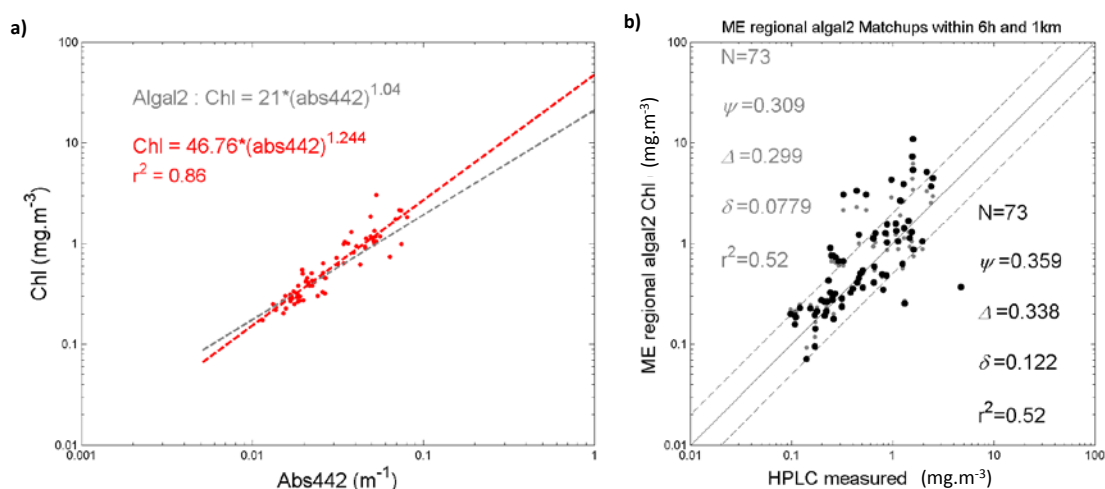


Figure 21 Regional adjustment of the equation 2.8 of the algal 2 Chl product, based on *in situ* absorption values at 442nm and Chl concentrations (a). Recalculation of match-up results using the regionally adjusted product, in black, and previous results of the standard product, in grey (b). A 6h time window was used in this analysis.

The two versions of the Chl product produced by the CoastColour Project (CC_NN and CC_QAA) yielded results which were similar between them, except for bias, which was much lower for the CC_QAA (Figure 22-b,d). The values of bias, coefficient of determination, RMS, and URMS (e.g. URMS=0.46; $r^2=0.43$, for CC_NN) were worse than the ones found for the standard products of

MERIS. The Relative and Absolute Percentage differences were especially poor for the CC_NN algorithm, yielding values higher than 500% of difference (see Table VII).

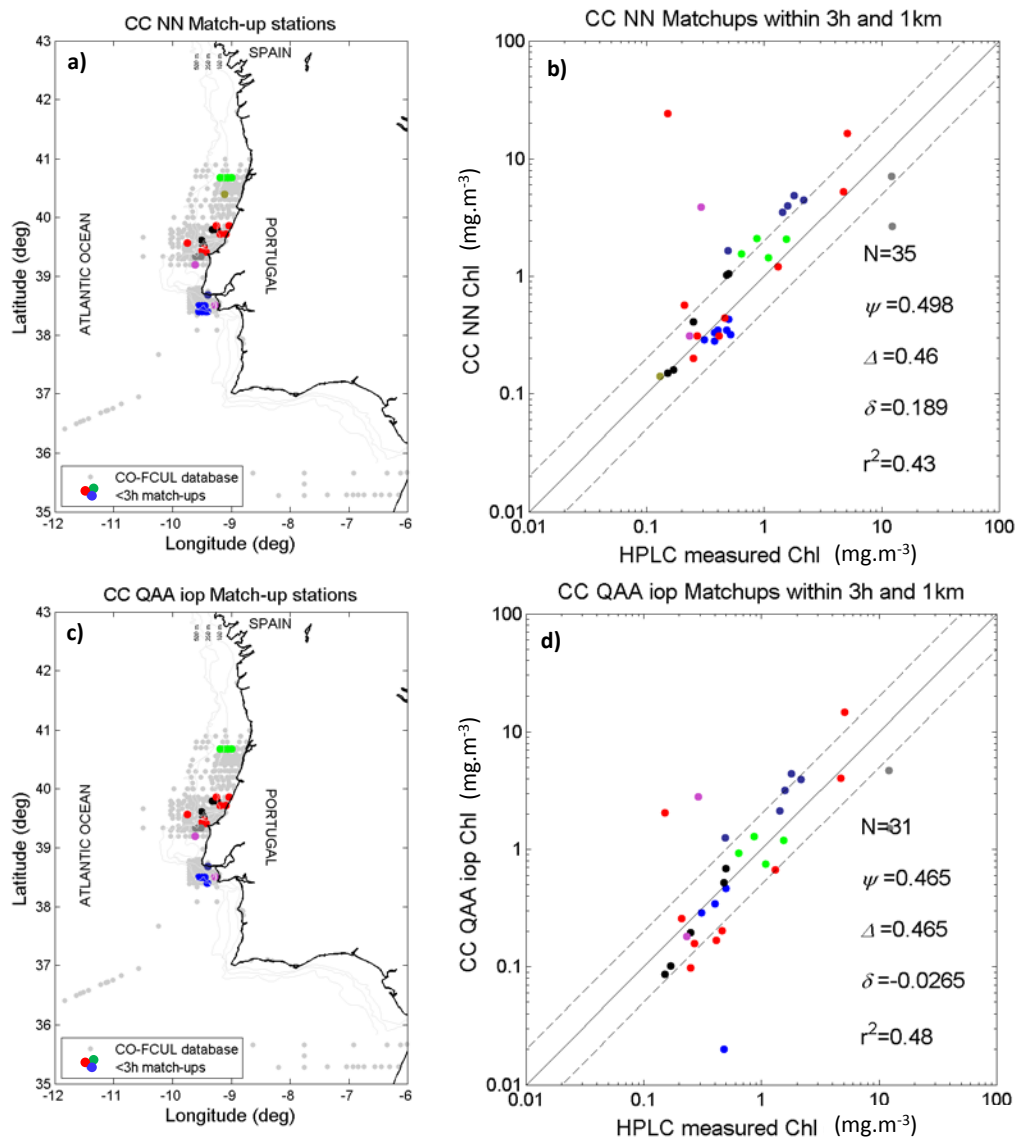


Figure 22 Match-up results obtained using the novel products developed in the CoastColour Project, using MERIS (CC_NN and CC_QAA). A 3h time difference was used in this analysis. **a)** and **c)** indicate the location of each sample considered for each analysis. **b)** and **d)** show the comparison between each product and *in situ* HPLC data. Colours refer to each cruise and are in accordance with Figure 11.

For the algorithms developed in the CoastColour Project, as also done for the algal 2 product, were regionally adjusted using the equation retrieved in Figure 21-a. Results are presented in Figure 23. From the comparison between the new products (CC_NN_{reg} and CC_QAA_{reg}) and the *in situ* HPLC data, it is possible to observe that this regional adjustment did not yield any improvement in the prediction of Chl concentrations (Figure 23-a,b) as was observed for the

regional adjustment of algal 2 (Figure 21-b). In fact, bias, RMS, URMS and RPD values were higher than the ones found with the original version, for both algorithms.

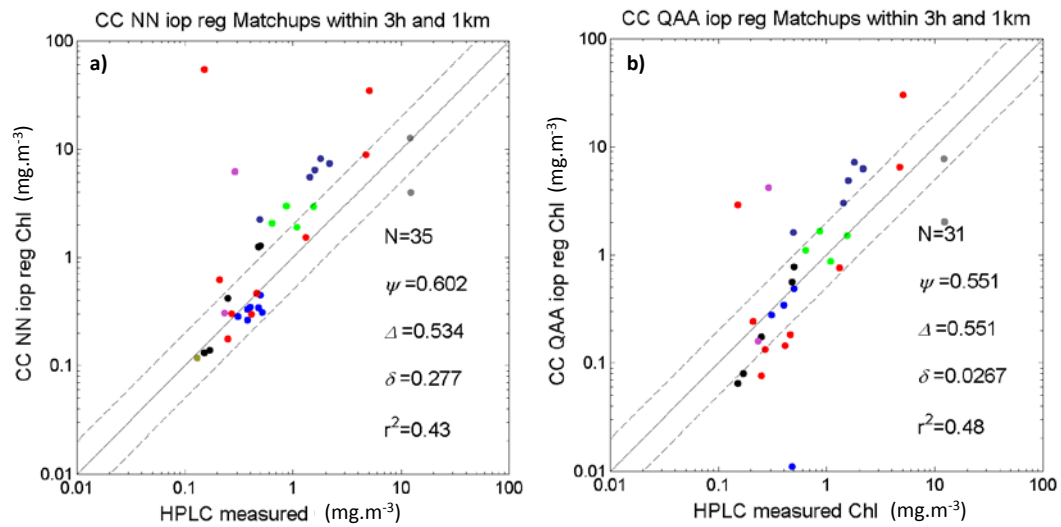


Figure 23 Match-up results obtained after regionally adjusting the novel products developed in the CoastColour Project, using MERIS (CC_NN and CC_QAA). A 3h time difference was used in this analysis. These results were obtained from the comparison between *in situ* HPLC data and the following products: **a)** CC_NN_{reg}; and **b)** CC_QAA_{reg}. Colours refer to each cruise and are in accordance with Figure 11.

The MLP-NN algorithm proposed by D’Alimonte et al. (2011), which was regionally adjusted for the Atlantic off Portugal (ATLP) by training the NN with JRC data collected during the GC11 cruise is here tested with the all *in situ* database. This algorithm was trained for both MERIS and MODIS bands allowing the input of Rrs data from both sensors (see section 2.2.2.3). Figure 24 presents the predicted Chl concentrations obtained through the application of the MLP_ATLP algorithm using MERIS radiometric data. Statistics indicate that this algorithm may have a better performance than the standard MERIS algorithms. The URMS value was much lower than the one obtained using algal 1 or algal 2, as well as the MODIS OC3M. The values of the Relative and Absolute percentage differences were similar with the ones obtained previously for algal 2 and much lower than the ones obtained for algal 1. The coefficient of determination is also high, especially considering the analysis using only data with novelty index < 3. This index can be seen as a measure of the applicability range of the algorithm (see section 2.2.2.3).

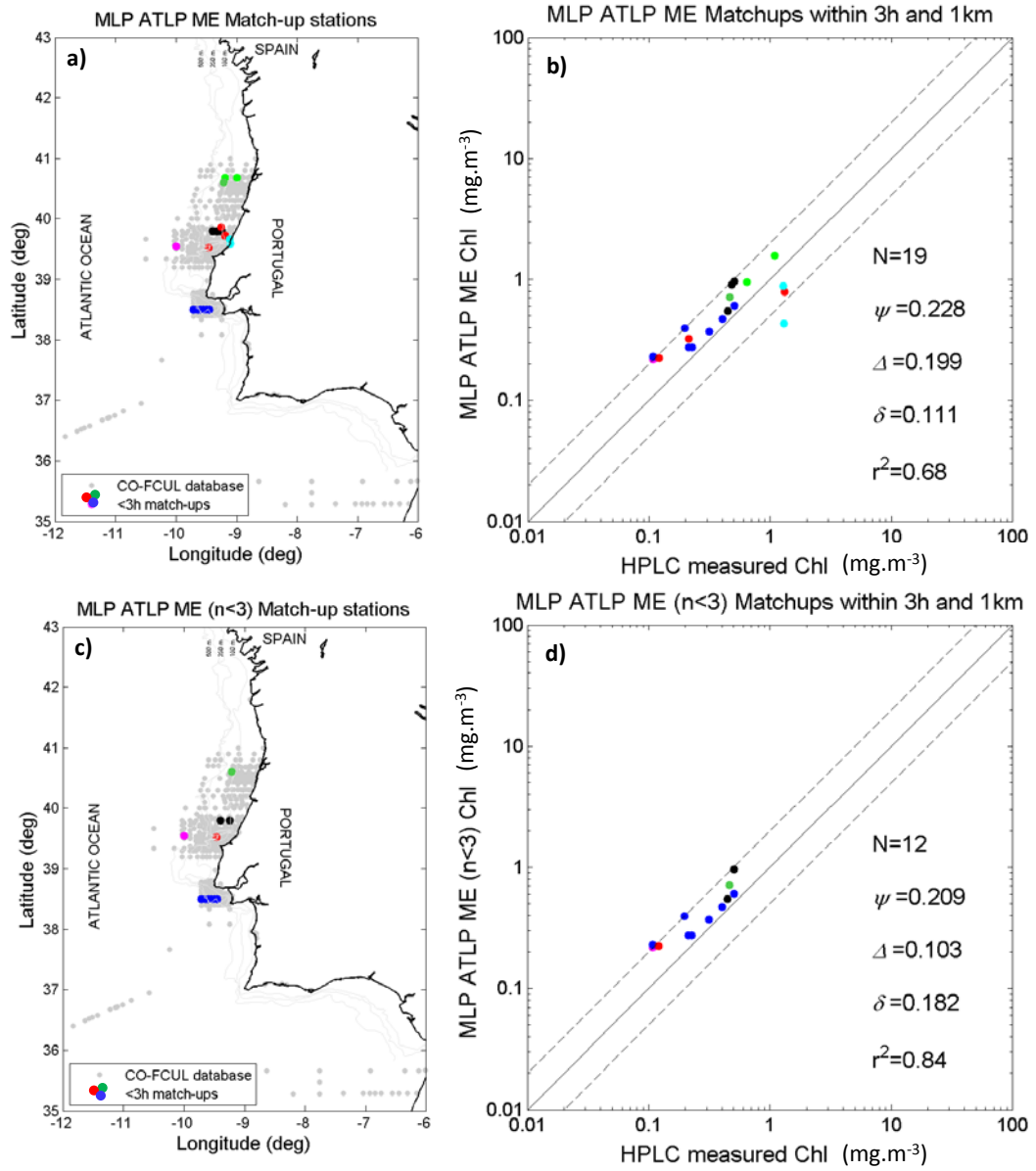


Figure 24 Match-up results obtained using the novel algorithms developed for the regionally adjusted MLP-NN, using MERIS (MLP_{ME}_ATLP). A 3h time difference was used in this analysis. **a)** and **c)** indicate the location of each sample considered for each analysis. **b)** and **d)** show the comparison between each product and *in situ* HPLC data. Results for all retrieved match-up data are presented in **a)** and **b)**. Results for matchups with low values of novelty (<3) are presented in **c)** and **d)**. Colours refer to each cruise and are in accordance with Figure 11.

The results obtained using an expanded temporal window, i.e. 6h time window, were similar to the results obtained considering only a 3h time difference (Figure 25). Although values of URMS for the 6h interval were higher than the ones found for the 3h interval, relative percentage of differences were lower (see Table VII). The number of valid pixels for this match-up analysis increased from 19 to 35 (the same as for MERIS algal 1, as radiometric data are the same).

Statistical results using novelty < 3 were also better, indicating an improved agreement between algorithm output and *in situ* HPLC data (Figure 25-d).

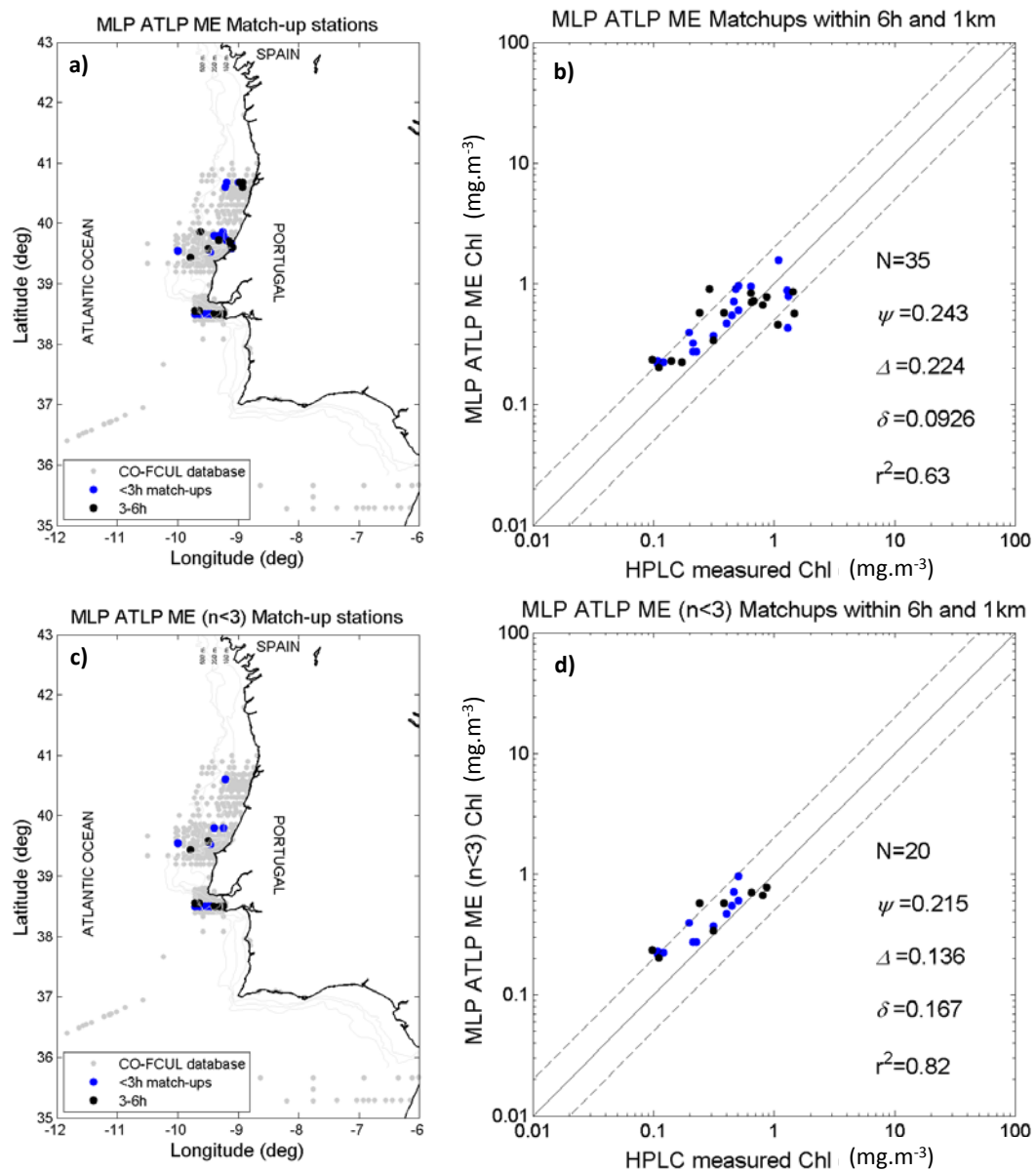


Figure 25 Match-up results obtained using the novel algorithms developed for the regionally adjusted MLP-NN, using MERIS (MLP_{ME}_ATLP). Two different time intervals are represented: 0 to 3h (black) and 3 to 6h (blue). **a)** and **c)** indicate the location of each sample considered for each analysis. **b)** and **d)** show the comparison between each product and *in situ* HPLC data. Results for all retrieved match-up data are presented in **a)** and **b)**. Results for matchups with low values of novelty (<3) are presented in **c)** and **d)**.

The MLP_{MO}_ATLP algorithm, is the MLP_ATLP using MODIS data as input. It also yielded a better agreement with the *in situ* HPLC data than the other novel algorithms (CC_NN and CC_QAA). The bias, URMS, RPD, APD and r^2 values were similar to the ones obtained using OC3M algorithm (Figure 26-b and Table VII). Using the novelty < 3 filter, results were even better for bias, URMS,

RPD and APD. The coefficient of determination was lower than the one obtained without the filter. However, this was caused by the reduced number of samples involved in this analysis (Figure 26-d).

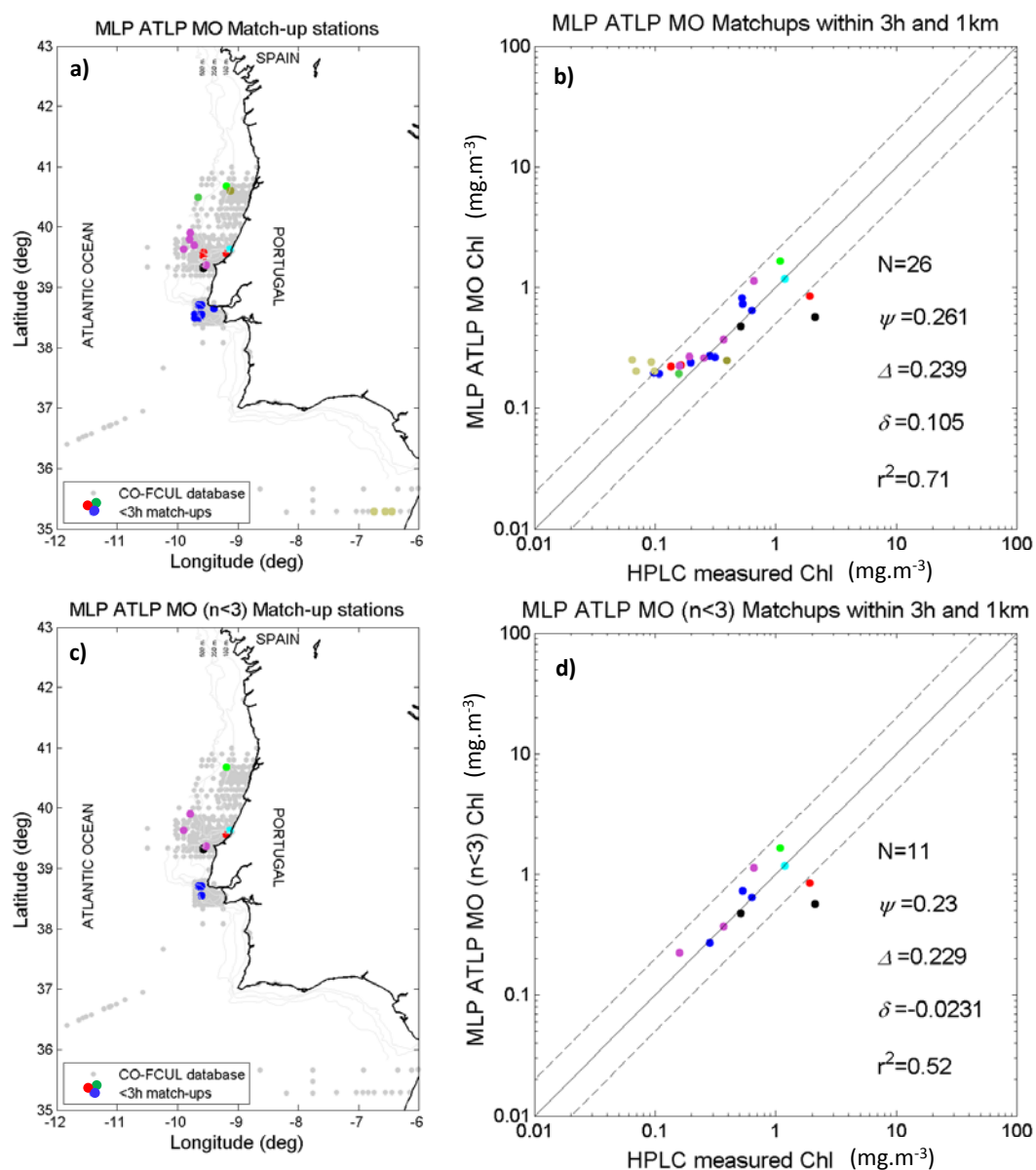


Figure 26 Match-up results obtained using the novel algorithm developed for regional adjusted MLP-NN, using MODIS (MLP_{MO}-ATLP). A 3h time difference was used in this analysis. **a)** and **c)** indicate the location of each sample considered for each analysis. **b)** and **d)** show the comparison between each product and in-situ HPLC data. Results for all retrieved match-up data are presented in **a)** and **b)**. Results for match-ups with low values of novelty (<3) are presented in **c)** and **d)**. Colours refer to each cruise and are in accordance with Figure 11.

Considering a time interval of 6h, the number of samples included increased, from 26 to 75 (in accordance to MODIS matchups). Statistical results were very similar with the ones obtained for

a 3h time interval, revealing that increasing the time window to 6h did not yield poorer predictions of Chl concentrations (Figure 27-b,d). Using the novelty < 3 filter resulted in lower values of error (bias, RMS, URMS, RPD and APD) and a similar value for the coefficient of determination (see Table VII).

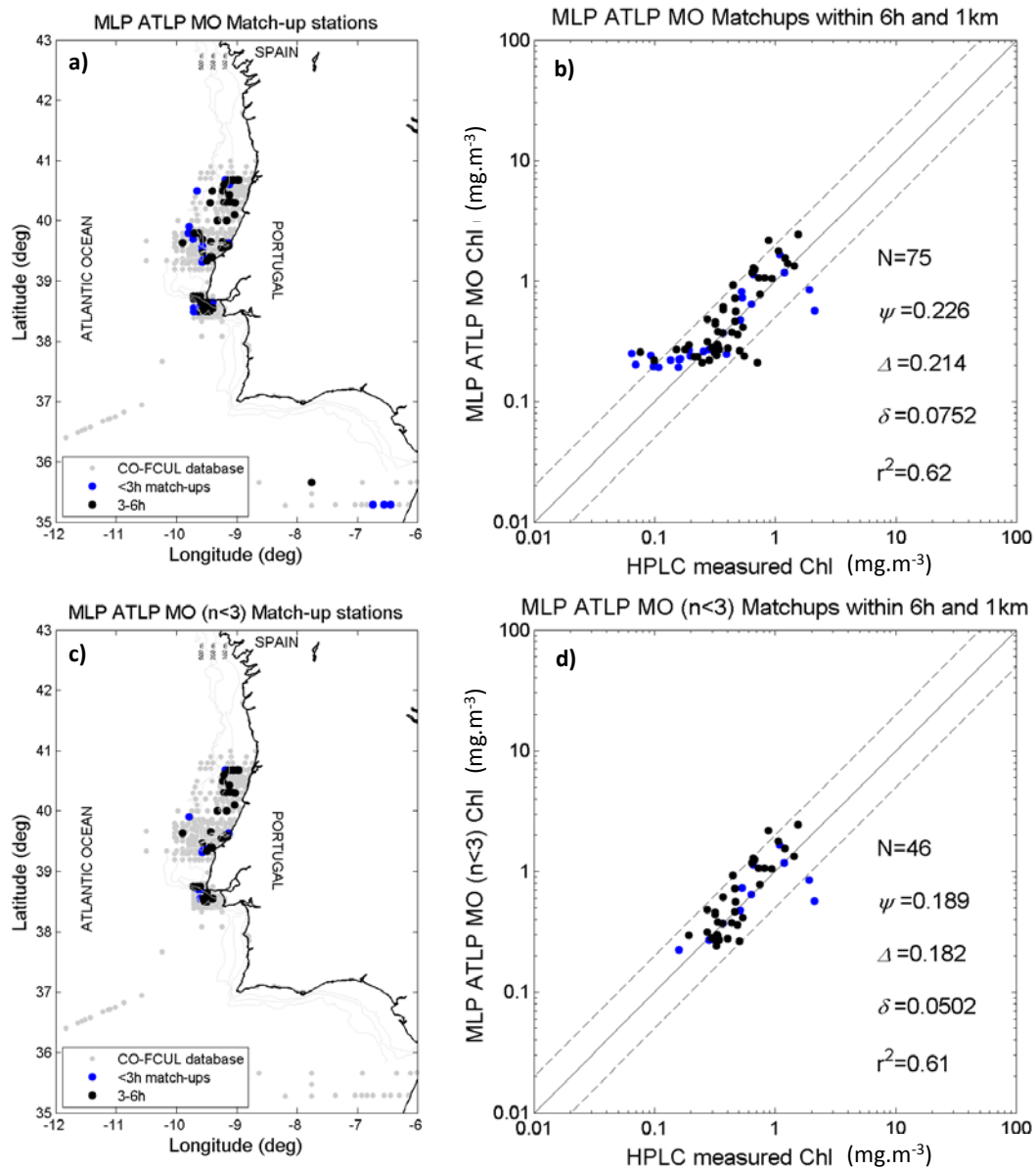


Figure 27 Match-up results obtained using the novel algorithms developed the regionally adjusted MLP-NN, using MODIS (MLP_{MO}-ATLP). Two different time intervals are represented: 0 to 3h (black) and 3 to 6h (blue). **a)** and **c)** indicate the location of each sample considered for each analysis. **b)** and **d)** show the comparison between each product and *in situ* HPLC data. Results for all retrieved match-up data are presented in **a)** and **b)**. Results for matchups with low values of novelty (<3) are presented in **c)** and **d)**.

The Chl product from the Climate Change Initiative Project (CCI) uses satellite data from MODIS, MERIS and SeaWiFS sensors. The number of available match-ups (n=139) is therefore much

higher than for the other algorithms (Figure 28; and Table VII). For a time window of 3h, the values of bias, RMS and URMS obtained were similar to the ones obtained for algal 1 and algal 2, and slightly higher than the ones obtained for OC3M and MLP_ATLP. The coefficient of determination was 0.74, i.e. within the range of values found for the standard product of MODIS and MERIS algal 1. However, relative and absolute percentage differences (RPD and APD) were approximately 100%, i.e. similar with what was obtained for algal 1 and much higher than what was obtained for OC3M, algal 2 and MLP_ATLP.

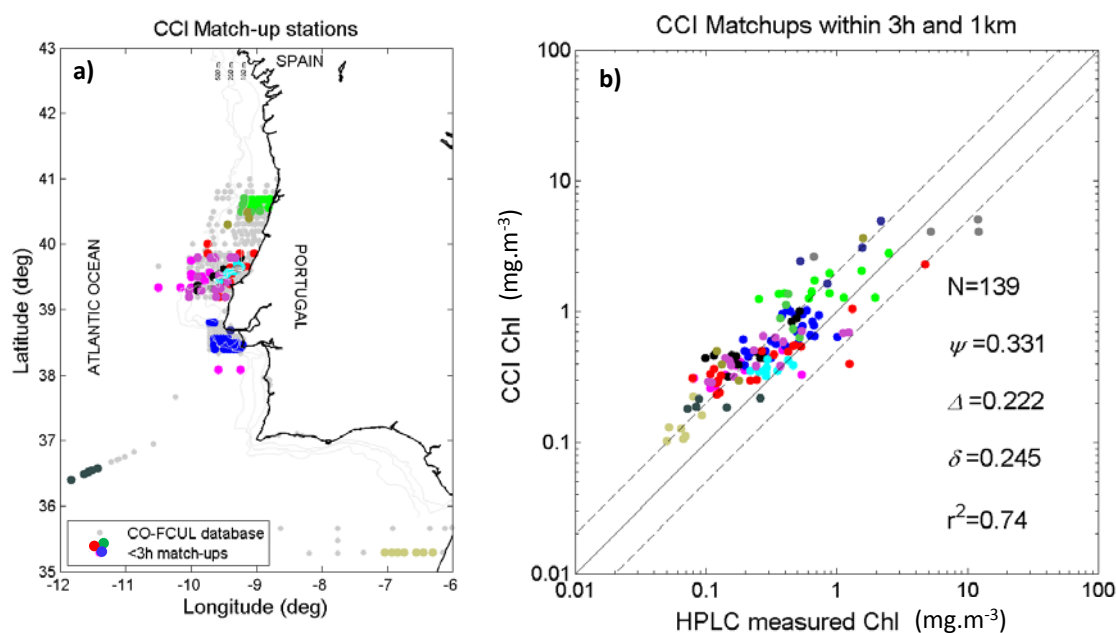


Figure 28 Match-up results obtained with the Chl CCI product. A 3h time difference was used in this analysis. **a)** Indicates the location of each sample. **b)** Shows the comparison between the product and *in situ* HPLC data. Colours refer to each cruise and are in accordance with Figure 11.

3.2.2 Comparisons between MERIS and MODIS Standard products

The matchups found for both MERIS products are presented in Figure 29. Given that each product, considers the use of different flags due to the use of different algorithms (algal 1 and algal 2), only 35 valid pixels were found for this analysis for a 6h window. The coefficient of determination was of 0.87. The bias value was -0.259, indicating an overestimation of Chl concentrations using algal 1, in comparison with algal 2. This is in agreement with the positive bias found for the comparisons between *in situ* and algal 1 Chl concentrations.

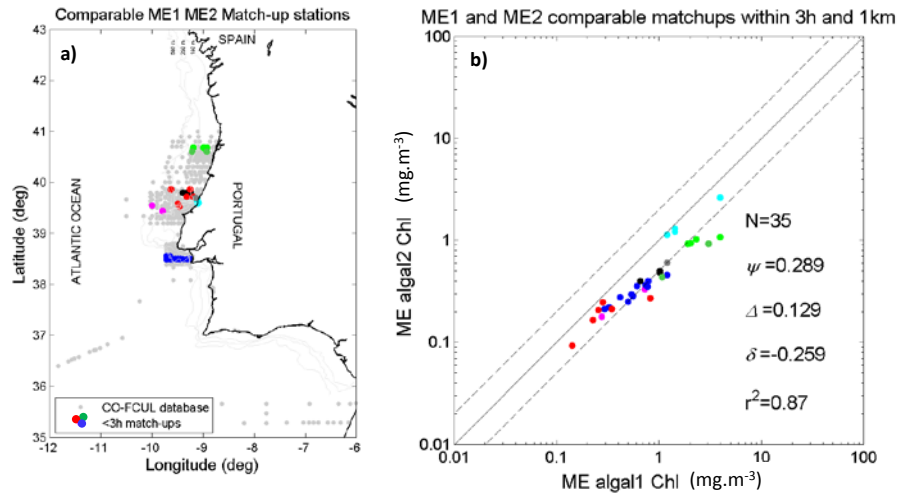


Figure 29 Location of common valid pixels using algal 1 and algal 2 MERIS algorithms (a); The comparison between the Chl product for these two algorithms is also presented (b). Colours refer to each cruise and are in accordance with Figure 11.

Only 13 concomitant samples were found between MODIS OC3M Chl product and MERIS algal 1 product (Figure 30) for a 6h time window. As previously mentioned, band-ratio algorithms as algal 1 and OC3M, are only suitable for Case 1 waters. Given the appropriateness for this study, only algal 1 was compared with MODIS standard product. The coefficient of determination was 0.95. The bias value was -0.101, indicating an overestimation of Chl concentrations using MERIS algal 1, in comparison with MODIS OC3M.

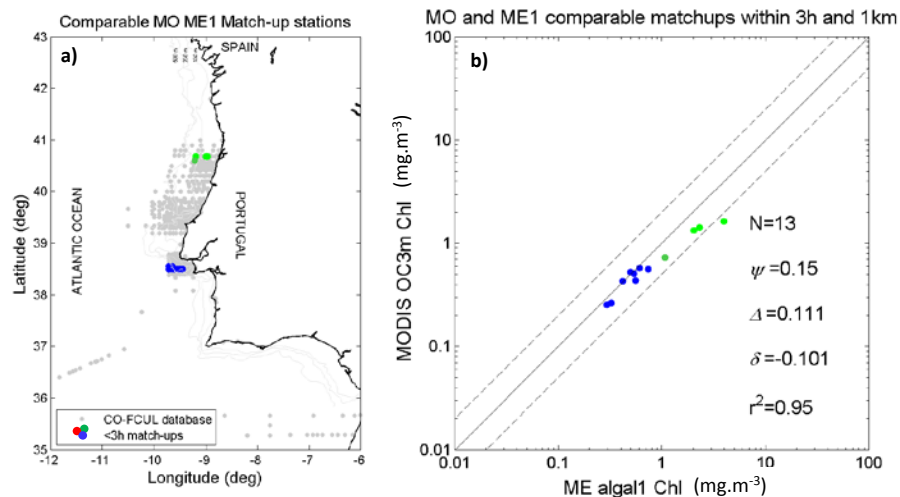


Figure 30 Location of common match-ups for MODIS and MERIS (algal 1) products, within a time window of 6h (a). The comparison between the Chl products for these two sensors is also presented (b). Colours refer to each cruise and are in accordance with Figure 11.

3.3 Water typology: case1 vs non-case1 waters

3.3.1 Optical properties off the Portuguese coast using *in situ* data

During the GC11 cruise, both apparent and inherent optical properties were measured. Although it is a very small dataset, these data are significant and capable of describing the bio-optical properties of the sampled area (see sampled area in Figure 11, cruise GC11). Analysing the absorption of the different optically active components: phytoplankton, CDOM and non-algal particles (NAP) in a ternary plot, we see that the total absorption is dominated by the absorption of the CDOM component (Figure 31). Remembering the classification scheme shown in Figure 6, majority of the sampled waters would be classified as CDOM dominated waters considering only the absorption properties.

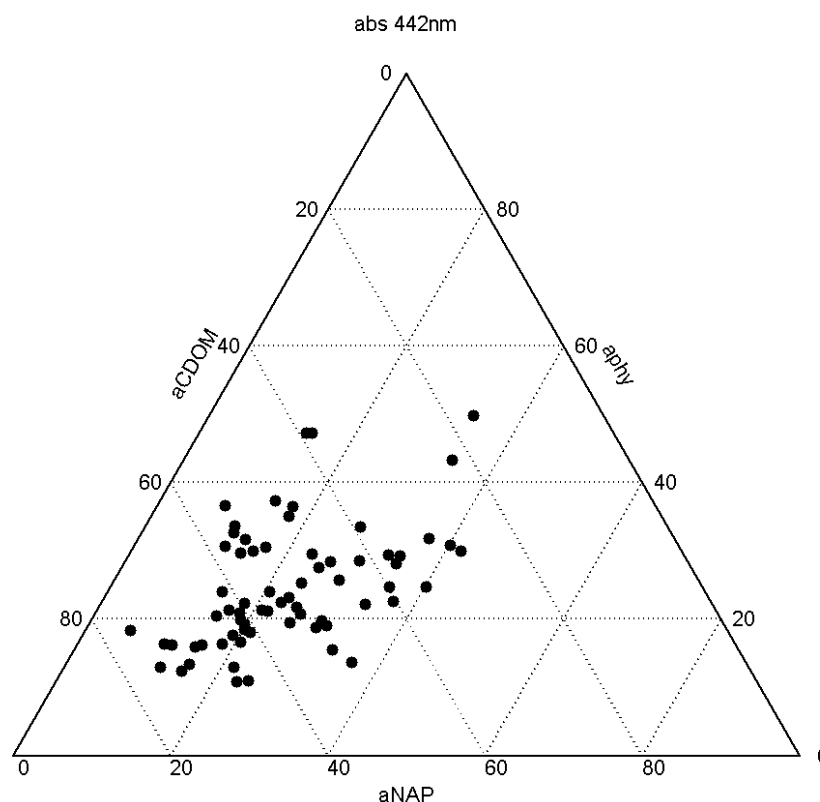


Figure 31 Ternary plot of absorption at 442nm of CDOM, non-algal particles and phytoplankton measured during the GC2011 cruise.

In fact, Chl is clearly not correlated with CDOM absorption (data not shown), which confirms that the waters sampled are not Chl dominated waters (Case 1). Analysing the AOPs and considering the Lee and Hu (2006) model, majority of sampled data fall within the thresholds

attributed to typical Case 1 waters when considering the Rrs555 condition (Figure 32-b), with only a few points surpassing the threshold. However, looking at the RR12 condition (Figure 32-a), majority of the data points are below or close the lower threshold set for typical Case 1 waters. This condition is a proxy of amount of CDOM per Chla, with lower values corresponding to higher CDOM per Chla conditions. Therefore, results are not in disagreement with the IOP (absorption) results.

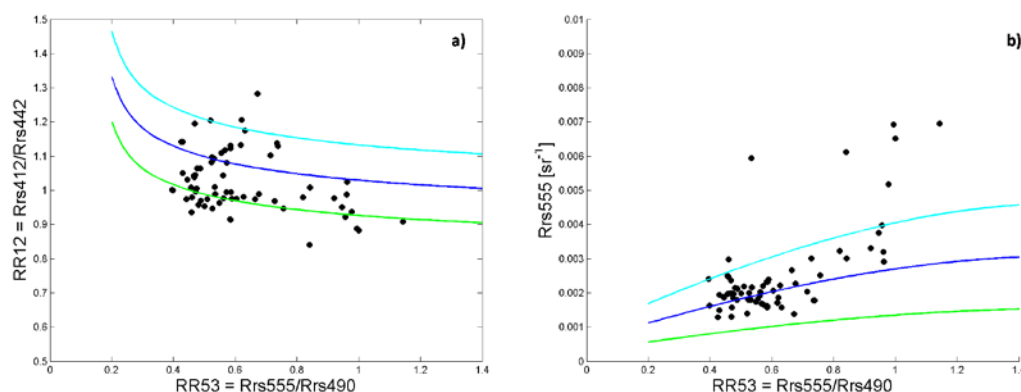


Figure 32 All *in situ* radiometric data collected during the GC11 cruise superimposed with Lee and Hu (2006) model: **a)** RR12_RR53 condition, **b)** Rrs555_RR53 condition.

Although these *in situ* data are relevant to characterize the sampled area, generalization is challenged by the small time and temporal scales. The analysis with remote sensing data was therefore attempted.

3.3.2 Water typology using remote sensing data

The Lee and Lu (2006) model described in Methods (section 2.6) is here used to attempt classification of type of water off the Portuguese coast and evaluate its spatial and temporal distribution. Model conditions were applied to daily and seasonal averaged Rrs MODIS data for a seven year period (2005-2011). As the model was originally applied to SeaWiFS, both sensors were initially tested. Figure 33 shows, as an example, the averaged ratio reflectances for the summer period of 2005 for both MODIS and SeaWiFS. These sensors have slightly different bands (i.e. SeaWiFS 412,443,490 and 555nm; MODIS 412,443,488 and 551nm) and different spatial resolution (i.e. SeaWiFS 4km and MODIS 1km) but general results were found similar, despite some observed differences.

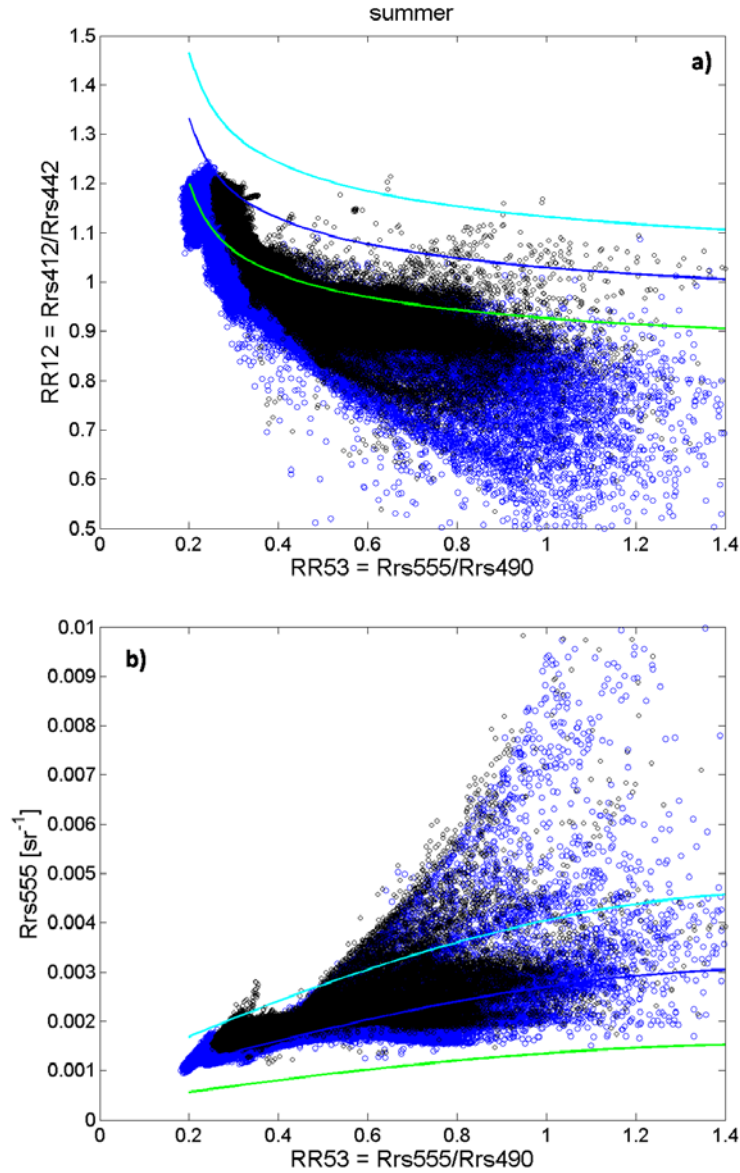


Figure 33 Reflectance ratios applied to MODIS (in blue) and SeaWiFS (in black) data off the Portuguese coast with superimposed Lee and Hu (2006) model for Case 1-waters (lines). Data presented are averaged Rrs data for the summer period of 2005.

Both MODIS RR12 ratio and Rrs555 reach lower values and are more dispersed than the retrieved data by SeaWiFS. To see how these differences can affect the map distribution of the water types, seasonal maps were generated applying: (1) only the first condition (equation 2.18), (2) only the second condition (equation 2.19) and (3) both conditions (equation 2.18 and 2.19).

For each daily image, every pixel was classified as Case 1 water or non-Case 1 water by applying each of the mentioned conditions. Percentage of times a pixel was considered as Case 1 water for a specific period was then mapped (Figures 34-35).

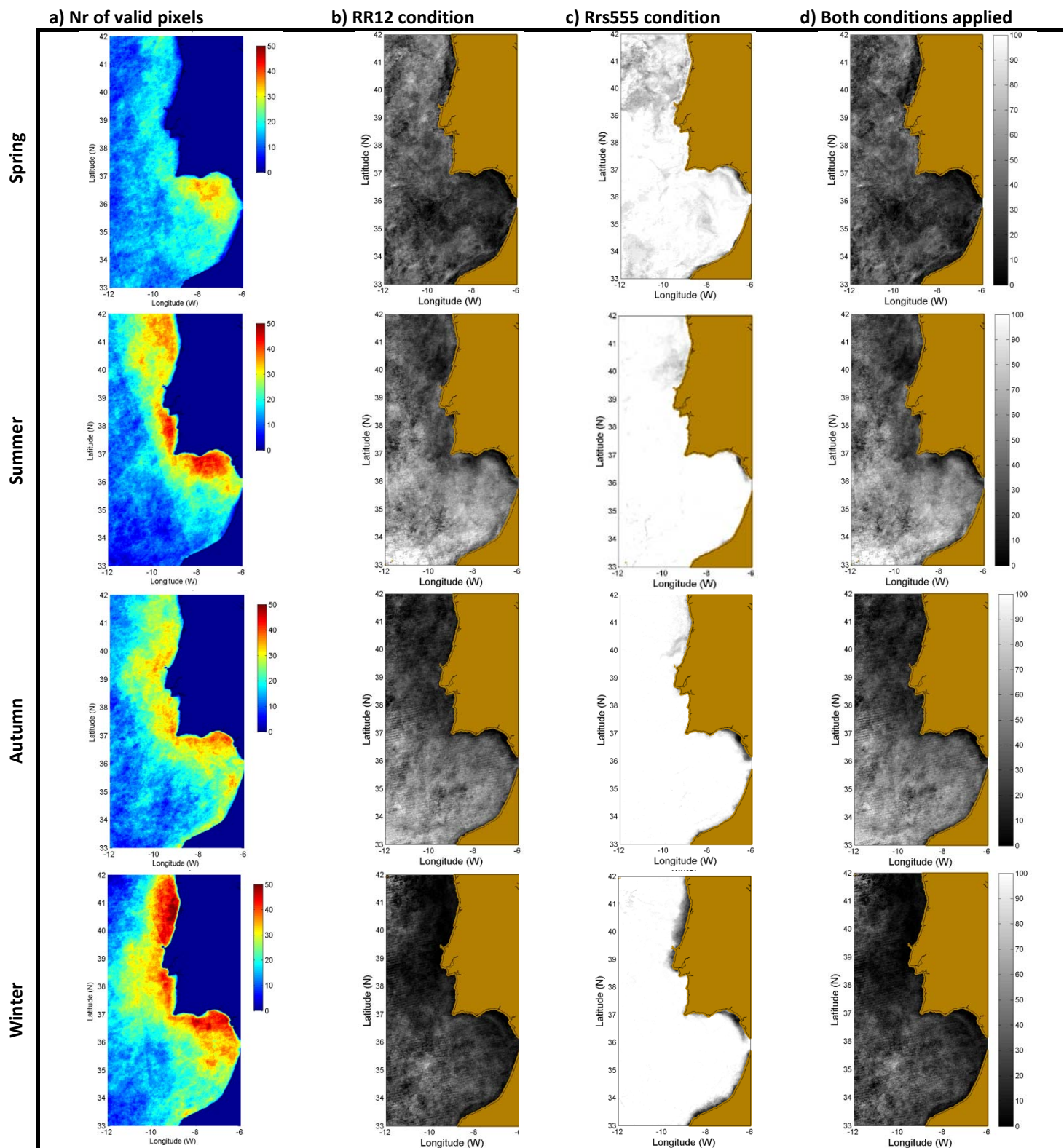


Figure 34 Maps of percentage of pixel classification as Case 1 waters according to Lee and Hu (2006) model conditions for MODIS data, considering the four seasons of 2005. For each season, the number of valid pixels is presented in **a**). Note that 50 was the maximum assigned value to the scale. The percentage of Case 1 pixel classification applying different criteria are presented in **b**) only the RR12_RR53 condition, **c**) only the Rrs555_RR53 condition, and **d**) with both conditions. Note that scale is in percentage (0-100%) and that pixels invalid for the considered time period are presented in brown.

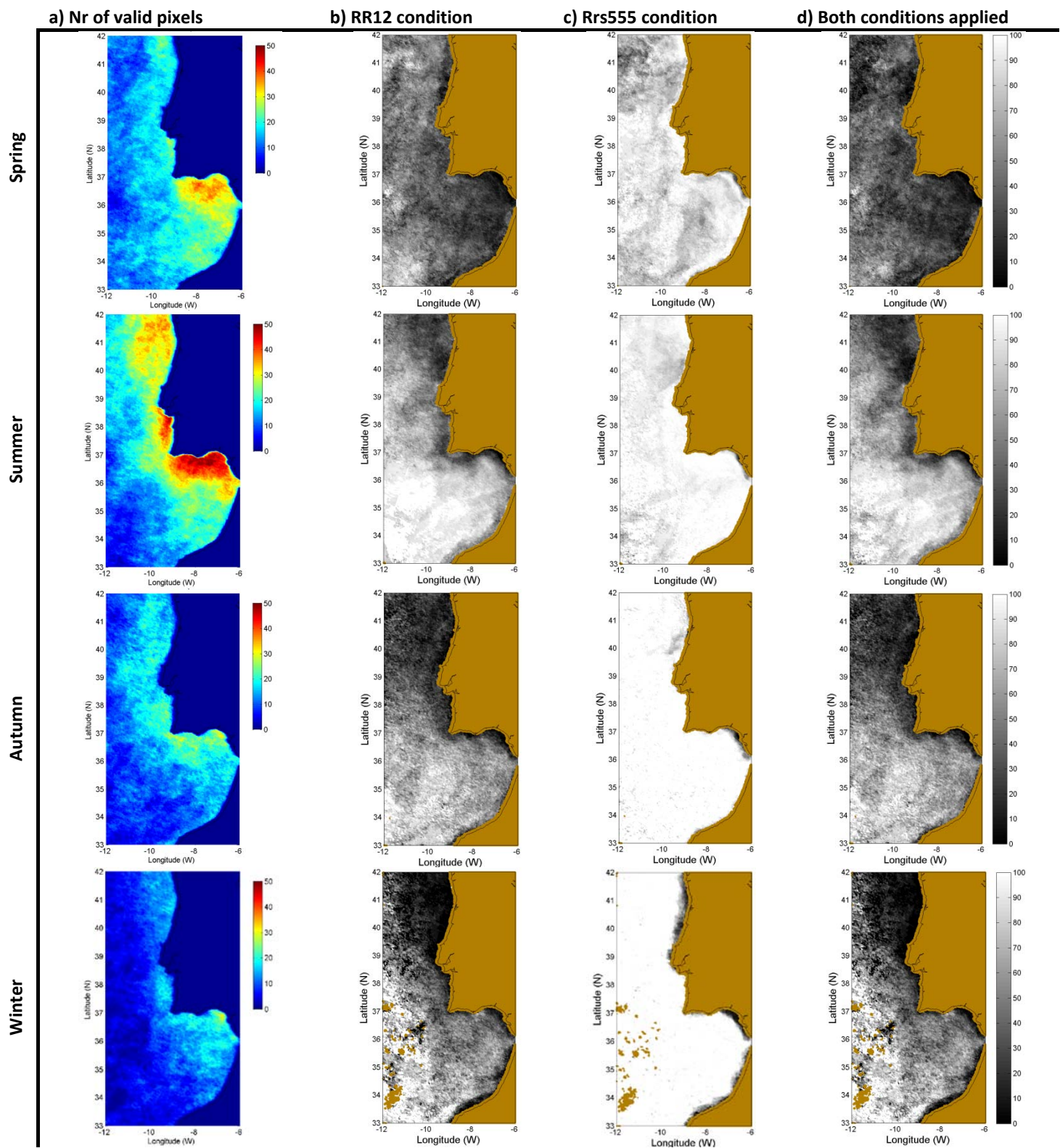


Figure 35 Maps of percentage of pixel classification as Case 1 waters according to Lee and Hu (2006) model conditions for SeaWiFS data, considering the four seasons of 2005. For each season, the number of valid pixels is presented in **a)**. Note that 50 was the maximum assigned value to the scale. The percentage of Case 1 pixel classification applying different criteria are presented in **b)** only the RR12_RR53 condition, **c)** only the Rrs555_RR53 condition, and **d)** with both conditions. Note that scale is in percentage (0-100%) and that pixels invalid for the considered time period are presented in brown.

For MODIS, and considering the four seasons, the highest number of valid pixels was observed in the summer and winter, and the lowest number of pixels was observed during spring (figure 34). Considering all cases, higher number of valid pixels was always found near the coast.

Considering the first condition (RR12 against RR53, equation 2.18), a high percentage of non-Case 1 waters (i.e. low percentage of Case 1 waters), represented in dark colours, were found throughout the whole Portuguese area selected for this study. This was observed for spring, summer, autumn and winter (Figure 34-b for all seasons). However, the highest percentages were found in winter.

Applying only the second condition (RRs555 against RR53, equation 2.19), most waters were frequently classified as Case 1 waters, represented in white and light grey colours (Figure 34-c for all seasons). The percentage of Case 1 waters in open waters was higher than 90% during summer, autumn and winter. A high spatio-temporal variability was found for the classification of Case 1 waters, using only the second condition: low percentages of Case 1 waters were found near the coast in winter, and lower percentages of typical Case 1 waters were also found in open water during spring.

The classification applying both conditions is quite similar to the classification using only the first condition (Figure 34-d for all seasons). The criteria for both conditions uses the “one out, all out” rule, i.e. if one pixel is classified as non-Case 1 waters for one condition, it will be automatically classified as non-Case 1 water. Therefore, the first condition strongly influences the final classification.

Given the similarity with these results obtained for the year 2005, the maps for the years from 2006 to 2011 are only presented in Annex II.

For SeaWiFS, the highest number of valid pixels were observed in summer and the lowest number during winter (Figure 35-a for all seasons). The spatial pattern found for the percentage of pixels classified as non-Case 1 waters was similar with what was observed using MODIS satellite data, both considering the first and the second condition. Considering the first condition, a lower percentage of pixels were classified as non-Case 1 waters, when compared with MODIS data (Figure 35-b for all seasons). The opposite trend was found when the second condition is considered (Figure 35-c for all seasons). However, it is important to note that differences are relatively small, as presented in the next sections (Figure 36-37 and Table VIII).

The map of differences between SeaWiFS and MODIS Case 1 water percentage classification are presented in Figures 36 and 37. Considering the first condition, the highest differences were found for summer and winter seasons (Figure 36-b and d). In the summer, 90.4% of pixels presented positive values for the differences ($\text{dif} > 0$), with a mean percentage difference of 22.9% (Table VIII). For the winter of 2005, 82.1% of pixels presented positive values for the differences, with a mean percentage difference of 27.9%. These results indicate that, applying the first condition, SeaWiFS classified a higher percentage of pixels as Case 1, compared to MODIS.

Considering only the second condition, the highest differences were found for spring and summer seasons (Figure 37-a and b). In this case, most differences observed were negative, indicating that SeaWiFS classified a lower percentage of pixels as Case 1 waters, compared to MODIS. In spring, 75.0% of pixels presented negative values for the differences ($\text{dif} < 0$), with a mean percentage difference of -9.4% (Table VIII). For the summer of 2005, 54.7% of pixels presented negative values for the differences, with a mean percentage difference of -4.5% (Figure 37-b; Table VIII). The seasons of autumn and winter presented a high percentage (~85%) of pixels with no differences between SeaWiFS and MODIS, i.e. $\text{dif} = 0$.

Table VIII Summary of the differences (diff) observed between the maps of SeaWiFS and MODIS classification for 2005. Results are presented for each season.

SW-MODIS	<i>Spring</i>	<i>Summer</i>	<i>Autumn</i>	<i>Winter</i>
1st condition (RR12vsRR53)				
N	355478	355845	356490	353498
% (diff>0)	72.7	90.4	77.54	82.1
% (diff<0)	24.0	7.4	20.6	14.9
% (diff=0)	3.2	2.2	1.8	3.0
Total % mean	10.5	22.9	13.8	27.9
Mean %(diff>0)	17.4	26.1	20.2	35.9
Mean %(diff<0)	-8.9	-8.0	-8.9	-11.2
2nd condition (Rrs555vsRR53)				
N	355478	355845	356490	353498
% (diff>0)	11.8	3.5	4.8	6
% (diff<0)	75.0	54.7	9.7	7.9
% (diff=0)	13.2	41.7	85.5	86.1
Total % mean	-9.4	-4.5	-0.6	-1.06
Mean %(diff>0)	7.5	5.6	6.9	7.9
Mean %(diff<0)	-13.7	-8.7	-9.3	-19.5

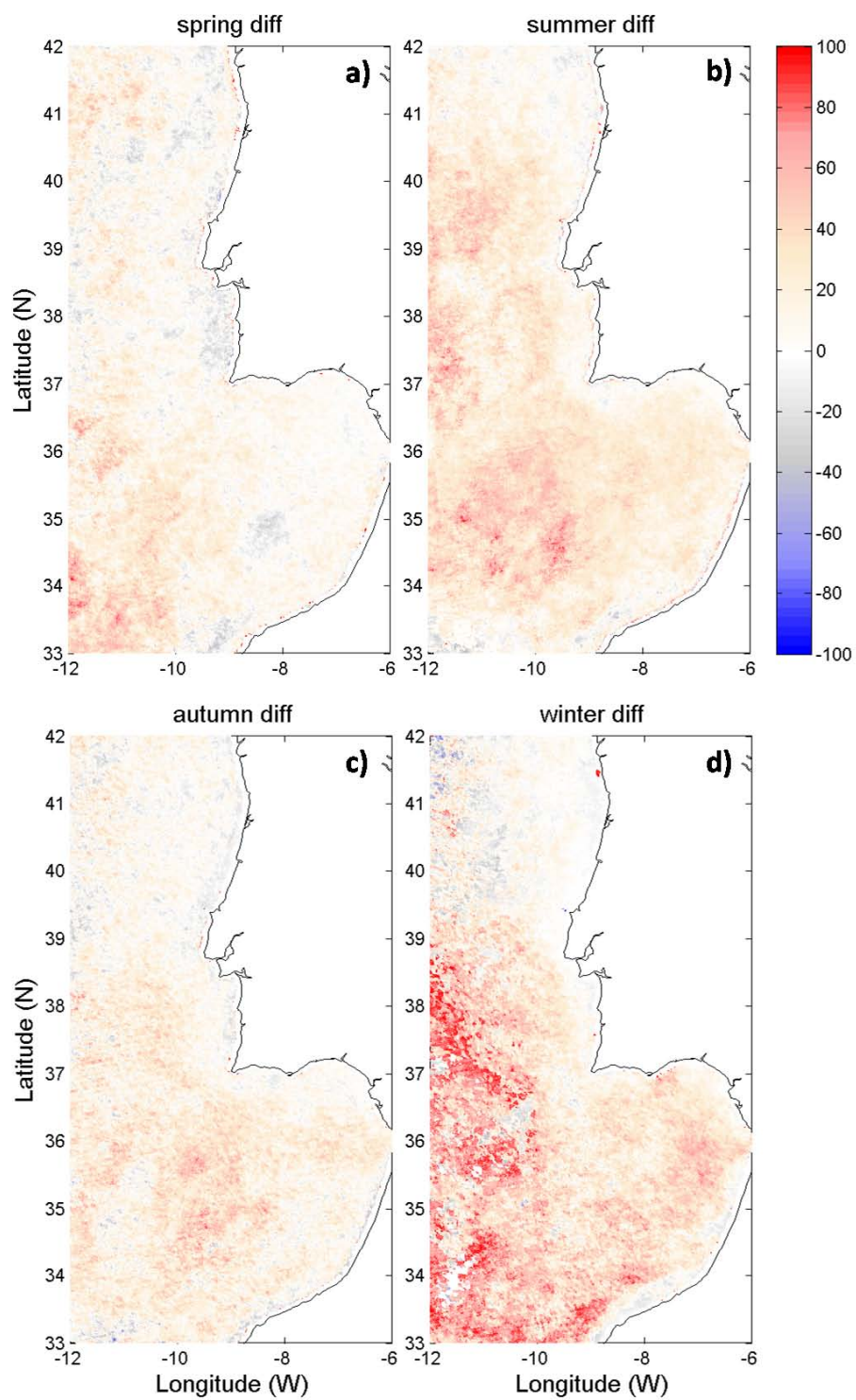


Figure 36 Maps of the difference between SeaWiFS and MODIS Case 1 waters percentage classification using only the RR12_RR53 condition for 2005: **a)** spring, **b)** summer, **c)** autumn and **d)** winter. Note that **b)** is the result of the difference between Figure 35 b) and Figure 34 b). Positive values result from higher percentage values for SeaWiFS classification and negative values from higher percentage values of MODIS classification.

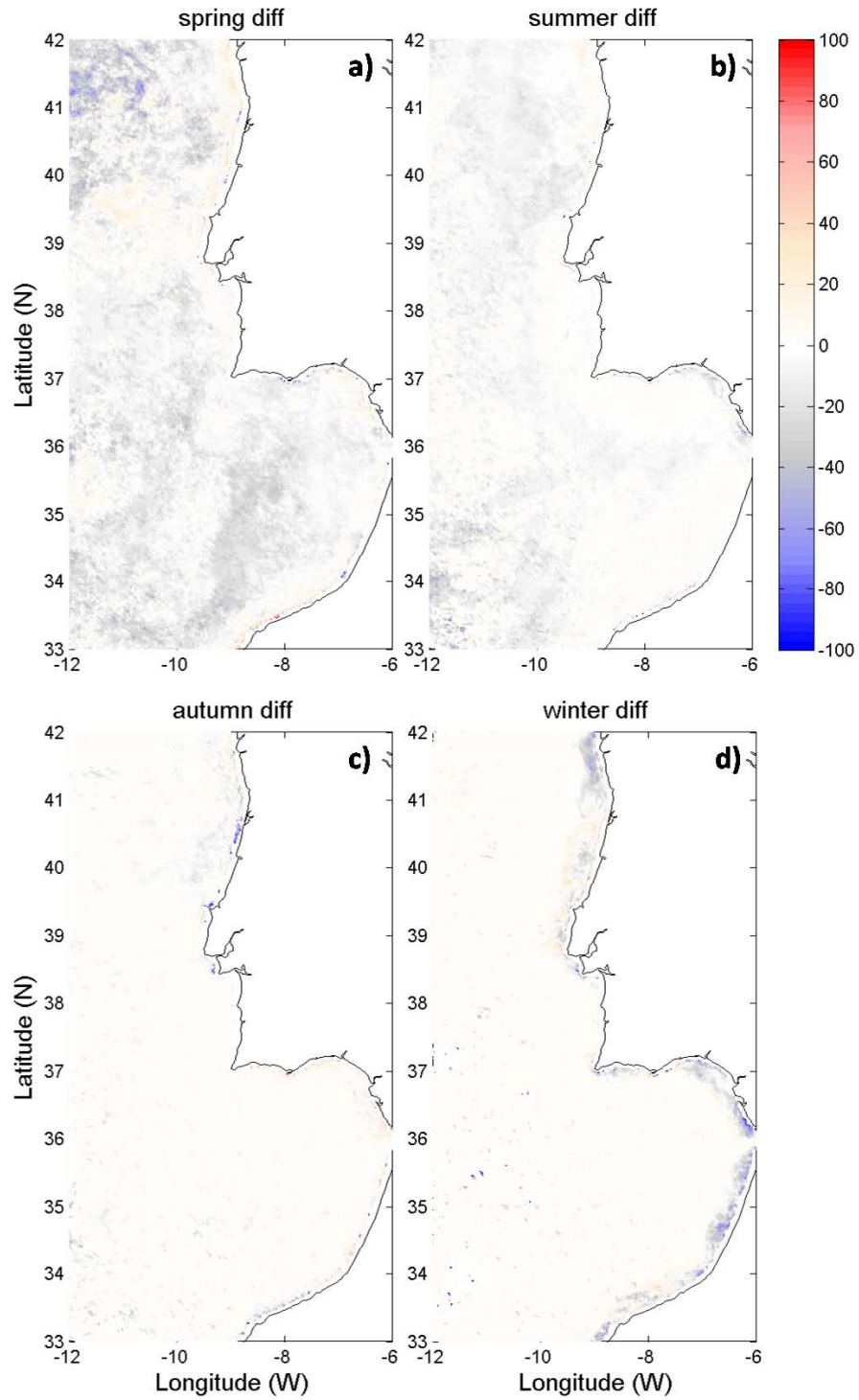


Figure 37 Maps of the difference between SeaWiFS and MODIS Case 1 waters percentage classification using only the Rrs555_RR53 condition for 2005: **a)** spring, **b)** summer, **c)** autumn and **d)** winter. Note that **b)** is the result of the difference between Figure 35 c) and Figure 34 c). Positive values result from higher percentage values for SeaWiFS classification and negative values from higher percentage values of MODIS classification.

3.3.3 Model constraints and applicability

In order to test the accuracy of MODIS and SeaWiFS radiometry, data were validated with *in situ* data matchups. NASAs database SeaBASS (available at <http://seabass.gsfc.nasa.gov/>) was used to perform the analysis. This database has worldwide open ocean data and match-ups can be provided for both MODIS and SeaWiFS sensors. Validation was performed for 412, 443, 488 (or 490), 551 (or 555) and 667 (or 665) bands (e.g. Figure 38-a,b,c,d,e). The final objective is to understand how inaccuracies in the bands used in Lee and Hu (2006) model can affect the water type classification. Therefore the RR12 and RR53 ratios were also tested (Figure 38-f,g) and data plotted with the model superimposed (e.g. Figure 38- h,i). For the MODIS match-ups (Figure 38) results show some dispersion of the data in all bands, more visible in the 667nm band (Figure 38-e). The RR53 agrees quite well with the *in situ* data (Figure 38-g), however the RR12 ratio shows a relevant bias (Figure 38-f). This bias impacts the water-type classification as sensor data fall below the threshold for Case 1 waters (red dots in Figure 38-g), while correspondent *in situ* data can still be within the Case 1 limits (black dots in Figure 38-g). In contrast, for the second condition (Rrs555_RR53) both datasets are in agreement. The same validation analysis was performed for SeaWiFS (Figure 39) with some relevant differences. The errors observed for the RR12 ratio seem to be restricted to a few data points (Figure 39-f,h), and not a generalized biased as seen for MODIS (Figure 38-f,h). This bias is more evident for lower values and is striking when compared to the small dataset collected in the GC2011 cruise (Figure 40-f). Twelve matchups were found with MODIS data for the cruise period and validation of radiometric data is shown in Figure 40.

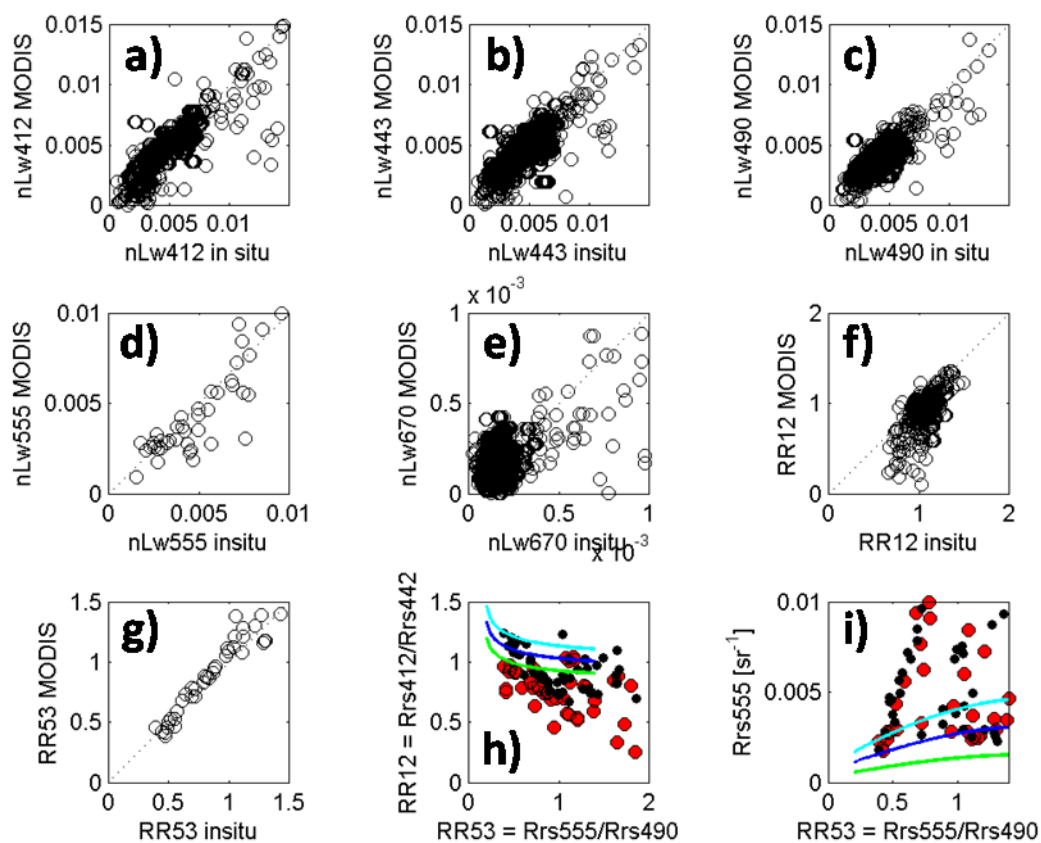


Figure 38 Validation of radiometric MODIS data with SeaBASS *in situ* database: for bands 412nm (a), 443nm (b), 488nm (c), 555nm (d) and 667nm (e). Validation is also performed for RR12 (f) and RR53 (g) ratios. Also presented are the sensor and *in situ* data results superimposed with Lee and Hu (2006) model for the RR12_RR53 condition (h) and the Rrs555_RR53 condition (i): *in situ* data in black, and sensor data in red.

Table IX Statistics of MODIS radiometric data comparison with the *in situ* SeaBASS database

MODIS	N	δ	Ψ	Δ	Slope	Offset	r^2	RPD (%)	APD (%)
nLw412	1232	-0.000	0.001	0.001	0.96	-0.000	0.69	-2.1	20.41
nLw443	3250	0.000	0.000	0.000	0.97	0.000	0.63	4.5	17.0
nLw488	3349	-0.000	0.000	0.000	0.89	0.000	0.66	-3.4	12.4
nLw551	51	-0.000	0.002	0.002	0.98	-0.000	0.88	-8.8	18.7
nLw667	2818	-0.000	0.000	0.000	1.02	-0.000	0.91	7.73	41.7
RR12	1175	-0.104	0.354	0.338	14.6	-14.7	0.05	-9.68	13.1
RR53	51	0.094	0.254	0.236	1.29	-0.19	0.77	8.25	13.4

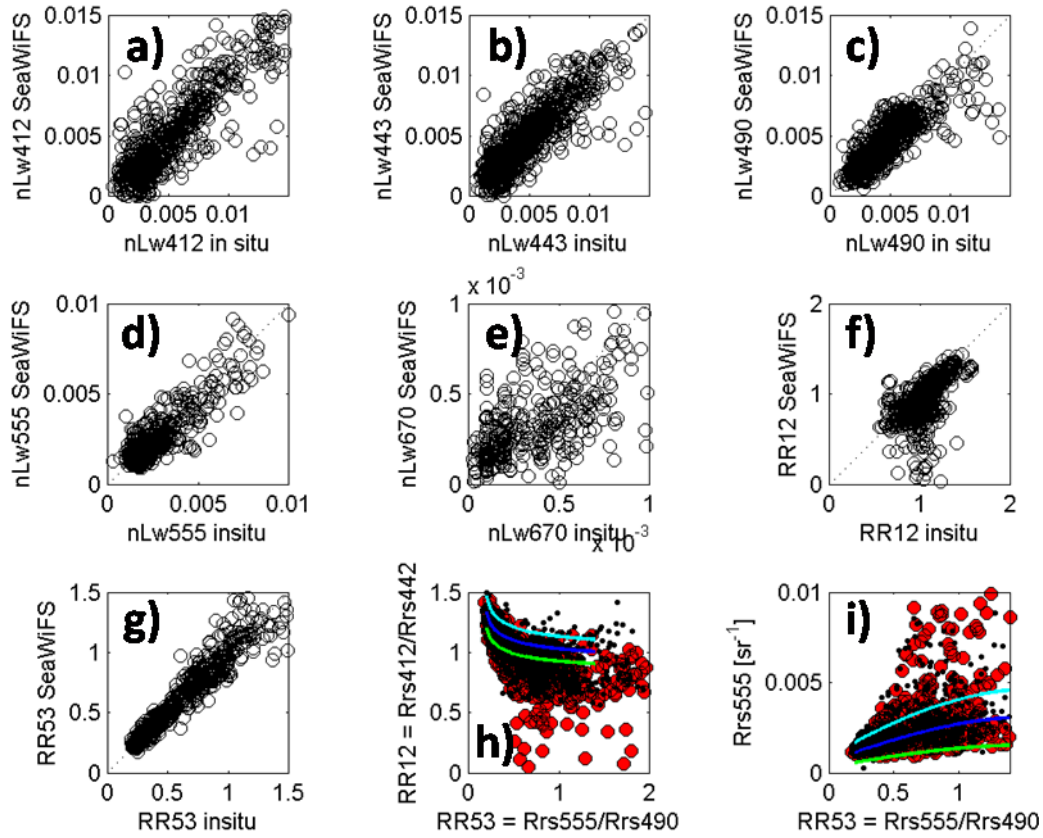


Figure 39 Validation of radiometric SeaWiFS data with SeaBaSS *in situ* database: for bands 412nm (a), 443nm (b), 488nm (c), 555nm (d) and 667nm (e). Validation is also performed for RR12 (f) and RR53 (g) ratios. Also presented are the sensor and *in situ* data results superimposed with Lee and Hu (2006) model for the RR12_RR53 condition (h) and the Rrs555_RR53 condition (i): *in situ* data in black, and sensor data in red.

Table X Statistics of SeaWiFS radiometric data comparison with the *in situ* SeaBASS database

SW	N	δ	Ψ	Δ	Slope	Offset	r^2	RPD (%)	APD (%)
nLw412	694	-0.000	0.002	0.002	0.93	-0.000	0.66	-1.8	35.3
nLw443	945	-0.000	0.002	0.002	0.91	0.000	0.68	0.37	26.6
nLw488	969	-0.000	0.002	0.002	0.79	0.000	0.73	-4.67	19.3
nLw551	709	-0.000	0.002	0.001	0.83	0.000	0.84	-2.44	21.8
nLw667	448	-0.000	0.001	0.001	0.86	0.000	0.83	17.9	55.7
RR12	695	-0.017	2.383	2.383	188	-197	0.01	-1.55	23.1
RR53	700	0.015	0.156	0.155	1.05	-0.02	0.87	3.07	11.2

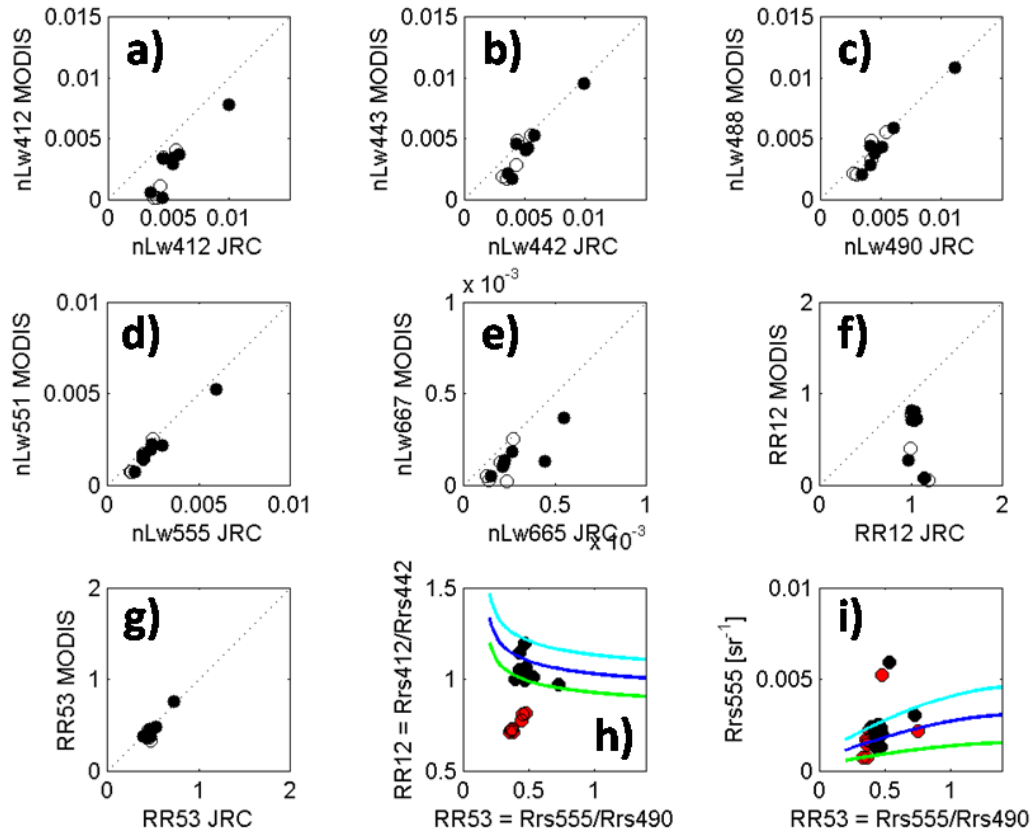


Figure 40 Validation of radiometric MODIS data with *in situ* data collected during the GC11 cruise: for bands 412nm (a), 443nm (b), 488nm (c), 555nm (d) and 667nm (e). Validation is also performed for RR12 (f) and RR53 (g) ratios. Also presented are the sensor and *in situ* data results superimposed with Lee and Hu (2006) model for the RR12_RR53 condition (h) and the Rrs555_RR53 condition (i): *in situ* data in black, and sensor data in red.

Table XI Statistics of MODIS radiometric data comparison with *in situ* data collected off the Portuguese coast (cruise GC11)

MODIS	N	δ	Ψ	Δ	Slope	Offset	r^2	RPD (%)	APD (%)
nLw412	12	-0.003	0.003	0.001	1.37	-0.005	0.81	-55.9	55.9
nLw443	12	-0.001	0.001	0.001	1.27	-0.002	0.89	-22.7	25.4
nLw488	12	-0.001	0.001	0.001	1.13	-0.001	0.94	-13.9	17.6
nLw551	12	-0.001	0.001	0.000	0.98	-0.000	0.96	-24.2	24.2
nLw667	12	-0.000	0.000	-0.000	0.75	-0.000	0.59	-51.8	51.8
RR12	12	-0.54	0.644	0.347	-6.7	7.6	0.42	-50.2	50.2
RR53	12	-0.05	0.069	0.045	1.35	-0.22	0.86	-11.7	12.3

For the GC11 cruise match-ups, the first two bands of MODIS underestimate the reflectance values, more markedly in the first band (i.e. 412nm). The RR12 totally fails to agree with the *in situ* RR12. However, and as seen for the SeaBASS database, the second condition shows good agreement between the datasets (Figure 40-i).

Based on this analysis, water-type classification based on the first condition is erroneous. This bias with RR12 ratio, although more evident, does not seem only associated to coastal stations (Figure 41).

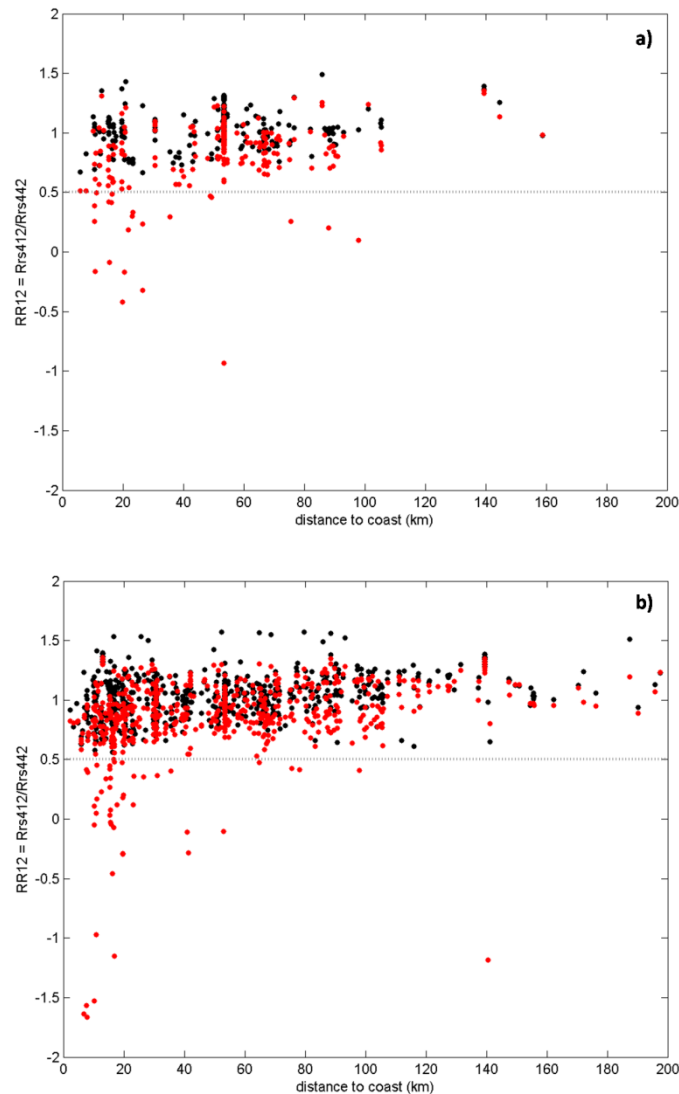


Figure 41 RR12 ratio variations with distance from coast (km)

Looking at the MODIS matchups retrieved for all the CO database, results reveal again low RR12 values, which are probably just an artefact of the atmospheric correction (Figure 42-a). The second condition seems, however, suitable for classification of Case 1 waters. We have to keep in mind that applying only this second condition, the total Case 1 waters will be overestimated,

as CDOM dominated waters might be included. Nevertheless, non-Case 1 waters due to high sediment particles in the water will be identified.

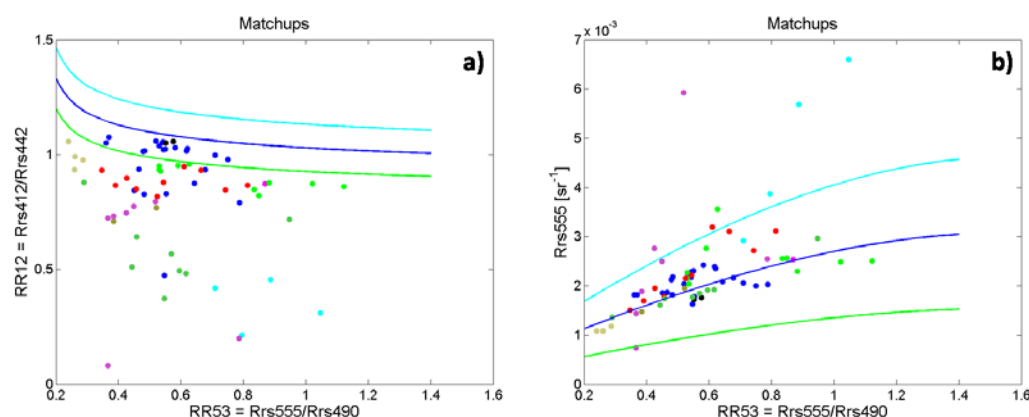


Figure 42 Radiometric MODIS match-ups with the CO database (n=75), for a 6h time window, plotted superimposed with the Lee and Hu 2006 model (lines). Colours refer to each cruise and are in accordance with Figure 11.

3.3.4 Temporal and Spatial variability of Case 1 waters

An overall analysis of the temporal and spatial variability of Case 1 waters was performed for the Portuguese region, over a period of 7 consecutive years, from 2005 to 2011. Results obtained after applying the first condition to classify Case 1 waters yielded high percentage of non-Case 1 waters, as seen in the previous sections. Given that it is considered to be a poor evaluation, these results were not considered in this analysis and are only presented in Annex II. Therefore, only the second condition was used to evaluate the temporal and spatial variability of Case 1 waters in this region (Figure 43). These results represent the percentage of pixels classified as Case 1 waters in the total number of images considered (daily images for 7 years). Higher percentages of Case 1 waters were always observed in open waters, except in Spring, where non-typical Case 1 waters were classified occasionally, i.e. with a frequency of 5 – 25% (Figure 42-a). Near the coast, the percentage of non-Case 1 waters is generally high (~50%) during autumn, winter and spring. In fact, during the winter, percentages of non-Case 1 waters could reach values of approximately 100%.

The variability of this classification was also assessed through an analysis of the standard deviation of data, for each season, over the 7-year period, from 2005 to 2011 (Figure 44). For offshore waters, the highest variability was found in the spring season, which is in accordance with the higher percentages of non-Case 1 waters found in Figure 43, indicating that spatial

distribution of these types of water are highly variable between years. This corresponds to a maximum standard deviation of ~20-25%.

In general, the highest standard deviations (Figure 44) were found where higher percentages of non-Case 1 waters were observed (Figure 43-44). As before, for non-Case 1 percentage, high standard deviations were also found near the shore for all seasons (Figure 44).

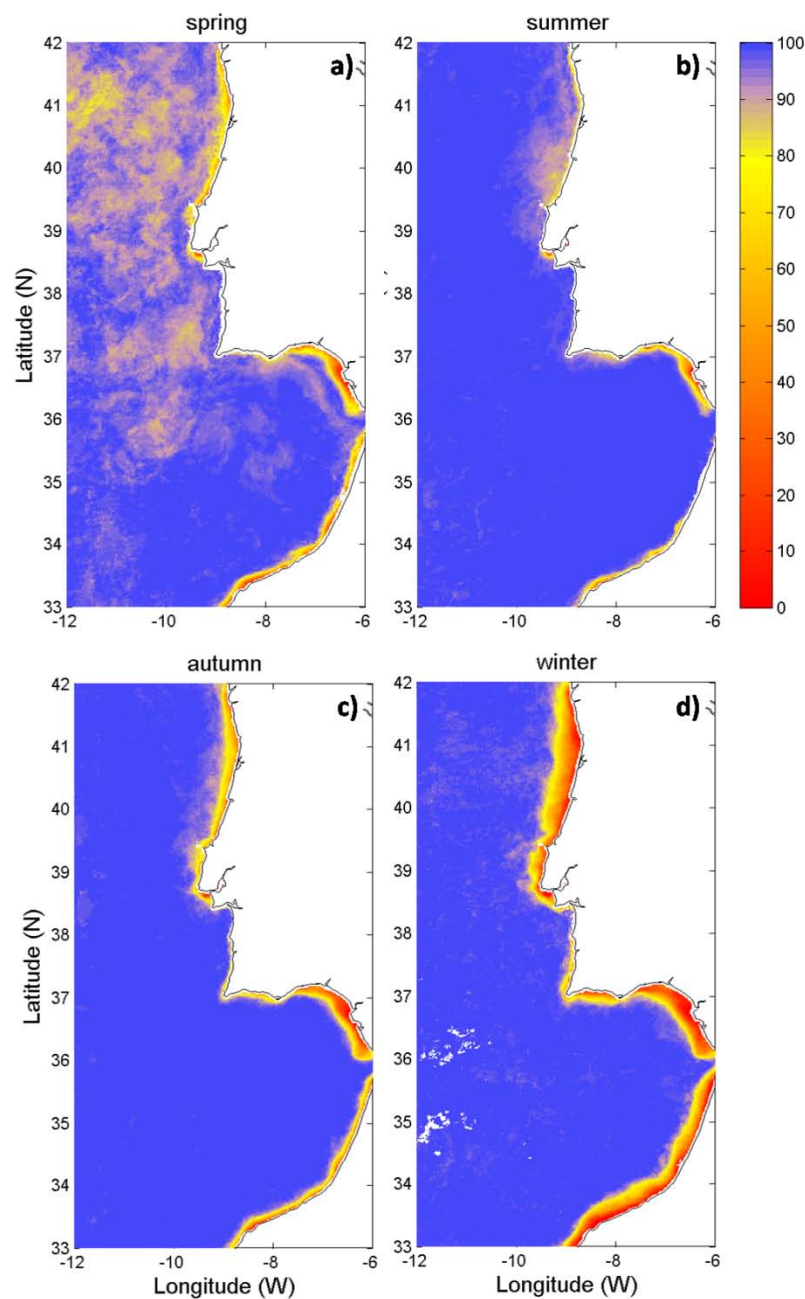


Figure 43 Seasonal maps of percentage of pixel classification as Case 1 waters according to Lee and Hu (2006) model conditions for the MODIS data for a 7 years period (2005-2011). The maps of the percentage that each pixel was classified as Case 1 for the analysed period applying only the Rrs555_RR53 condition for **a)** spring, **b)** summer **c)** autumn, and **d)** winter. Scale is in percentage (0-100%).

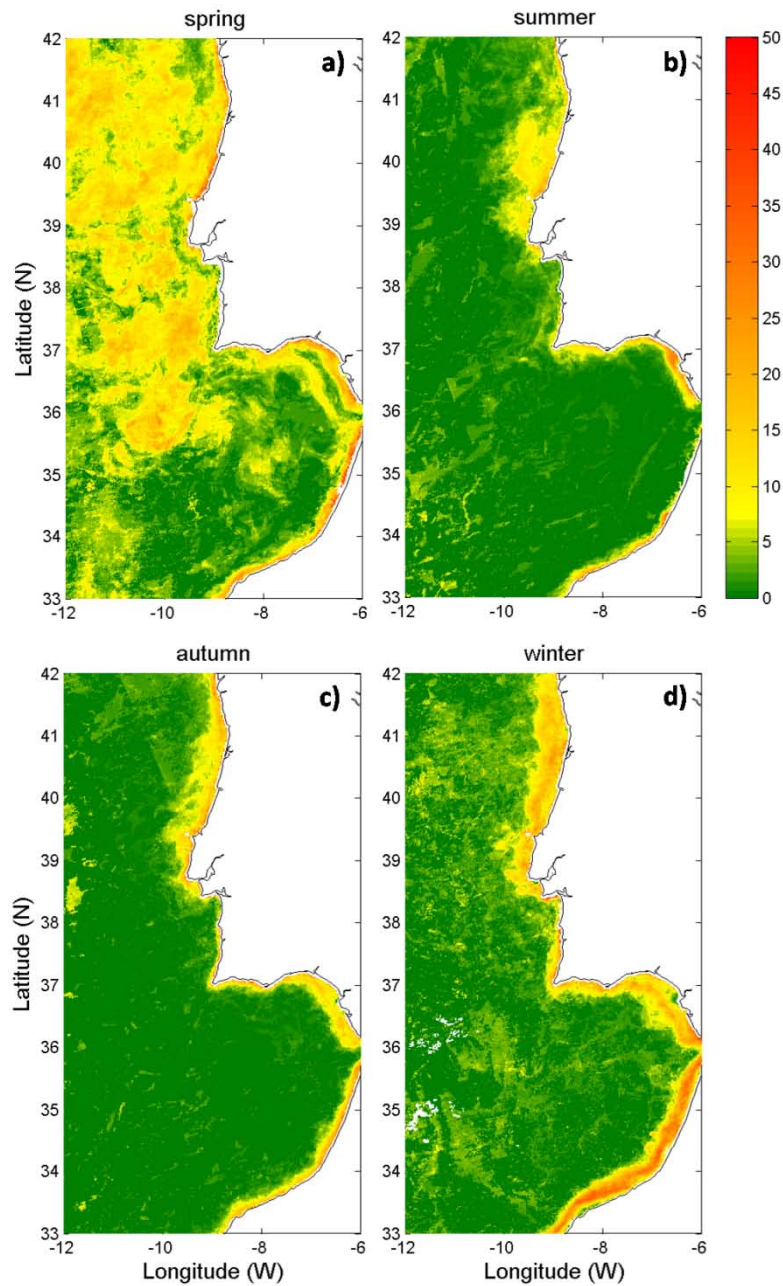


Figure 44 Maps of standard deviation of seasonal percentage of pixel classification as Case 1 waters according to Lee and Hu (2006) model (Rrs555_RR53 condition) for the MODIS data for a 7 years period (2005-2011). That is how variable are the pixels classified for each season of each year compared to the seasonal mean of the seven years for **a)** spring, **b)** summer **c)** autumn, and **d)** winter. Scale is in percentage (0-50%).

The second condition was also used to evaluate the variability of the classification of Case 1 waters in the Portuguese coastal waters throughout the years (Figure 44). This analysis was done including data from 2005 to 2011. It is possible to observe that summer is the season with the highest mean percentage of pixels classified as Case 1 waters, always higher than 96%. Winter is the season with the lowest percentage of pixels classified as Case 1 waters.

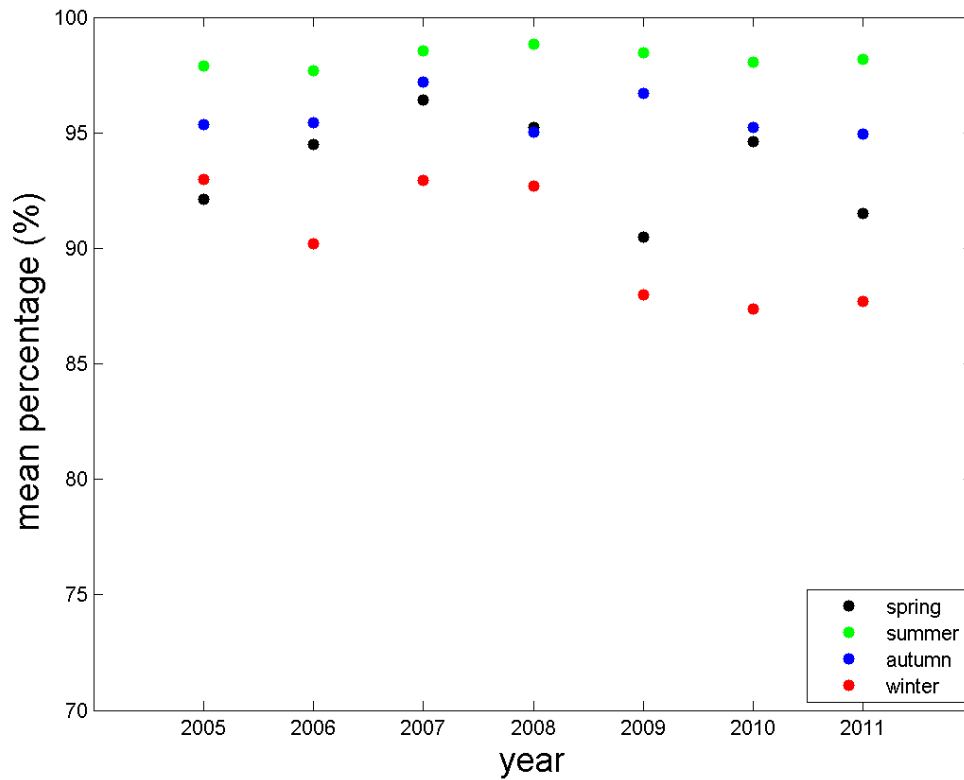


Figure 45 Mean percentage of total pixels between 2005 and 2011 for each season.

3.4 Factors affecting satellite percentage error

To have an insight on the factors affecting the Chl products accuracy, a set of parameters were considered to perform a multi-correlation analysis (Table IX). Parameters considered include: percentage error between sensor and *in situ* data (% error), reflectance ratio 412nm/443nm (RR12), reflectance at 555nm (Rrs555), index1 (Ind1), index2 (Ind2), index3 (Ind3), first optical depth ($Z_{1^{st}}$), distance to coast (D_{coast}), total chlorophyll (TChla), micro-sized fraction (*f_{micro}*), nano-sized fraction (*f_{nano}*), pico-sized (*f_{pico}*) and size index (SI). Indices 1,2,3 and SI are properly described in the Methods and correspond to equations 2.20, 2.21, 2.22 and 2.5, respectively.

For the MODIS match-up analysis, percentage error retrieved between the sensor and the *in situ* data are positively correlated to the Rrs555 and negatively correlated to biomass (TChla). Index 2 (Ind2) is positively correlated to the nano-sized fraction (*f_{nano}*), but negatively correlated with the pico-sized fraction (*f_{pico}*). The farther away from coast (i.e, increasing D_{coast}) a significant decrease in biomass is observed (TChla), with an increase in the nano-sized fraction of the phytoplankton community. Size-index (SI) is highly correlated to *f_{micro}*, as this parameter as a

high weight in its calculation (equation 2.5). First optical depth is highly inversely correlated to Chl, and positively correlated with %error.

For MERIS algal 1 matchups, error was found to be negatively correlated with RR12, Rrs555 and index 3. Similarly, was also negatively correlated to fpico and SI, but positively correlated to fnano (Table IX). Biomass (TChla) did not significantly correlate to algal 1 %error, but negatively correlated with MODIS and algal 2 %error data.

Algal2 product matchups, revealed error correlated negatively with RR12, and therefore also with Ind1 and Ind2. Distance to coast was negatively correlated with Rrs555 for all sensors, but only positively correlated with RR12 for algal 2 data.

Table XII Correlation matrices for MODIS and MERIS standard products matchups parameters. List of parameters evaluated include: percentage error between sensor and *in situ* data (% error), reflectance ratio 412nm/443nm (*RR12*), reflectance at 555nm (*Rrs555*), index1 (*Ind1*)*, index2 (*Ind2*)*, index3 (*Ind3*)*, first optical depth (*Z_1st*), distance to coast (*D_coast*), total chlorophyll *a* (*TChla*), micro-sized fraction (*fmicro*), nano-sized fraction (*fnano*), pico-sized (*fpico*) and size index (*SI*)*. Significant correlations appear in bold ($p < 0.05$). *see text for further details.

	%error	<i>RR12</i>	<i>Rrs555</i>	<i>Ind1</i>	<i>Ind2</i>	<i>Ind3</i>	<i>Z_1st</i>	<i>D_coast</i>	<i>TChla</i>	<i>Fmicro</i>	<i>fnano</i>	<i>fpico</i>	<i>SI</i>
MODIS													
% error	1.00												
<i>RR12</i>	0.09	1.00											
<i>Rrs555</i>	0.25	-0.09	1.00										
<i>Ind1</i>	0.11	-0.63	0.34	1.00									
<i>Ind2</i>	-0.12	-0.92	-0.14	0.62	1.00								
<i>Ind3</i>	0.17	-0.04	0.59	0.67	-0.05	1.00							
<i>Z_1st</i>	0.38	0.33	-0.53	-0.13	-0.06	-0.17	1.00						
<i>D_coast</i>	0.07	0.06	-0.46	-0.05	0.11	-0.23	0.53	1.00					
<i>TChla</i>	-0.38	-0.33	0.53	0.13	0.06	0.17	-1.00	-0.53	1.00				
<i>fmicro</i>	-0.15	-0.08	0.36	-0.06	-0.09	0.14	-0.52	-0.60	0.52	1.00			
<i>fnano</i>	0.14	-0.15	-0.28	0.16	0.24	-0.14	0.36	0.62	-0.36	-0.90	1.00		
<i>fpico</i>	0.15	0.49	-0.31	-0.21	-0.31	-0.07	0.59	0.15	-0.59	-0.57	0.26	1.00	
<i>SI</i>	-0.15	-0.10	0.37	-0.05	-0.08	0.14	-0.53	-0.59	0.53	1.00	-0.89	-0.59	1.00
	%error	<i>RR12</i>	<i>Rrs555</i>	<i>Ind1</i>	<i>Ind2</i>	<i>Ind3</i>	<i>Z_1st</i>	<i>D_coast</i>	<i>TChla</i>	<i>Fmicro</i>	<i>fnano</i>	<i>fpico</i>	<i>SI</i>
MERIS algal1													
% error	1.00												
<i>RR12</i>	-0.34	1.00											
<i>Rrs555</i>	-0.34	-0.26	1.00										
<i>Ind1</i>	0.12	-0.70	0.56	1.00									
<i>Ind2</i>	0.26	-0.85	0.16	0.76	1.00								
<i>Ind3</i>	-0.34	-0.02	0.66	0.49	-0.05	1.00							
<i>Z_1st</i>	0.28	0.51	-0.65	-0.56	-0.50	-0.27	1.00						
<i>D_coast</i>	0.31	0.25	-0.49	-0.35	-0.28	-0.23	0.53	1.00					
<i>TChla</i>	-0.28	-0.51	0.65	0.56	0.50	0.27	-1.00	-0.53	1.00				
<i>fmicro</i>	-0.60	-0.06	0.45	0.11	0.11	0.22	-0.65	-0.73	0.65	1.00			
<i>fnano</i>	0.59	-0.15	-0.40	-0.02	0.08	-0.31	0.42	0.67	-0.42	-0.86	1.00		
<i>fpico</i>	0.27	0.48	-0.38	-0.39	-0.49	-0.12	0.76	0.40	-0.76	-0.63	0.35	1.00	
<i>SI</i>	-0.60	-0.06	0.44	0.10	0.11	0.22	-0.65	-0.72	0.65	1.00	-0.86	-0.64	1.00
	%error	<i>RR12</i>	<i>Rrs555</i>	<i>Ind1</i>	<i>Ind2</i>	<i>Ind3</i>	<i>Z_1st</i>	<i>D_coast</i>	<i>TChla</i>	<i>Fmicro</i>	<i>fnano</i>	<i>fpico</i>	<i>SI</i>
MERIS algal2													
% error	1.00												
<i>RR12</i>	-0.27	1.00											
<i>Rrs555</i>	-0.03	-0.12	1.00										
<i>Ind1</i>	0.33	-0.63	0.54	1.00									
<i>Ind2</i>	0.25	-0.84	0.17	0.81	1.00								
<i>Ind3</i>	0.21	-0.13	0.77	0.69	0.23	1.00							
<i>Z_1st</i>	0.29	0.56	-0.57	-0.60	-0.62	-0.34	1.00						
<i>D_coast</i>	-0.14	0.49	-0.54	-0.59	-0.52	-0.50	0.59	1.00					
<i>TChla</i>	-0.29	-0.56	0.57	0.60	0.62	0.34	-1.00	-0.59	1.00				
<i>fmicro</i>	-0.14	-0.30	0.36	0.45	0.44	0.34	-0.62	-0.65	0.61	1.00			
<i>fnano</i>	0.08	0.14	-0.35	-0.37	-0.28	-0.42	0.44	0.63	-0.44	-0.90	1.00		
<i>fpico</i>	0.14	0.44	-0.26	-0.48	-0.56	-0.18	0.69	0.44	-0.69	-0.78	0.55	1.00	
<i>SI</i>	-0.15	-0.31	0.36	0.45	0.45	0.34	-0.62	-0.64	0.62	1.00	-0.89	-0.80	1.00

Chapter 4: Discussion

4.1 *In situ* dataset

In this section, different aspects of the phytoplankton pigment dataset will be considered. Discussion will focus on the applied methodologies and associated uncertainties, the representativeness of the dataset (i.e., temporal and spatial coverage) and its contribution to the current knowledge of the study site. This section intends also to provide a context for the validation analysis itself.

4.1.1 Chlorophyll *a* measurement uncertainties

Accuracy is telling a story truthfully, and precision is how similarly the story is repeated over and over again.

Accuracy and precision are the principal parameters for determining the performance of measurement methods. Although *in situ* data, in a validation exercise, are assumed to be the *truth*, these have also associated uncertainties. *In situ* data can be affected by several constraints related to equipment, operator, method or even natural variability of the parameter under analysis. Chlorophyll *a* (Chl) is a key monitoring parameter in oceanography and its *in situ* determination has long been subject of interest. Measurement methods (e.g., spectrometry, fluorometry) mainly rely on its capability of absorbing visible light in the blue and red part of the spectrum and emitting fluorescence in the red. However, Chl is inside phytoplankton cells that co-exist with other substances (e.g., sediments, detritus) that add difficulties to its *in vivo* measurement. Before laboratory *in vitro* quantification can be performed, filtration, storage and extraction procedures need to be undertaken. All of these have associated uncertainties. Phytoplankton pigments are very labile and, during these processes, degradation products can be generated. HPLC enables chemical separation (i.e. based on molecular polarity) and quantification of the pigments individually (i.e. even degradation products can be determined), allowing therefore a more accurate measurement. An accuracy for Chl in the order of <5% can be achieved with HPLC (Hooker et al., 2012). For satellite Chl validation activities, this has been the Space agencies' recommended technique. Several HPLC methods have however been developed and there is no external process or independent agency that certifies if an HPLC phytoplankton method is adequately performed. To understand method results comparability, evaluate uncertainties and promote method discussion, space agencies have organized round-robins. NASA's HPLC round-robins consist in the distribution of batches of samples identically processed to participants, who analyse them with their HPLC method and report the obtained

results for comparison. Our research centre (Centre of Oceanography, CO) participated in the round-robin SeaHARRE-5 in 2010. For the SeaHARRE-5, filtered field samples were collected in the coast of New England (USA) and Tasmania and were distributed to the ten participant laboratories (Hooker et al., 2012). In addition, a set of ampoules with a DHI pigment mixture were also distributed. These latter samples can be directly injected in the HPLC, avoiding the filter extraction processing. The comparison of the results obtained with the two sets of samples allows understanding the difference between extraction and instrument uncertainties. Reference value is calculated with results of the quality assured laboratories (i.e., Danish DHI Institute of Water, Environment and Health; NASA's Goddard Space Flight Centre; Laboratoire d'Océanographie de Villefranche; and the American Horn Point Laboratory). Statistical results obtained by each Laboratory, for each set of samples, were compared between each other and to the reference laboratory values, which always presented minimum percent errors.

Percentage of coefficient of variation for Chl pigment, obtained for the tested CO method (only C8 method was tested), was 8.8% for the field samples (results for the other laboratories varied from 4.1 % reference laboratory values, to 12.6%) and 1.4% for the pigments mixture (minimum 0.1% and maximum 8.7% for all the methods tested). The absolute percentage of differences (APD) for field samples was on average 18.5% (minimum 3.3% and maximum 33.6% for all the methods tested) and 6.3% for pigments mixture (minimum 0.1% and maximum 9.7% for all the methods tested). These results indicate that CO is just within the range of variation found for the other laboratories working with HPLC technique to assess phytoplankton pigments. According to these results, the uncertainty of the CO method is associated to the extraction method rather than to the HPLC method itself. In fact, the only participant using the same method of CO obtained % errors for the pigments mixture in the same range (i.e. 1.3% coefficient of variation and 6.5% for APD). However, this laboratory obtained better results for the filtered field samples (i.e. 8.2% and 6.3%). This laboratory uses acetone instead of methanol for pigments extraction and results of the laboratories used to calculate the reference values, all use acetone as extractor.

Tests conducted for establishing the CO method concluded that pigments extraction with acetone underestimated chlorophyll- c2 and pheophorbide-a, while methanol extraction underestimated pheophytins a and b-carotene (Cartaxana and Brotas, 2003). For long extraction times (6– 24 h), methanol generally yielded lower pigment concentrations, possibly due to isomerization and/or pigment degradation and acetone would be a better option if long extraction times were used. However, for shorter extraction times, methanol was more efficient

in extracting Chl (Figure 1 in Cartaxana and Brotas, 2003). CO method uses a 1h extraction time, and therefore methanol was the chosen solvent. There is, however, no ideal method for pigment extraction and results depend on several factors such as the phytoplankton community present in samples, or even operator.

After participation in the SeaHARRE-5, some updates were introduced in the CO method, namely the control of column temperature (25°C), the use of longer extraction times (30 min to 1 h), and the inclusion of an internal standard (trans- β -apo-8'-carotenal) (see Table IV).

To guarantee consistency and comparability of the HPLC results, a quality control based on the proportion of Chl and accessory pigments (adapted from Aiken et al., 2009) was applied. Only 50 samples were excluded, however, overall classification of cruises was variable (Table VI). Best results were obtained for cruises (i.e., PG06 and GC09) with smallest number of samples and conducted on a restricted temporal and spatial coverage. The worst results were found for the Cs monitoring program which spanned throughout a year (i.e. samples from different seasonal conditions). The dispersion of data may be only the result of the variability of the medium conditions as pigment composition of phytoplankton communities are highly variable and pigments proportions are dependent on several environmental parameters (e.g., light, nutrients availability; Ruivo et al., 2012). Pigment information can therefore contain ecological information (e.g., herbivory, light conditions, cell conditions). This analysis is out of the scope of this thesis, and specific analysis have been addressed elsewhere (e.g. Mendes et al., 2011).

4.1.2 Geographical and temporal coverage

A total number of 770 water samples were kept after quality control of HPLC pigment data. Chl values ranged between 0.013-10 mg m⁻³. These concentrations are representative of the variability observed along the coast throughout the year (Moita 2001), where maximum values are found in spring/summer during upwelling events. More than 50% of the samples were collected during summer season, with approximately 25% of the samples collected in late summer (i.e., early September). Samples collected during spring and late winter amounted to ~20% each. Interestingly, the highest Chl values were registered in late winter GC10 cruise during an upwelling wind-regime (Guerreiro et al., 2013). Upwelling has been identified as the major source of seasonal and spatial variability of phytoplankton in the Portuguese coast, associated with nutrient availability to the euphotic zone and alterations of the water column stability (Moita, 2001; Silva et al., 2009). Generally, the west coast of Portugal is characterized by

a strong and seasonal upwelling, determined by the coastal morphology, the continental shelf/upper slope bathymetry and local winds (Fiúza, 1983). Sustained upwelling conditions are generally observed from April to September, when persistent northerly winds occur (Fiúza et al., 1982), while advection of warmer oligotrophic oceanic waters is observed during autumn and winter, when southerly winds dominate, leading to downwelling conditions and an intensification of waters flowing poleward (Fiúza et al., 1982; Peliz et al., 2005). However, episodes of reverse winds can occur during both periods. In general, wind forcing circulation interacts with topography and coastline orientation, modifying the along-shore and cross-shelf flows at different levels, resulting in amplification and/or reduction of upwelling-downwelling (Kudela et al., 2005; Ryan et al., 2005).

A total of seven cruises were undertaken in one of the three afore mentioned upwelling centres (section 1.3, p35), around Capes Espichel and Carvoeiro, where high SST front probability (local SST gradient $>0.1^{\circ}\text{C Km}^{-1}$) were reported by Relvas et al. (2007). Persistent upwelling generates a clear contrast between the coastal cold, vertically mixed upwelled waters, and the warmer oceanic stratified waters (i.e. SST front). The maximum front probabilities were found in the vicinities of cape Carvoeiro, in the southern edge of the Nazaré canyon axis. As seen in Figure 16, eutrophic waters were mostly found near the coast, extending offshore at the Cape Carvoeiro region. Trophic status in this area was however variable, depending on time of sampling (i.e., season and year). More than 60% of the collected samples were within the Nazaré area by means of along- and across-coast transects. These transects can cover both coastal nutrient-rich eutrophic waters and offshore oligotrophic waters.

Other sampled oligotrophic areas included the Gorringe seamount, (i.e GC09 cruise), which is located in the Atlantic Ocean, around 125-150 miles west of Portugal between Azores and the Strait of Gibraltar (Alteriis et al., 2003) and is considered to be an oligotrophic region due to its low nutrient and biomass concentrations (Mendonça et al., 2012).

The areas south of Cape Carvoeiro and Cape Sao Vicente are characterized by major changes in coastline orientation, in clear contrast with the straight coast off Aveiro, where cruises NR06, HS10 and HS11 took place. The relatively weak upwelling signal on the outer shelf off Aveiro, and the low probability of fronts indicate that this area, together with the areas south of Capes Espichel and Sao Vicente, where some of the CSA stations were located, is retentive for biogenic material with small offshore advection (Relvas et al., 2007). The other CSA stations and Cs monitoring stations in the Bay of Lisbon, where NR05 cruise took place, are between the Capes Espichel and Carvoeiro strongly influenced by upwelling events, as mentioned. This area is also

influenced by the Tagus river outflow. It is important to note that all samples from Cs were taken during the ebb/high tide period to reduce the river influence.

A considerable amount of different areas was covered, from oligotrophic to eutrophic, with a clear dominance of samples collected in mesotrophic conditions (Figure 14). All seasons are included (e.g. weekly monitoring station) with predominance of samples collected during summer conditions. Several oceanographic conditions are therefore covered and dataset is considered well representative of variability present along the Portuguese coast.

It should be noticed that the Chl threshold used for classification of the oligo-, meso- and eutrophic waters (i.e., $\text{Chl} < 0.25 \text{ mgm}^{-3}$, $0.25 < \text{Chl} < 1.2 \text{ mgm}^{-3}$ and $\text{Chl} > 1.2 \text{ mgm}^{-3}$, respectively) is just conventional. These definitions are generally ecologically more complex (Claustre et al., 1994; Tett et al., 2007) and vary regionally due to natural Chl variability. The threshold used is based on Aiken et al. (2009), who reported data for the Atlantic ocean. Although similar, other authors have used slightly different thresholds. For example, Bricaud et al. (2004), classified oligotrophic waters when $\text{Chl} < 0.2 \text{ mg m}^{-3}$, mesotrophic when Chl values were between 0.2 and 2 mg m^{-3} , and eutrophic waters those with $\text{Chl} > 2 \text{ mg m}^{-3}$.

4.1.3 Contribution to current knowledge

The present analysis is the first comprehensive phytoplankton pigment dataset reported for the Portuguese coast. The compiled dataset was collected to comprise a representative spatial and temporal coverage of the coast, focusing mainly on its western part. Starting point objective was to collect useful data for satellite product validation and algorithm development activities, but that would also allow better understanding phytoplankton dynamics off and along the coast. By collecting information on a set of pigments rather than only Chl, the interpretation of phytoplankton dynamics can be pursued at a community level instead of biomass as a whole.

The phytoplankton classification, either based on size or function, has already been discussed in section 1.2.1 and caveats of the use of pigments as taxonomical markers have been introduced in section 1.2.2. Uncertainties related to the pigment-based size-class assignment, are due to two factors: on the one hand, the diagnostic pigments used are not all unique to the phytoplankton taxa with which they are mostly associated. For example fucoxanthin, the proxy for diatoms, is present in other classes such as coccolithophores, pelagophytes or chrysophytes; peridinin is not present in all dinoflagellate species and many picoeukaryotes contain

fucoxanthin and 19'-hexanoyloxyfucoxanthin (Roy et al., 2011). On the other hand, some phytoplankton taxa, which typically belong to a certain size class, may have species that belong to other classes. For example, diatoms, which are classified as microphytoplankton, have species belonging to nanophytoplankton. Some of these smaller diatoms (e.g. *Pseudonitzschia* spp. and *Thalassiosira* spp.) have been reported as common species from the study area (Mendes et al., 2011; Oliveira et al., 2009b; Silva et al., 2008; Silva et al., 2013). Nonetheless, pigments-based taxonomy has been validated for the study area (e.g. Mendes et al., 2011, Silva et al., 2008). In the Bay of Lisbon (Cs monitoring station), Silva et al. (2008) have reported fucoxanthin, peridinin and 19'-hexanoyloxyfucoxanthin as good indicators for diatoms, dinoflagellates and coccolithophores, respectively, with synchronized seasonal variations and significant positive correlations. Mendes et al. (2011), using the pigment data of DC06 cruise, proved the usefulness of relying in pigment analysis to study spatial distribution of phytoplankton groups in relation to a complex physical environment, the Nazaré canyon area. They have identified an area of high concentration of peridinin pigment with the presence of chain-forming toxic dinoflagellates. Furthermore, Brotas et al. (2013) using data from cruises GC09, NR05, PG06, DC06 and GC10, together with additional data from the Northeast Atlantic, were able to regionalize and validate the size-class model presented by Brewin et al. (2010). The model presented by Brotas et al. (2013) made further progress by estimating cell numbers in the studied area, producing maps of phytoplankton cell abundances. The authors combined a model for partitioning total chlorophyll-a into size classes based on diagnostic pigments (i.e. Uitz et al., 2006), with cell abundances measured using flow cytometry or microscope counts for large cells, to infer intracellular pigment concentrations. The results were consistent with values from the literature, hence providing some indirect validation for the pigment-based method. This reinforces the suitability of the use of Uitz et al. (2006) for size-index classification at the Portuguese coast.

Brewin et al. (2010) model applied at a global scale indicated dominance of micro-sized phytoplankton at Chl concentrations $> 1.3 \text{ mg m}^{-3}$, however, the regionalized version (Brotas et al., 2013), for the Eastern Atlantic, indicated higher (>50%) micro-sized fraction for much lower Chl concentrations threshold (i.e. $> 0.5 \text{ mg m}^{-3}$). These values are in agreement with the present dataset (Figure 16-b). For both model versions, nanoplankton fraction was higher than the picoplankton fraction for Chl levels $> 0.2 \text{ mg m}^{-3}$, which is also in agreement with this dataset (Figure 16-b). Differences in Chl levels obtained for microplankton dominance (i.e. diatoms and dinoflagellates) are probably related to optimal conditions available for their growth in coastal areas, where nutrient from river outflows and/or upwelling events promote their growth. For instance, nutrients seem to be mostly of riverine origin in the Cs monitoring station. By analysing

weekly collected samples during a year, Silva et al. (2008) concluded that silicates and phosphates were highly correlated to the Tagus river runoff. The seasonal variation of Chl was coincident with the seasonality of total phytoplankton with maxima occurring throughout the year, and major Chl peaks matching those of diatoms microscopic counts. Highest Chl value observed was 0.916 mg m^{-3} . For the Western coast in general, Moita (2001), identified coastal upwelling as the major source of seasonal and spatial phytoplankton abundance variability and assemblage composition.

In contrast to the coastal areas, small phytoplankton in open ocean are known to be common and often abundant (Sieracki et al., 1993), with micro-sized phytoplankton growth only taking place when optimum conditions occur. In the North Atlantic, according to classical theory (Sverdrup, 1953), the phytoplankton bloom is initiated when positive heat fluxes in spring cause a stratification of the water column that allow phytoplankton cells to remain enough time in optimum light conditions to compensate their respiration losses and grow. During the bloom, phytoplankton typically grow rapidly, reaching high Chl values. Sieracki et al. (1993) reported an increase in Chl from 0.5 mg m^{-3} to $> 2.5 \text{ mg m}^{-3}$ at 46°N , 18°W in a cruise conducted in 1989. Once diatoms deplete the silica nutrient, there is a shift in the phytoplankton community to small flagellates. At a global scale, micro-sized plankton can therefore be associated to high Chl levels. However, when including very coastal data, these Chl levels decrease for the presence of micro-phytoplankton. In fact, for the present dataset, maximum size index ($\text{SI} > 45$ out of 50) can be observed for a high range of Chl values (~ 0.1 to 10 mg m^{-3} ; Figure 18). This indicates that even those samples with Chl concentration of approximately 0.1 mg m^{-3} can be almost 100 % dominated by micro-phytoplankton. This coastal dataset contrasts with other oceanic water datasets, as the ones presented by Bricaud et al. (2004), where only Chl concentrations $> 2 \text{ mg m}^{-3}$ are associated with SI values higher than 45, i.e. with almost 100% micro-phytoplankton dominance. This dataset is therefore a relevant contribution not only to the knowledge of phytoplankton dynamics off the Portuguese coast, but also for understanding the constraints of the application of bio-optical models to regional and coastal areas. Bio-optical models' limitations can be identified by their application to such a dataset and improvements can then be performed, providing an important contribution to ocean-colour applications. In addition, limitations of these optical models can also provide insight on the specificities of the studied area and contribute for a better assessment of regional oceanographic events (Brito et al., 2013).

4.2 Match-ups

This section is focused on the results of the validation exercise. Constraints of the match-up analysis will be considered, and the integrated comparison of the Chl products statistical results will be analysed. The regional influence in the overall products performance will be discussed.

4.2.1 Analysis constraints

Match-up analysis need to be constrained to the temporal and spatial windows necessary to guarantee contemporaneity of *in situ* samples and satellite passage, and spatial comparison adequacy (see also section 2.3.2). A considerable amount of factors can affect the quality of a match-up (e.g. satellite viewing angle, time of satellite passage, presence of clouds, abnormal atmospheric correction, etc.). Application of quality flags to the satellite data reduces the amount of possible matchups but is the only way to guarantee its quality. Temporal and spatial restrictions are a trade-off between a perfect match and the number of match-ups necessary to perform statistical evaluation of results. Two different time-windows were considered in this analysis (< 3h and < 6h), which was restricted to standard products of two sensors. MODIS and MERIS were selected for being the operational sensors providing better resolution and covering all the time period of the *in situ* dataset. SeaWiFS standard data was excluded from the analysis as the mission ceased in December 2010 and only 4 km resolution data were available. However, CCI product, in the novel products tested, includes SeaWiFS data (see section 2.2.2.2).

As mentioned in methods section, match-ups were not retrieved on a single pixel analysis. A multi-pixel box approach was used to allow for the generation of simple statistics to assist in the evaluation of spatial stability, and homogeneity at the validation point. Average value of a 3x3 pixel box was calculated and only considered valid if variation coefficient of pixels was < 25 %.

For the initial 770 *in situ* samples available, the highest number of retrieved matchups was 139, for the CCI product, which is a combination of three sensors data, i.e SeaWiFS, MODIS and MERIS. This increases the amount of valid data available both temporally and spatially, even restricting match-ups to a 3h time window. All other products had less than 80 match-ups for a 6h time window. This low number of match-ups reflects the quality constraints of the satellite data and the fact that *in situ* samples were collected in limited periods of time.

Radiometric data were available for one cruise (i.e. GC11), with a limited number of retrieved matchups (i.e, 12 for MODIS). This small match-up dataset was compared to nLw MODIS data, and atmospheric correction is discussed in section 4.3.1, but limited the statistical validity of comparison results. Direct testing of the algorithms (i.e. without the atmospheric correction effect) was therefore not permitted. However, application of different algorithms to the same radiometric data can provide clues on their performance. Both MODIS and MERIS radiometry data were used to compare standard and regional products. Five of the evaluated products are directly computed from MERIS radiometric data (i.e. standard algal 1 and algal 2 algorithms and novel CoastColour neural network and QAA algorithms, and MLP_ATLP). Only two of the evaluated products are derived from MODIS radiometry (i.e. the standard OC3m and the MLP_ATLP). It should be noticed that algorithm regionalization is also constrained by limited radiometric dataset collected in GC11 cruise (i.e 68 optical stations) as it does not incorporate the necessary seasonal and/or spatial variability.

Location of match-ups, obtained for each product, differed from one another, meaning that the direct comparison of algorithms performance for the same samples is limited. In fact, no *in situ* sample was identified to have a valid match-up for all the analysed products. This means that performance of some Chl products is evaluated based on a different sub-set of the *in situ* data. Even though, for a 6h time window, comparison between standard MODIS and MERIS algal 1 product was possible (i.e. 13 match-ups) and both MERIS products were also compared (35 match-ups). It is remarked that the algal 1 and algal2 products are determined from fully independent processing, which explains the different number of match-ups. Algal 2 was designed to be applicable also in coastal waters and therefore the number of match-ups is considerably higher.

4.2.2 Assessment of algorithms effectiveness

To understand how the different Chl products compare with the *in situ* data, a set of statistical parameters was computed. All products were tested against the correspondent *in situ* match-ups and summary statistics are presented in Table VII. A suite of metrics was selected, since no single metric covers all the attributes of uncertainties needed to be characterized.

Selection of these metrics was based on: 1) metrics that have been commonly used in the literature, to facilitate comparisons with other work; 2) the need to separate random and systematic components of errors.

As a measure of the spread of the data, as compared to the best agreement, Root Mean Square Error (RMS, Ψ) was selected. It is commonly-used (IOCCG, 2006; Bailey and Werdell, 2006) for measuring errors or uncertainties, and it is often recommended for model – observation inter-comparisons in Earth Sciences. The interpretation of RMS is facilitated if the data (both observations and estimates) have normal distributions. In fact, it is known that bio-optical variables such as Chl approach a normal distribution when the data have been log-transformed (Campbell, 1995; Gregg and Casey, 2004). Uncertainty estimates were calculated with log-transformed data, except for the mean relative and absolute percentage of differences (RPD and APD), which were not transformed so that its interpretation could be more intuitive, given that the units of the other statistics are decades of log and are not easy to interpret.

As a measure of accuracy, bias (δ) was calculated. The bias is defined as the residual offset that remains when positive and negative errors are cancelled against each other (average off-set). RPD gives an estimate of the uncertainty as a function of the *in situ* value and can be thought as a relative bias. It is the mean percent of differences between satellite and *in situ* measurement normalized with the *in situ* measurement values. APD, as RPD, is the mean of the differences between the satellite estimate and the *in situ* measurement, weighted on the measured Chl value. Contrastingly, although the differences can be either positive or negative, it does not give any information about the direction of discrepancy, as it is the mean of the absolute values of the differences; it represents a sort of relative RMS.

The unbiased RMS (URMS, Δ) was also calculated (see section 2.5, equation 2.11). This parameter describes the error of the estimated values with respect to the measured ones, regardless of the average bias between the distributions, that is, it is the component of the total RMS not due to the bias. It is related to Ψ and δ according to $\Psi^2 = \Delta^2 + \delta^2$.

To analyse the correlation between the measurements, a Type-2 regression model was used to compute the slope and intercept of a linear equation relating the log-transformed *in situ* and satellite derived Chl concentrations. Type-1 regression typically assumes that the dependent variable (*in situ* data) is well known, when in reality the *in situ* data are also affected by uncertainties (e.g. problems with *in situ* data sampling techniques as discussed in section 4.1.1) that are difficult to quantify. Therefore, Type-2 regression was adopted (Glover et al., 2011, MATLAB function `lsqfitma.m`), which minimizes residual variance in both x and y dimensions, rather than in the y dimension only (as in Type-1 regression). The slope, intercept and the coefficient of determination (r^2) were obtained using this Type-2 regression model. The coefficient of determination indicates the overall degree of linear association between the log-transformed *in situ* and log-transformed satellite estimates, but it is not a measure of the algorithm performance by itself. Thus, the slope (closer to 1), the intercept (closer to 0) and the mentioned statistics are used to evaluate the performance of the tested algorithms.

Although match-ups retrieved for the different algorithms may be different, statistics on algorithm performance are assumed representative for the studied area.

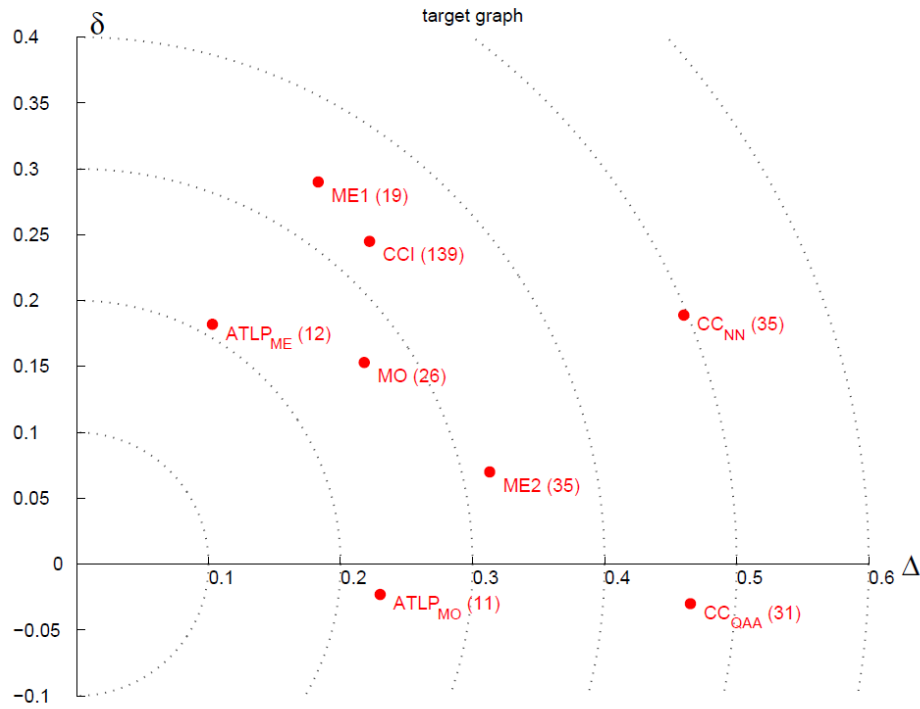


Figure 46 Target diagram for the relation of each Chl product with their correspondent *in situ* match-ups. ATLP_{ME} and ATLP_{MO} correspond to the regionalized version of MLP algorithm for the Atlantic off Portugal, calculated using MERIS and MODIS radiometric data, respectively. MO is the standard MODIS product; ME1 and ME2 are the MERIS algal 1 and algal 2 products; CC_{NN} and CC_{QAA} are the CoastColour products based on the Neural Network algorithm and the QAA algorithm. CCI is the product produced by the CCI project. URMS (Δ) is plotted in the x-axis, and bias (δ) in the y-axis. Dotted lines are isolines of RMS (Ψ), as according to equation $\Psi^2 = \Delta^2 + \delta^2$.

For better visualization and inter-comparison of results, summary statistic diagrams were used (i.e., target and Taylor diagrams). Target diagrams (Jolliff et al., 2009) are efficient in summarizing information about error by plotting URMS (Δ) and bias (δ) together (Figure 46). This diagram gives further information on the RMS (Ψ), which is the distance from the point of origin as determined by the relation $\Psi^2 = \Delta^2 + \delta^2$ (dotted lines in Figure 46). This means that the Chl products with better comparable results in relation to the *in situ* data will appear closer to the origin.

The Chl products which compared better with the *in situ* data were the regionalized MLP for the Atlantic Portuguese coast (ATLP). Specific results for MODIS and MERIS radiometric inputs indicate that ATLP_{MO} has low and slightly negative bias whereas ATLP_{ME} has higher positive bias, but smaller URMS. These differences may arise from the fact that sensor match-ups differ, but are in accordance to the results presented in Figure 30, where coincident match-ups of MODIS

and MERIS reveal an underestimation of MODIS in comparison to MERIS. ATLP results were however based on a very small match-up dataset.

For the other novel products tested, CoastColour had the worst URMS results; nevertheless, the QAA version had low negative bias. QAA CoastColour product version performed better than the NN one. CCI product had similar results to the standard MODIS and MERIS products, however, with more robust statistics as number of match-ups were much higher. MODIS standard product agreed better with the *in situ* data results than the algal1 MERIS product, but had more bias in comparison to the MERIS algal 2 product.

The Taylor diagram (Taylor, 2001) is used hereafter to summarize and discuss the correlations observed between the Chl products tested and the *in situ* data. Taylor diagrams specifically provide an illustration of the following parameters: 1) the level of correlation between the series of elements, 2) a comparison of their respective standard deviation, and, 3) the URMS (Figure 47). The *in situ* series of reference is represented on the x-axis of the 2-D diagram by the standard deviation. To allow comparison of the different algorithms performance, this standard deviation was normalized for the reference (i.e., the *in situ* data) so that the *in situ* data converged to the value 1 on the abscissa (black star in Figure 47). The datasets to be compared are represented by a point situated at the radial distance from the origin equal to the normalized standard deviation and the cosine of the angle between this radial and the x-axis is the correlation coefficient (r) between the datasets. The distance between the reference and the dataset point is, by construction, the URMS (see Taylor, 2001 for further details). In practice, the closer a dataset point is located with respect to the reference, the similar it is to the *in situ* data.

Concerning the parameters displayed in the Taylor diagram, both CoastColour products presented higher standard deviation compared to the reference. In fact, these were the products with the highest standard deviations. CoastColour products are also the less correlated to the reference. Best products were the MERIS algal1 and MODIS standard products, the CCI and the ATLP computed with MERIS radiometry data. The latter was the product with best correlation and URMS. MERIS algal2 and the ATLP computed with MODIS radiometry were less correlated than this group, to the *in situ* reference.

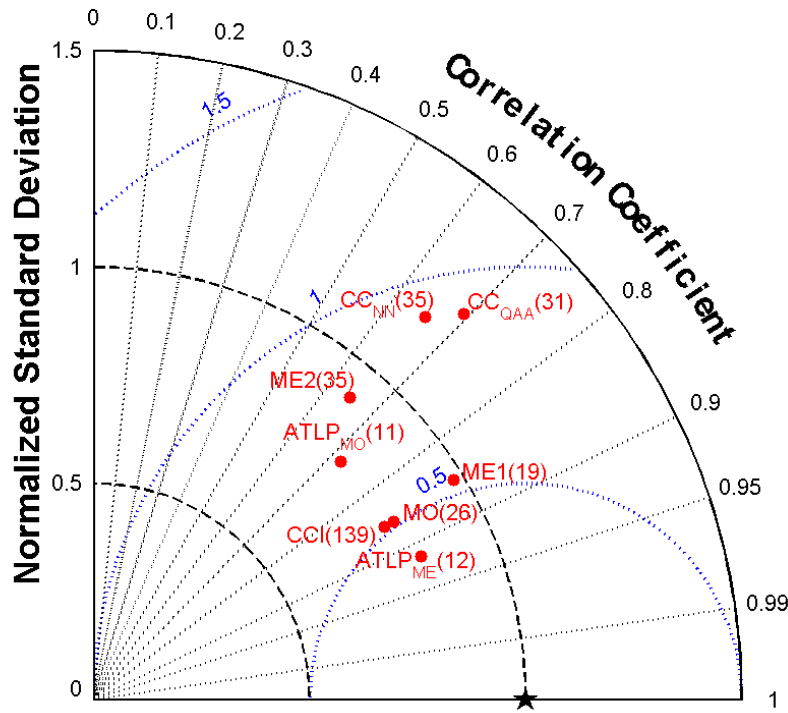


Figure 47 Taylor diagram for the relation of each Chl product with their correspondent *in situ* match-ups. $ATLP_{ME}$ and $ATLP_{MO}$ correspond to the regionalized version of MLP algorithm for the Atlantic off Portugal, calculated using MERIS and MODIS radiometric data, respectively. MO is the standard MODIS product; ME1 and ME2 are the MERIS algal 1 and algal 2 products; CC_{NN} and CC_{QAA} are the CoastColour products based on the Neural Network algorithm and the QAA algorithm. CCI is the product produced by the CCI project. Normalized standard deviation is plotted in the x-axis, and the angle corresponds to the correlation coefficient. Dashed black lines are isolines of normalized standard deviation, dotted black lines are correlation coefficient isolines and dotted blue lines are isolines of URMS (Δ).

Both diagrams have shown a better performance of MODIS standard product in comparison to the MERIS algal 1. Mean relative and absolute percentage differences (Table VII) revealed overestimation by both sensors, but approximately half the error for the MODIS product. As an example, MODIS RPD for a 3h time window was +57 % while RPD for MERIS algal 1 product was +111%. MERIS algal 1 algorithm has a semi-analytical component; however it is empirically based as MODIS OC3M. Differences in the *in situ* data used to derive the algorithms coefficients may be responsible for the results observed but are more likely to do with dissimilarities at the radiometry level. Zibordi et al. (2013), in a validation exercise for the European seas, also reported a major overestimation of Chl (i.e. +131%) for algal1 MERIS product in the range of approximately $0.05\text{--}20 \text{ mg m}^{-3}$. Similar results were retrieved by these authors for algal2 products. In the present analysis, however, overestimation was found significantly smaller for the algal 2 product (i.e +42% for a 3h time window).

Zibordi et al. (2013) explain the algal1 product Chl overestimation by the negative bias observed when comparing the *in situ* nLw data with the MERIS retrieved nLw. For the 3rd MERIS reprocessing data, these authors reported a 23% underestimation of the 443/560 band-ratio by the MERIS radiometric product. This underestimation is seen by the Chl standard algorithm as the presence of more phytoplankton absorbing in the blue range of the spectrum, resulting in an overestimation of the Chl product. Radiometric differences arise from the atmospheric correction. Both aerosol optical thickness at 869 nm and the Angstrom exponent α appear overestimated, leading to dissimilarities in the determination of the aerosol type and to an overestimate of the atmospheric radiance contribution to the top-of-atmosphere signal, with more pronounced effects at the blue bands (Zibordi et al., 2013). For the MODIS radiometry data, only a slight overestimation (i.e. +4%) is reported for the equivalent band-ratio (i.e., 443/547).

Dogliotti et al. (2009), in a validation exercise in the Patagonian Continental Shelf, showed a general underestimation of MODIS Chl standard product over the whole range analysed (i.e. - 32%), however with local differences. These differences reported for different areas emphasize the need for a regional validation, before any routine use of a satellite product. Volpe et al. (2007) found the need to develop an algorithm for the Mediterranean Sea, being able to achieve +3% of RPD with a regionalized empirical algorithm. Here, it is also presented an algorithm specially tuned for the Portuguese coast (MLP_ATLP), which provides the lowest relative and absolute percentage of differences of all the tested products (Table VII). Using MODIS and MERIS radiometric products, ATLP generated products with better performances than the standard satellite products. Results were further improved when restricting the novelty index to < 3 . This result emphasizes the need to account for the application limits of the algorithms, so that only reliable data is made available. It should be noticed that MLP_ATLP is an empirically derived NN algorithm trained with local surface *in situ* Chl data. Errors related to integrated Chl for the first optical depth (i.e. Chl “seen” by the satellite), or regional specificities of phytoplankton pigment absorption properties or/and other optically active substances are incorporated in the algorithm.

With respect to CoastColour, tested products provided very different performance results despite having the same atmospheric correction. Both QAA and NN CoastColour are inversion scheme algorithms which were developed to derive IOPs from the water-leaving radiances (AOPs). They however differ in its basis. CoastColour NN bio-optical model has to be trained with *in situ* data, and the QAA is an algebraic algorithm with theoretical fundamentals of hydrological

optics included, semi-analytically derived (IOCCG, 2006). CoastColour NN is therefore constrained by the range and specificities of *in situ* data used to train the bio-optical model, while the QAA algorithm should be applicable in any region. In an inter-comparison exercise (IOCCG, 2006), both the standard NN (algal2, Doerffer and Schiller, 2007) and the QAA algorithms (Lee et al., 2002 and Lee et al., 2005) were tested for their capability of retrieving IOPs correctly. Both algorithms were tested against a simulated dataset, with QAA and NN providing similar results for the total absorption, but QAA providing significantly better results for the absorption of the phytoplankton and CDOM components (IOCCG, 2006). CoastColour version of these algorithms was here compared against the same *in situ* match-ups dataset, number of match-ups only differing due to invalid data of QAA for four match-ups, which were valid for the NN algorithm. Better Chl agreement with the *in situ* data obtained with the QAA product version also confirms its capability to better determine the phytoplankton absorption at 442nm in comparison to the NN version.

The results of the comparison of each product against *in situ* data have been presented as a whole. However, *in situ* match-ups may vary with Chl product under analysis. This means that statistics may be affected by specificities of the different sampling area included in the match-ups. A regional analysis is conducted and is discussed in the following section.

4.2.3 Regional analysis

CoastColour algorithms had only a difference of four in the number of match-ups, which were retrieved as invalid for the QAA algorithm. The cruise contributing with more match-ups for these products was DC07 (in the Nazaré canyon) (Figure 48 a-b). The NN algorithm seems to work particularly well in the Bay of Lisbon (NR05 cruise), but showed poor performance in three cruises (GC10, GC11 and DC07), all in the Nazaré canyon area. Looking at Figure 22 a-b, it can be seen that the match-ups from these cruises are scattered, but only two match-ups (one for GC11 and one for DC07) are highly biased. These match-ups had also high bias for the QAA version (Figure 48-a), which might indicate errors at the radiometric level. Samples from the GC10 cruise have *in situ* values of Chl > 10 mg m⁻³, and corresponded to a winter upwelling event reported in Guerreiro et al. (2013). These samples corresponded therefore to particular oceanographic upwelling conditions with probably high phytoplankton absorption, and phytoplankton community dominated by diatoms and coccolithophores (Guerreiro et al., 2013), which may be

affecting the algorithms performance. Algal 2 also had low performance for the match-ups of this cruise (Figure 50-b).

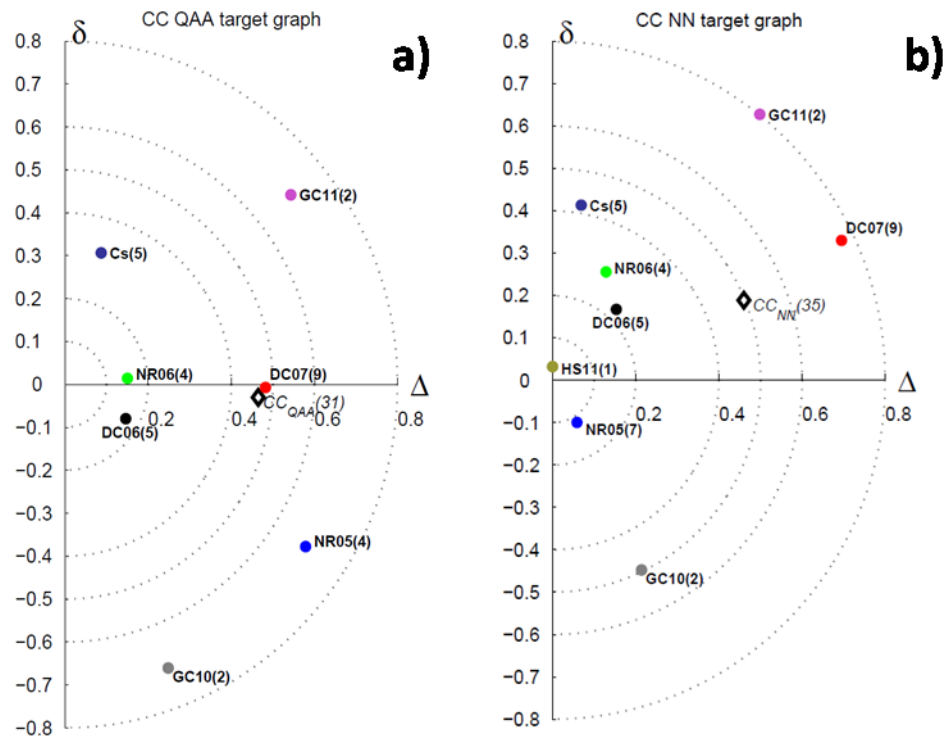


Figure 48 Target diagram for the relation of CoastColour QAA (a) and NN (b) Chl products with their correspondent *in situ* match-ups. Average is presented by an open black diamond and results obtain for each cruise are in colour according to Figure 11. Number of match-ups is presented in parenthesis.

MODIS performance was about the same for all cruises which had more than one match-up (Figure 49-a), except for DC06, where it performed worst for one of the match-ups (Figure 19 a-b). This particular match-up is negatively biased but no special conditions could be related to this result.

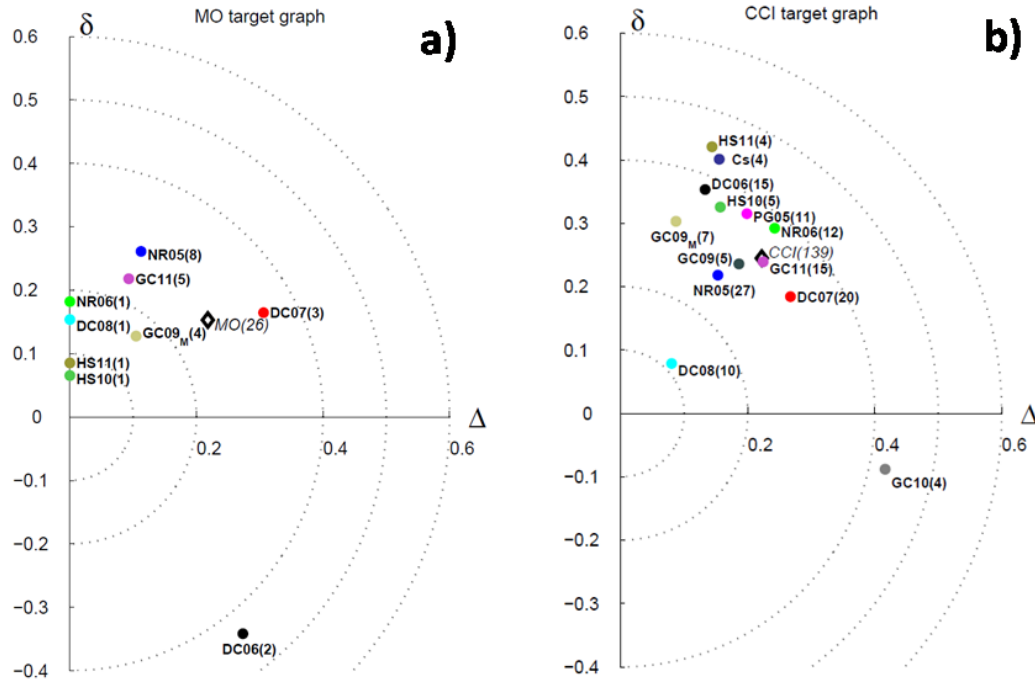


Figure 49 Target diagram for the relation of MODIS **(a)** and CCI **(b)** Chl products with their correspondent *in situ* match-ups. Average is presented by an open black diamond and results obtain for each cruise are in colour according to Figure 11. Number of match-ups is presented in parenthesis.

CCI had also uniform performances for all cruises, although underestimated for GC10 upwelling conditions and was particularly good in matching Chl values for the DC08 cruise (Figure 49-b). The retrieved matchups for this cruise correspond to a very restricted Chl range $\sim 0.3 \text{ mg m}^{-3}$ (Figure 28), which may be within the optimal performance range of the algorithm.

MERIS algal1 performed worst for the match-ups in the Aveiro area, which corresponded to the match-ups with higher Chl concentrations (Figure 50-a). Algal2, in contrast, performed very well for this region, but failed to match-ups the GC10 Chl values, as already mentioned. Atmospheric correction problems may be the cause for algal1 bias in the Aveiro area, as in the ATLP MERIS version, novelty index < 3 eliminates these match-ups, as well as DC08, from the comparison (Figure 51-b). This may be an indication of abnormal nLw data. The fact that algal2 product has better performance also supports this argument, as algal2 and algal1 have independent atmospheric correction procedures.

ATLP MERIS version performs uniformly for all matched-up cruises; however the MODIS version (Figure 51-a) retrieved values with higher bias for the DC07 cruise than the MODIS standard version and gives similar poor results for the DC06 cruise, both cruises located in the Nazaré area.

This regional analysis is very important to understand how the various algorithms perform in the different conditions included in the dataset, and reveals that overall statistics may be affected by poor performance for only one specific cruise. This analysis also gives indication of the areas of optical interest, and areas where sampling effort should be directed to. The Nazaré canyon area, being an area oceanographically very dynamic, reveals different algorithm performances for different cruises in the region, and is identified as an area of interest for algorithm validation. For validation purposes, areas where temporal or spatial optical variability throughout the year is highest, are preferable as to obtain a validation dataset covering the widest dynamic range of optical variability possible (IOCCG, 2009).

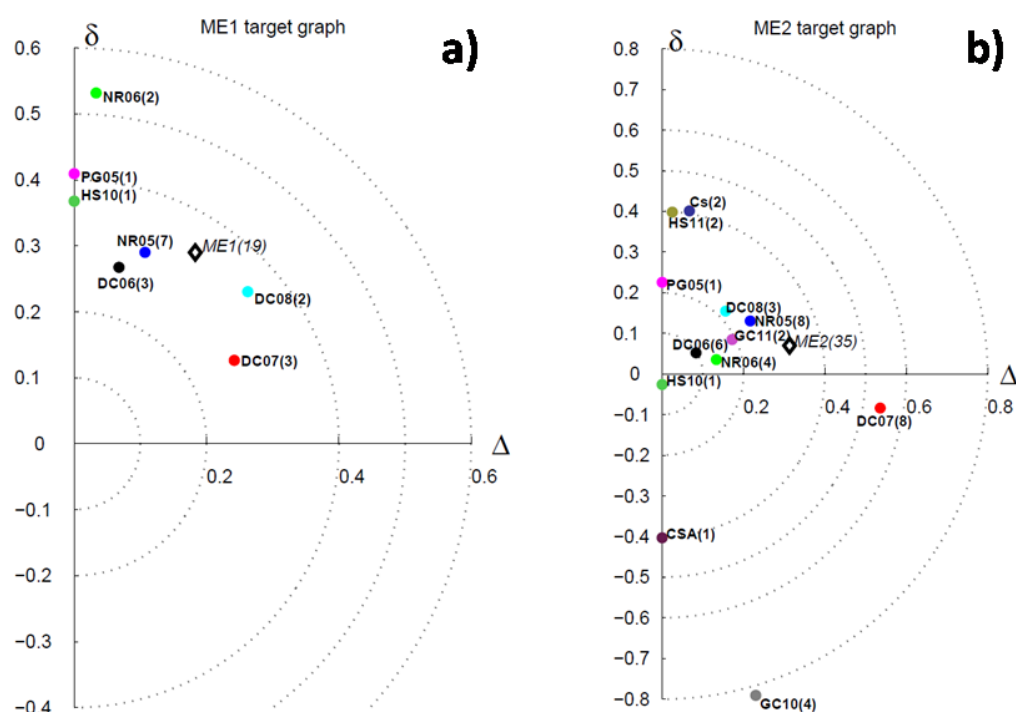


Figure 50 Target diagram for the relation of MERIS algal1 **(a)** and algal2 **(b)** Chl products with their correspondent *in situ* match-ups. Average is presented by an open black diamond and results obtain for each cruise are in colour according to Figure 11. Number of match-ups is presented in parenthesis. Note the different scales.

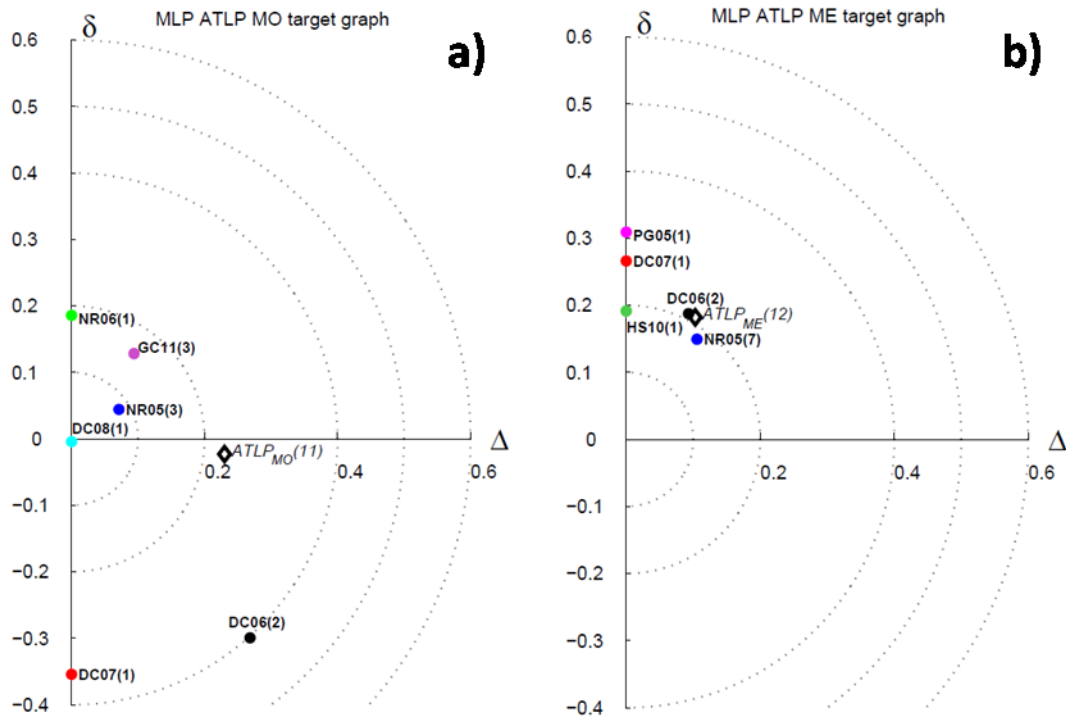


Figure 51 Target diagram for the relation of MLP_ATLP MO (a) and ME (b) Chl products (novelty index < 3) with their correspondent *in situ* match-ups. Average is presented by an open black diamond and results obtain for each cruise are in colour according to Figure 11. Number of match-ups is presented in parenthesis.

4.3 Assessment of water typology: case 1 vs non-case 1 waters

Commonly, Case 1 waters are those whose inherent optical properties (Preisendorfer, 1976) can be adequately described by phytoplankton (represented by chlorophyll concentration, or Chl), whereas Case-2 waters are otherwise (see section 1.1.2). In this section the implications of water typology on algorithm performance will be discussed. The results obtained regarding the optical properties of the study area will be analysed, and the limitations of water-type classification using a remote sensing model will be considered. Focus will be given to the atmospheric correction constraints. The spatial and temporal distribution of water type in the study area will then be interpreted.

4.3.1 Implications of water typology

It is widely accepted that a universal bio-optical algorithm applicable for all water types is not feasible (IOCCG, 2009). The historic example is the difference between Case-1 and Case-2 waters (Morel and Prieur 1977; IOCCG 2000). In Case-1 waters, the optical properties are dominated by phytoplankton, whereas in Case-2 waters the optical properties are governed by other constituents, such as suspended sediments and/or coloured dissolved organic matter (see also section 1.1.2). In the recent decades, many bio-optical models, remote-sensing algorithms for Chl retrieval, and applications in ocean-colour remote sensing have been developed specifically for Case-1 waters (e.g., O'Reilly et al., 1998; Morel and Maritorena, 2001). Algorithms specifically developed for Case-1 waters often fail or return inaccurate retrievals in Case-2 waters. Among Case-2 waters, however, there are many different substances that affect the optical properties of the waters. The optical properties of these substances can further vary regionally. Thus, different Case-2 algorithms have been derived for local waters, or for specific environmental regimes such as CDOM dominated or sediment-dominated waters (IOCCG, 2009). In fact, there has been a lot of effort devoted to developing Case-2 algorithms, as demonstrated by projects like CoastColour. However, a single ocean-colour image scene, can display multiple water types with differing optical properties, which in turn require different algorithms. A first attempt to classify waters based on optical characteristics with the subsequently objective of selecting and blending different bio-optical algorithms was presented by Moore et al. (2001). The approach is based on a fuzzy logic classification scheme applied to the satellite-derived water-leaving radiance data, and was tested using an ocean-colour satellite image of the northwest Atlantic shelf. Local *in situ* bio-optical data were used by the authors to characterize optically-distinct water classes *a priori* and to parameterize algorithms for each class. More simple approaches, can rely on simple case1, non-case1 classification (Lee and Hu, 2006), or, as proposed by D'Alimonte et al. (2003), to determine solely the applicability range of the algorithm in use. Both these latter methods were here tested for the study area. D'Alimonte et al. (2003) method of novelty detection was included and tested in the MLP-ATLP algorithms. As mentioned, this method is based on the assumption that the level of accuracy of the algorithm output depends on the representativeness of inputs in the training dataset. The obtained results with an algorithm can therefore be supported by its range of applicability. A novelty index < 3 was here selected (D'Alimonte et al., 2013). This novelty index filter was applied successfully, revealing improved algorithm performance results (Table VII). However, this method does not provide a water-type distribution perspective. In order to generate maps of water typology (i.e., Case1 and non-case1 water) for the studied area, Lee and Hu (2006) model was used. This model, which is

an inclusive Case 1 water criterion applied to remote sensing reflectances, is based on the latest bio-optical models for Case1 waters developed from extensive measurements (Morel and Maritorena, 2001). This criterion implies two conditions, one based on the CDOM abundance per Chl expected in typical Case 1 waters, and the other based on the suspended sediments abundance per Chl. Both conditions were used here to provide a distribution perspective of Case1 waters and its seasonal variations for the study area.

At present, the use of optical classification schemes to refine and constrain ocean-colour radiometric algorithms is a topic of ongoing research and requires specific attention to ensure awareness and applicability of the method (IOCCG, 2009). Use of satellites for coastal monitoring requires regular validation of data products (e.g. Zibordi et al., 2006) and, in operation, characterization of the water type under observation to ensure appropriate algorithms are used. Ideally, concurrent measurements of both optical properties (absorption and scattering) and Chl are required to map the distribution of Case-1 waters. The mapping of water-type classification may help understand algorithms applicability and restrict areas of algorithm applicability

4.3.2 Understanding regional optical properties

Recently, coastal ocean optics have been the topic of numerous studies (e.g. Babin et al., 2003; Tilstone et al., 2005; Groom et al., 2009; Vantrepotte et al., 2007), highlighting that bio-optical measurements at regional scale are a crucial step in improving the accuracy of coastal bio-optical algorithms. *In situ* radiometric data were collected during the GC11 cruise, which allowed to optically characterize the sampling area.

The total absorption coefficient is affected by the presence of both suspended and dissolved material in water, and its decomposition into its different components allows the monitoring of phytoplankton and the remaining absorbing materials (see also section 1.1.2). A ternary plot (Figure 31), although not providing absolute values of the absorption coefficients, is a useful method for identifying a water mass and its associated absorption process. By defining the percent contribution of each of the components, a water mass can be defined by which component controls the absorption budget (IOCCG, 2006). Arnone et al. (2004) emphasize that the absorption parameters are very sensitive to biological and chemical processes and can be related to different biogeochemical processes.

Freshwater inputs are assumed to be the major source of CDOM in coastal waters, although biological sources have also to be considered (e.g. from phytoplankton and/or bacterioplankton). The CDOM absorption and spectral signature can change over time and space, in relation to its composition and origin, with processes such as bacterial degradation, photodegradation, coagulation or selective sedimentation (see Vantrepotte et al., 2007 and references therein). In certain cases, phytoplankton may also represent the main contributor to the overall absorption in coastal waters, generally associated to the establishment of optimal conditions for phytoplankton growth (e.g. upwelling events). Suspended sediments absorption tends to be seasonal (Vantrepotte et al., 2007).

Ternary plot in Figure 31, reveals dominance of CDOM absorption (>60%) for the analysed samples, with some contribution of suspended sediments (<40%) and phytoplankton absorption (<50%). These results evidence the presence of riverine origin substances, and/or generated in biological degradation processes. The contribution of sediment absorption reveals the sedimentary dynamic component of the Nazaré canyon region. Quaresma et al. (2007) report the importance of internal waves activity in summer in the resuspension of sediments in the area. Additionally, strong semi-diurnal bottom currents occur in all parts of the canyon, particularly in its upper and middle sections (commonly exceeding 30 cm s^{-1}) which, along with the ample supply of fine-grained sediments from the shelf, result in the permanent haze of suspended matter in the upper canyon (De Stigter et al., 2007). It should be noticed the short time and spatial scale of the presented absorption results. In the South coast of Portugal, for three stations analysed seasonally from 2008-2012, Icely et al. (2013), reported highly variable results, reflecting probably the temporal scale, even though with ~40% of the samples having been also considered CDOM absorption dominated waters. However, reported results, revealed residual contribution of suspended sediments. Samples were classified as either CDOM or phytoplankton absorption dominated waters. Their study area is located at the extreme southwest coast, where no river plumes are observed and coastal drainage from the coastal region is restricted to occasional rainstorms (Goela et al., 2013). CDOM is therefore likely of biological origin, but analysis of these results is still subject of undergoing research. Phytoplankton blooms are frequent in the area, especially from spring to late summer, when favourable north westerly and westerly winds promote upwelling events (Relvas and Barton, 2002). Phytoplankton absorption absolute values reported by Goela et al. (2013), at 440nm, for a two year period (2008-2009) varied between 0.010 and 0.152 m^{-1} , comparable to the values determined for our area, which varied between 0.012 and 0.081 m^{-1} at 442 nm. Absorption coefficient of CDOM and suspended sediments during GC11 cruise, varied between 0.022-0.17

m^{-1} and $0.008\text{-}0.089 \text{ m}^{-1}$, respectively. Absolute values from the South coast were not available for comparison, but Groom et al. (2009), for the L4 monitoring station in the English Channel, at 440 nm and a two year period (2003-2004), reported similar CDOM absorption coefficients (i.e. $\sim 0.02\text{-}0.2 \text{ m}^{-1}$), but highly variable suspended sediment absorption coefficients (i.e. $\sim 0.0026\text{-}0.112 \text{ m}^{-1}$). In comparison to the various European seas (Zibordi et al., 2011), averaged phytoplankton absorption data retrieved in the West coast of Portugal (0.033 m^{-1} at 442nm), is comparable to the averaged values obtained for the Ligurian Sea ($0.050 \pm 0.048 \text{ m}^{-1}$) and the northern Adriatic Sea ($0.052 \pm 0.034 \text{ m}^{-1}$). Results were higher compared to the Eastern Mediterranean Sea ($0.007 \pm 0.005 \text{ m}^{-1}$) and lower compared to the Baltic, the Eastern English Channel or the Black Sea ($0.193 \pm 0.254 \text{ m}^{-1}$, $0.124 \pm 0.067 \text{ m}^{-1}$ and $0.156 \pm 0.202 \text{ m}^{-1}$, respectively). CDOM and suspended sediments absorption coefficients found for GC11 cruise, at 412nm, 0.1 and 0.038 m^{-1} , respectively, were also comparable for the Ligurian ($0.092 \pm 0.056 \text{ m}^{-1}$ and $0.038 \pm 0.029 \text{ m}^{-1}$) and northern Adriatic Seas ($0.131 \pm 0.056 \text{ m}^{-1}$ and $0.075 \pm 0.091 \text{ m}^{-1}$). CDOM and suspended sediments absorption coefficients were also higher than those found for the Eastern Mediterranean Sea ($0.047 \pm 0.117 \text{ m}^{-1}$ and $0.009 \pm 0.003 \text{ m}^{-1}$), and lower than the ones found for the Baltic ($0.391 \pm 0.181 \text{ m}^{-1}$ and $0.106 \pm 0.138 \text{ m}^{-1}$), the Eastern English Channel ($0.252 \pm 0.162 \text{ m}^{-1}$ and $0.083 \pm 0.048 \text{ m}^{-1}$) and the Black Sea ($0.281 \pm 0.162 \text{ m}^{-1}$ and $0.055 \pm 0.098 \text{ m}^{-1}$). It should be noticed that data collected for the various European basins were gathered from 2000-2009, during several cruises (Zibordi et al., 2011). The limited dataset collected for the western Portuguese coast, during the GC11 cruise, although representative of the sampling area is both spatially and temporally restricted.

Remote sensing data were analysed with the Lee and Hu (2006) model to have an overview of the water typology distribution in the considered study area. This scheme was originally applied to SeaWiFS ocean-colour data. However, because the final goal was to infer on how the water type could affect the performance of the Chl algorithms, the model was applied to MODIS sensor data. As sensors have slightly different wavelength bands, water typology classification results were mapped using both sensors data for 2005 (Figure 33-35) in order to compare differences (Figure 36-37 and Table VIII). Water typology classification was performed using only one of the Lee and Hu model conditions (columns b and c in Figure 34 and 35, for MODIS and SeaWiFS, respectively), and using both conditions (column d in Figure 34 and 35, for MODIS and SeaWiFS, respectively). Classification maps are presented as the percentage that each pixel was considered as Case 1 for the analysed period.

Maps of water type classification, for both sensors, and all applied classification schemes, revealed seasonal variations. The classification scheme using both conditions is mainly driven by the results obtained by the first condition, as classification is based on a “one out, all out” rule and show overall classification of the waters as non-case 1 waters. This is particularly evident during winter and spring. The models identify the water as having more CDOM per Chl than typical Case 1 waters, and this might be due to the presence of biogenic material (in Spring as degradation of phytoplankton blooms and of riverine origin in winter), however, overall spread and presence at some degrees away from the coast, may indicate atmospheric problems in the first two bands (RR12) of both sensors. Case 1 waters were only identified in southern and offshore regions during autumn and summer seasons. For SeaWiFS, Case 1 waters were identified in the same regions in summer, autumn, as well as in winter. On the contrary, the application of the second condition only, which relies on the thresholds imposed on the ~555 nm band, indicate that non-case 1 waters were only present closer to coast, and mainly in the northern portion of the coast, for all seasons. Exception is seen in spring, when northern off-shore waters are classified as having more sediment load per Chl than typical case 1 waters. The coastal non-case 1 waters were particularly evident in the winter season, northern to Cape Espichel, where the influence of the outflow of the main Portuguese rivers is evident (i.e, Minho, Douro, Mondego and Tagus rivers). For MODIS, this analysis was performed from 2005-2011 (figures presented in annex II). Classification patterns were found quite stable and similar to the ones described for 2005, however, high pattern variability was observed for the spring season.

Differences between MODIS and SeaWiFS water-type classification maps, obtained by the application of the first and second model conditions, were mapped. Classification using MODIS data underestimated case 1 waters in comparison to the maps using SeaWiFS data for the first condition (Figure 36). This underestimation was mainly seen in off-shore regions, during winter and summer seasons, but more evident in winter, when atmospheric correction problems due to cloud presence may be more frequent. In contrast, for the second condition, classification using MODIS data overestimated case 1 waters in comparison to the classification maps provided using SeaWiFS data (Figure 37). This overestimation was observed for off-shore waters in spring and summer seasons, and for coastal waters in autumn and winter seasons. The contrasting differences observed, for the two classification schemes, indicated that atmospheric correction accuracy is both sensor- and wavelength-specific. Atmospheric correction will be further discussed in the following section.

4.3.3 Water typology remote sensing model constraints: atmospheric correction

The model of Lee and Hu (2006) makes use of radiometric ocean-colour data to provide a practical Case 1/non-Case 1 water classification. This classification uses remote sensing reflectance data at four different wavelengths to describe theoretical case 1 water optical properties. Both 412/443 (RR12) and 555/490 (RR53) Rrs band-ratios and Rrs555 are used to characterize the case 1 typical variations. As explained in the methods chapter, the RR12 ratio is used as a measure of CDOM per Chl, Rrs555 as a measure of particle backscattering and RR53 is viewed as a measure of Chl. This means that accurate radiometric data are needed at the four bands used (i.e., 412 nm, 443 nm, 490 nm and 555 nm). Applicability of this model to remote sensing data can therefore be compromised by incorrect atmospheric correction at these bands.

Atmospheric correction is the term usually used to refer the process of removal of the signal component that reaches an ocean-colour sensor that is not the water-leaving signal. This component to be removed is approximately 90% of the visible radiation observed by earth-viewing satellite sensors (Franz et al., 2012). It includes the sunlight radiation reflected by air molecules and aerosols in the atmosphere (see Figure 3 in section 1.1.1) and other contributions associated with light reflected by the ocean surface that does not interact with the water column and thus carries no information on the concentrations of water column constituents. Being the water-leaving contribution such a small component of the total observed radiance, Rrs(λ) retrievals from sensors are very sensitive to errors or inconsistencies in the atmospheric correction algorithm and the sensor calibration. In fact, 1% error at this stage can be translated into a 10% difference in the water-leaving reflectance, which can result in even larger differences in derived geophysical parameters, e.g., Chl (Franz et al., 2012).

SeaWiFS and MODIS data share a common atmospheric correction code (i.e. SeaDAS) and equivalent processing solutions. The standard atmospheric correction approach for both sensors is that of Gordon and Wang (1994), with a number of significant updates, including, among others, the use of a revised set of aerosol models and aerosol selection (Ahmad et al., 2010). Bailey et al. (2010) also improved correction for non-zero water-leaving radiances in the near-infra red spectral region. Any differences between MODIS and SeaWiFS data are therefore likely to be associated to differences in sensor design, polarization, band position, overpass time, and band choice in algorithms. For example, one of the atmospheric correction bands (750nm) for MODIS avoids the oxygen absorption in the atmosphere, while the corresponding SeaWiFS band is centered at 765nm, covering the entire oxygen absorption and therefore requiring additional correction (Zhang et al., 2006).

In fact, Zibordi et al. (2013), reported similar validation statistics for both SeaWiFS and MODIS sensors radiometric products, at the 490 nm, 555 nm and 670nm bands. SeaWiFS match-ups exhibited values of bias equal to ~~10~~0% at 490 nm and 555 nm, and to -21% at 670 nm. Correspondingly, MODIS match-ups exhibited values of bias equal to -4% at 488 nm, -6% at 547 nm, and -36% at 667 nm. Increased bias in the red part of the spectrum (667-670 nm), is related to the very low signal in clear waters, becoming the instrumental noise more significant. However, at the 412nm and 443nm bands, SeaWiFS match-ups exhibited bias values equal to +7% and +9%, respectively; while MODIS, for the same bands, exhibited bias values equal to -15% and -2%.

Franz et al. (2012) reported higher mean absolute percentage differences in the blue bands (16%) for the NASA ocean-colour sensors data in comparison to *in situ* data. Values are more significant when match-ups from coastal waters are included in the analysis. Elevated concentrations of CDOM and Chl lessen the signal-to-noise ratio at 412 nm. Thus, the signal is more affected by the instrumental noise and calibration error in that band. The higher differences observed in the blue bands are further complicated by uncertainties in the atmospheric correction algorithm due to the presence of absorbing aerosols (dust, smoke, soot) from terrestrial sources and human activity, and turbid or highly productive waters that reflect significantly in the NIR (Franz et al., 2012). Reflectance values in the NIR should be zero for clear waters. Non-zero in the NIR lead to failure of aerosol determination by the atmospheric correction algorithm, and the bio-optical model described in Bailey et al. (2010) is applied in these cases, which also adds uncertainty to measurements. Franz et al. (2012) further explained that SeaWiFS and MODIS data alone do not allow to discern the absorbing aerosols from the non-absorbing ones. Therefore the effect of the absorbing aerosols is not identified or removed by the current atmospheric correction algorithm, leading to increased negative bias in the $R_{rs}(\lambda)$ retrievals, especially in the shortest wavelengths (i.e, blue bands). The uncertainty values found for SeaWiFS and MODIS in the blue band are however different. Franz et al. (2012), for sensors' common match-ups, reported mean absolute percentage differences between sensors data of 22.94% for 412 nm, 13.64 % for 443 nm, 8.20% for 555-547nm, and 8.94% for 670-667nm. Zibordi et al. (2013) also found considerable differences between sensors (see above), with MODIS sensor underestimating in comparison to SeaWiFS. These differences were not considered significant by the authors considering the variability of the sampled areas, the various *in situ* methodologies applied, and the inter-annual dependence of biases (Zibordi et al., 2013; 2012). For the purpose of this study however, such differences explain the dissimilarities observed between the water classification maps when Lee and Hu (2006) model is applied to

MODIS and SeaWiFS. Results demonstrated that application of the Lee and Hu model first condition to remote sensing data is not recommended, at least for the present atmospheric correction, as shown by figures 38, 39 and 40. The differences found herein are higher for coastal stations, but are still very significant in off-shore regions, for MODIS sensor data. Given what was discussed above, only the second condition was used to analyse the spatial and temporal variability of the water typology, as well as to map non-Case 1 water masses.

4.3.4 Water type temporal and spatial distribution

The seasonal variability and spatial distribution of non-Case 1 waters was analysed by applying only the second condition of the Lee and Hu (2006) model (see discussion in the previous section 4.3.3). Using only the second condition, one has to keep in mind that Case 1 waters will be overestimated, as some of the water masses may have CDOM load per Chl higher than expected for typical Case 1 waters. Even though, the non-case 1 waters due to higher suspended sediments per Chl are identified. Sediments scatter and back-scattering increase reflectance in the whole spectrum domain, but are better detected in the green part, where absorption is at its minimum.

Morel and Bélanger (2006) also provide a model on the expected limits of sediments per Chl concentration typical of Case 1 waters. Both models are based on Morel and Maritorena, (2001) however, theoretical lines present significant differences (Figure 52). Comparing only the theoretical model of Lee and Hu (2006; blue line) with the modeled limit for Case 1 waters following Morel and Bélanger (2006; in red), differences are observed for $\text{Chl} > 0.1 \text{ mg m}^{-3}$. However, it is important to note that Lee and Hu (2006) indicated that the blue line is for theoretical conditions, and natural variability is expected. The upper limit (cyan line) is inclusive in comparison to Morel and Bélanger (2006) until $\text{Chl} > 2 \text{ mg m}^{-3}$. For higher Chl concentrations, the classification with the Lee and Hu (2006) second condition is slightly lower. However, as seen in the example provided by Figure 52, only very small amount of pixels would be differently classified.

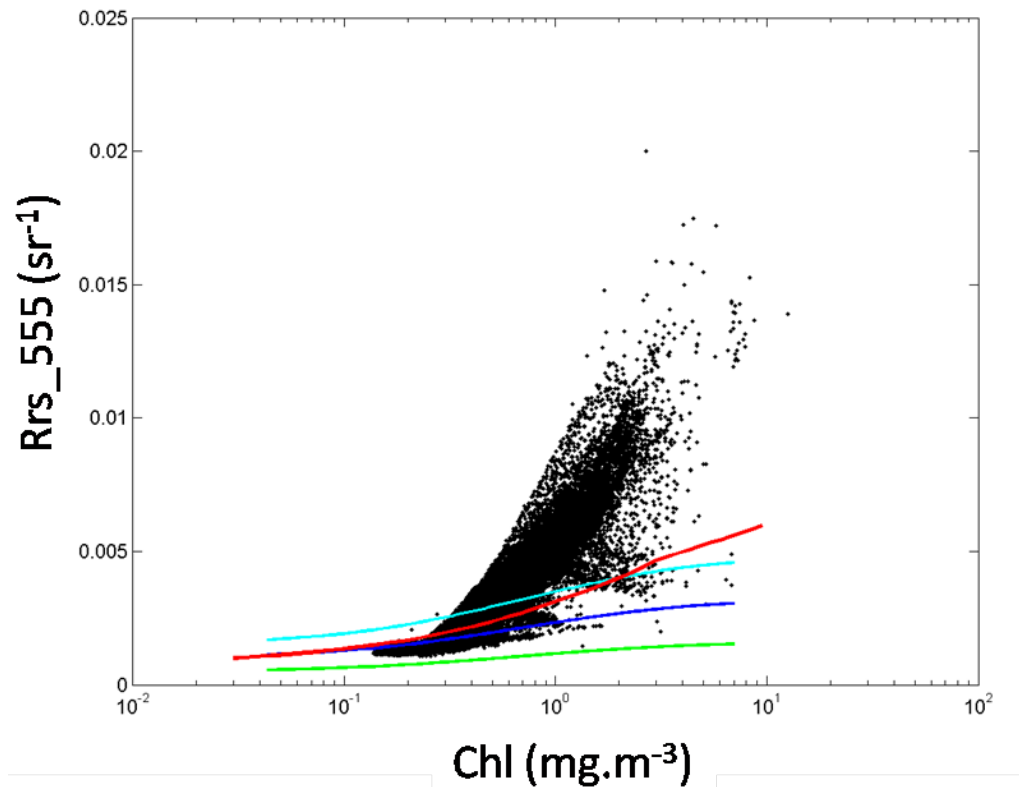


Figure 52 Morel and Bélanger (2006) model superimposed (for sun-zenith angle of 45°) to satellite data and Lee and Hu (2006) second condition model. Data presented are averaged R_{rs} data for the summer period of 2005.

A seven-year period was analysed and percentage maps were generated for each season. Maps represent the number of times (in percentage) that each pixel was classified as Case 1 water. It should be noted that no averages were applied to generate these seasonal maps (Figure 43). Red colour represents the pixels that were always classified as non-Case 1 (i.e., 0% in the color bar), and blue colour represents the pixels that were always classified as Case 1 waters (100% in the color bar).

The seasonal variability revealed persistent sediment loaded coastal waters in winter (red colour pixels), mainly for the South coast and north of Cape Espichel on the West coast. These sediments are probably of riverine origin as these are the areas with major rivers drain. The non-case 1 water band observed along the northern coast can extend to > 50 km off the coast. Same pattern is seen during autumn, however, more restricted to coast, and with lower maximum percentages of non-Case 1 classification (~ 70 -80%).

Summer is the season with fewer pixels classified as non-case 1 waters. This season is typically dry, and persistent non-case 1 waters are only found in the mouth of Tagus river, which has an

average annual outflow of $350 \text{ m}^3 \text{ s}^{-1}$ (Costa et al., 2007), reaching maximum in winter ($700 \text{ m}^3 \text{ s}^{-1}$) and minimum in Summer ($100 \text{ m}^3 \text{ s}^{-1}$).

In spring, non-case 1 waters were found off-shore, being most probably related to the North Atlantic phytoplankton Spring blooms. The model here applied is based on Morel and Maritorena (2001) bio-optical case1 water model that has been developed with a maximum of 10 mg m^{-3} Chl concentrations. In the North Atlantic bloom events can reach concentrations higher than this, and model condition applied here can misclassify the phytoplankton as sediment. Morel and Bélanger (2006) should be tested for spring, has it is more conservative for Chl concentrations $> 2 \text{ mg m}^{-3}$. Phytoplankton particles increase light scattering with increasing Chl (Gordon and Morel 1983). Sediments are only considered to be dominant in the water when the model threshold limit is reached. However, on specific phytoplankton blooms, this threshold can be surpassed and yet waters are still phytoplankton dominated. For instance, coccolithophore blooms may occur in the open ocean with typical high reflectance values, caused by the strong backscattering efficiency of the cells covered by calcite plates, and to the numerous detached calcite liths. In such waters the formal criterion for classification as Case 1 waters (phytoplankton dominated with no terrestrial influence) is still met, however, may look like turbid, sediment loaded waters. Their location, if clearly offshore, can remove the ambiguity concerning their interpretation (Morel and Antoine, 2011). *Trichodesmium* blooms (Subramanian et al., 1999), *Phaeocystis*, or *Synechococcus* blooms (Morel, 1997), can also be encountered off-shore leading to strong deviations from the Case 1 typical properties.

In the water-type classification, the high variability associated to these off-shore non-case 1 waters, seen by the standard deviation presented in Figure 44, supports the interpretation of these water masses being transient phytoplankton blooms. For all seasons, temporal variability for the patterns of the non-case 1 waters can be observed.

Considering the area analysed in this study as a whole (Figure 45), the lowest inter-annual variability is found in summer, and the highest is found in winter and spring. Winter season has the lowest pixels classified as Case 1 waters. Uncertainties related to the atmospheric correction, which have a seasonal component (Zibordi et al., 2012) can further contribute for the differences observed. However, it should be noticed that winter non-Case 1 distribution pattern closely follows the continental shelf limit-line.

4.4 Factors affecting chlorophyll product accuracy

4.4.1 Index water type

The specificities of chlorophyll algorithms make them more suitable for use in waters for which they have been developed, i.e. different optical-types of water such as Case 1 and non-Case 1 waters. For instance, chlorophyll algorithms of the blue-to-green ratio type (e.g. MODIS OC3M and MERIS algal 1) were developed for Case 1 waters and are likely to have a reduced performance in CDOM or sediment loaded waters. Based on the Lee and Hu (2006) model, three water-type indices were determined and computed for all the match-ups obtained with MODIS, MERIS algal 1 and algal 2. First index (Ind_1) is based on both model conditions: it is the product of the differences between the theoretical RR12 and the satellite RR12 measurement, and the theoretical Rrs555 and the satellite Rrs555 measurement (equation 2.20). The first difference calculated to compute ind_1, i.e. between theoretical and satellite-derived RR12, was considered to be index 2 (ind_2) and the second difference was considered index 3 (ind_3), equations 2.21 and 2.22, respectively).

Spearman correlation coefficients were determined to analyse how the Chl percentage error of each product in comparison to the *in situ* data, varied with the calculated indices (first six lines of Table XII). It should be noticed, that both Ind_1 and Ind_2 were always significantly negatively correlated to RR12. This is true for all the tested products. These results indicate, as expected and already discussed, that the theoretical RR12 values are always higher than the measured values, suggesting atmospheric problems in the blue bands. Given that Ind_1 is the product of Ind_2 and Ind_3, it was found to be positively correlated to both indices separately. Reflectance at 547-560 nm is always positively correlated to Ind_1 and Ind_3.

For MODIS, percent error was found to have a significant positive relationship with Rrs555 ($r_s=0.25$) and a significant negative relationship with Chl ($r_s=-0.38$). It was positively related to the reflectance at the 547 nm MODIS band, but no significant correlations were found for any of the computed indices. The reflectance values in the green band are related to particles scattering. This scattering can be either from the phytoplankton cells or the inorganic sediment particles. In fact, Rrs547 is positively and significantly correlated to Chl ($r_s=0.53$). However, as mentioned, the percent error is negatively correlated to Chl ($r_s=-0.38$). This indicates that the error might be related to increased Rrs547 due to the presence of sediments in the water.

Percent error determined for algal 1 MERIS was significantly correlated with RR12 ($r_s=-0.34$), Rrs at 560 nm ($r_s=-0.34$) and Ind_3 ($r_s=-0.34$), however not significantly correlated to Ind_1 nor Ind_2. All correlations were negative; therefore an increase in error is associated to a decrease in these parameters. These may indicate the decreased performance of the algorithm closer to shore. The use of Ind_3 seems to be suitable to restrict application of the algorithm.

Algal 2 product percent error was significantly associated to both RR12 ratio and indices 1 and 2. It was inversely correlated to the ratio RR12 ($r_s=-0.27$), but positively correlated with the indices 1 and 2 (r_s Ind_1 = 0.33 and Ind_2 = 0.25). The positive correlation with the indices, but negative correlation with the measured RR12 ratio, indicates that the difference between the theoretical RR12 was always higher than the measured ratio, which is in accordance to what has been discussed and again suggesting atmospheric correction problems on the measured RR12. The negative correlation with the RR12 ratio indicates that this algorithm is able to cope with CDOM loaded waters (i.e. coastal waters) but performs worst in clearer waters. In fact, the percent error is negatively correlated to Chl ($r_s=-0.29$). The Ind_1 was the parameter found to have the highest correlation coefficient with the percent error for this Chl product and may be used to restrict algorithm application.

4.4.2 Phytoplankton size classes

In order to analyse the impact of the phytoplankton community composition in the Chl products accuracy, Spearman correlation coefficients (r_s) were determined for all size fractions and size index (SI). The micro-phytoplankton fraction (f_{micro}) is highly correlated to the SI parameter ($r_s=1$) as f_{micro} was dominant for all products match-ups datasets (>50%), furthermore it is the component with the highest weight (i.e., 50) in the SI calculation formula (see equation 2.5). Nano and pico-sized phytoplankton fractions (f_{nano} and f_{pico} , respectively) were both negatively correlated to the micro-sized fraction, and the SI, but positively correlated with each other. For all tested products, both Chl and Rrs547-560 nm were significantly and positively correlated to f_{micro} and significantly and negatively correlated to f_{nano} and f_{pico} . Conversely, f_{nano} and f_{pico} are positively correlated to the distance from coast and f_{micro} is inversely correlated to it. This is in accordance to what has been shown in Figure 16, where f_{micro} was mostly encountered near the coast, as opposed to f_{nano} and f_{pico} , which were mostly found off-shore. Biomass and scattering, as f_{micro} are also higher near the coast, explaining the positive correlation found between these parameters.

For MODIS match-ups, f_{nano} was significantly correlated to Ind_2, while f_{pico} was negatively correlated. F_{pico} was found to be significantly correlated to RR12, and this was true for all the products analysed. Negative correlations were found between RR12 and f_{micro} , for all products, but these were only significant for the algal 2 product.

Considering the percent error determined for each Chl product, significant correlation with phytoplankton size-fractions were only found for the algal 1 product. For this product, the percent error was significantly and positively related to the f_{micro} and SI; and significantly but negatively for f_{nano} . Interestingly, the correlation found with Chl was not statistically significant. Algal 2 and MODIS algorithms, on the other hand, were significantly correlated to Chl but not to the phytoplankton size-fractions. Differences could be related to particular characteristics of each algorithm match-up dataset; however no differences were found between the averages SI of each dataset (i.e., $29 \mu\text{m} \pm 10.36$ for MODIS, $28 \mu\text{m} \pm 11.12$ for algal 1 and $30 \mu\text{m} \pm 11.15$ for algal 2). This indicates that the size-composition of the phytoplankton community influenced the performance of algal 1 algorithm, and, at least for this dataset, this was not clearly related to the Chl absolute value.

As stated in the introduction, Chl is an ubiquitous pigment, however, other pigments present in phytoplankton composition, which were here associated to specific size-groups (Uitz et al., 2006), can change in type and amount relative to Chl concentration. This can affect substantially the phytoplankton absorption spectra, to a factor of 6 in the blue-green ratio (Hoepffner and Sathyendranath, 1992), and therefore influence Chl product accuracy. The retrieved results may be related to algal 1 algorithm specificities; however, further investigation has to be conducted with an increased number of match-ups.

4.4.3 Other parameters

The performance of Chl products was also evaluated considering the distance of the match-ups location from coast and the first optical depth (Z_1^{st}). It should be noticed that the first optical depth (Z_1^{st}) was calculated based on the euphotic depth (Z_{eu} , equation 2.24), which has been derived directly from surface Chl concentration (equation 2.23). These parameters (i.e., Z_1^{st} and Chl) are therefore inversely correlated and have equal Spearman correlation coefficients, but opposed signs. As found for Chl, Z_1^{st} was found to be significantly associated to the percentage error of both MODIS and MERIS algal 2 Chl products. No significance was found for the algal 1 product.

First optical depth was found to be significantly related to match-ups location, with Z_1^{st} increasing with increasing distance from coast. Closer to coast, water turbidity is increased and light penetration in the water column is reduced. This implies shallower euphotic and first optical depths. However, contrasting results were found for percentage error of the analysed Chl products with distance from coast of the match-ups. Although not statistically significant, both MODIS and MERIS algal 1 products were positively related to the location of the match-ups ($r_s=0.07$ and $r_s=0.31$, respectively). Errors found in the Chl retrieval of these products increase when match-ups are further off-shore. In contrast, the correlation found for the percentage error of algal 2 Chl product are negatively related to the match-ups distance from coast ($r_s=-0.14$). These results were not expected as algal 2 was developed to achieve better performance in coastal waters, and MODIS OC3M and MERIS algal 1 are expected to operate better in oceanic clear waters. For the algal 2 product, these results may be only an artefact introduced by a specific cruise or Chl patchiness on the match-ups data set, as Chl was found to be significantly and inversely correlated to the distance from coast, and also inversely correlated to percentage error for all products. In fact, for all products, error was inversely and significantly correlated to Chl. This means that, for all products, errors are greater in more oceanic waters, as Chl is inversely related to the distance from coast. As mentioned, this result is in accordance to what was expected for algal 2 product, but not for MODIS OC3m and algal 1. The increase in percentage error with distance from coast is related to the fact that Chl was only collected at surface and not integrated in the water column to the first optical depth. Therefore the satellite is “seeing” more chlorophyll than the measured in the collected sample. This difference is only evident when water column is stratified and a deep-chlorophyll maximum develops associated to the optimum light depth. When this happens, surface Chl is not representative of the Chl in the first optical depth. Stramska & Stramki (2005) concluded, using modeling exercises, that the contribution of a non-uniform vertical Chl profile is negligible when surface Chl content is greater than 0.4 mg.m^{-3} , at least for deep Chl maximum (DCM) between 20 and 45 m, situation verified for the majority of the off-shore stratified stations. Errors due to a non-uniform Chl profile therefore increase at lower Chl concentrations. This explains why the error obtained here for all products is inversely correlated to Chl. In fact, Figure 53 shows that for higher the Z_{eu} (i.e., the higher the Z_1^{st} , see equation 2.24) the deeper the DCM is, the percent error increases, meaning that surface Chl is less representative of the Chl within the first optical depth (the Chl seen by the ocean colour sensor).

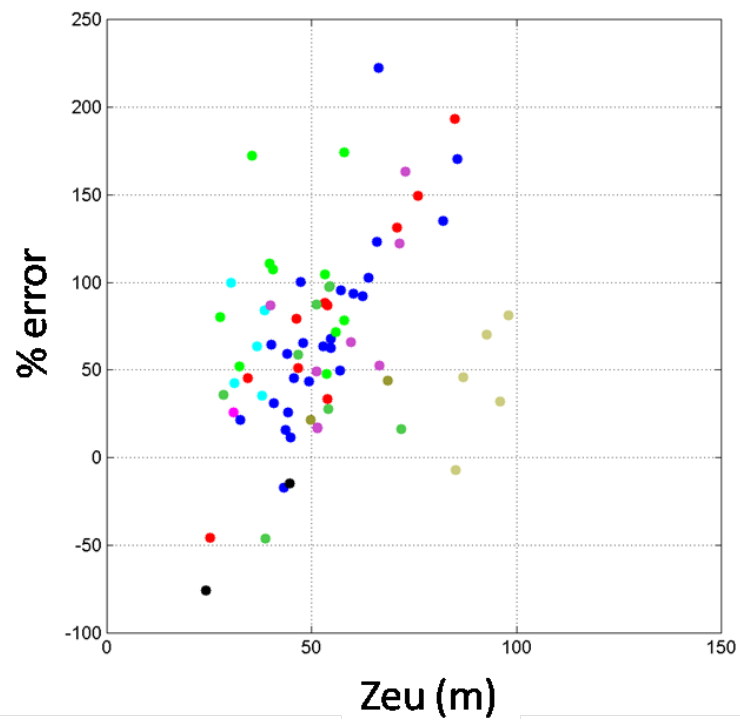


Figure 53 Variation of percentage error of MODIS matchups with the euphotic depth (m). Colours correspond to the different cruises, according to Figure 11.

Chapter 5: Final Remarks

5.1 General considerations

Ocean-colour remote sensing is the only available tool providing continuous and synoptic view of the oceans. However, the coefficients used in empirical algorithms are derived from datasets that do not necessarily represent all natural variations. The performance of such algorithms is always subject to compatibility between the waters under study and the waters from which data were obtained for algorithm development (IOCCG, 2006). Therefore, for monitoring purposes, uncertainties have to be considered and it is crucial to understand the region under analysis.

The main objective of this thesis was to evaluate the standard MERIS and MODIS chlorophyll products off the Portuguese coast and identify the factors influencing its performance when compared to *in situ* data. Algorithm regionalization was intended and validation of novel products was also included in the analysis. Four tasks were initially purposed: (1) to gather a comprehensive *in situ* pigment dataset; (2) to validate and compare Chl products for the Portuguese coast; (3) to regionally parameterize algal2 MERIS algorithm and MLP algorithm; and (4) to provide a classification of the water types off and along the coast and retrieve its spatial and seasonal distribution. All tasks were conducted successfully, as described below.

The pigments information collected throughout the years allowed to achieve specific objective 1. This work allowed to gather information on different regions of the coast, and indirectly, to identify areas of special interest for ocean-colour validation purposes. Areas such as the Nazaré canyon, were highly dynamic with optically active substances varying both spatially and temporally. This was evidenced by the phytoplankton communities variability observed, and the differences obtained in the products performance for the various cruises undertaken in the area.

To fulfill the second objective, a set of Chl products were tested against contemporaneous *in situ* data. Generalized overestimation by satellite products was observed, however, with regional differences. The high number of samples necessary to retrieve a reasonable amount of match-ups should be emphasized. There is the need to conduct campaigns specifically driven for the validation/algorithm development activity. Further efforts to collect additional radiometric data would help improving the determination of the uncertainty components related to the Chl algorithm itself, and the atmospheric correction component.

An optical campaign (i.e. 68 optical stations) conducted in the Nazaré region during the spring season, allowed to regionally train a bio-optical algorithm, which improved Chl estimates in the area, thus allowing to achieve the specific objective 3. The absorption coefficients of CDOM

were found to be dominant, with ranges comparable to the average values measured in the northern Adriatic sea and in the Ligurian sea, both in the Mediterranean basin. Although the significant contribution provided by this work, an investment in radiometric data collection would very much improve our knowledge on the optical properties in the area. It is essential to understand its spatial and temporal variability, because, as shown by results, the use of remote sensing for water type classification requires improved atmospheric correction.

The specific objective 4 was achieved through the classification of the water type. It was based in the relation of the three optically active components (i.e., CDOM, suspended sediments and phytoplankton) contribution to the water-leaving signal, using proxies for their estimate following Lee and Hu (2006). The proxy used for CDOM is based on the ratio of the first two bands in the blue part of the spectrum. However, atmospheric correction spectrally perturbs the derived water-leaving radiance data in this part of the spectrum (i.e., 412 and 443 nm bands), and this introduces biases in their band-ratios. Nonetheless, seasonal maps of non-case 1 waters were produced considering only the contribution of suspended sediments (green band: 555 nm). A marked seasonal variability was verified in the spatial distribution of this water type, which emphasizes the importance of restricting algorithms area of applicability.

The biases found in the blue bands were not significantly influential in Chl products performance. Mainly because the 412 nm band is not used in the band-ratio Chl algorithms and other spectral uncertainties, less marked in the other bands, were probably mitigated by the ratio itself. However, algorithms designed to operate in coastal waters were found to retrieve Chl values with lower bias than the standard blue-green ratio algorithms, when compared to *in situ* data. Better statistical results were achieved by the regionalized MLP algorithm (Figure 54). These results suggest that the optical properties of the study site are better represented by this algorithm. Additionally, this algorithm provides novelty indices to the output data, which proved to correctly provide algorithm range of applicability.

Understanding products range of applicability and uncertainties in relation to the study area are essential to make adequate use of satellite products and to accurately interpret its information. The results presented in this thesis are therefore a contribution to that knowledge, for the coast off Portugal. It is key contribution for understanding the applicability of such valuable monitoring tool.

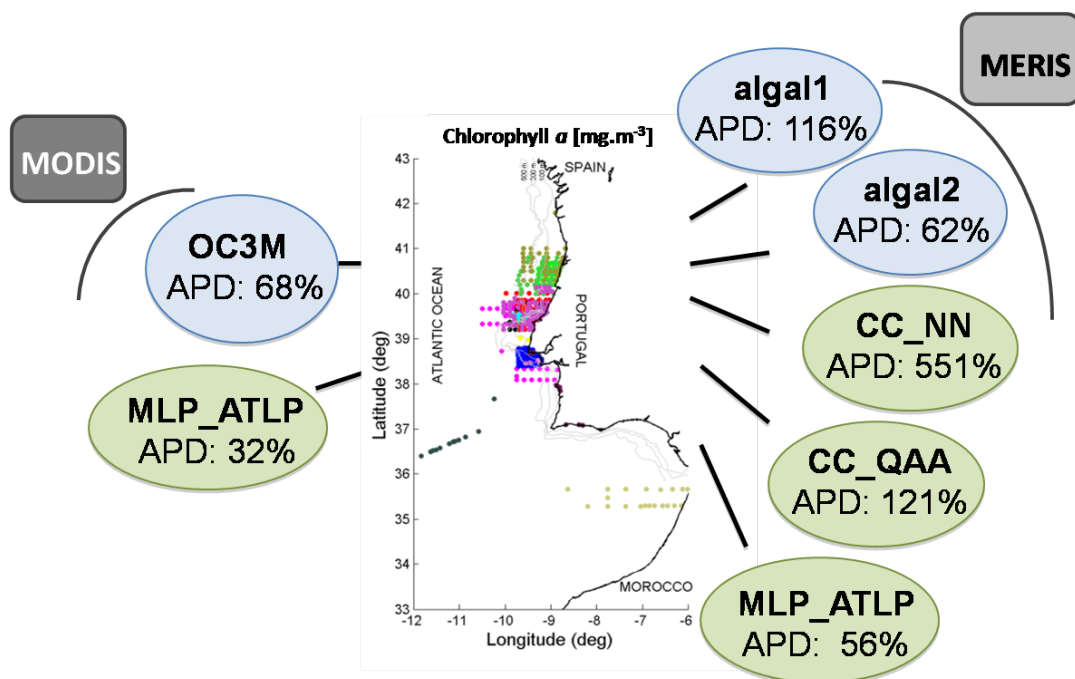


Figure 54 Summary scheme of comparison between satellite Chl products and the *in situ* dataset. Absolute percentage of difference (APD) is presented for each of the standard (in blue) and novel (in green) products tested.

5.2 Future perspectives

Standard chlorophyll satellite products were found to generally overestimate concentrations in comparison to *in situ* data. This overestimation was significantly reduced when using a regionally tuned algorithm. The applicability of this algorithm is restricted, because regionalization was based on the limited dataset acquired during the GC11 cruise. Nevertheless, improved results are encouraging. A large set of high quality *in-situ* optical data is mandatory for these studies, being set as a priority. Efforts are in course to keep updating the *in situ* database, in order to incorporate as much as possible the temporal and spatial variability of the study area.

Validation activities are a continuous process which needs dedicated sampling campaigns and multidisciplinary teams. Joint efforts have recently come together to create a consistent validation program of ocean colour products off the Portuguese coast in the form of a consortium, OCPortugal (ocportugal.org). Meris validation work performed by the University of Algarve, the work presented here for the West coast and the optical modelling component of

the Nova University - intend to contribute to future ocean-colour missions and integrate the Sentinel-3 validation team.

The existence of a high precision satellite Chl product enables a series of very important applications. Phytoplankton are the basis of oceanic food webs and therefore may have significant implications in terms of fisheries management. Being in the lower trophic level, phytoplankton chlorophyll has become an important indicator of the quality status of marine open waters and the health of ecosystem. The importance of knowing Chl products uncertainties is therefore crucial for establishing critical biomass thresholds, which are generally defined based on historical data. Further studies would greatly increase the potential benefits of these remote methodologies. In addition, chlorophyll is also a determinant factor for computing ocean primary productions, providing further insight into global biogeochemical cycles.

Results from scientific research more often raise further questions rather than provide clear answers. The basis has however been set and further studies, especially focused on phytoplankton size classes will emerge (e.g., Brotas et al., 2013; Brito et al., 2013). Moreover, the development of spectral absorption models to differentiate specific phytoplankton groups, such as the Harmful Algal Blooms (HABs), will also be the focus of increased research during the near future. HABs are a public health problem and may cause the loss of a significant number of animals in aquaculture farms. In recent years, a couple of European projects have been approved to develop such models, as is the EU FP7 AQUA_USERS, in which our research team is a partner. These contributions will provide important support for the progress of new technology.

Besides the validation activity, pigment information can be further explored with concomitant chemical and physical data to retrieve biological indicators and provide insight on phytoplankton communities dynamics (e.g., Mendes et al., 2011; Silva et al. 2008)

Chapter 6: References

References

- Ahmad, Z., Franz, B.A., McClain, C.R., Kwiatkowska, E.J., Werdell, J., Shettle, E.P., Holben, B.N. (2010). New aerosol models for the retrieval of aerosol optical thickness and normalized water-leaving radiances from the SeaWiFS and MODIS sensors over coastal regions and Open Oceans. *Applied Optics*, 49, 5545 - 60.
- Aiken, J., Moore, G. (2000). Algorithm Theoretical Basis Document ATBD 2.8 CASE 2 Anomalous scattering and Gelbstoff waters flags. Doc no. PO-TN-MEL-GS-0005.
- Aiken, J., Moore, G.F., Trees, C.C., Hooker, S.B., Clark, D.K. (1995). The SeaWiFS CZCS-Type Pigment Algorithm. NASA Tech. Memo. 104566, 29, in: Hooker, S.B., Firestone, E.R. (Eds.), NASA Goddard Space Flight Center, Greenbelt, Maryland, 34 pp.
- Aiken, J., Pradhan, Y., Barlow, R., Lavender, S., Poulton, A., Holligan, P., Hardman-Mountford, N.J. (2009). Phytoplankton pigments and functional types in the Atlantic Ocean: A decadal assessment, 1995-2005. *AMT Special Issue. Deep-Sea Research Part II*, 56, 899 - 917.
- Alteriis, G., Passaro, S., Tonielli, R. (2003). New, high resolution swath bathymetry of Gettysburgh and Ormonde Seamounts (Gorringe Bank, eastern Atlantic) and first geological results. *Marine Geophysical Researches*, 24, 223 - 244.
- Alvain, S., Moulin, C., Dandonneau, Y., Breon, F.M. (2005). Remote sensing of phytoplankton groups in case 1 waters from global SeaWiFS imagery. *Deep-Sea Research Part I*, 1, 1989-2004.
- Amorim, A., Palma, A.S., Sampayo, M.A., Moita, M.T. (2001). On a *Lingulodinium polyedrum* bloom in Setúbal bay, Portugal. In: *Harmful Algal Blooms 2000*, (Ed. by G.M. Hallegraeff, S.I. Blackburn, C.J. Bolch & R.J. Lewis). Intergovernmental Oceanographic Commission of UNESCO. 133-136 pp.
- Amorim, A., Moita, M.T., Oliveira, P. (2004). Dinoflagellate blooms related to coastal upwelling plumes off Portugal. In: *Harmful Algae 2002*, (Ed. by K.A. Steindinger, J.H. Landsberg, C.R. Tomas & G.A. Vargo). Florida Fish and Wildlife Conservation Commission, Florida Institute of Oceanography, and Intergovernmental Oceanographic Commission of UNESCO. 89-91pp.
- Antoine, D., Morel, A. (1999). A multiple scattering algorithm for atmospheric correction of remotely-sensed ocean colour (MERIS instrument): principle and implementation for

- atmospheres carrying various aerosols including absorbing ones. *International Journal of Remote Sensing*, 20, 1875 - 1916.
- Arnone, R.A., Wood, A.M., Gould, R.W.Jr. (2004). The Evolution of Optical Water Mass Classification. *Oceanography*, 17, 14 – 15.
- Babin, M., Stramski, D., Ferrari, G.M., Claustre, H., Bricaud, A., Obolensky, G., Hoepffner, N., (2003). Variations in the light absorption coefficients of phytoplankton, non-algal particles, and dissolved organic matter in coastal waters around Europe. *Journal of Geophysical Research*, 108, 3211.
- Bailey, S.W., Werdell, P.J. (2006). A multi-sensor approach for the on-orbit validation of ocean color satellite data products. *Remote Sensing of Environment*, 102, 12 - 23.
- Bailey, S.W., Franz, B.A., Werdell, P.J. (2010). Estimation of near-infrared water-leaving reflectance for satellite ocean color data processing. *Optics Express*, 18, 7521 - 7527.
- Balch, W.M., Kilpatrick, K.A., Holligan, P.M., Trees, C. (1996). The 1991 coccolithophore bloom in the central north Atlantic. I: Optical properties and factors affecting their distribution. *Limnology and Oceanography*, 41, 1669 - 1683.
- Barlow, R., Stuart, V., Lutz, V., Sessions, H., Sathyendranath, S., Platt, T., Kyewalyanga, M., Clementson, L., Fukasawa, M., Watanabe, S., Devred, E. (2007). Seasonal pigment patterns of surface phytoplankton in the subtropical Southern Hemisphere. *Deep-Sea Research Part I*, 54, 1687-1703.
- Barlow, R., Kyewalyanga, M., Sessions, H., van den Berga, M., Morris, T. (2008). Phytoplankton pigments, functional types, and absorption properties in the Delagoa and Natal Bights of the Agulhas ecosystem. *Estuarine, Coastal and Shelf Science*, 80, 201 - 211.
- Behrenfeld, M.J., O'Malley, R., Siegel, D., McClain, C., Sarmiento, J., Feldman, G., Milligan, A., Falkowski, P., Letelier, R., Boss, E. (2006). Climate-driven trends in contemporary ocean productivity. *Nature*, 444, 752 – 755.
- Blackford, J.C., Allen, J.I., Gilbert, F.J. (2004). Ecosystem dynamics at six contrasting sites: A generic modelling study. *Journal of Marine Systems*, 52, 191 – 215.
- Bouman, H., Platt, T., Sathyendranath, S., Stuart, V. (2005). Dependence of light-saturated photosynthesis on temperature and community structure. *Deep Sea Research Part I*, 52, 1284 – 1299.

- Bourg, L., Lerebourg, C., Mazeran, C., Bruniquel, V., Barker, K., Jackson, J., Kent, C., Lavender, S., Moore, G., Brockmann, C., Bouvet, M., Delwart, S., Goryl, P., Huot, J-P., Kwiatkowska, E., Fisher, J., Ramon, D., Doerffer, R., Gabron, N., Antoine, D., Zagolski, F., Santer, R., Dash, J., Hooker, S., Brotas, V., Muller-Krager, F., Kratzer, S. (2011). MERIS 3rd data Reprocessing: Software and ADF updates, Report n.A879.NT.008.ACRI-ST, 21091/07/I-OL. 73pp. Available in the website:

<http://earth.eo.esa.int/pcs/envisat/meris/documentation>.
- Bowler, C., Karl, D.M., Colwell, R. (2009). Microbial oceanography in a sea of opportunity. *Nature*, 459, 180 – 184.
- Brewin, R.J.W., Sathyendranath, S., Hirata, T., Lavender, S., Barciela, R.M., Hardman-Mountford, N.J. (2010). A three-component model of phytoplankton size class for the Atlantic Ocean. *Ecological Modelling*, 221, 1472-1483.
- Brewin, R.J.W., Hardman-Mountford, N.J., Lavender, S.J., Raitsos, D.E., Hirata, T., Uitz, J., Devred, E., Bricaud, A., Ciotti, A., Gentili, B. (2011). An intercomparison of bio-optical techniques for detecting dominant phytoplankton size class from satellite remote sensing. *Remote Sensing of Environment*, 115, 325 – 339.
- Bricaud, A., Claustre, H., Ras, J., Oubelkheir, K. (2004). Natural variability of phytoplanktonic absorption in oceanic waters: influence of the size structure of algal populations. *Journal of Geophysical Research*, 109, C11010.
- Brito, A., Sá, C., Brotas, V., Vitorino, J., Platt, T., Sathyendranath, S. (2013). Understanding bio-optical properties of phytoplankton in the western Iberian coast: application of theoretical models. *Remote Sensing of Environment*, under revision.
- Brotas, V., Plante-Cuny, M.R. (1996). Identification et quantification des pigments chlorophylliens et caroténoïdes des sédiments marins: un protocole d'analyse par HPLC. *Oceanologica Acta*, 19, 623-634.
- Brotas, V., Brewin, R.J.W., Sá, C., Brito, A.C., Silva, A., Mendes, C.R., Diniz, T., Kaufmann, M., Tarran, G., Groom, S.B., Platt, T., Sathyendranath, S. (2013). Deriving phytoplankton size classes from satellite data: validation along a trophic gradient in the eastern Atlantic Ocean. *Remote Sensing of Environment*, 134, 66 - 77.
- Brown, C.W., Podestá, G.P. (1997). Remote sensing of Coccolithophore blooms in the Western South Atlantic Ocean. *Remote Sensing of Environment*, 60, 83 - 91.

- Brunet, C., Lizon, F. (2003). Tidal and diel periodicities of size fractionated phytoplankton pigment signatures at an offshore station in the South-Eastern English Channel. *Estuarine, Coastal and Shelf Science*, 56, 1 - 11.
- Campbell, J.W. (1995). The lognormal distribution as a model for bio-optical variability in the sea. *Journal of Geophysical Research*, 100, 13237 – 13254.
- Carder, K.L., Chen, F.R., Lee, Z.P., Hawes, S.K., Kamykowski, D. (1999). Semi-analytic MODIS algorithms for chlorophyll a and absorption with bio-optical domains based on nitrate-depletion temperatures. *Journal of Geophysical Research*, 104, 5403 - 5421.
- Cartaxana, P., Brotas, V. (2003). Effects of extraction on HPLC quantification of major pigments from benthic microalgae. *Archiv für Hydrobiologie*, 157, 339 - 349.
- Ciotti, A., Bricaud, A. (2006). Retrievals of a size parameter for phytoplankton and spectral light absorption by colored detrital matter from water-leaving radiances at SeaWiFS channels in a continental shelf region off Brazil. *Limnology and Oceanography: Methods*, 4, 237 - 253.
- Ciotti, A., Lewis, M.R., Cullen J.J. (2002). Assessment of the relationships between dominant cell size in natural phytoplankton communities and the spectral shape of the absorption coefficient. *Limnology and Oceanography*, 42, 406 - 417.
- Clark, G.L., Ewing, G.C., Lorenzen, C.J. (1970). Spectra of backscattered light from the sea obtained from aircraft as a measure of chlorophyll concentration. *Science*, 167, 1119 - 1121.
- Claustre, H. (1994). Phytoplankton pigment signatures of the trophic status in various oceanic regimes. *Limnology and Oceanography*, 39, 1206-1211.
- Costa, M.J., Vasconcelos, R., Costa, J.L., Cabral H.N. (2007). River flow influence on the fish community of the Tagus estuary (Portugal). *Hydrobiologia*, 587, 113 – 123.
- D'Alimonte, D., Zibordi, G. (2003). Phytoplankton determination in an optically complex coastal region using a multilayer perceptron neural network. *Geoscience and Remote Sensing, IEEE Transactions*, 41, 2861 - 2868.
- D'Alimonte, D., Mélin, F., Zibordi, G., Berthon, J.F. (2003). Use of the novelty detection technique to identify the range of applicability of empirical ocean color algorithms. *Geoscience and Remote Sensing, IEEE Transactions*, 41, 2833 - 2843.
- D'Alimonte, D., Zibordi, G., Berthon, J.F. (2004). Determination of CDOM and NPPM absorption coefficient spectra from coastal water remote sensing reflectance. *Geoscience and Remote Sensing, IEEE Transactions* 42, 1770 - 1777.

- D'Alimonte, D., Zibordi, G., Berthon, J.-F., Canuti, E., Kajiyama, T. (2011). Bio-optical algorithms for european seas: Performance and applicability of neural-net inversion schemes. JRC-IES Scientific and Technical Research Reports, Technical Report. JRC 66326.
- D'Alimonte, D., Zibordi, G., Kajiyama, T., Berthon, J.-F. (2014). Comparison between MERIS and regional high-level products in European seas. *Remote Sensing of Environment*, 140, 378 – 395.
- Da Silva, J.C.B., New, A.L., Srokosz, M.A., Smith, T.J. (2002). On the Observability of internal tidal waves in remotely-sensed ocean colour data. *Geophysical Research Letters*, 29, 1569.
- Dandonneau, Y., Deschamps, P.-Y., Nicolas, J.-M., Loisel, H., Blanchot, J., Montel, Y., Thieuleux, F., Bécu, G. (2004). Seasonal and interannual variability of ocean color and composition of phytoplankton communities in the North Atlantic, equatorial Pacific and South Pacific. *Deep-Sea Research Part II*, 51, 303–318.
- De Stigter, H., Boer, W., Mendes, P., Jesus, C., Thomsen, L., van den Bergh, G., van Weering, T. (2007). Recent sediment transport and deposition in the Nazaré Canyon, Portuguese continental margin. *Marine Geology* 256, 144 - 164.
- Devred, E., Sathyendranath, S., Stuart, V., Platt, T. (2011). A three component classification of phytoplankton absorption spectra: Application to ocean-color data. *Remote Sensing of Environment*, 115, 2255 – 2266.
- Doerffer R. (2002). Protocols for the validation of MERIS water products. European Space Agency. Doc. No. PO-TN-MEL-GS-0043.
- Doerffer, R., Schiller, H. (2007). The MERIS Case 2 water algorithm. *International Journal of Remote Sensing*, 28, 517 – 535.
- Dogliotti, A.I., Schloss, I.R., Almandoz, G.O., Gagliardini, D.A. (2009). Evaluation of SeaWiFS and MODIS chlorophyll-a products in the Argentinean Patagonian Continental Shelf (38°S-55°S). *International Journal of Remote Sensing*, 30, 251 - 273.
- Falkowski P.G., Raven, J.A. (1997). *Aquatic photosynthesis*. Blackwell Science, 375 pp.
- Field, C.B., Behrenfeld, M.J., Randerson, J.T., Falkowski, P. (1998). Primary Production of the Biosphere: Integrating Terrestrial and Oceanic Components. *Science*, 281 – 237.
- Fiúza, A.F.G. (1983). Upwelling patterns off Portugal. In: Suess, E., Thied, J. (Eds.), *Coastal Upwelling, its Sediment Record. Part A. Responses of the Sedimentary Regime to Present Coastal Upwelling*. Plenum, New York, 85–98 pp.

- Fiúza, A.F.G., Macedo, M.E., Guerreiro, M.R. (1982). Climatological space and time variation of the Portuguese coastal upwelling. *Oceanologica Acta*, 5, 31 – 40.
- Folkestad, A., Pettersson, L.H., Durand, D.D. (2007). Inter-comparison of ocean colour data products during algal blooms in the Skagerrak. *International Journal of Remote Sensing*, 28, 569 - 592.
- Forel, F.A. (1890). "Couleur de L'eau" in *Optique, Le Lman. Monographie Limnologique*, 2, 462-487 (Slatkins, Genve, 1895).
- Franz, B.A., Bailey, S.W., Meister, G., Werdell, P.J. (2012). Consistency of the NASA Ocean Color Data Record. *Proceedings of Ocean Optics*, Glasgow, Scotland, 8-12 October.
- Garcia, C.A.E., Garcia, V.M.T., McClain, C.R. (2005). Evaluation of SeaWiFS chlorophyll algorithms in the Southwestern Atlantic and Southern Oceans. *Remote Sensing of Environment*, 95, 125 - 137.
- Garver, S.A., Siegel, D.A. (1997). Inherent optical property inversion of ocean color spectra and its biogeochemical interpretation: 1. time series from the Sargasso Sea. *Journal of Geophysical Research*, 102, 18607 - 18625.
- Gibson, P.J., Keating, J., Power, C.J. (2000). *Introductory Remote Sensing Principles and concepts*. Routledge, London 216 pp.
- Glover, D.M., Jenkins, W.J., Doney, S.C. (2011). *Modeling Methods for Marine Science*. Cambridge Univeristy Press. 571 pp.
- Goela, P.C., Icely, J., Cristina, S., Newton, A., Moore, G., Cordeiro, C. (2013). Specific absorption coefficient of phytoplankton off the Southwest coast of the Iberian Peninsula: A contribution to algorithm development for ocean colour remote sensing. *Continental Shelf Research*, 52, 119 -132.
- Gordon, H.R. (1997). Atmospheric correction of ocean color imagery in the earth observing system era. *Journal of Geophysical Research*, 102, 17081-17106.
- Gordon, H.R. (2005). Normalized water-leaving radiance: revisiting the influence of surface roughness. *Applied Optics*, 44, 241 - 248.
- Gordon, H.R., McCluney, W.R. (1975). Estimation of the depth of sunlight penetration in the sea for remote sensing. *Applied Optics*, 14, 413 - 416.
- Gordon, H.R., Clark, D.K. (1980). Remote sensing optical properties of a stratified ocean: an improved interpretation. *Applied Optics*, 19, 3428 - 3430.

- Gordon, H.R., Morel, A.Y. (1983). Remote Assessment of Ocean Colour for Interpretation of Satellite Visible Imagery. *Lecture Notes on Coastal and Estuarine Studies*: Springer-Verlag, Berlin.4, 114 pp.
- Gordon, H.R., Wang, M. (1994). Retrieval of water-leaving radiance and aerosol optical thickness over the oceans with SeaWiFS: A preliminary algorithm. *Applied Optics*, **33**, 443 – 452.
- Gordon, H.R., Clark, D.K., Brown, J.W., Brown, O.B., Evans, R.H., Broenkow, W.W. (1983). Phytoplankton pigment concentrations in the Middle Atlantic Bight: comparison of ship determinations and CZCS estimates. *Applied Optics*, **22**, 20 - 36.
- Gregg, W.W., Casey, N.W. (2004). Global and regional evaluation of the SeaWiFS Chlorophyll data set. *Remote Sensing of Environment*, **93**, 463 – 479.
- Groom, S., Martinez-Vicente, V., Fishwick, J., Tilstone, G., Moore, G., Smyth, T., Harbour, D. (2009). The Western English Channel observatory: optical characteristics of station L4. *Journal of Marine Systems*, **77**, 278 – 295.
- Guerreiro, C., Oliveira, A., de Stigter, H., Cachão, M., Sá, C., Borges, C., Cros, L., Santos, A., Fortuño, J-M., Rodrigues, A. (2013) Late winter coccolithophore bloom off central Portugal in response to river discharge and upwelling. *Continental Shelf Research*, **59**, 65 - 83.
- Haltrin, V.A. (1999). Chlorophyll-based model of seawater optical properties. *Applied Optics*, **38**, 6826 – 6832.
- Hirata, T., Aiken, J., Smyth, T.J., Hardman-Mountford, N., Barlow, R.G. (2008). An absorption model to derive phytoplankton size classes from satellite ocean colour. *Remote Sensing of Environment*, **112**, 3153-3159.
- Hirata, T., Hardman-Mountford, N.J., Brewin, R.J.W., Aiken, J., Barlow, R., Suzuki, K., Isada, T., Howell, E., Hashioka, T., Noguchi-Aita, M., Yamanaka, Y. (2011). Synoptic relationships between surface chlorophyll-a and diagnostic pigments specific to phytoplankton functional types. *Biogeosciences*, **8**, 311 – 327.
- Hirata, T., Hardman-Mountford, N.J., Brewin, R.J.W. (2012). Comparing satellite-based phytoplankton classification methods. *EOS, Transactions American Geophysical Union*, **93**, 59 – 60.
- Hoepffner, N., Sathyendranath, S. (1992). Bio-optical characteristics of coastal waters: Absorption spectra of phytoplankton and pigment distribution in the western North Atlantic. *Limnology and Oceanography*, **37**, 1660 – 1679.

- Hooker, S.B., Clementson, L., Thomas, C.S., Schlüter, L., Allerup, M., Ras, J., Claustre, H., Normandeau, C., Cullen, J., Kienast, M., Kozłowski, W., Vernet, S., Chakraborty, S., Lohrenz, S., Tuel, M., Redalje, D., Cartaxana, P., Mendes, C.R., Brotas, V., Prabhu Matondkar, S.G., Neeley, A., Skarstad, E. (2012). The Fifth SeaWiFS HPLC Analysis Round-Robin Experiment (SeaHARRE-5). NASA Technical Memorandum 2012-217503, NASA Goddard Space Flight Center, Greenbelt, Maryland.
- Hoppenrath, M., Elbrächter, M., Drebes, G. (2009). Marine phytoplankton. Selected microphytoplankton species from the North Sea around Helgoland and Sylt. Kleine Senckenberg-Reihe Band 49, Germany. 264 pp.
- Icelly, J.D., Moore, G.F., Cristina, S.C., Goela, P.C., Newton, A. (2013). Linking MERIS validation at Sagres, SW Portugal with validation of OLCI and SLSTR sensors on Sentinel-3. Poster presentation at ESA Living Planet Symposium, 2013 Edinburgh, UK, 9-13th September.
- IOCCG (2000). Remote Sensing of Ocean Colour in Coastal, and Other Optically-Complex, Waters. Sathyendranath, S. (ed.), Reports of the International Ocean-Colour Coordinating Group, No. 3, IOCCG, Dartmouth, Canada. 145 pp.
- IOCCG (2006). Remote Sensing of Inherent Optical Properties: Fundamentals, Tests of Algorithms, and Applications. Lee, Z.-P. (ed.), Reports of the International Ocean-Colour Coordinating Group, No. 5, IOCCG, Dartmouth, Canada. 122 pp.
- IOCCG (2009). Partition of the Ocean into Ecological Provinces: Role of Ocean-Colour Radiometry. Dowell, M. and Platt, T. (eds.), Reports of the International Ocean-Colour Coordinating Group, No. 9, IOCCG, Dartmouth, Canada. 109 pp.
- IOCCG (2012). Mission Requirements for Future Ocean-Colour Sensors. McClain, C. and Meister, G. (ed.), Reports of the International Ocean-Colour Coordinating Group, No. 13, IOCCG, Dartmouth, Canada. 115 pp.
- Jeffrey, S.W., Vesk, M. (1997). Introduction to marine phytoplankton and their pigment signatures. In: Jeffrey, S.W., Mantoura, R.F.C., Wright, S.W. (Eds.), *Phytoplankton Pigments in Oceanography: Guidelines to Modern Methods*. : UNESCO Monogr.Oceanogr. Methodol., Vol. 10. UNESCO Publishing, Paris, 37 – 84 pp.
- Jolliff, J.K., Kindle, J.C., Shulman, I., Penta, B., Friedrichs, M.A.M., Helber, R., Arnone, R.A. (2009). Summary diagrams for coupled hydrodynamic-ecosystem model skill assessment. *Journal of Marine Systems*, 76, 64 – 82.

- Kahru, M., Mitchell, B.G. (1999). Empirical chlorophyll algorithm and preliminary SeaWiFS validation for the Californian Current. *International Journal of Remote Sensing*, 20, 3423 - 3429.
- Kahru, M., Kudela, R.M., Manzano-Sarabia, M., Mitchell, B.G. (2012). Trends in the surface chlorophyll of the California Current: Merging data from multiple ocean color satellites. *Deep-Sea Research Part II*, 77-80, 89 – 98.
- Kirk, J.T.O. (1994). *Light and photosynthesis in aquatic ecosystems*. Cambridge University Press, Cambridge. 662 pp.
- Komick, N.M., Costa, M.P.F., Gower, J. (2009). Bio-optical algorithm evaluation for MODIS for western Canada coastal waters: An exploratory approach using in situ reflectance. *Remote Sensing of Environment*, 113, 794 - 804.
- Kostadinov, T. S., Siegel, D. A., Maritorena, S. (2009). Retrieval of the particle size distribution from satellite ocean color observations. *Journal of Geophysical Research*, 114, C09015.
- Kraay, G.W., Zapata, M., Veldhuis, M.J.W. (1992). Separation of chlorophylls c1, c2, and c3 of marine phytoplankton by reversed-phase-C18-high-performance liquid chromatography. *Journal of Phycology*, 28, 708-712.
- Kudela, R., Pitcher, G., Probyn, T., Figueiras, F., Moita, T., Trainer, V. (2005). Harmful algal blooms in coastal upwelling systems. *Oceanography* 18, 184 – 197.
- Kywalyanga, M.S., Naik, R., Hegde, S., Raman, M., Barlow, R. and Roberts, M. (2007). Phytoplankton biomass and primary production in Delagoa Bight Mozambique: Application of Remote Sensing. *Estuarine, Coastal and Shelf Science*, 74, 429 - 436.
- Le Quéré, C., Harrison, S.P., Prentice, I.C., Buitenhuis, E.T., Aumont, O., Bopp, L., Claustre, H., Cotrim da Cunha, L., Geider, R., Giraud, X., Klaas, C., Kohfeld, K.E., Legendre, L., Manizza, M., Platt, T., Rivkin, R.B., Sathyendranath, S., Uitz, J., Watson, A., Wolf-Gladrow, A. (2005). Ecosystem dynamics based on plankton functional types for global ocean biogeochemistry models. *Global Change Biology*, 11, 2016-2040.
- Leal, M.C., Sá, C., Nordez, S., Brotas, V., Paula, J. (2009). Distribution and vertical dynamics of planktonic communities at Sofala Bank, Mozambique. *Estuarine, Coastal and Shelf Science*, 84, 605 - 616.
- Lee, Z-P., Hu, C. (2006). Global distribution of Case-1 waters: An analysis from SeaWiFS measurements. *Remote Sensing of Environment*, 101, 270 - 276.

- Lee, Z.-P., Carder, K.L., Arnone R.A. (2002). Deriving inherent optical properties from water color: a multiband quasi-analytical algorithm for optically deep waters. *Applied Optics*, 41, 5755 – 5772.
- Lee, Z.-P., Darecki, M., Carder, K.L., Davis, C.O., Stramski, D., Rhea, W.J. (2005). Diffuse attenuation coefficient of downwelling irradiance: An evaluation of remote sensing methods. *Journal of Geophysical Research*, 110, C02017.
- Loisel, H., Morel, A. (1998). Light scattering and chlorophyll concentration in case 1 waters: a re-examination. *Limnology and Oceanography*, 43, 847 - 857.
- Longhurst, A. (1998). *Ecological geography of the sea*. Academic Press, San Diego. pp. 398 ISBN 0-12-455558-6.
- Maritorena, S., Siegel, D.A. (2005). Consistent merging of satellite ocean color data using a semi-analytical model. *Remote Sensing of Environment*, 94, 429 - 440.
- Maritorena, S., Siegel, D.A., Peterson, A.R. (2002). Optimization of a semianalytical ocean color model for global-scale applications. *Applied Optics-LP*, 41, 2705 - 2714.
- Martin, S. (2004). *An introduction to ocean remote sensing*. Cambridge University Press, Cambridge, UK. 476 pp.
- Mason, E., Coombs, S., Oliveira, P.B. (2005). An overview of the literature concerning the oceanography of the eastern North Atlantic region. *Relat. Cient. Téc. IPIMAR, Série digital nº 33*, 58 pp. Available in the website: <http://ipimar-iniap.ipimar.pt>
- McClain, C.R. (2009). A Decade of Satellite Ocean Color Observations. *The Annual Review of Marine Science*, 1, 19-42.
- McClain, C.R., Christian, J.R., Signorini, S.R., Lewis, M.R., Asanuma, I., Turk, D., Dupouy-Douchement, C. (2002). Satellite ocean color observations of the tropical Pacific Ocean. *Deep Sea Research Part II*, 49, 2533 - 2560.
- Mendes, C.R., Cartaxana P., Brotas, V. (2007). HPLC determination of microalgae pigments: comparing resolution and sensitivity of a C18 and a C8 method. *Limnology and Oceanography: Methods*, 5, 363 - 370.
- Mendes, C.R., Sá, C., Vitorino, J., Borges, C., Brotas, V. (2011). Spatial distribution of phytoplankton communities in the Nazaré submarine canyon region (Portugal): HPLC-CHEMTAX approach. *Journal of Marine Systems*, 87, 90-101.

- Mendonça, A., Figueiredo, M., Bashmachnikov, I., Couto, A., Lafon, V., Aristegui, J. (2010). Evaluation of ocean color and sea surface temperature sensors algorithms using in situ data: a case study of temporal and spatial variability on two northeast Atlantic seamounts. *Journal of Applied Remote Sensing*, 4, 043506.
- Mendonça, A., Aristegui, J., Vilas, J.C., Montero, M.F., Ojeda, A., Espino, M., Martins, A. (2012). Is there a Seamount effect on microbial community structure and biomass? The case of Seine and Sedlo Seamounts (Northeast Atlantic). *Plos One*, 7, 29526.
- Mitchell, B.G., Bricaud, A., Carder, K., Cleveland, J., Ferrari, G., Gould, R., Kahru, M., Kishino, M., Maske, H., Moisan, T., Moore, L., Nelson, N., Phinney, D., Reynolds, R., Sosik, H., Stramski, D., Tassan, S., Trees, C., Weidemann, A., Wieland J., Vodacek, A. (2000). Determination of spectral absorption coefficients of particles, dissolved material and phytoplankton for discrete water samples. In: *Ocean Optics Protocols For Satellite Ocean Color Sensor Validation*. NASA/TM-2000-209966, 125 - 153.
- Mobley, C.D., Stramski, D., Bissett, W.P., Boss, E. (2004). Optical Modeling of Ocean Waters: Is the Case 1 - Case 2 Classification Still Useful? *Oceanography Journal*, 17, 60-67.
- Moita, M.T. (2001). Structure, variability and dynamics of phytoplankton from the Portuguese continental coast. PhD dissertation, University of Lisbon, Lisbon. 272pp.
- Moore, T.S., Campbell, J.W., Feng, H. (2001). A Fuzzy Logic Classification Scheme for Selecting and Blending Satellite Ocean Color Algorithms. *IEEE Transactions on Geoscience and Remote Sensing*, 39, 1764 – 1776.
- Morel, A. (1988). Optical modeling of the upper ocean in relation to its biogenous matter content (case 1 water). *Journal of Geophysical Research*, 93, 749 - 768.
- Morel, A. (1997). Consequences of a *Synechococcus* bloom upon the optical properties of oceanic (case 1) waters. *Limnology and Oceanography*, 42, 1746 - 1754.
- Morel, A., Prieur, L. (1977). Analysis of variations in ocean color. *Limnology and Oceanography* 22, 709 - 722.
- Morel, A., Maritorena, S. (2001). Bio-optical properties of oceanic waters: A reappraisal. *Journal of Geophysical Research*, 10, 7163 - 7180.
- Morel, A., Bélanger, S. (2006). Improved Detection of turbid waters from Ocean Color information. *Remote Sensing of Environment*, 102, 237 – 249.
- Morel, A., Antoine, D. (2011). Algorithm theoretical basis document 2.9: Pigment index retrieval in Case 1 waters. Available in the website: <http://envisat.esa.int/instruments/meris/pdf/>

- Morel, A., Huot, Y., Gentili, B., Werdell, P.J., Hooker, S.B., Franz, B.A. (2007). Examining the consistency of products derived from various ocean color sensors in open ocean (case 1) waters in the perspective of a multi-sensor approach. *Remote Sensing of Environment*, 111, 69-88.
- Muacho, S., da Silva, J.C.B., Brotas, V., Oliveira, P.B. (2013). Effect of internal waves on near-surface chlorophyll concentration and primary production in the Nazaré Canyon (west of the Iberian Peninsula). *Deep Sea Research Part I: Oceanographic Research Papers*, 81, 89 – 96.
- Nair, A., Sathyendranath, S., Platt, T., Morales, J., Stuart, V., Forget, M.-H., Devred, E., Bouman, H. (2008). Remote sensing of phytoplankton functional types. *Remote Sensing of Environment*, 112, 3366 – 3375.
- Ohde, T., Siegel, H., Gerth, M. (2007). Validation of MERIS Level-2 products in the Baltic Sea, the Namibian coastal area and the Atlantic Ocean. *International Journal of Remote Sensing*, 28, 609 - 624.
- Oliveira, P.B., Nolasco, R., Dubert, J., Moita, T., Peliz, A. (2009a). Surface temperature, chlorophyll and advection patterns during a summer upwelling event off central Portugal. *Continental Shelf Research*, 29, 759 - 774.
- Oliveira P.B., Moita M.T., Silva A., Monteiro I.T., Palma, S. (2009b). Summer diatom and dinoflagellate blooms in Lisbon Bay from 2002 to 2005: pre-conditions inferred from wind and satellite data. *Progress in Oceanography*, 83, 270 – 277.
- O'Reilly, J.E., Maritorena, S., Mitchell, B.G., Siegel, D.A., Carder, K.L., Garver, S.A., Kahru, M., McClain, C. (1998). Ocean color chlorophyll algorithms for SeaWiFS. *Journal of Geophysical Research*, 103, 24937 - 24953.
- O'Reilly, J.E., Maritonema, S., O'Brien, M., Siegel, D., Toole, D., Menzies, D., Smith, R., Muller, J., Mitchell, B.G., Kahru, M., Chavez, F., Strutton, P., Cota, G., Hooker, S., McClain, C., Carder, K., Miller-Karger, F., Harding, L., Magnuson, A., Phinney, D., Moore, G., Aiken, J., Arrigo, K., Letelier, R., Culver, M., (2000). SeaWiFS Postlaunch Calibration and Validation Analyses, Part 3. *NASA Tech. Memo. 2000-206892, Vol. 11*, S.B. Hooker and E.R. Firestone, Eds., NASA Goddard Space Flight Center, 49 pp.
- Peliz, A., Dubert, J., Haidvogel, D.B., Le Cann, B. (2003). Generation and Unstable Evolution of a Density-Driven Eastern Poleward Current: The Iberian Poleward Current. *Journal of Geophysical Research*, 108 (C8), 3268.

- Peliz, A., Dubert, J., Santos, A.M.P., Oliveira, P.B., Le Cann, B. (2005). Winter upper ocean circulation in the Western Iberian Basin — Fronts, Eddies and Poleward Flows: an overview. *Deep Sea Research I*, 52, 621 – 646.
- Preisendorfer, R.W. (1961). Application of radiative transfer theory to light measurements in the sea. *International Union of Geodesy and Geophysical Monographs*, 10, 11 - 30.
- Prieur, L., Sathyendranath, S. (1981). An optical classification of coastal and oceanic waters based on the specific spectral absorption curves of phytoplankton pigments, dissolved organic matter, and other particulate materials. *Limnology and Oceanography*, 26, 671 - 689.
- Quaresma, L.S., Vitorino, J., Oliveira, A., Da Silva, J.C.B. (2007). Evidence of sediment resuspension by nonlinear internal waves on the western Portuguese mid shelf. *Marine Geology*, 246, 123 – 143.
- Raitsos, D.E., Lavender, S.J., Maravelias, C.D., Haralambous, J., Richardson, A.J., Reid, P.C. (2008). Identifying four phytoplankton functional types from space: An ecological approach. *Limnology and Oceanography*, 53, 605 - 613.
- Relvas, P., Barton, E.D. (2002). Mesoscale patterns in the Cape São Vicente (Iberian Peninsula) upwelling region. *Journal of Geophysical Research*, 107(C10), 3164.
- Relvas, P., Barton, E.D., Dubert, J., Oliveira, P.B., Peliz, Á., Da Silva, J.C.B., Santos, A.M.P. (2007). Physical oceanography of the western Iberia ecosystem: latest views and challenges. *Progress in Oceanography*, 74, 149 – 173.
- Ribeiro, S., Amorim, A. (2008). Community structure and seasonality of dinoflagellate cysts in recent sediments from a coastal site in the North-East Atlantic (Lisbon Bay), Portugal. *Marine Micropaleontology*, 68, 156 – 178.
- Ribeiro, A.C., Peliz, A., Santos, A.M.P. (2005). A study of the response of chlorophyll-a biomass to a winter upwelling event off Western Iberia using SeaWiFS and in situ data. *Journal of Marine Systems*, 53, 87 - 107.
- Robinson, I. S. (2004). *Measuring the oceans from space*. Praxis Publishing Ltd, Chichester, UK. 660pp.
- Roesler, C.S. (1998). Theoretical and experimental approaches to improve the accuracy of particulate absorption coefficients derived from the quantitative filter technique. *Limnology and Oceanography*, 43, 1649 - 1660.

- Roy, S., Llewellyn, C., Egelund, E. S., Johnsen, G. (2011). Phytoplankton pigments: Characterization and applications in oceanography. Cambridge University Press. 874pp.
- Ruivo, M., Amorim A., Cartaxana, P. (2011). Effects of growth phase and irradiance on phytoplankton pigment ratios: implications for chemotaxonomy in coastal waters. *Journal of Plankton Research*, 33, 1012-1022.
- Ryan, J.P., Dierssen, H.M., Kudela, R.M., Scholin, C.A., Johnson, K.S., Sullivan, J.M., Fischer, A.M., Rienecker, E.V., McEnaney, P.R., Chavez, F.P. (2005). Coastal ocean physics and red tides: an example from Monterey Bay, California. *Oceanography* 18, 246 - 255.
- Sá C., Da Silva J.C.B., Oliveira P.B., Brotas V. (2008). Comparison of MERIS (ALGAL_1 and ALGAL_2) and MODIS (OCM3) of chlorophyll products and validation with HPLC *in situ* data collected off the Western Iberian Peninsula. Proceedings of '2nd MERIS/(A)ATSR Workshop' (Eds. H. Lacoste & L. Ouwehand), ESA, SP-666 (CD_ROM), European Space Agency, Noordwijk, The Netherlands.
- Sá, C., Leal, M.C., Silva, A., Nordez, S., André, E., Paula, J., Brotas, V. (2013). Variation of phytoplankton assemblages along the Mozambique coast as revealed by HPLC and microscopy. *Journal of Sea Research*, 79, 1 - 11.
- Sathyendranath, S., Stuart, V., Cota, G., Maass, H., Platt, T. (2001). Remote sensing of phytoplankton pigments: A comparison of empirical and theoretical approaches. *International Journal of Remote Sensing*, 22, 249 – 273.
- Sathyendranath, S., Watts, L., Devred, E., Platt, T., Caverhill, C., Maass, H. (2004). Discrimination of diatoms from other phytoplankton using ocean-colour data. *Marine Ecology Progress Series*, 272, 59 – 68.
- Secchi, P.A. (1866). Relazione della esperienze fatte a bordo della Pontificia Pirocorvetta L'Immacolata Concezione per determinare la trasparenza del mare. Translation available, Dept. of the Navy, Office of Chief of Naval Operations, O.N.I. Trans. No. A-655, Op-923 M4B, 21 Dec 1955.
- Sieburth, J.N., Smetacek, V., Lenz, J. (1978). Pelagic ecosystem structure: Heterotrophic compartments of the plankton and their relationship to size fractions. *Limnology and Oceanography*, 23, 1256 – 1263.
- Siegel, D.A., Wang, M., Maritorena, S., Robinson, W. (2000). Atmospheric correction of satellite ocean color imagery: The black pixel assumption. *Applied Optics*, 39, 3582 – 2591.

- Sieracki, M.E., Verity, P.G., Stoecker, D.K. (1993). Plankton community response to sequential silicate and nitrate depletion during the 1989 North Atlantic spring bloom. *Deep-Sea Research Part II*, 40, 213 - 225.
- Silva, A., Mendes, C.R., Palma, S., Brotas, V. (2008). Short time variation of phytoplankton succession, during one year, in Lisbon Bay (Portugal) as revealed by microscopy cells counts and HPLC pigment analysis. *Estuarine, Coastal and Shelf Science*, 79, 230 - 238.
- Silva, A., Palma, S., Oliveira, P.B., Moita, M.T. (2009). Composition and interannual variability of phytoplankton in a coastal upwelling region (Lisbon Bay, Portugal). *Journal of Sea Research*, 62, 238 – 249.
- Silva, A., Brotas, V., Valente, A., Sá, C., Diniz, T., Patarra, R.F., Álvaro, N., Neto, A. (2013). Coccolithophores species as indicators of oceanographic conditions in the Azores region. *Estuarine, Coastal and Shelf Science*, 118, 50 - 59.
- Siokou-Frangou, I., Christaki, U., Mazzocchi, M.G., Montresor, M., Ribera D'Alcala, M., Vaque, D., Zingone, A. (2009). Plankton in the open Mediterranean Sea: A review. *Biogeosciences D.*, 6 (6), 11 187–11 293.
- Smith, R.C., Wilson, W.H. (1981). Ship and satellite bio-optical research in the California Bight, in: *Oceanography From Space*, Gower, J.F.R. (Ed.) Plenum, New York, 281 - 294.
- Smyth, T.J., Tilstone, G.H., Groom, S.B. (2005). Integration of radiative transfer into satellite models of ocean primary production. *Journal of Geophysical Research*, 110, C10014.
- Šolić, M., Krstulović, N., Kušpilić, G., Ninčević Gladan, Ž., Bojanić, N., Šestanović, S., Šantić, D., Ordulj, M. (2010). Changes in microbial food web structure in response to changed environmental trophic status: A case study of the Vranjic Basin (Adriatic Sea). *Marine Environmental Research*, 70, 239 – 249.
- Sorensen, K., Aas, E., Hokedal, J. (2007). Validation of MERIS water products and bio-optical relationships in the Skagerrak. *International Journal of Remote Sensing*, 28, 555 - 568.
- Stramska, M., Stramski, D. (2005) Effects of a nonuniform vertical profile of chlorophyll concentration on remote-sensing reflectance of the ocean. *Applied Optics*, 44, 1735 - 1747.
- Stramski, D., Kiefer, D.A. (1991). Light scattering by microorganisms in the open ocean. *Progress in Oceanography*, 28, 343 - 383.

- Subramaniam, A., Carpenter, E.J., Karentz, D., Falkowski, P.G. (1999). Bio-optical properties of the marine diazotrophic cyanobacteria *Trichodesmium* spp. I. Absorption and photosynthetic action spectra. *Limnology and Oceanography*, 44, 608 - 617.
- Subramaniam, A., Brown, C.W., Hood, R.R., Carpenter, E.J., Capone, D.G. (2002). Detecting *Trichodesimum* blooms in SeaWiFS imagery. *Deep Sea Research Part II*, 49, 107 – 121.
- Sverdrup, H.U. (1953). On conditions for the vernal blooming of phytoplankton. *Journal du Conseil Permanent International Pour L'Exploration de la Mer*, 18, 287 – 295.
- Tassan, S., Ferrari, G.M. (1995). An alternative approach to absorption measurements of aquatic particles retained on filters. *Limnology and Oceanography*, 40, 1358 - 1368.
- Tassan, S., Ferrari, G.M., Bricaud, A., Babin, M. (2000). Variability of the amplification factor of light absorption by filter-retained aquatic particles in the coastal environment. *Journal of Plankton Research*, 22, 639 - 657.
- Taylor, K.E. (2001). Summarizing multiple aspects of model performance in a single diagram. *Journal of Geophysical Research*, 106, D7, 7183 - 7192.
- Tett, P., Gowen, R., Mills, D., Fernandes, T., Gilpin, L., Huxham, M., Kennington, K., Read, P., Service, M., Wilkinson, M., Malcolm, S. (2007). Defining and detecting undesirable disturbance in the context of marine eutrophication. *Marine Pollution Bulletin*, 55, 282 – 297.
- Tilstone, G.H., Smyth, T.J., Gowen, R.J., Martinez-Vicente, V., Groom, S.B. (2005). Inherent optical properties of the Irish Sea and their effect on satellite primary production algorithms. *Journal of Plankton Research*, 27, 1127 - 1148.
- Trees, C.C., Clark, D.K., Bidigare, R.R., Ondrusek, M.E., Mueller, J.L. (2000). Accessory pigments versus chlorophyll a concentration within the euphotic zone: an ubiquitous relationship. *Limnology and Oceanography*, 45, 1130 - 1143.
- Uitz, J., Claustre, H., Morel, A., Hooker, S.B. (2006). Vertical distribution of phytoplankton communities in open ocean: An assessment based on surface chlorophyll. *Journal of Geophysical Research*, 111, CO8005.
- Valente, A., Da Silva, J.C.B. (2009). On the observability of the fortnightly cycle of the Tagus estuary turbid plume using Modis ocean colour images. *Journal of Marine Systems*, 75, 131 – 137.
- Vantrepotte, V., Brunet, C., Mériaux, X., Lécuyer, E., Vellucci, V., Santer, R. (2007). Bio-optical properties of coastal waters in the Eastern English Channel. *Estuarine, Coastal and Shelf Science*, 72, 201 - 212.

- Vidussi, F., Claustre, H., Manca, B.B., Luchetta, A., Marty, J.C. (2001). Phytoplankton pigment distribution in relation to upper thermocline in the eastern Mediterranean Sea during winter. *Journal of Geophysical Research*, 106, 19939 - 19956.
- Volpe, G., Santoleri, R., Velluci, V., Ribera d'Alcalà, M., Marullo, S., D'Ortenzio, F. (2007). The colour of the Mediterranean Sea: Global versus regional bio-optical algorithms evaluation and implication for satellite chlorophyll estimates. *Remote Sensing of Environment*, 107, 625 - 638.
- Werdell, P.J., Bailey, S.W., Franz, B.A., Harding, L.W., Feldman, G.C., McClain, C.R. (2009). Regional and seasonal variability of chlorophyll-a in Chesapeake Bay as observed by SeaWiFS and MODIS-Aqua. *Remote Sensing of Environment*, 113, 1319 - 1330.
- Worden, A.Z., Not, F. (2008). Ecology and diversity of picoeukaryotes. In D. L. Kirchman (Ed.), *Microbial ecology of the oceans*, 2nd ed. John Wiley & Sons, 159-205 pp.
- Wright, S.W., Jeffrey, S.W. (2006). Pigment markers for phytoplankton production. In: Volkmann, J.K. (Ed.), *Marine Organic Matter: Biomarkers, Isotopes and DNA*. Springer-Verlag, Berlin, 71–104 pp.
- Yoder, J.A., Kennelly, M.A., Doney, S.C., Lima, I.D. (2010). Are trends in SeaWiFS chlorophyll time-series unusual relative to historic variability? *Acta Oceanologica Sinica*, 29, 1 – 4.
- Zapata, M., Rodriguez, F., Garrido, J.L. (2000). Separation of chlorophylls and carotenoids from marine phytoplankton: A new HPLC method using a reversed phase C8 column and pyridine-containing mobile phases. *Marine Ecology Progress Series*, 195, 29-45.
- Zhang, X., Lewin, M.R., Johnson, B. (1998). The influence of bubbles on scattering of light in the Ocean. *Applied Optics*, 37, 6525-6536.
- Zhang, C., Hu, C., Shang, S., Müller-Karger, F.E., Li, Y., Dai, M., Huang, B., Ning, X., Hong, H. (2006). Bridging between SeaWiFS and MODIS for continuity of chlorophyll-a concentration assessments off Southeastern China. *Remote Sensing of Environment*, 102, 250 – 263.
- Zibordi, G., Berthon, J.-F., Doyle, J.P., Grossi, S., van der Linde, D., Targa, C., Alberotanza, L. (2002). Coastal Atmosphere and Sea Time Series (CoASTS), Part 1: A long-term measurement program. NASA Tech. Memo. 2002-206892, v. 19, edited by: Hooker, S. B. and Firestone, E. R., NASA Goddard Space Flight Center, Greenbelt, Maryland, 29 pp.
- Zibordi, G., Mélin, F., Hooker, S. B., D'Alimonte, D., Holben, B. (2004). An autonomous above-water system for the validation of ocean color radiance data. *IEEE Transactions, Geoscience and Remote Sensing*, 42, 401 – 415.

- Zibordi, G., Berthon, J.-F., Mélin, F., D'Alimonte, D. (2011). Cross-site consistent in situ measurements for satellite ocean color applications: The BiOMaP radiometric dataset. *Remote Sensing of Environment*, 115, 2104 – 2115.
- Zibordi, G., Mélin, F., Berthon, J.-F. (2012). Intra-annual variations of biases in remote sensing primary ocean color products at a coastal site. *Remote Sensing of Environment*, 124, 627 – 636.
- Zibordi, G., Mélin, F., Berthon, J.-F., Canuti, E. (2013). Assessment of MERIS ocean color data products for European seas, *Ocean Science*, 9, 521 – 533.

Annex I: Dataset

Phytoplankton pigment data used in this thesis after quality control

Data Policy

The full dataset used in this thesis is presented here after. This dataset was obtained through the collaboration with several Institutions. I declare that I participated in the sampling planning of all projects presented here. In addition, I was also actively involved in the laboratory processing activities.

These data can be used for research purposes. However, authorization from Principal Investigator is mandatory. Researchers interested in using these data need to contact directly the PI. Co-authorship of any publication should be offered.

Abbreviation index

Ref – Sample reference number

CC – Cruise code

TChla – Total Chlorophyll *a* (DvChla+mvChla+epimers+alomers+chlorophyllide)

Fuc - Fucoxanthin

Per - Peridin

Hex - Hexanthin

But – 19'Butanoyloxyfucoxanthin

Alo - Aloxanthin

Clb – Chlorophyll *b*

Zea – Zeaxanthin

Cruise: RV Pelagia 2005 (PG05)

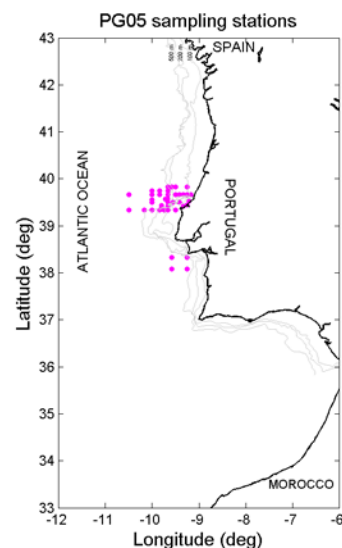
Cruise host: NIOZ

Chief Scientist: Dr. Henko De Stigter

Methods summary: GF/F filters (47mm), 4-5 L filtered, HPLC C18

Samples collected and filtered by: Carolina Sá

Samples processed by: Carolina Sá, Rafael Mendes



Ref	CC	Date (dd-mm-yy)	Time (UTC)	Latitude (N)	Longitude (W)	Sample Depth (m)	Pigments concentration ($\mu\text{g L}^{-1}$)							
							TChla	Fuc	Per	Hex	But	Alo	Clb	Zea
1	1	28/04/05	14:40	39.566	-9.717	5	0.54	0.29	0.01	0.08	0.02	0.02	0.04	0.01
2	1	29/04/05	16:21	39.439	-9.792	5	0.38	0.08	0.01	0.23	0.03	0.01	0.03	0.01
3	1	29/04/05	16:21	39.439	-9.792	5	0.24	0.04	0.01	0.15	0.02	0.00	0.02	0.01
4	1	03/05/05	19:27	39.667	-9.167	5	0.22	0.04	0.01	0.05	0.01	0.00	0.05	0.00
5	1	03/05/05	20:15	39.667	-9.333	5	0.17	0.02	0.01	0.08	0.01	0.00	0.04	0.00
6	1	03/05/05	21:03	39.667	-9.500	5	0.16	0.02	0.01	0.05	0.01	0.00	0.04	0.00
7	1	03/05/05	21:54	39.667	-9.667	5	0.12	0.02	0.01	0.07	0.01	0.00	0.01	0.01
8	1	03/05/05	22:40	39.667	-9.833	5	0.18	0.01	0.01	0.06	0.01	0.00	0.03	0.04
9	1	03/05/05	23:30	39.667	-10.000	5	0.13	0.03	0.01	0.07	0.01	0.01	0.01	0.05
10	1	04/05/05	02:01	39.667	-10.500	5	0.15	0.01	0.01	0.09	0.01	0.00	0.02	0.04
11	1	04/05/05	18:58	39.333	-9.500	5	1.20	0.69	0.01	0.06	0.01	0.01	0.06	0.00
12	1	04/05/05	20:37	39.333	-9.833	5	1.10	0.57	0.02	0.11	0.01	0.01	0.14	0.01
13	1	04/05/05	21:38	39.333	-10.000	5	0.20	0.04	0.01	0.05	0.00	0.00	0.05	0.01
14	1	04/05/05	22:35	39.333	-10.167	5	0.17	0.02	0.01	0.07	0.01	0.00	0.05	0.01
15	1	05/05/05	00:25	39.333	-10.500	5	0.18	0.02	0.00	0.08	0.04	0.00	0.03	0.03
16	1	05/05/05	22:05	39.500	-9.833	5	0.14	0.01	0.01	0.09	0.01	0.00	0.02	0.02
17	1	05/05/05	23:03	39.333	-9.833	5	0.69	0.33	0.01	0.11	0.01	0.00	0.10	0.01
18	1	05/05/05	23:27	39.333	-9.750	5	1.40	1.08	0.02	0.09	0.01	0.00	0.09	0.01
19	1	05/05/05	23:53	39.333	-9.667	5	2.12	1.17	0.02	0.11	0.01	0.01	0.13	0.01
20	1	06/05/05	00:33	39.417	-9.667	5	0.56	0.21	0.01	0.11	0.01	0.00	0.11	0.01
21	1	06/05/05	01:10	39.500	-9.667	5	0.25	0.06	0.01	0.06	0.01	0.00	0.04	0.01
22	1	06/05/05	01:45	39.583	-9.667	5	0.21	0.03	0.01	0.07	0.01	0.00	0.06	0.01
23	1	06/05/05	02:20	39.667	-9.667	5	0.13	0.02	0.01	0.06	0.01	0.00	0.05	0.01
24	1	06/05/05	02:53	39.750	-9.667	5	0.23	0.02	0.01	0.10	0.02	0.00	0.05	0.02
25	1	06/05/05	03:25	39.833	-9.667	5	0.21	0.02	0.01	0.08	0.01	0.00	0.05	0.01
26	1	06/05/05	03:52	39.833	-9.583	5	0.19	0.03	0.01	0.06	0.01	0.00	0.05	0.01
27	1	06/05/05	04:15	39.833	-9.500	5	0.30	0.03	0.01	0.12	0.01	0.00	0.09	0.01
28	1	06/05/05	05:15	39.667	-9.500	5	0.28	0.05	0.01	0.10	0.02	0.00	0.06	0.01
29	1	07/05/05	01:26	39.667	-9.333	5	0.42	0.19	0.01	0.06	0.01	0.00	0.08	0.01
30	1	07/05/05	03:00	39.417	-9.333	5	2.72	1.54	0.02	0.06	0.00	0.00	0.11	0.00
31	1	07/05/05	04:38	39.667	-9.250	5	0.45	0.19	0.01	0.04	0.01	0.00	0.06	0.01
32	1	07/05/05	05:27	39.833	-9.250	5	0.24	0.07	0.01	0.05	0.01	0.00	0.04	0.01

Ref	CC	Date (dd-mm-yy)	Time (UTC)	Latitude (N)	Longitude (W)	Sample Depth (m)	Pigments concentration (μgL^{-1})							
							Tchl a	Fuc	Per	Hex	But	Alo	Clb	Zea
33	1	09/05/05	21:53	39.525	-9.208	5	0.45	0.26	0.01	0.06	0.00	0.00	0.05	0.01
34	1	10/05/05	01:22	39.450	-9.250	5	0.71	0.46	0.01	0.06	0.00	0.00	0.07	0.01
35	1	10/05/05	03:50	39.667	-9.417	5	0.19	0.02	0.01	0.09	0.01	0.00	0.03	0.01
36	1	10/05/05	04:50	39.500	-9.417	5	0.28	0.11	0.01	0.08	0.01	0.00	0.04	0.01
37	1	11/05/05	21:14	39.333	-10.000	5	0.07	0.00	0.01	0.02	0.00	0.00	0.02	0.00
38	1	11/05/05	22:21	39.500	-10.000	5	0.12	0.00	0.01	0.03	0.01	0.00	0.03	0.00
39	1	11/05/05	00:00	39.750	-10.000	5	0.08	0.00	0.02	0.04	0.01	0.00	0.01	0.00
40	1	12/05/05	00:48	39.750	-9.833	5	0.13	0.02	0.01	0.06	0.01	0.00	0.02	0.03
41	1	12/05/05	01:16	39.667	-9.833	5	0.20	0.05	0.01	0.06	0.01	0.00	0.02	0.03
42	1	12/05/05	03:07	39.500	-9.667	5	0.14	0.01	0.01	0.04	0.00	0.00	0.03	0.01
43	1	12/05/05	04:08	39.667	-9.667	5	0.10	0.01	0.01	0.05	0.01	0.00	0.01	0.00
44	1	13/05/05	10:00	39.500	-9.551	5	0.20	0.05	0.01	0.07	0.00	0.00	0.02	0.01
45	1	15/05/05	09:10	39.550	-10.000	5	0.11	0.01	0.01	0.04	0.01	0.00	0.01	0.00
46	1	16/05/05	20:55	38.333	-9.250	5	0.46	0.17	0.06	0.10	0.02	0.01	0.07	0.04
47	1	16/05/05	22:50	38.333	-9.583	5	0.93	0.27	0.11	0.19	0.01	0.02	0.17	0.04
48	1	17/05/05	02:15	38.083	-9.583	5	0.16	0.04	0.01	0.06	0.02	0.00	0.01	0.01
49	1	17/05/05	03:54	38.083	-9.250	5	0.15	0.05	0.01	0.06	0.02	0.00	0.01	0.01

Cruise: NR Noruega 2005 (NR05)

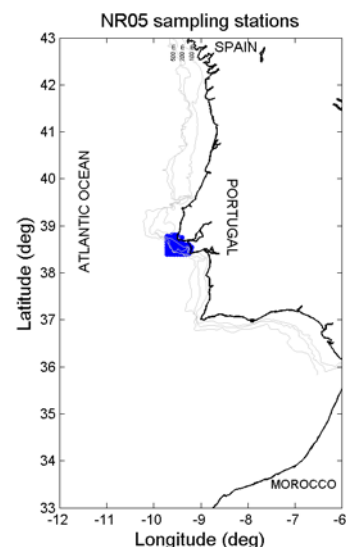
Cruise host: IPIMAR

Chief Scientist: Dra. Teresa Moita

Methods summary: GF/F filters (47mm), 4-5 L filtered, HPLC C18

Samples collected and filtered by: Carolina Sá, Miguel Leal, Rafael Mendes

Samples processed by: Carolina Sá, Rafael Mendes



Ref	CC	Date (dd-mm-yy)	Time (UTC)	Latitude (N)	Longitude (W)	Sample Depth (m)	Pigments concentration ($\mu\text{g L}^{-1}$)							
							TChla	Fuc	Per	Hex	But	Alo	Clb	Zea
50	2	30/08/05	07:15	38.410	-9.257	1	0.42	0.16	0.01	0.06	0.01	0.01	0.02	0.07
51	2	30/08/05	08:05	38.400	-9.302	1	0.44	0.22	0.01	0.06	0.01	0.00	0.02	0.04
52	2	30/08/05	09:01	38.400	-9.359	1	0.54	0.29	0.00	0.05	0.01	0.02	0.02	0.02
53	2	30/08/05	10:20	38.400	-9.404	1	0.48	0.20	0.00	0.04	0.01	0.00	0.02	0.03
54	2	30/08/05	11:33	38.400	-9.447	1	0.38	0.14	0.00	0.06	0.00	0.00	0.02	0.06
55	2	30/08/05	12:52	38.400	-9.501	1	0.38	0.14	0.02	0.09	0.01	0.01	0.01	0.06
56	2	30/08/05	13:54	38.400	-9.546	1	0.52	0.23	0.02	0.06	0.01	0.02	0.02	0.04
57	2	30/08/05	15:01	38.400	-9.595	1	0.17	0.05	0.01	0.03	0.01	0.00	0.01	0.03
58	2	30/08/05	16:09	38.400	-9.642	1	0.21	0.06	0.01	0.05	0.01	0.01	0.01	0.02
59	2	30/08/05	17:33	38.390	-9.711	1	0.08	0.00	0.00	0.02	0.00	0.00	0.00	0.05
60	2	30/08/05	18:41	38.450	-9.713	1	0.14	0.03	0.00	0.03	0.01	0.00	0.01	0.06
61	2	30/08/05	19:43	38.450	-9.648	1	0.20	0.07	0.00	0.04	0.01	0.00	0.02	0.03
62	2	30/08/05	20:39	38.450	-9.597	1	0.24	0.09	0.00	0.04	0.02	0.00	0.02	0.04
63	2	30/08/05	21:30	38.450	-9.553	1	0.40	0.20	0.01	0.06	0.01	0.00	0.02	0.05
64	2	30/08/05	22:15	38.450	-9.500	1	0.58	0.23	0.01	0.06	0.01	0.02	0.03	0.05
65	2	30/08/05	23:22	38.450	-9.452	1	0.40	0.20	0.00	0.05	0.00	0.00	0.02	0.05
66	2	31/08/05	00:30	38.450	-9.404	1	0.83	0.44	0.02	0.08	0.01	0.01	0.04	0.07
67	2	31/08/05	01:15	38.450	-9.351	1	0.63	0.30	0.01	0.07	0.01	0.01	0.03	0.04
68	2	31/08/05	02:11	38.450	-9.300	1	0.49	0.23	0.00	0.04	0.00	0.00	0.02	0.03
69	2	31/08/05	03:07	38.450	-9.250	1	0.67	0.24	0.03	0.07	0.01	0.03	0.03	0.04
70	2	31/08/05	03:46	38.450	-9.217	1	1.01	0.35	0.03	0.09	0.01	0.06	0.04	0.05
71	2	31/08/05	04:31	38.500	-9.205	1	0.57	0.17	0.03	0.10	0.01	0.02	0.04	0.06
72	2	31/08/05	05:16	38.500	-9.253	1	0.86	0.42	0.02	0.07	0.01	0.01	0.03	0.02
73	2	31/08/05	06:07	38.500	-9.298	1	0.65	0.33	0.01	0.06	0.01	0.01	0.02	0.04
74	2	31/08/05	06:52	38.500	-9.354	1	0.67	0.33	0.02	0.07	0.01	0.01	0.03	0.06
75	2	31/08/05	07:48	38.500	-9.400	1	0.80	0.38	0.02	0.09	0.01	0.02	0.03	0.07
76	2	31/08/05	08:33	38.500	-9.455	1	0.31	0.18	0.00	0.04	0.00	0.00	0.01	0.05
77	2	31/08/05	09:18	38.500	-9.498	1	0.50	0.26	0.01	0.05	0.01	0.00	0.02	0.05
78	2	31/08/05	10:09	38.500	-9.554	1	0.40	0.19	0.01	0.05	0.01	0.01	0.02	0.07
79	2	31/08/05	10:54	38.500	-9.596	1	0.23	0.08	0.00	0.04	0.01	0.00	0.01	0.03
80	2	31/08/05	10:54	38.500	-9.596	5	0.21	0.07	0.01	0.03	0.01	0.00	0.01	0.03
81	2	31/08/05	12:01	38.500	-9.642	1	0.20	0.07	0.00	0.04	0.01	0.00	0.01	0.04

Ref	CC	Date (dd-mm-yy)	Time (UTC)	Latitude (N)	Longitude (W)	Sample Depth (m)	Pigments concentration ($\mu\text{g L}^{-1}$)							
							TChla	Fuc	Per	Hex	But	Alo	Clb	Zea
82	2	31/08/05	13:26	38.500	-9.711	1	0.11	0.01	0.00	0.02	0.00	0.00	0.01	0.06
83	2	31/08/05	14:39	38.550	-9.711	1	0.10	0.01	0.00	0.02	0.01	0.00	0.00	0.07
84	2	31/08/05	15:41	38.550	-9.650	1	0.31	0.15	0.00	0.05	0.01	0.01	0.02	0.03
85	2	31/08/05	16:43	38.550	-9.604	1	0.28	0.12	0.00	0.04	0.01	0.00	0.02	0.03
86	2	31/08/05	17:39	38.550	-9.552	1	0.34	0.11	0.00	0.04	0.00	0.00	0.02	0.03
87	2	31/08/05	18:18	38.550	-9.503	1	0.19	0.14	0.00	0.04	0.00	0.01	0.01	0.03
88	2	31/08/05	19:03	38.550	-9.447	1	0.49	0.22	0.01	0.05	0.00	0.01	0.02	0.07
89	2	31/08/05	19:43	38.550	-9.398	1	0.43	0.22	0.01	0.04	0.00	0.00	0.02	0.05
90	2	31/08/05	20:22	38.550	-9.351	1	2.04	1.15	0.03	0.07	0.01	0.02	0.08	0.02
91	2	31/08/05	21:01	38.550	-9.301	1	1.90	1.16	0.04	0.08	0.01	0.06	0.10	0.03
92	2	31/08/05	21:41	38.550	-9.252	1	1.08	0.57	0.01	0.07	0.01	0.02	0.05	0.04
93	2	31/08/05	22:20	38.550	-9.201	1	0.94	0.18	0.07	0.08	0.01	0.15	0.03	0.03
94	2	31/08/05	23:05	38.600	-9.254	1	0.93	0.39	0.02	0.05	0.01	0.02	0.04	0.03
95	2	31/08/05	23:39	38.600	-9.299	1	2.14	1.12	0.05	0.09	0.01	0.08	0.09	0.03
96	2	01/09/05	00:18	38.600	-9.349	1	2.12	0.82	0.04	0.07	0.01	0.16	0.07	0.04
97	2	01/09/05	00:58	38.600	-9.399	1	0.75	0.33	0.03	0.05	0.01	0.03	0.04	0.03
98	2	01/09/05	01:37	38.600	-9.449	1	0.39	0.19	0.00	0.04	0.00	0.00	0.02	0.05
99	2	01/09/05	02:16	38.600	-9.501	1	0.29	0.14	0.00	0.03	0.01	0.00	0.01	0.02
100	2	01/09/05	03:01	38.600	-9.549	1	0.21	0.10	0.00	0.04	0.01	0.00	0.01	0.03
101	2	01/09/05	03:46	38.600	-9.602	1	0.24	0.10	0.00	0.05	0.01	0.00	0.02	0.02
102	2	01/09/05	04:31	38.600	-9.650	1	0.22	0.08	0.00	0.04	0.01	0.00	0.01	0.02
103	2	01/09/05	05:16	38.600	-9.713	1	0.16	0.04	0.00	0.03	0.01	0.00	0.01	0.06
104	2	01/09/05	06:13	38.650	-9.716	1	0.40	0.17	0.01	0.06	0.01	0.01	0.02	0.01
105	2	01/09/05	07:09	38.650	-9.650	1	0.35	0.14	0.01	0.07	0.01	0.00	0.02	0.02
106	2	01/09/05	07:54	38.650	-9.599	1	0.28	0.11	0.00	0.05	0.00	0.00	0.02	0.03
107	2	01/09/05	08:39	38.650	-9.548	1	0.25	0.11	0.00	0.04	0.01	0.00	0.02	0.04
108	2	01/09/05	09:18	38.650	-9.495	1	0.54	0.26	0.01	0.04	0.01	0.00	0.02	0.03
109	2	01/09/05	09:58	38.650	-9.448	1	0.44	0.19	0.00	0.05	0.01	0.00	0.02	0.03
110	2	01/09/05	10:31	38.650	-9.398	1	0.52	0.23	0.00	0.04	0.01	0.01	0.02	0.06
111	2	01/09/05	12:13	38.750	-9.399	1	1.18	0.47	0.02	0.06	0.01	0.03	0.06	0.06
112	2	01/09/05	13:31	38.680	-9.499	1	2.30	0.83	0.05	0.07	0.01	0.17	0.07	0.04
113	2	01/09/05	14:11	38.680	-9.546	1	0.63	0.30	0.00	0.05	0.01	0.01	0.03	0.04
114	2	01/09/05	14:50	38.700	-9.603	1	0.63	0.36	0.01	0.04	0.01	0.01	0.03	0.03
115	2	01/09/05	15:35	38.700	-9.650	1	0.53	0.26	0.01	0.04	0.01	0.01	0.02	0.03
116	2	01/09/05	16:20	38.700	-9.717	1	0.55	0.27	0.01	0.05	0.01	0.01	0.02	0.03
117	2	01/09/05	17:16	38.750	-9.722	1	0.45	0.16	0.01	0.05	0.01	0.01	0.02	0.02
118	2	01/09/05	18:13	38.750	-9.655	1	0.65	0.30	0.01	0.05	0.01	0.01	0.02	0.02
119	2	01/09/05	18:52	38.750	-9.601	1	1.06	0.49	0.01	0.08	0.01	0.04	0.05	0.04
120	2	01/09/05	19:37	38.750	-9.552	1	2.22	1.05	0.04	0.11	0.02	0.04	0.08	0.05
121	2	01/09/05	20:56	38.800	-9.504	1	2.77	1.10	0.04	0.09	0.02	0.15	0.09	0.03
122	2	01/09/05	21:30	38.800	-9.552	1	1.97	1.10	0.05	0.16	0.02	0.04	0.10	0.04
123	2	01/09/05	23:50	38.800	-9.606	1	0.88	0.46	0.02	0.08	0.02	0.02	0.04	0.03
124	2	02/09/05	00:35	38.780	-9.647	1	0.73	0.36	0.01	0.06	0.01	0.01	0.03	0.03
125	2	02/09/05	01:20	38.780	-9.714	1	0.55	0.23	0.02	0.09	0.02	0.02	0.03	0.02

Cruise: RV Pelagia 2006 (PG06)

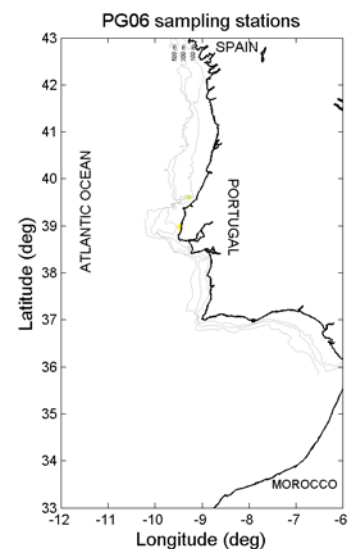
Cruise host: NIOZ

Chief Scientist: Dr. Henko De Stigter

Methods summary: GF/F filters (47mm), 4-5 L filtered, HPLC C18

Samples collected and filtered by: Sérgio Muacho

Samples processed by: Carolina Sá, Rafael Mendes



Ref	CC	Date (dd-mm-yy)	Time (UTC)	Latitude (N)	Longitude (W)	Sample Depth (m)	Pigments concentration ($\mu\text{g L}^{-1}$)							
							TChla	Fuc	Per	Hex	But	Alo	Clb	Zea
126	3	05/09/06	20:48	38.980	-9.487	5	2.67	0.70	1.43	0.15	0.06	0.03	0.06	0.03
127	3	10/09/06	21:27	39.612	-9.292	5	0.32	0.06	0.02	0.05	0.03	0.00	0.04	0.16
128	3	10/09/06	23:28	39.612	-9.291	5	0.15	0.03	0.01	0.03	0.02	0.00	0.02	0.08
129	3	11/09/06	01:23	39.612	-9.292	5	0.18	0.03	0.02	0.03	0.02	0.00	0.02	0.09
130	3	11/09/06	03:26	39.612	-9.292	5	0.20	0.03	0.01	0.04	0.02	0.00	0.02	0.09
131	3	11/09/06	05:32	39.612	-9.292	5	0.18	0.03	0.01	0.03	0.02	0.00	0.02	0.08
132	3	11/09/06	06:42	39.612	-9.292	5	0.24	0.04	0.01	0.04	0.02	0.00	0.02	0.10
133	3	11/09/06	08:59	39.611	-9.291	5	0.20	0.03	0.02	0.03	0.02	0.00	0.02	0.09

Cruise: NR Noruega 2006 (NR06)

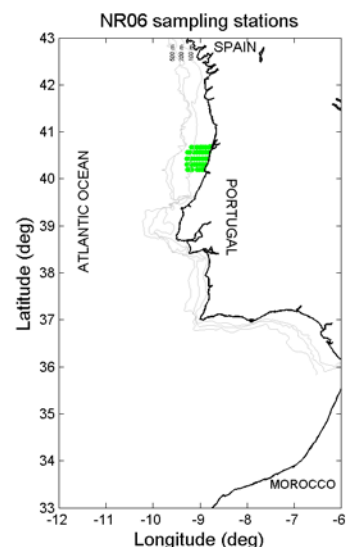
Cruise host: IPIMAR

Chief Scientist: Dra. Teresa Moita

Methods summary: GF/F filters (47mm), 4-5 L filtered, HPLC C18

Samples collected and filtered by: Rafael Mendes, Mónica, Mariana e Marta D.

Samples processed by: Carolina Sá, Rafael Mendes



Ref	CC	Date (dd-mm-yy)	Time (UTC)	Latitude (N)	Longitude (W)	Sample Depth (m)	Pigments concentration ($\mu\text{g L}^{-1}$)							
							TChla	Fuc	Per	Hex	But	Alo	Clb	Zea
134	4	14/09/06	22:00	40.200	-8.927	1	2.20	0.25	1.33	0.27	0.08	0.08	0.15	0.08
135	4	15/09/06	23:00	40.200	-8.967	1	0.90	0.15	0.46	0.12	0.04	0.03	0.12	0.05
136	4	15/09/06	00:00	40.200	-9.017	1	0.41	0.09	0.10	0.06	0.03	0.01	0.06	0.04
137	4	15/09/06	00:30	40.200	-9.068	1	0.20	0.06	0.02	0.05	0.03	0.00	0.03	0.06
138	4	15/09/06	02:00	40.200	-9.164	1	0.16	0.04	0.02	0.03	0.02	0.00	0.02	0.03
139	4	15/09/06	02:45	40.200	-9.172	1	0.30	0.06	0.04	0.05	0.03	0.01	0.03	0.06
140	4	15/09/06	03:40	40.200	-9.216	1	0.47	0.07	0.07	0.09	0.05	0.01	0.06	0.09
141	4	15/09/06	04:40	40.200	-9.267	1	0.25	0.05	0.03	0.06	0.03	0.00	0.03	0.07
142	4	15/09/06	12:40	40.310	-8.887	1	0.86	0.13	0.22	0.26	0.05	0.04	0.09	0.07
143	4	15/09/06	12:10	40.310	-8.936	1	0.51	0.08	0.06	0.15	0.04	0.02	0.07	0.08
144	4	15/09/06	11:20	40.310	-8.976	1	0.34	0.05	0.03	0.06	0.03	0.01	0.03	0.10
145	4	15/09/06	10:15	40.310	-9.019	1	0.23	0.04	0.02	0.04	0.02	0.00	0.02	0.07
146	4	15/09/06	09:45	40.310	-9.072	1	0.33	0.06	0.05	0.07	0.02	0.01	0.03	0.04
147	4	15/09/06	09:00	40.310	-9.116	1	0.27	0.06	0.12	0.05	0.02	0.00	0.02	0.04
148	4	15/09/06	08:00	40.310	-9.179	1	0.30	0.05	0.09	0.04	0.02	0.00	0.03	0.08
149	4	15/09/06	07:00	40.310	-9.216	1	0.33	0.08	0.05	0.11	0.05	0.01	0.04	0.06
150	4	15/09/06	05:55	40.310	-9.273	1	0.35	0.09	0.04	0.12	0.05	0.01	0.03	0.05
151	4	15/09/06	13:35	40.430	-8.851	1	2.83	0.34	2.66	0.33	0.12	0.05	0.09	0.04
152	4	15/09/06	14:25	40.430	-8.879	1	0.48	0.10	0.11	0.27	0.03	0.02	0.06	0.05
153	4	15/09/06	15:10	40.430	-8.930	1	0.34	0.06	0.02	0.09	0.03	0.01	0.04	0.09
154	4	15/09/06	16:00	40.430	-8.970	1	0.31	0.04	0.05	0.06	0.02	0.00	0.03	0.09
155	4	15/09/06	16:45	40.430	-9.019	1	0.31	0.05	0.04	0.07	0.02	0.00	0.03	0.09
156	4	15/09/06	17:30	40.430	-9.066	1	0.30	0.07	0.04	0.07	0.03	0.01	0.03	0.11
157	4	15/09/06	18:15	40.430	-9.130	1	0.27	0.06	0.02	0.06	0.03	0.00	0.02	0.09
158	4	15/09/06	19:00	40.430	-9.178	1	0.40	0.09	0.02	0.09	0.05	0.01	0.03	0.10
159	4	15/09/06	19:20	40.430	-9.211	1	0.33	0.08	0.03	0.12	0.05	0.01	0.03	0.07
160	4	15/09/06	20:20	40.430	-9.273	1	0.24	0.06	0.02	0.08	0.03	0.00	0.02	0.05
161	4	16/09/06	04:30	40.560	-8.819	1	2.48	0.73	0.80	0.43	0.00	0.09	0.08	0.08
162	4	16/09/06	03:40	40.560	-8.877	1	1.79	0.35	0.36	0.49	0.04	0.07	0.17	0.07
163	4	16/09/06	03:10	40.560	-8.927	1	0.48	0.07	0.03	0.13	0.04	0.01	0.05	0.05
164	4	16/09/06	02:20	40.560	-8.967	1	0.25	0.04	0.02	0.08	0.02	0.00	0.02	0.03
165	4	16/09/06	01:45	40.560	-9.017	1	0.61	0.10	0.07	0.30	0.04	0.02	0.05	0.06

Ref	CC	Date (dd-mm-yy)	Time (UTC)	Latitude (N)	Longitude (W)	Sample Depth (m)	Pigments concentration (μgL^{-1})							
							TChla	Fuc	Per	Hex	But	Alo	Clb	Zea
166	4	16/09/06	01:00	40.560	-9.072	1	0.40	0.06	0.08	0.23	0.03	0.01	0.02	0.03
167	4	16/09/06	00:10	40.560	-9.127	1	0.36	0.06	0.05	0.24	0.02	0.01	0.02	0.03
168	4	15/09/06	22:45	40.560	-9.221	1	0.27	0.05	0.02	0.18	0.03	0.01	0.02	0.05
169	4	15/09/06	22:00	40.560	-9.272	1	0.21	0.03	0.01	0.09	0.02	0.00	0.02	0.05
170	4	16/09/06	05:45	40.690	-8.793	1	1.95	0.62	0.47	0.39	0.04	0.08	0.06	0.08
171	4	16/09/06	06:10	40.680	-8.822	1	1.12	0.26	0.18	0.31	0.01	0.03	0.05	0.10
172	4	16/09/06	06:45	40.680	-8.882	1	0.88	0.17	0.21	0.34	0.02	0.02	0.04	0.06
173	4	16/09/06	07:10	40.680	-8.931	1	0.64	0.14	0.07	0.26	0.02	0.01	0.04	0.08
174	4	16/09/06	07:45	40.680	-8.970	1	0.67	0.19	0.04	0.28	0.02	0.01	0.05	0.09
175	4	16/09/06	08:20	40.680	-8.996	1	0.64	0.16	0.10	0.27	0.02	0.01	0.04	0.06
176	4	16/09/06	09:05	40.680	-9.057	1	1.54	0.37	0.50	0.79	0.05	0.06	0.12	0.12
177	4	16/09/06	10:00	40.680	-9.128	1	0.87	0.15	0.21	0.48	0.03	0.02	0.06	0.04
178	4	16/09/06	11:00	40.680	-9.186	1	1.08	0.19	0.10	0.71	0.03	0.03	0.06	0.06

Cruise: NRP D.Carlos I 2006 (**DC06**)

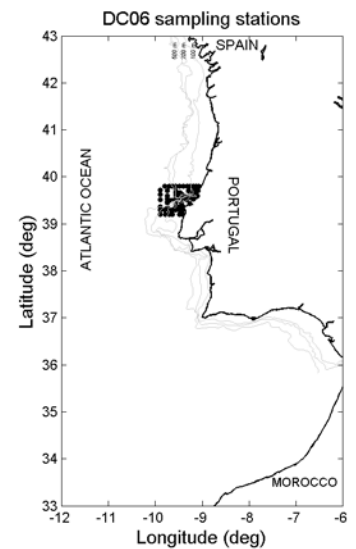
Cruise host: IH

Chief Scientist: Dr. João Vitorino

Methods summary: GF/F filters (47mm), 4-5 L filtered, HPLC C18

Samples collected and filtered by: Carolina Sá, Rafael Mendes, Inês Félix

Samples processed by: Carolina Sá, Rafael Mendes



Ref	CC	Date (dd-mm-yy)	Time (UTC)	Latitude (N)	Longitude (W)	Sample Depth (m)	Pigments concentration ($\mu\text{g L}^{-1}$)							
							TChla	Fuc	Per	Hex	But	Alo	Clb	Zea
179	5	26/06/06	03:27	39.720	-9.900	5	0.17	0.02	0.01	0.04	0.01	0.00	0.01	0.08
180	5	26/06/06	22:59	39.630	-9.900	5	0.22	0.03	0.01	0.06	0.02	0.00	0.02	0.11
181	5	25/06/06	18:48	39.510	-9.900	5	0.18	0.02	0.02	0.05	0.02	0.00	0.02	0.10
182	5	25/06/06	07:51	39.370	-9.900	5	0.24	0.04	0.02	0.06	0.02	0.01	0.02	0.07
183	5	25/06/06	06:25	39.300	-9.900	5	0.26	0.03	0.01	0.07	0.02	0.01	0.03	0.08
184	5	24/06/06	02:16	39.200	-9.900	5	0.14	0.02	0.01	0.04	0.01	0.00	0.01	0.04
185	5	24/06/06	01:31	39.200	-9.780	5	1.20	0.25	0.30	0.15	0.01	0.05	0.05	0.04
186	5	24/06/06	00:46	39.200	-9.700	5	0.74	0.15	0.13	0.13	0.01	0.02	0.04	0.03
187	5	24/06/06	00:08	39.200	-9.630	5	0.93	0.23	0.05	0.13	0.02	0.04	0.10	0.02
188	5	23/06/06	22:42	39.200	-9.480	5	0.34	0.09	0.00	0.05	0.01	0.01	0.02	0.04
189	5	23/06/06	21:43	39.200	-9.410	5	1.12	0.30	0.06	0.17	0.03	0.02	0.08	0.04
190	5	24/06/06	17:48	39.300	-9.410	5	0.59	0.22	0.09	0.12	0.01	0.03	0.06	0.05
191	5	24/06/06	18:28	39.300	-9.480	5	0.11	0.06	0.02	0.06	0.00	0.01	0.02	0.03
192	5	24/06/06	19:18	39.300	-9.570	5	2.83	0.63	0.75	0.21	0.06	0.34	0.15	0.02
193	5	24/06/06	20:18	39.300	-9.630	5	1.43	0.35	0.26	0.12	0.03	0.15	0.10	0.03
194	5	24/06/06	20:58	39.300	-9.700	5	0.28	0.06	0.04	0.08	0.01	0.01	0.02	0.04
195	5	25/06/06	01:54	39.300	-9.800	5	0.14	0.03	0.02	0.05	0.01	0.00	0.01	0.03
196	5	26/06/06	05:47	39.800	-9.800	5	0.18	0.02	0.00	0.06	0.02	0.00	0.01	0.06
197	5	26/06/06	15:38	39.800	-9.080	5	2.37	0.70	0.11	0.36	0.07	0.08	0.46	0.19
198	5	26/06/06	14:46	39.800	-9.130	5	1.13	0.27	0.14	0.32	0.07	0.03	0.16	0.15
199	5	26/06/06	14:05	39.800	-9.190	5	0.78	0.10	0.18	0.16	0.05	0.01	0.07	0.13
200	5	26/06/06	13:21	39.800	-9.250	5	0.50	0.09	0.07	0.16	0.04	0.01	0.06	0.11
201	5	26/06/06	12:27	39.800	-9.320	5	0.48	0.08	0.05	0.16	0.04	0.01	0.06	0.11
202	5	26/06/06	11:24	39.800	-9.400	5	0.44	0.08	0.02	0.21	0.07	0.01	0.08	0.06
203	5	26/06/06	10:44	39.800	-9.480	5	0.23	0.03	0.01	0.09	0.03	0.00	0.02	0.10
204	5	26/06/06	09:22	39.800	-9.570	5	0.20	0.03	0.01	0.07	0.02	0.00	0.01	0.06
205	5	26/06/06	08:37	39.800	-9.630	5	0.22	0.03	0.01	0.08	0.02	0.00	0.02	0.07
206	5	26/06/06	07:27	39.800	-9.700	5	0.20	0.02	0.01	0.08	0.02	0.00	0.01	0.06
207	5	03/07/06	19:54	39.700	-9.570	5	0.21	0.04	0.02	0.05	0.01	0.00	0.03	0.03
208	5	01/07/06	06:25	39.700	-9.300	5	0.32	0.04	0.02	0.09	0.02	0.00	0.03	0.08
209	5	26/06/06	17:16	39.700	-9.190	5	0.49	0.09	0.03	0.12	0.03	0.01	0.06	0.11
210	5	26/06/06	16:38	39.700	-9.130	5	2.16	0.52	0.61	0.23	0.06	0.06	0.26	0.16

Ref	CC	Date (dd-mm-yy)	Time (UTC)	Latitude (N)	Longitude (W)	Sample Depth (m)	Pigments concentration (μgL^{-1})							
							TChla	Fuc	Per	Hex	But	Alo	Clb	Zea
211	5	27/06/06	04:20	39.700	-9.090	5	2.06	0.55	0.75	0.12	0.03	0.09	0.17	0.07
212	5	27/06/06	03:19	39.630	-9.140	5	1.02	0.20	0.25	0.17	0.03	0.03	0.07	0.11
213	5	27/06/06	02:18	39.590	-9.160	5	1.13	0.28	0.22	0.12	0.02	0.05	0.07	0.08
214	5	27/06/06	01:07	39.570	-9.170	5	1.46	0.40	0.40	0.11	0.03	0.05	0.13	0.07
215	5	27/06/06	00:03	39.530	-9.190	5	2.17	0.70	0.57	0.08	0.04	0.06	0.25	0.06
216	5	27/06/06	05:34	39.578	-9.119	5	1.02	0.32	0.19	0.08	0.02	0.04	0.10	0.05
217	5	27/06/06	05:54	39.588	-9.116	5	3.21	0.33	2.43	0.12	0.07	0.31	0.08	0.03
218	5	27/06/06	08:16	39.608	-9.112	5	4.25	0.44	3.29	0.15	0.06	0.14	0.09	0.06
219	5	01/07/06	23:34	39.590	-9.100	5	1.02	0.21	0.20	0.04	0.01	0.04	0.12	0.03
220	5	01/07/06	00:20	39.590	-9.140	5	1.25	0.35	0.17	0.17	0.02	0.03	0.16	0.06
221	5	01/07/06	01:09	39.600	-9.190	5	1.14	0.25	0.12	0.17	0.03	0.04	0.18	0.05
222	5	26/06/06	17:47	39.646	-9.184	5	0.41	0.06	0.03	0.11	0.03	0.01	0.04	0.09
223	5	26/06/06	19:38	39.624	-9.194	5	0.32	0.05	0.02	0.09	0.03	0.01	0.03	0.09
224	5	26/06/06	21:46	39.607	-9.202	5	0.24	0.04	0.01	0.08	0.02	0.00	0.03	0.08
225	5	27/06/06	23:21	39.586	-9.210	5	0.26	0.04	0.02	0.08	0.02	0.01	0.03	0.08
226	5	01/07/06	01:47	39.620	-9.210	5	1.01	0.23	0.15	0.12	0.04	0.03	0.15	0.06
227	5	01/07/06	02:38	39.630	-9.240	5	1.28	0.27	0.14	0.20	0.06	0.03	0.14	0.06
228	5	01/07/06	03:32	39.616	-9.285	5	1.22	0.29	0.14	0.27	0.09	0.03	0.13	0.06
229	5	01/07/06	04:32	39.590	-9.350	5	0.17	0.02	0.01	0.04	0.01	0.00	0.01	0.02
230	5	01/07/06	08:06	39.640	-9.270	5	0.33	0.07	0.02	0.08	0.02	0.00	0.03	0.05
231	5	01/07/06	10:12	39.610	-9.260	5	0.34	0.11	0.03	0.06	0.02	0.01	0.04	0.06
232	5	01/07/06	11:38	39.560	-9.240	5	0.85	0.18	0.24	0.12	0.02	0.01	0.04	0.04
233	5	01/07/06	13:25	39.430	-9.270	5	1.23	0.71	0.30	0.14	0.03	0.07	0.10	0.03
234	5	01/07/06	14:52	39.510	-9.330	5	0.26	0.05	0.02	0.07	0.02	0.00	0.01	0.03
235	5	01/07/06	15:23	39.540	-9.360	5	0.14	0.02	0.01	0.04	0.01	0.00	0.01	0.02
236	5	01/07/06	16:43	39.580	-9.390	5	0.11	0.02	0.01	0.03	0.01	0.00	0.01	0.03
237	5	01/07/06	18:42	39.600	-9.410	5	0.13	0.03	0.00	0.05	0.01	0.00	0.01	0.02
238	5	01/07/06	20:30	39.630	-9.430	5	0.20	0.03	0.02	0.06	0.01	0.00	0.03	0.10
239	5	01/07/06	21:46	39.670	-9.470	5	0.17	0.02	0.02	0.06	0.01	0.00	0.03	0.02
240	5	02/07/06	00:18	39.580	-9.430	5	0.09	0.02	0.01	0.05	0.01	0.00	0.01	0.02
241	5	02/07/06	01:33	39.540	-9.450	5	0.16	0.02	0.01	0.06	0.01	0.00	0.01	0.03
242	5	02/07/06	05:58	39.390	-9.430	5	1.58	0.69	0.18	0.10	0.02	0.01	0.03	0.04
243	5	02/07/06	07:01	39.450	-9.450	5	0.22	0.03	0.02	0.05	0.02	0.00	0.03	0.08
244	5	02/07/06	08:27	39.510	-9.480	5	0.25	0.03	0.01	0.07	0.03	0.00	0.05	0.09
245	5	02/07/06	12:26	39.550	-9.490	5	0.15	0.02	0.01	0.05	0.01	0.00	0.01	0.02
246	5	02/07/06	13:24	39.610	-9.510	5	0.17	0.02	0.02	0.06	0.02	0.00	0.02	0.02
247	5	02/07/06	02:54	39.520	-9.510	5	0.15	0.02	0.01	0.06	0.01	0.00	0.01	0.06
248	5	02/07/06	14:51	39.530	-9.550	5	0.25	0.03	0.03	0.08	0.02	0.00	0.04	0.08
249	5	02/07/06	16:14	39.510	-9.580	5	0.27	0.04	0.02	0.09	0.02	0.00	0.04	0.08
250	5	02/07/06	19:53	39.500	-9.660	5	0.11	0.01	0.01	0.03	0.01	0.00	0.01	0.03
251	5	04/07/06	10:32	39.320	-9.570	5	2.10	1.28	0.09	0.11	0.02	0.00	0.03	0.04
252	5	04/07/06	11:14	39.350	-9.570	5	0.51	0.19	0.02	0.07	0.02	0.00	0.03	0.06
253	5	04/07/06	06:57	39.410	-9.570	5	0.84	0.37	0.07	0.13	0.03	0.01	0.03	0.05
254	5	04/07/06	05:49	39.470	-9.570	5	0.13	0.02	0.01	0.04	0.01	0.00	0.01	0.03
255	5	04/07/06	05:14	39.480	-9.570	5	0.12	0.01	0.01	0.04	0.01	0.00	0.01	0.04
256	5	04/07/06	03:33	39.510	-9.570	5	0.12	0.02	0.01	0.04	0.01	0.00	0.02	0.04
257	5	04/07/06	02:11	39.510	-9.570	5	0.15	0.02	0.01	0.05	0.01	0.00	0.01	0.04

Ref	CC	Date (dd-mm-yy)	Time (UTC)	Latitude (N)	Longitude (W)	Sample Depth (m)	Pigments concentration (μgL^{-1})							
							TChla	Fuc	Per	Hex	But	Alo	Clb	Zea
258	5	04/07/06	23:45	39.530	-9.570	5	0.14	0.02	0.01	0.06	0.01	0.00	0.01	0.04
259	5	03/07/06	22:13	39.580	-9.570	5	0.13	0.02	0.02	0.04	0.01	0.00	0.02	0.05
260	5	03/07/06	20:42	39.640	-9.570	5	0.14	0.02	0.01	0.04	0.01	0.00	0.03	0.03
261	5	06/07/06	23:16	39.390	-9.560	5	0.26	0.07	0.01	0.03	0.01	0.00	0.02	0.04
262	5	05/07/06	22:02	39.370	-9.470	5	0.47	0.26	0.02	0.04	0.00	0.00	0.01	0.05
263	5	05/07/06	21:27	39.360	-9.430	5	1.93	0.91	0.31	0.10	0.02	0.08	0.02	0.04
264	5	03/07/06	18:24	39.700	-9.750	5	0.10	0.01	0.01	0.01	0.00	0.00	0.01	0.07
265	5	03/07/06	15:00	39.600	-9.750	5	0.10	0.01	0.01	0.03	0.00	0.00	0.01	0.03
266	5	03/07/06	11:51	39.530	-9.750	5	0.13	0.01	0.02	0.03	0.01	0.00	0.01	0.03
267	5	03/07/06	07:26	39.480	-9.750	5	0.13	0.01	0.01	0.04	0.01	0.00	0.01	0.05
268	5	03/07/06	03:47	39.440	-9.750	5	0.13	0.01	0.01	0.04	0.01	0.00	0.01	0.05
269	5	03/07/06	01:24	39.370	-9.750	5	0.21	0.04	0.02	0.06	0.02	0.00	0.03	0.12

Cruise: NRP D.Carlos I 2007 (**DC07**)

Cruise host: IH

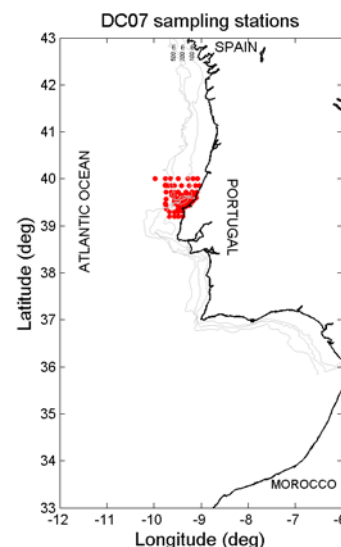
Chief Scientist: Dr. João Vitorino

Methods summary: GF/F filters (47mm), 4-5 L filtered, HPLC C18

Samples collected and filtered by: Carolina Sá, Rafael Mendes, André Valente,

André Couto, Sgt. Mourinho

Samples processed by: Carolina Sá, Rafael Mendes



Ref	CC	Date (dd-mm-yy)	Time (UTC)	Latitude (N)	Longitude (W)	Sample Depth (m)	Pigments concentration ($\mu\text{g L}^{-1}$)							
							TChla	Fuc	Per	Hex	But	Alo	Clb	Zea
270	6	13/06/07	07:09	39.201	-9.679	5	0.30	0.07	0.01	0.06	0.01	0.00	0.05	0.04
271	6	13/06/07	08:19	39.199	-9.569	5	0.33	0.09	0.01	0.05	0.01	0.01	0.05	0.03
272	6	13/06/07	09:19	39.199	-9.483	5	1.24	0.41	0.63	0.08	0.03	0.07	0.04	0.02
273	6	13/06/07	10:18	39.201	-9.390	5	0.60	0.27	0.08	0.08	0.02	0.01	0.03	0.01
274	6	13/06/07	11:14	39.304	-9.390	5	0.33	0.14	0.03	0.04	0.01	0.01	0.03	0.02
275	6	13/06/07	12:21	39.301	-9.481	5	0.39	0.20	0.03	0.05	0.02	0.01	0.03	0.02
276	6	13/06/07	13:46	39.302	-9.569	5	0.39	0.19	0.03	0.05	0.02	0.01	0.04	0.02
277	6	13/06/07	14:59	39.300	-9.679	5	0.35	0.10	0.01	0.05	0.01	0.01	0.06	0.04
278	6	13/06/07	16:46	39.371	-9.750	5	0.13	0.02	0.00	0.06	0.02	0.00	0.01	0.03
279	6	13/06/07	20:44	39.439	-9.749	5	0.12	0.02	0.00	0.06	0.02	0.00	0.01	0.03
280	6	13/06/07	23:16	39.471	-9.755	5	0.13	0.02	0.00	0.05	0.02	0.00	0.01	0.03
281	6	14/06/07	09:28	39.570	-9.750	5	0.15	0.02	0.00	0.05	0.02	0.00	0.01	0.02
282	6	14/06/07	14:39	39.721	-9.750	5	0.13	0.02	0.00	0.04	0.01	0.00	0.01	0.03
283	6	14/06/07	18:11	39.860	-9.751	5	0.13	0.02	0.00	0.04	0.02	0.00	0.01	0.04
284	6	14/06/07	21:04	40.006	-9.752	5	0.13	0.02	0.01	0.04	0.02	0.00	0.01	0.03
285	6	15/06/07	23:04	40.004	-9.647	5	0.15	0.03	0.01	0.05	0.02	0.00	0.01	0.03
286	6	15/06/07	00:52	40.005	-9.483	5	0.20	0.03	0.01	0.08	0.03	0.00	0.01	0.02
287	6	15/06/07	02:53	40.005	-9.276	5	0.25	0.03	0.01	0.07	0.02	0.01	0.01	0.03
288	6	15/06/07	04:15	40.004	-9.176	5	0.16	0.02	0.01	0.06	0.02	0.00	0.01	0.03
289	6	15/06/07	05:26	40.004	-9.075	5	0.21	0.03	0.02	0.06	0.01	0.00	0.03	0.03
290	6	15/06/07	06:36	40.005	-9.980	5	0.54	0.09	0.10	0.11	0.01	0.01	0.12	0.03
291	6	15/06/07	07:56	39.862	-9.034	5	0.41	0.07	0.04	0.11	0.01	0.00	0.08	0.03
292	6	15/06/07	09:00	39.862	-9.110	5	0.35	0.03	0.03	0.07	0.01	0.00	0.09	0.03
293	6	15/06/07	10:24	39.860	-9.249	5	0.27	0.06	0.00	0.04	0.01	0.01	0.01	0.03
294	6	15/06/07	11:59	39.861	-9.416	5	0.06	0.01	0.00	0.03	0.01	0.01	0.01	0.00
295	6	15/06/07	13:26	39.861	-9.570	5	0.15	0.02	0.00	0.05	0.02	0.00	0.01	0.03
296	6	15/06/07	14:08	39.860	-9.630	5	0.15	0.02	0.01	0.05	0.02	0.00	0.01	0.02
297	6	15/06/07	15:29	39.860	-9.700	5	0.16	0.02	0.00	0.05	0.02	0.00	0.01	0.03
298	6	15/06/07	20:02	39.655	-9.627	5	0.13	0.02	0.00	0.05	0.02	0.00	0.01	0.02
299	6	15/06/07	21:12	39.720	-9.630	5	0.12	0.02	0.00	0.05	0.02	0.00	0.01	0.02
300	6	15/06/07	21:59	39.721	-9.570	5	0.13	0.02	0.01	0.06	0.02	0.00	0.01	0.03
301	6	15/06/07	22:49	39.654	-9.571	5	0.16	0.02	0.00	0.06	0.03	0.00	0.01	0.02

Ref	CC	Date (dd-mm-yy)	Time (UTC)	Latitude (N)	Longitude (W)	Sample Depth (m)	Pigments concentration ($\mu\text{g L}^{-1}$)							
							TChla	Fuc	Per	Hex	But	Alo	Clb	Zea
302	6	16/06/07	00:16	39.719	-9.480	5	0.12	0.01	0.01	0.05	0.02	0.00	0.01	0.02
303	6	16/06/07	01:34	39.654	-9.400	5	0.13	0.01	0.00	0.06	0.02	0.00	0.01	0.02
304	6	16/06/07	02:51	39.720	-9.319	5	0.15	0.02	0.00	0.05	0.01	0.00	0.02	0.04
305	6	16/06/07	04:12	39.721	-9.186	5	0.15	0.02	0.00	0.06	0.01	0.00	0.01	0.03
306	6	16/06/07	05:02	39.719	-9.089	5	0.60	0.25	0.04	0.10	0.01	0.01	0.05	0.01
307	6	16/06/07	05:44	39.657	-9.112	5	0.33	0.06	0.03	0.09	0.01	0.01	0.05	0.02
308	6	16/06/07	06:24	39.618	-9.132	5	0.23	0.05	0.02	0.07	0.01	0.00	0.03	0.02
309	6	16/06/07	07:58	39.586	-9.145	5	0.42	0.17	0.02	0.07	0.01	0.01	0.03	0.01
310	6	16/06/07	08:30	39.574	-9.151	5	0.31	0.09	0.02	0.07	0.01	0.01	0.03	0.02
311	6	16/06/07	09:00	39.554	-9.159	5	0.27	0.09	0.02	0.07	0.01	0.00	0.03	0.02
312	6	16/06/07	10:21	39.593	-9.105	5	0.77	0.23	0.04	0.16	0.02	0.03	0.08	0.02
313	6	16/06/07	13:24	39.590	-9.125	5	0.51	0.17	0.04	0.12	0.01	0.01	0.02	0.02
314	6	16/06/07	13:58	39.591	-9.134	5	0.34	0.11	0.02	0.08	0.01	0.01	0.04	0.02
315	6	16/06/07	17:04	39.581	-9.163	5	0.26	0.05	0.01	0.09	0.03	0.01	0.03	0.02
316	6	16/06/07	20:02	39.594	-9.178	5	0.24	0.05	0.01	0.08	0.03	0.00	0.02	0.02
317	6	17/06/07	2:01	39.656	-9.149	5	0.22	0.04	0.01	0.08	0.02	0.00	0.02	0.02
318	6	17/06/07	03:13	39.654	-9.188	5	0.25	0.03	0.02	0.11	0.03	0.00	0.03	0.03
319	6	17/06/07	16:05	39.654	-9.147	5	0.13	0.02	0.01	0.05	0.01	0.00	0.01	0.02
320	6	18/06/07	17:05	39.655	-9.189	5	0.11	0.01	0.01	0.05	0.02	0.00	0.01	0.02
321	6	18/06/07	18:30	39.658	-9.234	5	0.10	0.01	0.00	0.03	0.01	0.00	0.01	0.01
322	6	18/06/07	20:23	39.661	-9.280	5	0.14	0.02	0.01	0.06	0.03	0.00	0.01	0.02
323	6	18/06/07	22:58	39.621	-9.266	5	0.11	0.01	0.00	0.04	0.01	0.00	0.01	0.02
324	6	19/06/07	00:21	39.603	-9.257	5	0.13	0.01	0.00	0.06	0.02	0.00	0.01	0.02
325	6	19/06/07	05:50	39.562	-9.193	5	0.41	0.13	0.01	0.12	0.01	0.00	0.06	0.01
326	6	19/06/07	06:53	39.531	-9.176	5	0.50	0.15	0.02	0.13	0.01	0.00	0.08	0.01
327	6	19/06/07	07:49	39.486	-9.218	5	0.34	0.09	0.01	0.10	0.02	0.00	0.04	0.02
328	6	19/06/07	09:23	39.557	-9.262	5	1.20	0.63	0.04	0.15	0.02	0.01	0.07	0.01
329	6	19/06/07	13:35	39.608	-9.308	5	0.14	0.02	0.00	0.05	0.01	0.00	0.01	0.01
330	6	19/06/07	18:50	39.592	-9.346	5	0.11	0.01	0.00	0.04	0.01	0.00	0.01	0.01
331	6	19/06/07	20:35	39.573	-9.339	5	0.13	0.02	0.00	0.06	0.02	0.00	0.01	0.02
332	6	19/06/07	22:26	39.508	-9.308	5	0.11	0.02	0.00	0.04	0.01	0.00	0.01	0.01
333	6	20/06/07	00:09	39.433	-9.268	5	0.39	0.12	0.02	0.13	0.01	0.00	0.07	0.02
334	6	20/06/07	01:01	39.404	-9.334	5	0.45	0.15	0.02	0.15	0.01	0.00	0.09	0.02
335	6	20/06/07	02:25	39.461	-9.354	5	0.47	0.13	0.02	0.14	0.01	0.00	0.08	0.02
336	6	20/06/07	04:13	39.537	-9.382	5	0.11	0.01	0.01	0.04	0.01	0.00	0.01	0.02
337	6	20/06/07	05:32	39.488	-9.411	5	0.17	0.04	0.01	0.05	0.01	0.00	0.02	0.01
338	6	20/06/07	07:18	39.420	-9.406	5	0.53	0.16	0.02	0.15	0.01	0.01	0.08	0.02
348	6	20/06/07	08:05	39.395	-9.406	5	0.47	0.14	0.02	0.15	0.01	0.01	0.08	0.02
349	6	20/06/07	08:44	39.410	-9.435	5	0.46	0.13	0.02	0.13	0.01	0.00	0.07	0.03
350	6	20/06/07	09:20	39.423	-9.470	5	0.41	0.14	0.01	0.11	0.02	0.00	0.05	0.03
351	6	20/06/07	09:57	39.438	-9.501	5	0.27	0.08	0.01	0.08	0.02	0.00	0.03	0.03
352	6	20/06/07	10:46	39.466	-9.468	5	0.25	0.06	0.01	0.08	0.02	0.00	0.03	0.03
353	6	20/06/07	22:17	39.557	-9.390	5	0.12	0.01	0.00	0.05	0.01	0.00	0.01	0.02
354	6	21/06/07	00:58	39.590	-9.394	5	0.08	0.01	0.00	0.04	0.01	0.00	0.00	0.01
355	6	21/06/07	04:21	39.641	-9.400	5	0.12	0.01	0.00	0.05	0.01	0.00	0.01	0.02
356	6	21/06/07	06:19	39.568	-9.440	5	0.13	0.02	0.00	0.05	0.02	0.00	0.01	0.02
357	6	21/06/07	12:15	39.528	-9.469	5	0.12	0.01	0.00	0.04	0.01	0.00	0.01	0.02

Ref	CC	Date (dd-mm-yy)	Time (UTC)	Latitude (N)	Longitude (W)	Sample Depth (m)	Pigments concentration (μgL^{-1})							
							TChla	Fuc	Per	Hex	But	Alo	Clb	Zea
358	6	03/07/07	07:05	39.861	-9.410	5	0.16	0.06	0.01	0.03	0.01	0.00	0.01	0.02
359	6	03/07/07	08:26	39.860	-9.253	5	1.31	0.75	0.10	0.05	0.04	0.00	0.03	0.06
360	6	03/07/07	09:43	39.861	-9.110	5	1.32	0.87	0.03	0.07	0.02	0.00	0.03	0.04
361	6	03/07/07	10:44	39.860	-9.037	5	4.72	2.72	0.14	0.13	0.04	0.05	0.15	0.05
362	6	03/07/07	11:55	39.720	-9.091	5	5.09	2.67	0.31	0.15	0.05	0.09	0.21	0.07
363	6	03/07/07	12:51	39.720	-9.192	5	0.21	0.07	0.01	0.03	0.01	0.00	0.01	0.04
364	6	03/07/07	14:04	39.721	-9.317	5	0.17	0.06	0.01	0.03	0.01	0.00	0.01	0.03
365	6	03/07/07	14:49	39.662	-9.282	5	0.18	0.07	0.01	0.03	0.01	0.00	0.01	0.03
366	6	03/07/07	17:19	39.621	-9.266	5	0.38	0.20	0.01	0.04	0.01	0.00	0.02	0.02
367	6	03/07/07	18:41	39.604	-9.260	5	1.34	0.73	0.13	0.09	0.05	0.01	0.09	0.06
368	6	04/07/07	00:11	39.614	-9.191	5	1.51	0.50	0.19	0.18	0.03	0.08	0.15	0.06
369	6	04/07/07	03:03	39.595	-9.176	5	0.48	0.19	0.03	0.08	0.01	0.01	0.04	0.05
370	6	04/07/07	05:43	39.583	-9.167	5	0.60	0.19	0.05	0.10	0.02	0.02	0.04	0.05
371	6	04/07/07	08:00	39.593	-9.136	5	0.89	0.26	0.06	0.11	0.02	0.02	0.13	0.07
372	6	04/07/07	08:33	39.591	-9.127	5	1.00	0.26	0.10	0.16	0.04	0.02	0.10	0.09
373	6	04/07/07	10:48	39.593	-9.108	5	1.74	0.27	0.27	0.14	0.04	0.11	0.31	0.11
374	6	04/07/07	11:57	39.654	9.113	5	1.90	0.34	0.32	0.08	0.02	0.13	0.25	0.07
375	6	04/07/07	12:41	39.616	-9.132	5	1.47	0.20	0.31	0.09	0.01	0.11	0.21	0.10
376	6	04/07/07	13:35	39.587	-9.146	5	0.83	0.21	0.06	0.11	0.03	0.05	0.11	0.09
377	6	04/07/07	14:18	39.556	-9.163	5	0.79	0.23	0.08	0.16	0.03	0.02	0.07	0.08
378	6	04/07/07	14:42	39.526	-9.177	5	0.77	0.22	0.06	0.13	0.03	0.02	0.07	0.06
379	6	04/07/07	15:29	39.564	-9.195	5	1.92	0.35	0.19	0.22	0.02	0.27	0.10	0.06
380	6	04/07/07	17:26	39.556	-9.259	5	0.94	0.33	0.08	0.10	0.02	0.02	0.09	0.08
381	6	04/07/07	18:47	39.482	-9.227	5	0.83	0.22	0.07	0.13	0.02	0.03	0.13	0.06
382	6	04/07/07	19:19	39.432	-9.271	5	1.14	0.26	0.11	0.15	0.04	0.05	0.21	0.08
383	6	04/07/07	20:50	39.515	-9.315	5	0.38	0.19	0.02	0.05	0.02	0.01	0.05	0.01
384	6	04/07/07	22:16	39.570	-9.344	5	0.89	0.42	0.05	0.09	0.02	0.01	0.07	0.05
385	6	04/07/07	22:59	39.542	-9.402	5	0.58	0.27	0.03	0.07	0.02	0.01	0.04	0.05
386	6	05/07/07	00:53	39.477	-9.390	5	0.19	0.07	0.01	0.04	0.01	0.00	0.01	0.03
387	6	05/07/07	02:26	39.399	-9.377	5	0.90	0.23	0.06	0.17	0.03	0.05	0.16	0.08
388	6	05/07/07	03:34	39.492	-9.435	5	0.58	0.27	0.02	0.09	0.02	0.01	0.04	0.04
389	6	05/07/07	05:28	39.394	-9.475	5	0.41	0.14	0.02	0.10	0.02	0.01	0.03	0.04
390	6	05/07/07	06:51	39.331	-9.497	5	0.78	0.28	0.06	0.14	0.02	0.02	0.06	0.03
391	6	05/07/07	09:16	39.471	-9.570	5	0.33	0.14	0.01	0.06	0.01	0.00	0.02	0.03
392	6	05/07/07	11:59	39.520	-9.572	5	0.16	0.06	0.01	0.03	0.01	0.00	0.01	0.03
393	6	05/07/07	14:35	39.581	-9.570	5	0.13	0.05	0.00	0.02	0.01	0.00	0.01	0.02
394	6	05/07/07	16:46	39.694	-9.573	5	0.32	0.18	0.01	0.04	0.01	0.00	0.01	0.03
395	6	05/07/07	17:53	39.656	-9.430	5	0.33	0.18	0.02	0.04	0.01	0.01	0.01	0.03
396	6	05/07/07	21:01	39.597	-9.412	5	0.14	0.06	0.01	0.03	0.01	0.00	0.01	0.02
397	6	06/07/07	23:39	39.582	-9.497	5	0.39	0.22	0.01	0.04	0.01	0.00	0.01	0.03
398	6	06/07/07	03:19	39.528	-9.469	5	0.19	0.07	0.01	0.04	0.01	0.00	0.02	0.03

Cruise: NRP D.Carlos I 2008 (DC08)

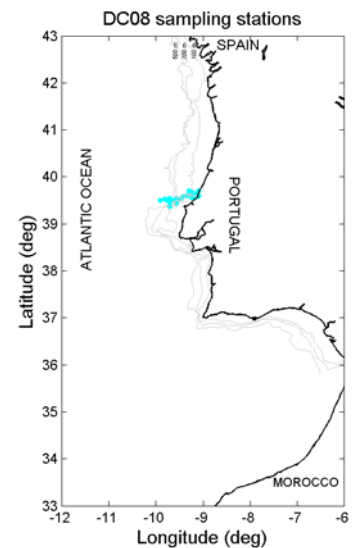
Cruise host: IH

Chief Scientist: Dr. João Vitorino

Methods summary: GF/F filters (47mm), 4-5 L filtered, HPLC C18

Samples collected and filtered by: Carolina Sá, Sgt. Mourinho

Samples processed by: Carolina Sá, Rafael Mendes



Ref	CC	Date (dd-mm-yy)	Time (UTC)	Latitude (N)	Longitude (W)	Sample Depth (m)	Pigments concentration ($\mu\text{g L}^{-1}$)							
							TChla	Fuc	Per	Hex	But	Alo	Clb	Zea
399	7	02/03/08	03:10	39.505	-9.903	5	0.46	0.02	0.01	0.20	0.04	0.01	0.04	0.18
400	7	02/03/08	06:39	39.531	-9.805	5	0.51	0.03	0.01	0.26	0.04	0.00	0.05	0.00
401	7	02/03/08	10:04	39.498	-9.752	5	0.53	0.03	0.01	0.28	0.05	0.01	0.05	0.11
402	7	02/03/08	12:27	39.468	-9.699	5	0.48	0.02	0.01	0.22	0.04	0.01	0.05	0.12
403	7	02/03/08	14:30	39.505	-9.660	5	0.60	0.03	0.01	0.27	0.04	0.02	0.07	0.15
404	7	02/03/08	18:29	39.512	-9.580	5	0.58	0.06	0.01	0.21	0.05	0.01	0.10	0.10
405	7	02/03/08	20:09	39.522	-9.561	5	0.52	0.06	0.01	0.17	0.05	0.01	0.08	0.08
406	7	02/03/08	21:51	39.518	-9.506	5	1.06	0.44	0.02	0.08	0.02	0.03	0.14	0.08
407	7	02/03/08	23:11	39.524	-9.482	5	2.02	0.89	0.02	0.12	0.03	0.04	0.16	0.08
408	7	03/03/08	00:27	39.545	-9.452	5	1.76	0.73	0.02	0.10	0.02	0.03	0.16	0.08
409	7	03/03/08	01:53	39.580	-9.430	5	0.99	0.43	0.02	0.08	0.02	0.02	0.13	0.08
410	7	03/03/08	04:40	39.591	-9.348	5	0.64	0.15	0.02	0.08	0.02	0.02	0.14	0.03
411	7	03/03/08	06:56	39.615	-9.287	5	1.10	0.35	0.02	0.12	0.03	0.03	0.14	0.06
412	7	03/03/08	09:14	39.621	-9.210	5	0.67	0.16	0.01	0.08	0.02	0.02	0.10	0.05
413	7	03/03/08	11:05	39.581	-9.161	5	0.72	0.18	0.07	0.05	0.01	0.02	0.10	0.02
414	7	03/03/08	12:44	39.594	-9.117	5	0.65	0.20	0.10	0.03	0.01	0.02	0.08	0.01
415	7	03/03/08	13:22	39.594	-9.104	5	0.95	0.31	0.12	0.03	0.01	0.02	0.10	0.02
416	7	03/03/08	13:53	39.596	-9.092	5	0.41	0.18	0.04	0.02	0.01	0.01	0.04	0.01
417	7	03/03/08	17:34	39.699	-9.090	6.4	0.85	0.35	0.06	0.03	0.01	0.02	0.06	0.01
418	7	06/03/08	07:11	39.551	-9.181	7	0.62	0.28	0.01	0.02	0.01	0.01	0.03	0.01
419	7	06/03/08	09:01	39.579	-9.159	5	0.72	0.33	0.01	0.03	0.01	0.01	0.04	0.01
420	7	06/03/08	10:53	39.629	-9.131	5	1.19	0.54	0.02	0.04	0.01	0.01	0.06	0.02
421	7	06/03/08	12:18	39.665	-9.115	5	1.28	0.60	0.03	0.04	0.01	0.02	0.05	0.01
422	7	06/03/08	13:45	39.593	-9.103	5	1.29	0.67	0.02	0.03	0.01	0.01	0.04	0.01
423	7	06/03/08	14:27	39.595	-9.089	5	1.07	0.61	0.02	0.02	0.00	0.01	0.03	0.02
424	7	06/03/08	14:59	39.608	-9.112	5	1.43	0.71	0.05	0.03	0.00	0.02	0.04	0.01
425	7	06/03/08	16:58	39.577	-9.117	5	0.84	0.40	0.02	0.03	0.01	0.02	0.05	0.01
426	7	06/03/08	17:31	39.590	-9.141	5	1.26	0.56	0.05	0.03	0.01	0.03	0.06	0.02
427	7	06/03/08	18:14	39.581	-9.160	5	0.81	0.37	0.02	0.03	0.01	0.01	0.05	0.01
428	7	06/03/08	19:00	39.601	-9.186	5	0.75	0.32	0.01	0.03	0.01	0.01	0.04	0.01
429	7	06/03/08	20:48	39.630	-9.244	5	0.27	0.07	0.01	0.03	0.01	0.01	0.05	0.01
430	7	06/03/08	22:03	39.617	-9.284	5	0.26	0.07	0.01	0.03	0.01	0.01	0.05	0.01

Ref	CC	Date (dd-mm-yy)	Time (UTC)	Latitude (N)	Longitude (W)	Sample Depth (m)	Pigments concentration ($\mu\text{g L}^{-1}$)							
							TChla	Fuc	Per	Hex	But	Alo	Clb	Zea
431	7	07/03/08	00:20	39.561	-9.242	5	0.23	0.06	0.01	0.03	0.01	0.01	0.04	0.01
432	7	07/03/08	04:09	39.671	-9.286	5	0.26	0.08	0.00	0.03	0.01	0.01	0.04	0.01
433	7	07/03/08	04:46	39.700	-9.300	5	0.22	0.06	0.01	0.03	0.01	0.01	0.04	0.01
434	7	07/03/08	07:12	39.672	-9.225	5	0.23	0.08	0.00	0.03	0.01	0.00	0.04	0.01
435	7	07/03/08	07:47	39.659	-9.238	5	0.29	0.10	0.01	0.03	0.01	0.01	0.05	0.01
436	7	07/03/08	10:06	39.605	-9.314	5	0.29	0.08	0.01	0.05	0.02	0.01	0.04	0.01
437	7	07/03/08	11:11	39.593	-9.344	5	0.29	0.07	0.01	0.04	0.01	0.01	0.05	0.02
438	7	07/03/08	13:40	39.580	-9.427	5	0.35	0.08	0.01	0.05	0.01	0.02	0.05	0.02
439	7	07/03/08	15:29	39.545	-9.453	5	0.25	0.05	0.00	0.03	0.01	0.01	0.04	0.01
440	7	07/03/08	16:16	39.522	-9.479	5	0.29	0.07	0.01	0.03	0.01	0.02	0.05	0.01
441	7	07/03/08	17:56	39.426	-9.569	7	0.42	0.14	0.03	0.04	0.01	0.01	0.08	0.01
442	7	07/03/08	18:20	39.451	-9.571	7	0.46	0.14	0.03	0.04	0.01	0.02	0.09	0.02
443	7	07/03/08	18:43	39.471	-9.570	5	0.28	0.08	0.01	0.04	0.01	0.01	0.05	0.01
444	7	08/03/08	00:52	39.521	-9.511	5	0.27	0.07	0.01	0.05	0.02	0.01	0.05	0.01
445	7	08/03/08	03:09	39.502	-9.660	5	0.27	0.02	0.01	0.15	0.05	0.00	0.02	0.04
446	7	08/03/08	05:03	39.548	-9.705	5	0.29	0.02	0.01	0.17	0.04	0.01	0.02	0.03
447	7	08/03/08	07:52	39.500	-9.699	5	0.31	0.02	0.01	0.18	0.05	0.01	0.02	0.03
448	7	08/03/08	09:51	39.472	-9.701	5	0.24	0.02	0.00	0.12	0.05	0.00	0.02	0.03
449	7	08/03/08	11:44	39.444	-9.701	5	0.27	0.02	0.00	0.15	0.05	0.01	0.02	0.04
450	7	08/03/08	14:46	39.398	-9.701	5	0.37	0.07	0.01	0.15	0.04	0.01	0.02	0.03
451	7	08/03/08	15:30	39.367	-9.700	5	0.21	0.02	0.00	0.10	0.03	0.01	0.03	0.03
452	7	07/03/08	17:43	39.499	-9.752	5	0.25	0.03	0.00	0.11	0.03	0.00	0.02	0.03
453	7	07/03/08	22:43	39.536	-9.570	5	0.43	0.12	0.01	0.11	0.03	0.01	0.03	0.03
454	7	07/03/08	21:19	39.521	-9.569	5	0.46	0.17	0.00	0.04	0.02	0.01	0.03	0.01
455	7	07/03/08	03:22	39.638	-9.272	5	0.22	0.07	0.00	0.02	0.01	0.00	0.04	0.01
456	7	07/03/08	02:17	39.623	-9.266	5	0.26	0.08	0.01	0.03	0.01	0.01	0.05	0.01
457	7	07/03/08	00:58	39.596	-9.255	5	0.24	0.07	0.01	0.05	0.01	0.01	0.04	0.01

Cruise: NRP Almirante Gago Coutinho 2009 (GC_M09)

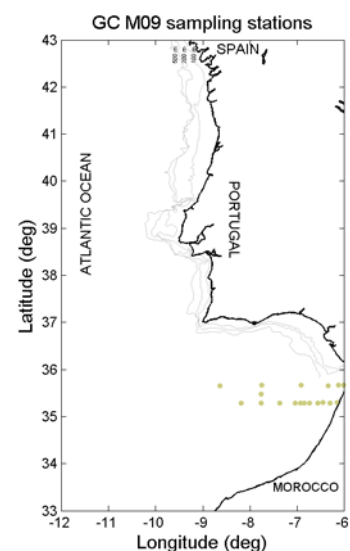
Cruise host: IH

Chief Scientist: Dr. João Vitorino

Methods summary: GF/F filters (25mm), 2-3 L filtered, HPLC C8

Samples collected and filtered by: Sgt. Mourinho, Dra. Anabela Oliveira

Samples processed by: Carolina Sá, Rafael Mendes



Ref	CC	Date (dd-mm-yy)	Time (UTC)	Latitude (N)	Longitude (W)	Sample Depth (m)	Pigments concentration ($\mu\text{g L}^{-1}$)							
							TChla	Fuc	Per	Hex	But	Alo	Clb	Zea
458	8	15/06/09	20:10	35.668	-6.014	5	0.70	0.25	0.06	0.11	0.03	0.02	0.11	0.10
459	8	15/06/09	21:30	35.661	-6.128	5	1.90	1.11	0.07	0.31	0.06	0.03	0.16	0.04
460	8	15/06/09	23:40	35.659	-6.350	5	0.08	0.00	0.00	0.03	0.01	0.00	0.00	0.04
461	8	16/06/09	08:15	35.663	-6.918	5	0.09	0.01	0.00	0.03	0.00	0.00	0.00	0.03
462	8	16/06/09	18:55	35.662	-7.757	5	0.08	0.01	0.00	0.03	0.01	0.00	0.00	0.04
463	8	17/06/09	00:05	35.659	-8.634	5	0.05	0.00	0.00	0.03	0.00	0.00	0.00	0.04
464	8	17/06/09	08:45	35.471	-7.765	5	0.07	0.00	0.00	0.02	0.00	0.00	0.01	0.05
465	8	18/06/09	08:30	35.294	-6.152	5	0.46	0.15	0.05	0.08	0.02	0.01	0.07	0.04
466	8	18/06/09	10:15	35.291	-6.307	5	0.08	0.01	0.00	0.03	0.01	0.00	0.01	0.05
467	8	18/06/09	11:30	35.294	-6.454	5	0.09	0.01	0.00	0.03	0.00	0.00	0.01	0.05
468	8	18/06/09	12:23	35.289	-6.559	5	0.06	0.01	0.00	0.03	0.01	0.00	0.00	0.03
469	8	18/06/09	13:52	35.289	-6.744	5	0.07	0.00	0.00	0.02	0.00	0.00	0.02	0.03
470	8	18/06/09	16:00	35.289	-6.744	5	0.10	0.02	0.00	0.05	0.00	0.00	0.00	0.06
471	8	18/06/09	20:00	35.290	-6.848	5	0.07	0.01	0.00	0.04	0.00	0.00	0.00	0.05
472	8	19/06/09	00:50	35.289	-6.936	5	0.05	0.00	0.00	0.02	0.00	0.00	0.00	0.04
473	8	19/06/09	02:10	35.287	-7.036	5	0.05	0.00	0.00	0.01	0.00	0.00	0.00	0.04
474	8	19/06/09	05:30	35.286	-7.364	5	0.06	0.00	0.00	0.01	0.00	0.00	0.00	0.03
475	8	19/06/09	10:00	35.280	-7.763	5	0.05	0.00	0.00	0.01	0.00	0.00	0.00	0.03
476	8	19/06/09	13:50	35.279	-8.194	5	0.01	0.00	0.00	0.00	0.00	0.00	0.00	0.01

Cruise: NRP Almirante Gago Coutinho 2009 (GC09)

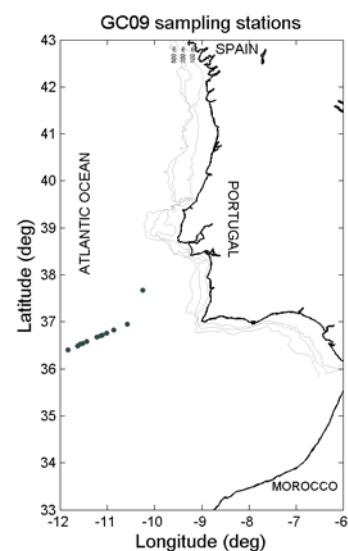
Cruise host: IH

Chief Scientist: Dr. João Vitorino

Methods summary: GF/F filters (25mm), 2-3 L filtered, HPLC C8

Samples collected and filtered by: Carolina Sá, Rafael Mendes, Sgt. Mourinho

Samples processed by: Carolina Sá, Rafael Mendes



Ref	CC	Date (dd-mm-yy)	Time (UTC)	Latitude (N)	Longitude (W)	Sample Depth (m)	Pigments concentration ($\mu\text{g L}^{-1}$)							
							TChla	Fuc	Per	Hex	But	Alo	Clb	Zea
477	9	02/06/09	05:40	37.672	-10.244	5	0.14	0.01	0.00	0.04	0.02	0.00	0.01	0.04
478	9	03/06/09	02:30	36.950	-10.580	5	0.11	0.01	0.00	0.04	0.01	0.00	0.01	0.01
479	9	03/06/09	02:30	36.950	-10.580	5	0.07	0.01	0.00	0.03	0.01	0.00	0.01	0.00
480	9	03/06/09	08:20	36.824	-10.867	5	0.09	0.01	0.01	0.02	0.01	0.00	0.01	0.01
481	9	03/06/09	12:18	36.757	-11.018	5	0.07	0.01	0.01	0.02	0.01	0.00	0.01	0.01
482	9	04/06/09	19:10	36.721	-11.101	5	0.03	0.00	0.01	0.01	0.00	0.00	0.00	0.00
483	9	03/06/09	16:50	36.706	-11.135	5	0.09	0.01	0.01	0.02	0.01	0.00	0.01	0.01
484	9	04/06/09	20:30	36.707	-11.135	5	0.05	0.01	0.00	0.02	0.00	0.00	0.00	0.01
485	9	04/06/09	22:30	36.671	-11.217	5	0.08	0.01	0.01	0.03	0.01	0.00	0.01	0.01
486	9	05/06/09	02:50	36.582	-11.430	5	0.07	0.01	0.00	0.02	0.01	0.00	0.00	0.01
487	9	05/06/09	04:40	36.541	-11.513	5	0.08	0.01	0.00	0.03	0.01	0.00	0.01	0.01
488	9	05/06/09	06:10	36.520	-11.572	5	0.26	0.02	0.01	0.10	0.04	0.00	0.03	0.02
489	9	05/06/09	07:50	36.489	-11.633	5	0.09	0.01	0.01	0.03	0.01	0.00	0.01	0.01
490	9	05/06/09	17:45	36.403	-11.833	5	0.14	0.02	0.01	0.04	0.01	0.00	0.01	0.02
491	9	05/06/09	17:45	36.403	-11.833	5	0.08	0.01	0.01	0.03	0.01	0.00	0.01	0.02

Cruise: NRP Almirante Gago Coutinho 2010 (GC10)

Cruise host: IH

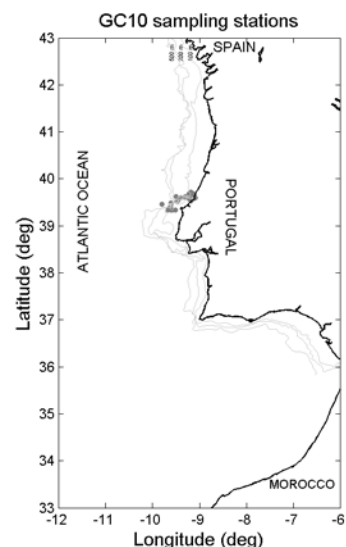
Chief Scientist: Dr. João Vitorino

Methods summary: GF/F filters (25mm), 2-3 L filtered, HPLC C8

Samples collected and filtered by: Carolina Sá, Márcio Souza, Catarina Guerreiro,

Sgt. Mourinho

Samples processed by: Carolina Sá, Dra. Ana Brito



Ref	CC	Date (dd-mm-yy)	Time (UTC)	Latitude (N)	Longitude (W)	Sample Depth (m)	Pigments concentration ($\mu\text{g L}^{-1}$)							
							TChla	Fuc	Per	Hex	But	Alo	Clb	Zea
492	10	06/03/10	23:42	39.630	-9.236	5	0.40	0.12	0.02	0.07	0.01	0.02	0.10	0.01
493	10	07/03/10	01:21	39.617	-9.198	5	0.19	0.08	0.01	0.05	0.01	0.01	0.05	0.00
494	10	07/03/10	02:02	39.601	-9.186	5	0.09	0.04	0.00	0.04	0.00	0.00	0.02	0.00
495	10	07/03/10	03:40	39.589	-9.140	5	0.17	0.06	0.01	0.06	0.01	0.01	0.03	0.00
496	10	07/03/10	05:17	39.593	-9.103	5	0.16	0.06	0.02	0.06	0.01	0.01	0.03	0.00
497	10	07/03/10	06:01	39.595	-9.089	5	0.22	0.10	0.02	0.07	0.01	0.01	0.04	0.00
498	10	07/03/10	06:48	39.577	-9.117	5	0.16	0.06	0.03	0.05	0.00	0.01	0.03	0.00
499	10	07/03/10	07:52	39.593	-9.113	5	0.20	0.09	0.03	0.05	0.01	0.01	0.03	0.00
500	10	07/03/10	14:27	39.608	-9.112	5	0.22	0.09	0.02	0.08	0.01	0.02	0.06	0.00
501	10	07/03/10	16:02	39.665	-9.115	5	0.25	0.11	0.02	0.09	0.01	0.01	0.07	0.00
502	10	07/03/10	18:33	39.579	-9.159	5	0.28	0.07	0.02	0.06	0.01	0.01	0.06	0.00
503	10	07/03/10	20:12	39.531	-9.190	5	0.26	0.09	0.02	0.09	0.01	0.01	0.06	0.00
504	10	07/03/10	21:14	39.577	-9.224	5	0.32	0.10	0.02	0.09	0.01	0.02	0.08	0.00
505	10	07/03/10	23:31	39.618	-9.199	5	0.33	0.10	0.03	0.08	0.01	0.02	0.08	0.00
506	10	08/03/10	03:18	39.684	-9.211	5	0.23	0.09	0.02	0.06	0.01	0.01	0.06	0.00
507	10	08/03/10	05:04	39.645	-9.244	5	0.42	0.11	0.02	0.08	0.01	0.02	0.09	0.01
508	10	08/03/10	06:09	39.617	-9.283	5	0.45	0.08	0.02	0.06	0.01	0.01	0.10	0.00
509	10	08/03/10	07:09	39.630	-9.236	5	0.33	0.11	0.05	0.10	0.01	0.02	0.07	0.00
510	10	08/03/10	08:56	39.618	-9.199	5	0.28	0.09	0.03	0.07	0.01	0.02	0.05	0.00
511	10	08/03/10	09:40	39.601	-9.185	5	0.31	0.05	0.02	0.04	0.01	0.01	0.05	0.00
512	10	08/03/10	11:20	39.590	-9.141	5	0.28	0.10	0.04	0.09	0.01	0.02	0.05	0.00
513	10	08/03/10	13:56	39.593	-9.103	5	0.33	0.00	0.03	0.06	0.01	0.01	0.06	0.00
514	10	08/03/10	16:57	39.577	-9.117	5	0.45	0.14	0.05	0.11	0.01	0.02	0.09	0.00
515	10	08/03/10	17:58	39.593	-9.113	5	0.34	0.13	0.02	0.09	0.01	0.02	0.08	0.00
516	10	08/03/10	19:13	39.608	-9.112	5	0.36	0.14	0.03	0.07	0.01	0.02	0.07	0.00
517	10	08/03/10	20:00	39.665	-9.115	5	0.25	0.08	0.02	0.06	0.01	0.01	0.06	0.00
518	10	08/03/10	21:57	39.579	-9.159	5	0.29	0.09	0.05	0.08	0.01	0.01	0.06	0.00
519	10	08/03/10	23:39	39.531	-9.190	5	0.32	0.13	0.02	0.08	0.01	0.01	0.08	0.00
520	10	09/03/10	00:20	39.577	-9.225	5	0.24	0.11	0.02	0.08	0.01	0.01	0.05	0.00
521	10	09/03/10	02:27	39.618	-9.199	5	0.29	0.10	0.03	0.09	0.01	0.02	0.07	0.00
522	10	09/03/10	05:07	39.698	-9.150	5	0.29	0.09	0.04	0.07	0.01	0.01	0.06	0.00
523	10	09/03/10	05:52	39.713	-9.187	5	0.26	0.09	0.02	0.09	0.01	0.01	0.07	0.00

Ref	CC	Date (dd-mm-yy)	Time (UTC)	Latitude (N)	Longitude (W)	Sample Depth (m)	Pigments concentration ($\mu\text{g L}^{-1}$)							
							TChla	Fuc	Per	Hex	But	Alo	Clb	Zea
524	10	09/03/10	06:58	39.684	-9.211	5	0.32	0.13	0.03	0.09	0.01	0.01	0.07	0.00
525	10	09/03/10	17:26	39.617	-9.284	5	0.67	0.27	0.02	0.09	0.01	0.02	0.17	0.01
526	10	09/03/10	18:43	39.629	-9.236	5	0.35	0.14	0.02	0.09	0.01	0.01	0.11	0.01
527	10	09/03/10	20:54	39.618	-9.199	5	0.26	0.09	0.01	0.07	0.01	0.01	0.07	0.00
528	10	09/03/10	21:37	39.601	-9.186	5	0.22	0.07	0.01	0.06	0.01	0.01	0.06	0.00
529	10	09/03/10	22:18	39.581	-9.160	5	0.22	0.10	0.02	0.14	0.01	0.01	0.06	0.00
530	10	09/03/10	23:56	39.593	-9.113	5	0.22	0.09	0.01	0.05	0.00	0.01	0.05	0.00
531	10	10/03/10	00:45	39.593	-9.103	5	0.58	0.16	0.00	0.07	0.01	0.09	0.06	0.00
532	10	10/03/10	02:35	39.577	-9.117	5	0.27	0.12	0.01	0.05	0.01	0.01	0.04	0.00
533	10	10/03/10	04:49	39.591	-9.111	5	0.24	0.09	0.01	0.06	0.01	0.01	0.04	0.00
534	10	10/03/10	05:52	39.608	-9.112	5	0.32	0.08	0.08	0.06	0.01	0.01	0.05	0.00
535	10	10/03/10	08:14	39.607	-9.149	5	0.29	0.08	0.04	0.07	0.01	0.01	0.05	0.00
536	10	10/03/10	09:09	39.579	-9.159	5	0.33	0.09	0.06	0.07	0.01	0.01	0.05	0.00
537	10	10/03/10	11:32	39.551	-9.182	5	0.40	0.13	0.03	0.07	0.01	0.03	0.07	0.01
538	10	10/03/10	11:57	39.531	-9.190	5	0.23	0.11	0.01	0.05	0.01	0.02	0.06	0.00
539	10	10/03/10	12:51	39.577	-9.224	5	0.39	0.09	0.03	0.07	0.01	0.04	0.06	0.00
540	10	10/03/10	14:51	39.617	-9.199	5	0.47	0.13	0.04	0.10	0.01	0.03	0.11	0.01
541	10	10/03/10	16:41	39.655	-9.174	5	0.43	0.13	0.03	0.09	0.01	0.01	0.11	0.01
542	10	10/03/10	17:15	39.676	-9.162	5	0.57	0.19	0.02	0.09	0.01	0.01	0.15	0.01
543	10	10/03/10	17:48	39.697	-9.150	5	0.52	0.24	0.02	0.10	0.01	0.01	0.15	0.00
544	10	10/03/10	20:13	39.713	-9.186	5	0.69	0.27	0.04	0.10	0.01	0.02	0.20	0.01
545	10	10/03/10	20:50	39.697	-9.201	5	0.53	0.17	0.03	0.10	0.01	0.01	0.15	0.01
546	10	10/03/10	21:51	39.672	-9.225	5	0.50	0.14	0.02	0.12	0.01	0.01	0.15	0.01
547	10	10/03/10	22:56	39.640	-9.247	5	0.33	0.11	0.02	0.08	0.01	0.01	0.10	0.00
548	10	11/03/10	00:06	39.606	-9.316	5	0.64	0.33	0.03	0.11	0.01	0.02	0.16	0.01
549	10	11/03/10	02:43	39.601	-9.409	5	0.49	0.22	0.04	0.08	0.01	0.02	0.09	0.01
550	10	11/03/10	05:50	39.546	-9.452	5	0.44	0.19	0.03	0.08	0.01	0.02	0.10	0.01
551	10	11/03/10	08:39	39.521	-9.479	5	0.61	0.16	0.03	0.24	0.03	0.02	0.10	0.01
552	10	15/03/10	10:57	39.342	-9.678	5	11.9	7.25	0.05	0.16	0.04	0.03	0.22	0.00
553	10	15/03/10	11:57	39.342	-9.608	5	12.1	7.31	0.03	0.15	0.04	0.03	0.23	0.00
554	10	15/03/10	12:26	39.342	-9.575	5	5.25	3.43	0.08	0.06	0.01	0.03	0.09	0.00
555	10	15/03/10	13:36	39.342	-9.515	5	12.3	7.58	0.18	0.16	0.04	0.07	0.26	0.01
556	10	15/03/10	23:34	39.623	-9.498	7	4.47	2.64	0.09	0.22	0.04	0.02	0.14	0.02
557	10	16/03/10	19:52	39.492	-9.609	5	8.48	6.16	0.52	0.15	0.04	0.03	0.18	0.00
558	10	17/03/10	05:02	39.406	-9.623	5	9.50	5.82	0.14	0.11	0.03	0.02	0.11	0.00
559	10	16/03/10	22:01	39.459	-9.608	5	4.05	3.14	0.08	0.07	0.02	0.00	0.09	0.00
560	10	18/03/10	20:46	39.459	-9.800	5	2.79	2.19	0.06	0.05	0.01	0.00	0.03	0.01

Cruise: RV Mytilus (HS10)

Cruise host: IPIMAR, HABSPOT project

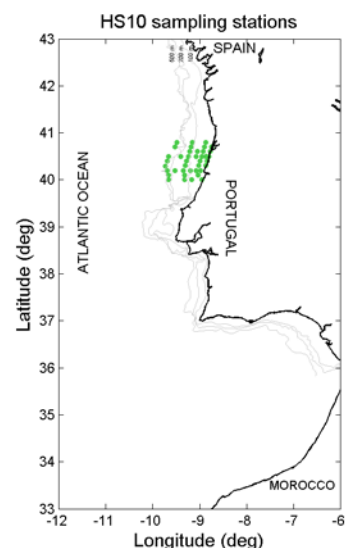
Chief Scientist: Dra. Teresa Moita

Methods summary: GF/F filters (25mm), 2-3 L filtered, HPLC C8

Samples collected and filtered by: Teresa Silva, Vera Veloso, Dra. Ana Amorim,

Teresa Quental

Samples processed by: Carolina Sá, Dra. Ana Brito, Teresa Silva



Ref	CC	Date (dd-mm-yy)	Time (UTC)	Latitude (N)	Longitude (W)	Sample Depth (m)	Pigments concentration ($\mu\text{g L}^{-1}$)							
							TChla	Fuc	Per	Hex	But	Alo	Clb	Zea
561	11	30/08/10	13:34	40.800	-8.866	5	3.43	1.20	0.71	0.79	0.08	0.34	0.20	0.04
562	11	30/08/10	16:27	40.798	-9.151	5	2.18	0.74	0.27	0.97	0.13	0.07	0.32	0.09
563	11	30/08/10	20:06	40.799	-9.484	5	0.64	0.25	0.05	0.32	0.07	0.00	0.07	0.05
564	11	30/08/10	21:27	40.698	-9.522	5	0.24	0.13	0.00	0.09	0.02	0.00	0.00	0.03
565	11	31/08/10	01:20	40.700	-9.188	5	0.52	0.21	0.06	0.26	0.03	0.00	0.06	0.06
566	11	31/08/10	03:52	40.701	-8.904	5	2.36	0.70	0.94	0.34	0.04	0.07	0.27	0.07
567	11	31/08/10	05:22	40.699	-8.753	5	2.39	0.68	0.80	0.67	0.03	0.08	0.22	0.15
568	11	31/08/10	06:19	40.599	-8.773	5	0.55	0.30	0.21	0.12	0.00	0.04	0.07	0.03
569	11	31/08/10	07:57	40.599	-8.924	5	1.46	0.51	0.36	0.41	0.08	0.04	0.15	0.09
570	11	31/08/10	10:29	40.600	-9.208	5	0.46	0.16	0.00	0.23	0.07	0.00	0.04	0.03
571	11	31/08/10	18:08	40.499	-9.406	5	0.71	0.34	0.00	0.27	0.10	0.00	0.05	0.12
572	11	31/08/10	19:42	40.500	-9.239	5	0.37	0.15	0.00	0.16	0.05	0.00	0.02	0.03
573	11	31/08/10	21:17	40.499	-9.080	5	0.40	0.13	0.00	0.17	0.05	0.00	0.03	0.04
574	11	31/08/10	22:29	40.501	-8.956	5	0.42	0.18	0.00	0.21	0.08	0.00	0.00	0.06
575	11	31/08/10	23:30	40.499	-8.862	5	0.70	0.27	0.00	0.34	0.12	0.00	0.05	0.09
576	11	01/09/10	00:10	40.500	-8.807	5	4.73	2.00	2.07	0.94	0.08	0.16	0.26	0.07
577	11	01/09/10	01:11	40.400	-8.841	5	3.29	1.87	0.94	0.55	0.06	0.09	0.18	0.06
578	11	01/09/10	02:49	40.400	-8.990	5	0.93	0.41	0.00	0.50	0.12	0.00	0.09	0.07
579	11	01/09/10	05:16	40.400	-9.274	5	0.46	0.23	0.00	0.27	0.09	0.00	0.00	0.03
580	11	01/09/10	08:53	40.402	-9.692	5	0.18	0.04	0.00	0.06	0.02	0.00	0.00	0.04
581	11	01/09/10	10:15	40.298	-9.724	5	0.26	0.10	0.00	0.13	0.04	0.00	0.00	0.04
582	11	01/09/10	14:08	40.299	-9.308	5	1.62	1.14	0.23	0.52	0.16	0.07	0.24	0.04
583	11	01/09/10	16:29	40.299	-9.023	5	1.44	0.49	0.16	0.87	0.15	0.03	0.16	0.07
584	11	01/09/10	18:02	40.299	-8.876	5	2.51	1.52	0.50	0.62	0.08	0.08	0.23	0.05
585	11	01/09/10	19:43	40.199	-8.980	5	0.47	0.17	0.04	0.40	0.07	0.00	0.05	0.05
586	11	01/09/10	20:45	40.198	-9.071	5	0.45	0.12	0.04	0.30	0.07	0.00	0.04	0.04
587	11	01/09/10	22:04	40.200	-9.196	5	0.39	0.14	0.00	0.21	0.07	0.00	0.02	0.03
588	11	01/09/10	23:32	40.199	-9.354	5	0.40	0.20	0.00	0.17	0.07	0.00	0.03	0.03
589	11	02/09/10	01:15	40.197	-9.523	5	0.38	0.13	0.00	0.12	0.05	0.00	0.03	0.06
590	11	02/09/10	02:55	40.200	-9.687	5	0.22	0.05	0.03	0.14	0.03	0.00	0.00	0.04
591	11	02/09/10	04:17	40.098	-9.659	5	0.79	0.24	0.11	0.36	0.11	0.02	0.09	0.06
592	11	02/09/10	07:25	40.100	-9.322	5	0.58	0.23	0.00	0.28	0.09	0.00	0.03	0.03

Ref	CC	Date (dd-mm-yy)	Time (UTC)	Latitude (N)	Longitude (W)	Sample Depth (m)	Pigments concentration ($\mu\text{g L}^{-1}$)							
							TChla	Fuc	Per	Hex	But	Alo	Clb	Zea
593	11	02/09/10	09:50	40.100	-9.039	5	0.32	0.07	0.02	0.18	0.03	0.00	0.02	0.04
594	11	02/09/10	15:23	39.999	-8.949	5	1.58	0.71	1.12	0.36	0.03	0.09	0.32	0.09
595	11	02/09/10	17:28	39.999	-9.166	5	0.32	0.05	0.06	0.15	0.02	0.00	0.04	0.09
596	11	02/09/10	19:03	39.999	-9.323	5	0.32	0.06	0.03	0.17	0.03	0.00	0.04	0.05
597	11	02/09/10	22:05	40.000	-9.658	5	0.36	0.14	0.00	0.17	0.07	0.00	0.04	0.08
598	11	04/09/10	08:34	40.599	-9.050	5	0.07	0.02	0.00	0.03	0.00	0.00	0.00	0.04
599	11	04/09/10	15:50	40.499	-9.660	5	0.16	0.03	0.00	0.04	0.01	0.00	0.00	0.04
600	11	04/09/10	18:33	40.499	-9.405	5	0.40	0.15	0.00	0.23	0.05	0.00	0.03	0.02
601	11	04/09/10	20:10	40.500	-9.240	5	0.22	0.09	0.00	0.11	0.02	0.00	0.00	0.03
602	11	04/09/10	21:51	40.500	-9.080	5	1.52	0.64	0.05	0.63	0.15	0.00	0.11	0.06
603	11	04/09/10	23:17	40.500	-8.956	5	1.89	1.01	0.33	1.10	0.19	0.05	0.27	0.07
604	11	05/09/10	00:21	40.500	-8.865	5	0.93	0.36	0.00	0.47	0.10	0.00	0.07	0.04

Cruise: NRP Almirante Gago Coutinho (GC11)

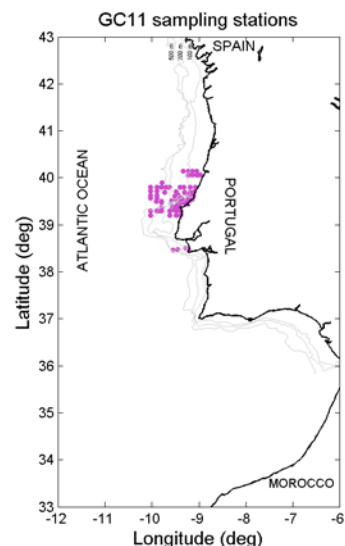
Cruise host: IH

Chief Scientist: Dr. João Vitorino

Methods summary: GF/F filters (25mm), 2-3 L filtered, HPLC C8

Samples collected and filtered by: Carolina Sá, Bruno Ribeiro

Samples processed by: Carolina Sá, Dra. Ana Brito



Ref	CC	Date (dd-mm-yy)	Time (UTC)	Latitude (N)	Longitude (W)	Sample Depth (m)	Pigments concentration ($\mu\text{g L}^{-1}$)							
							TChla	Fuc	Per	Hex	But	Alo	Clb	Zea
605	12	30/03/11	11:45	39.570	-10.030	5	0.88	0.66	0.01	0.21	0.03	0.01	0.05	0.00
606	12	30/03/11	14:35	39.630	-10.030	3	0.51	0.09	0.00	0.40	0.03	0.03	0.07	0.01
607	12	30/03/11	15:16	39.720	-10.030	1	0.60	0.10	0.04	0.49	0.03	0.05	0.02	0.01
608	12	30/03/11	21:45	39.800	-10.030	5	0.55	0.13	0.03	0.49	0.03	0.04	0.02	0.02
609	12	31/03/11	05:10	39.800	-9.900	5	0.54	0.61	0.00	0.08	0.05	0.00	0.04	0.00
610	12	31/03/11	07:30	39.720	-9.900	1	0.36	0.24	0.00	0.18	0.03	0.00	0.06	0.00
611	12	31/03/11	09:05	39.629	-9.900	1	0.37	0.12	0.00	0.21	0.02	0.01	0.06	0.00
612	12	31/03/11	11:00	39.629	-9.900	1	0.37	0.13	0.00	0.20	0.03	0.00	0.08	0.00
613	12	31/03/11	12:35	39.570	-9.900	1	1.01	0.79	0.00	0.15	0.03	0.01	0.02	0.00
614	12	31/03/11	14:40	39.570	-9.900	1	1.86	1.89	0.00	0.15	0.00	0.00	0.04	0.00
615	12	01/04/11	00:00	39.300	-9.900	5	0.65	0.47	0.00	0.30	0.02	0.00	0.06	0.00
616	12	01/04/11	03:15	39.301	-9.800	5	0.50	0.30	0.00	0.03	0.08	0.00	0.02	0.00
617	12	01/04/11	04:10	39.370	-9.800	5	0.59	0.63	0.00	0.05	0.00	0.00	0.02	0.00
618	12	01/04/11	07:30	39.470	-9.800	5	1.35	1.16	0.02	0.06	0.00	0.00	0.02	0.02
619	12	01/04/11	10:30	39.500	-9.800	5	0.60	0.71	0.00	0.06	0.03	0.00	0.00	0.01
620	12	09/04/11	14:45	39.799	-9.800	5	0.19	0.13	0.00	0.04	0.06	0.00	0.00	0.00
621	12	09/04/11	12:00	39.901	-9.788	1	0.16	0.12	0.00	0.04	0.00	0.00	0.01	0.01
622	12	10/04/11	00:30	39.799	-9.080	5	1.99	1.78	0.09	0.12	0.04	0.06	0.08	0.04
623	12	09/04/11	23:10	39.800	-9.190	5	0.21	0.15	0.04	0.05	0.00	0.00	0.02	0.00
624	12	09/04/11	22:05	39.798	-9.320	5	0.10	0.05	0.03	0.03	0.00	0.00	0.00	0.00
625	12	09/04/11	21:15	39.799	-9.400	5	0.11	0.10	0.00	0.02	0.00	0.00	0.00	0.00
626	12	09/04/11	19:05	39.799	-9.630	5	0.37	0.11	0.00	0.28	0.01	0.00	0.00	0.02
627	12	09/04/11	18:40	39.800	-9.700	5	0.15	0.11	0.00	0.07	0.00	0.00	0.00	0.01
628	12	10/04/11	06:45	39.699	-9.490	5	0.26	0.22	0.02	0.04	0.00	0.00	0.00	0.00
629	12	10/04/11	03:20	39.698	-9.189	5	0.67	0.61	0.08	0.14	0.02	0.01	0.08	0.01
630	12	10/04/11	01:20	39.700	-9.096	5	0.66	0.53	0.05	0.06	0.00	0.00	0.05	0.00
631	12	12/04/11	19:20	39.630	-9.140	5	1.44	0.94	0.21	0.09	0.02	0.04	0.10	0.01
632	12	12/04/11	20:30	39.589	-9.161	5	1.18	1.08	0.05	0.02	0.02	0.01	0.02	0.02
633	12	12/04/11	21:10	39.550	-9.180	5	1.07	0.64	0.11	0.04	0.01	0.01	0.07	0.00
634	12	13/04/11	01:00	39.625	-9.235	5	0.35	0.28	0.04	0.03	0.00	0.00	0.02	0.00
635	12	13/04/11	07:30	39.562	-9.238	5	0.45	0.32	0.06	0.04	0.00	0.00	0.03	0.00
636	12	13/04/11	08:40	39.503	-9.211	5	1.23	0.61	0.47	0.02	0.00	0.01	0.04	0.00

Ref	CC	Date (dd-mm-yy)	Time (UTC)	Latitude (N)	Longitude (W)	Sample Depth (m)	Pigments concentration ($\mu\text{g L}^{-1}$)							
							TChla	Fuc	Per	Hex	But	Alo	Clb	Zea
637	12	13/04/11	10:55	39.437	-9.274	5	1.01	0.83	0.07	0.02	0.00	0.01	0.02	0.00
638	12	13/04/11	12:20	39.489	-9.310	5	0.40	0.32	0.08	0.04	0.00	0.00	0.03	0.00
639	12	13/04/11	15:55	39.547	-9.368	5	0.18	0.09	0.07	0.02	0.00	0.00	0.00	0.00
640	12	13/04/11	17:30	39.564	-9.382	5	0.20	0.13	0.03	0.05	0.00	0.00	0.01	0.00
641	12	13/04/11	20:15	39.600	-9.411	5	0.15	0.10	0.05	0.02	0.00	0.00	0.00	0.00
642	12	13/04/11	21:10	39.637	-9.441	5	0.08	0.06	0.03	0.02	0.00	0.00	0.00	0.00
643	12	31/03/01	16:00	39.506	-9.904	1	1.11	1.01	0.01	0.07	0.02	0.01	0.02	0.01
644	12	14/04/11	18:20	39.330	-9.548	5	1.22	0.89	0.18	0.07	0.01	0.00	0.06	0.01
645	12	14/04/11	19:45	39.374	-9.494	5	0.36	0.35	0.07	0.04	0.01	0.00	0.03	0.00
646	12	14/04/11	21:00	39.416	-9.443	5	0.34	0.20	0.06	0.03	0.00	0.00	0.02	0.00
647	12	14/04/11	22:20	39.456	-9.390	5	0.20	0.16	0.04	0.03	0.00	0.00	0.02	0.00
648	12	14/04/11	23:15	39.388	-9.423	5	1.32	1.09	0.00	0.02	0.00	0.00	0.00	0.00
649	12	15/04/11	01:00	39.470	-9.456	5	0.21	0.16	0.03	0.03	0.00	0.00	0.02	0.00
650	12	15/04/11	05:55	39.525	-9.477	5	0.23	0.15	0.06	0.05	0.00	0.00	0.02	0.00
651	12	15/04/11	08:30	39.610	-9.512	5	0.09	0.12	0.00	0.05	0.00	0.00	0.00	0.00
652	12	15/04/11	11:25	39.580	-9.429	5	0.19	0.15	0.02	0.05	0.01	0.00	0.00	0.00
653	12	15/04/11	21:10	39.389	-9.561	5	0.40	0.33	0.06	0.05	0.00	0.00	0.04	0.00
654	12	15/04/11	22:30	39.361	-9.443	5	0.89	0.87	0.02	0.03	0.00	0.00	0.03	0.00
655	12	15/04/11	23:00	39.300	-9.386	5	0.98	0.84	0.09	0.04	0.00	0.00	0.03	0.00
656	12	16/04/11	00:12	39.300	-9.479	5	0.22	0.26	0.00	0.03	0.00	0.00	0.02	0.00
657	12	16/04/11	01:30	39.301	-9.623	5	0.39	0.31	0.02	0.03	0.00	0.00	0.03	0.00
658	12	16/04/11	03:45	39.299	-9.842	5	0.16	0.22	0.02	0.03	0.00	0.00	0.00	0.00
659	12	16/04/11	06:40	39.300	-10.030	5	0.16	0.13	0.00	0.06	0.00	0.00	0.00	0.01
660	12	16/04/11	07:55	39.200	-10.030	5	0.24	0.26	0.03	0.03	0.01	0.00	0.00	0.00
661	12	16/04/11	13:17	39.201	-9.622	5	0.23	0.24	0.00	0.03	0.00	0.00	0.00	0.01
662	12	16/04/11	15:15	39.201	-9.479	5	0.14	0.13	0.03	0.04	0.00	0.00	0.00	0.00
663	12	16/04/11	16:25	39.200	-9.388	5	0.37	0.41	0.05	0.05	0.00	0.01	0.02	0.01
664	12	10/04/11	11:40	39.695	-9.727	5	0.25	0.08	0.02	0.15	0.01	0.00	0.00	0.04
665	12	10/04/11	05:00	39.698	-9.302	5	0.21	0.17	0.05	0.00	0.00	0.00	0.00	0.00
666	12	07/04/11	07:40	40.148	-9.328	1	0.28	0.10	0.02	0.05	0.00	0.00	0.03	0.01
667	12	07/04/11	11:50	40.143	-9.045	1	0.67	0.35	0.16	0.04	0.00	0.01	0.04	0.00
668	12	06/04/11	12:00	38.507	-9.281	1	0.29	0.24	0.02	0.03	0.01	0.00	0.01	0.00
669	12	06/04/11	14:10	38.474	-9.226	1	0.26	0.27	0.00	0.03	0.00	0.00	0.00	0.00
670	12	06/04/11	15:30	38.473	-9.454	1	0.34	0.33	0.06	0.05	0.00	0.00	0.00	0.00
671	12	06/04/11	16:55	38.462	-9.546	1	0.37	0.31	0.03	0.02	0.00	0.00	0.01	0.00
672	12	06/04/11	18:05	38.462	-9.546	1	0.65	0.58	0.03	0.04	0.00	0.01	0.02	0.00
673	12	07/04/11	09:20	40.144	-9.225	1	0.33	0.16	0.08	0.06	0.00	0.00	0.04	0.00
674	12	07/04/11	10:35	40.146	-9.137	1	0.29	0.16	0.04	0.05	0.00	0.00	0.04	0.01
675	12	07/04/11	13:15	40.057	-8.967	1	1.87	1.22	0.07	0.12	0.02	0.07	0.10	0.02
676	12	07/04/11	14:35	40.057	-9.025	1	0.86	0.55	0.03	0.06	0.00	0.02	0.08	0.01
678	12	07/04/11	15:00	40.059	-9.051	1	0.85	0.57	0.02	0.07	0.01	0.03	0.07	0.01
679	12	07/04/11	16:15	40.057	-9.137	1	0.39	0.21	0.17	0.06	0.00	0.00	0.04	0.00
680	12	07/04/11	17:25	40.054	-9.221	1	0.46	0.15	0.13	0.04	0.00	0.00	0.05	0.00
681	12	08/04/11	16:30	39.521	-9.585	1	0.21	0.20	0.00	0.04	0.00	0.00	0.00	0.00
682	12	08/04/11	17:20	39.521	-9.575	1	0.27	0.28	0.05	0.04	0.00	0.00	0.00	0.00
683	12	11/04/11	11:19	39.453	-9.450	1	0.23	0.22	0.03	0.03	0.00	0.00	0.00	0.00
684	12	11/04/11	12:55	39.368	-9.524	1	0.66	0.66	0.03	0.02	0.00	0.00	0.02	0.00

Ref	CC	Date (dd-mm-yy)	Time (UTC)	Latitude (N)	Longitude (W)	Sample Depth (m)	Pigments concentration (μgL^{-1})							
							TChla	Fuc	Per	Hex	But	Alo	Clb	Zea
685	12	12/04/11	12:00	39.546	-9.143	1	0.70	0.48	0.08	0.01	0.00	0.01	0.01	0.00
686	12	12/04/11	15:00	39.607	-9.112	1	0.87	0.31	0.42	0.03	0.00	0.01	0.05	0.00
687	12	02/04/11	11:00	39.584	-9.146	1	0.40	0.34	0.00	0.07	0.00	0.00	0.02	0.00
688	12	02/04/11	12:40	39.551	-9.356	1	0.44	0.33	0.09	0.04	0.00	0.00	0.02	0.00

Cruise: RV Mytilus (HS11)

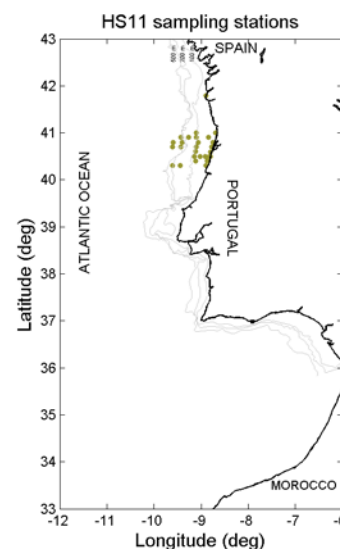
Cruise host: IPIMAR : HABSPOT project

Chief Scientist: Dra. Teresa Moita

Methods summary: GF/F filters (25mm), 2-3 L filtered, HPLC C8

Samples collected and filtered by: Teresa Silva, Vera Veloso, Bernardo

Samples processed by: Carolina Sá, Dra. Ana Brito, Teresa Silva



Ref	CC	Date (dd-mm-yy)	Time (UTC)	Latitude (N)	Longitude (W)	Sample Depth (m)	Pigments concentration ($\mu\text{g L}^{-1}$)							
							TChla	Fuc	Per	Hex	But	Alo	Clb	Zea
689	13	09/09/11	17:24	41.799	-8.904	5	3.15	1.99	0.08	0.03	0.01	0.01	0.01	0.00
690	13	10/09/11	00:52	40.999	-8.691	5	4.60	2.40	0.33	0.10	0.02	0.04	0.02	0.00
691	13	10/09/11	06:34	41.000	-9.101	5	0.23	0.17	0.03	0.12	0.02	0.00	0.00	0.00
692	13	10/09/11	18:30	40.899	-9.431	5	0.18	0.03	0.00	0.10	0.03	0.00	0.00	0.01
693	13	10/09/11	20:47	40.900	-9.264	5	0.34	0.05	0.00	0.12	0.03	0.00	0.01	0.02
694	13	10/09/11	22:49	40.901	-9.097	5	0.09	0.03	0.01	0.09	0.02	0.00	0.00	0.01
695	13	11/09/11	01:37	40.901	-8.838	5	0.30	0.13	0.04	0.11	0.01	0.03	0.00	0.01
696	13	11/09/11	05:03	40.800	-8.743	5	1.05	0.48	0.18	0.17	0.02	0.02	0.09	0.02
697	13	11/09/11	09:33	40.801	-9.068	5	0.25	0.04	0.00	0.08	0.01	0.00	0.02	0.00
698	13	11/09/11	13:49	40.800	-9.401	5	0.15	0.03	0.00	0.09	0.02	0.00	0.00	0.01
699	13	11/09/11	16:20	40.802	-9.596	5	0.18	0.02	0.05	0.13	0.03	0.00	0.03	0.01
700	13	11/09/11	20:47	40.699	-9.601	5	0.11	0.01	0.00	0.05	0.01	0.00	0.02	0.01
701	13	11/09/11	23:44	40.701	-9.432	5	0.22	0.02	0.02	0.11	0.03	0.00	0.02	0.01
702	13	12/09/11	03:20	40.701	-9.106	5	0.10	0.03	0.00	0.07	0.02	0.00	0.00	0.01
703	13	12/09/11	06:44	40.700	-8.780	5	0.10	0.06	0.02	0.05	0.00	0.00	0.02	0.00
704	13	12/09/11	08:50	40.599	-8.803	5	1.16	0.41	0.07	0.17	0.02	0.01	0.08	0.01
705	13	12/09/11	11:59	40.600	-9.120	5	0.39	0.08	0.01	0.20	0.05	0.00	0.04	0.02
706	13	13/09/11	02:38	40.500	-9.145	5	0.12	0.03	0.00	0.10	0.03	0.00	0.02	0.01
707	13	13/09/11	03:49	40.499	-9.019	5	0.20	0.07	0.00	0.10	0.02	0.00	0.02	0.01
708	13	13/09/11	04:58	40.499	-8.909	5	1.01	0.33	0.05	0.21	0.03	0.01	0.06	0.01
709	13	13/09/11	05:51	40.500	-8.835	5	2.16	1.05	0.16	0.21	0.04	0.03	0.10	0.00
710	13	13/09/11	06:17	40.499	-8.808	5	1.59	0.96	0.09	0.19	0.05	0.02	0.09	0.01
711	13	13/09/11	07:31	40.400	-8.865	5	2.49	0.70	0.20	0.36	0.06	0.00	0.17	0.00
712	13	13/09/11	10:39	40.400	-9.114	5	0.13	0.05	0.00	0.06	0.01	0.00	0.00	0.00
713	13	14/09/11	17:44	40.302	-9.603	5	0.04	0.00	0.00	0.03	0.01	0.00	0.00	0.01
714	13	14/09/11	19:32	40.301	-9.440	5	0.18	0.01	0.00	0.07	0.01	0.00	0.02	0.00
715	13	15/09/11	01:34	40.300	-8.902	5	1.68	0.77	0.18	0.39	0.06	0.04	0.13	0.01

Cruise: Cascais monitoring program (Cs)

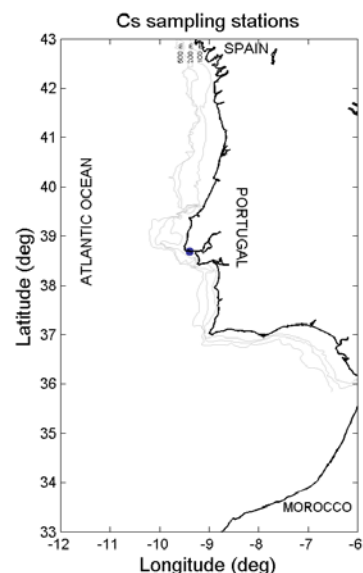
Cruise host: IPIMAR

Chief Scientist: Dra. Teresa Moita

Methods summary: GF/F filters (25mm), 2 L filtered, HPLC C8

Samples collected and filtered by: IPIMAR team, Carolina Sá, Dra. Ana Brito

Samples processed by: Carolina Sá, Dra. Ana Brito



Ref	CC	Date (dd-mm-yy)	Time (UTC)	Latitude (N)	Longitude (W)	Sample Depth (m)	Pigments concentration (μgL^{-1})							
							TChla	Fuc	Per	Hex	But	Alo	Clb	Zea
716	14	15/03/11	10:40	38.683	-9.400	5	0.85	0.23	0.42	0.02	0.01	0.03	0.05	0.01
717	14	22/03/11	15:40	38.683	-9.400	5	3.11	0.44	1.31	0.18	0.02	0.13	0.21	0.02
718	14	29/03/11	10:30	38.683	-9.400	5	0.53	0.40	0.13	0.02	0.00	0.01	0.07	0.00
719	14	05/04/11	14:30	38.683	-9.400	5	0.49	0.60	0.00	0.02	0.00	0.01	0.03	0.00
720	14	13/04/11	09:15	38.683	-9.400	5	1.35	0.70	0.13	0.05	0.01	0.04	0.12	0.02
721	14	19/04/11	13:30	38.683	-9.400	5	1.40	0.47	0.20	0.20	0.02	0.11	0.17	0.02
722	14	26/04/11	09:00	38.683	-9.400	5	0.95	0.43	0.03	0.10	0.03	0.04	0.17	0.04
723	14	03/05/11	13:30	38.683	-9.400	5	1.53	1.13	0.06	0.03	0.00	0.02	0.13	0.01
724	14	11/05/11	08:15	38.683	-9.400	5	1.43	1.03	0.10	0.05	0.01	0.03	0.13	0.01
725	14	17/05/11	13:35	38.683	-9.400	5	0.97	0.81	0.06	0.06	0.01	0.02	0.06	0.01
726	14	31/05/11	14:40	38.683	-9.400	5	0.34	0.24	0.00	0.00	0.00	0.04	0.04	0.03
727	14	09/06/11	08:20	38.683	-9.400	5	0.52	0.33	0.00	0.01	0.02	0.02	0.09	0.01
728	14	15/06/11	14:00	38.683	-9.400	5	1.79	1.90	0.00	0.00	0.00	0.00	0.02	0.02
729	14	28/06/11	11:40	38.683	-9.400	5	0.88	0.77	0.05	0.06	0.01	0.01	0.04	0.01
730	14	04/07/11	15:30	38.683	-9.400	5	1.77	2.63	0.00	0.07	0.08	0.01	0.02	0.01
731	14	11/07/11	10:00	38.683	-9.400	5	1.46	1.41	0.00	0.02	0.00	0.01	0.04	0.01
732	14	18/07/11	15:20	38.683	-9.400	5	1.13	0.80	0.07	0.02	0.01	0.06	0.10	0.01
733	14	26/07/11	10:00	38.683	-9.400	5	2.16	1.53	0.04	0.01	0.00	0.02	0.12	0.00
734	14	01/08/11	14:30	38.683	-9.400	5	2.12	1.43	0.30	0.06	0.02	0.02	0.08	0.00
735	14	08/08/11	08:45	38.683	-9.400	5	0.72	0.49	0.20	0.07	0.00	0.02	0.03	0.01
736	14	16/08/11	15:00	38.683	-9.400	5	0.57	0.19	0.08	0.05	0.01	0.01	0.04	0.01
737	14	31/08/11	15:00	38.683	-9.400	5	1.89	0.77	0.34	0.15	0.04	0.06	0.15	0.01
738	14	13/09/11	14:00	38.683	-9.400	5	1.59	0.71	0.26	0.11	0.02	0.01	0.12	0.00
739	14	21/09/11	08:00	38.683	-9.400	5	0.75	0.32	0.08	0.14	0.01	0.01	0.06	0.00
740	14	28/09/11	14:00	38.683	-9.400	5	0.67	0.27	0.12	0.09	0.02	0.02	0.05	0.01
741	14	28/10/11	14:15	38.683	-9.400	5	0.45	0.21	0.04	0.04	0.02	0.01	0.05	0.00
742	14	03/11/11	09:00	38.683	-9.400	5	0.68	0.33	0.05	0.03	0.03	0.02	0.08	0.01
743	14	09/11/11	12:30	38.683	-9.400	5	1.16	0.28	0.26	0.08	0.02	0.08	0.16	0.00
744	14	15/11/11	16:10	38.683	-9.400	5	0.31	0.15	0.04	0.02	0.00	0.03	0.07	0.01
745	14	23/11/11	11:22	38.683	-9.400	5	0.25	0.18	0.03	0.02	0.00	0.01	0.04	0.00
746	14	29/11/11	16:50	38.683	-9.400	5	1.40	0.29	0.24	0.01	0.01	0.06	0.15	0.00
747	14	06/12/11	10:45	38.683	-9.400	5	0.44	0.21	0.02	0.05	0.01	0.02	0.07	0.00

Ref	CC	Date (dd-mm-yy)	Time (UTC)	Latitude (N)	Longitude (W)	Sample Depth (m)	Pigments concentration (μgL^{-1})							
							TChla	Fuc	Per	Hex	But	Alo	Clb	Zea
748	14	19/12/11	09:15	38.683	-9.400	5	0.89	0.28	0.07	0.05	0.01	0.04	0.14	0.00
749	14	27/12/11	15:30	38.683	-9.400	5	0.81	0.32	0.03	0.04	0.01	0.04	0.09	0.01
750	14	04/01/12	15:40	38.683	-9.400	5	1.57	0.72	0.08	0.09	0.02	0.04	0.10	0.02
751	14	13/01/12	09:00	38.683	-9.400	5	0.46	0.25	0.11	0.00	0.02	0.03	0.08	0.00
752	14	19/01/12	09:40	38.683	-9.400	5	0.70	0.25	0.06	0.10	0.01	0.05	0.07	0.00

Cruise: Fisheries monitoring project (CSA)

Cruise host: CO

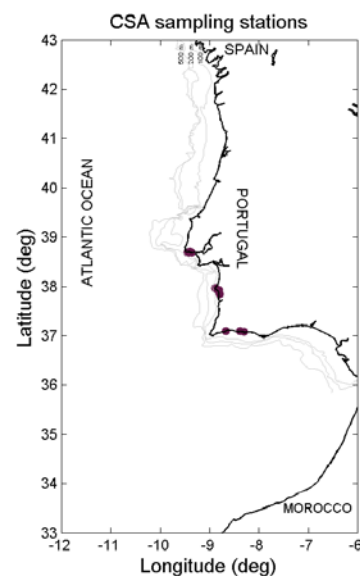
Chief Scientist: Dr. Henrique Cabral

Methods summary: GF/F filters (25mm), 2 L filtered, HPLC C8

Samples collected and filtered by: Sofia Henriques, Miguel Pais, Carolina Sá,

Dra. Ana Brito

Samples processed by: Carolina Sá, Dra. Ana Brito



Ref	CC	Date (dd-mm-yy)	Time (UTC)	Latitude (N)	Longitude (W)	Sample Depth (m)	Pigments concentration ($\mu\text{g L}^{-1}$)							
							TChla	Fuc	Per	Hex	But	Alo	Clb	Zea
753	15	04/08/10	16:00	38.700	-9.414	1	2.48	3.03	0.09	0.06	0.02	0.03	0.08	0.01
754	15	04/08/10	16:00	38.701	-9.399	1	4.80	4.36	0.08	0.08	0.03	0.03	0.08	0.01
755	15	04/08/10	16:00	38.688	-9.365	1	3.72	3.00	0.16	0.06	0.01	0.02	0.06	0.02
756	15	04/08/10	16:00	38.689	-9.426	1	2.29	2.39	0.06	0.06	0.02	0.01	0.05	0.01
757	15	04/08/10	16:00	38.694	-9.445	1	3.00	2.83	0.07	0.08	0.02	0.02	0.04	0.01
758	15	20/05/10	15:00	37.947	-8.858	1	2.02	2.23	0.03	0.04	0.01	0.02	0.04	0.01
759	15	20/05/10	15:00	37.950	-8.865	1	2.20	2.52	0.05	0.06	0.02	0.02	0.05	0.01
760	15	20/05/10	12:30	37.926	-8.814	1	4.58	5.92	0.13	0.05	0.03	0.04	0.04	0.02
761	15	20/05/10	12:30	37.921	-8.811	1	2.07	2.21	0.04	0.09	0.03	0.02	0.06	0.02
762	15	09/09/11	15:00	37.921	-8.811	1	1.19	0.78	0.10	0.07	0.00	0.00	0.05	0.00
763	15	20/05/10	12:30	37.849	-8.801	1	2.35	2.59	0.08	0.14	0.04	0.01	0.03	0.01
764	15	09/09/11	15:00	37.849	-8.801	1	1.03	0.73	0.09	0.06	0.01	0.01	0.05	0.00
765	15	09/09/11	15:00	37.873	-8.806	1	0.44	0.44	0.13	0.08	0.02	0.01	0.03	0.00
766	15	09/09/11	10:43	37.962	-8.887	1	1.16	0.62	0.04	0.21	0.05	0.02	0.09	0.02
767	15	09/09/11	13:19	37.966	-8.880	1	0.70	0.43	0.06	0.11	0.03	0.01	0.05	0.01
768	15	15/07/11	09:00	37.091	-8.669	1	1.42	0.51	0.00	0.03	0.00	0.02	0.25	0.00
769	15	15/07/11	10:00	37.075	-8.312	1	0.79	0.33	0.04	0.01	0.00	0.01	0.10	0.01
770	15	15/07/11	11:00	37.096	-8.386	1	1.23	0.19	0.03	0.10	0.02	0.04	0.37	0.02

Annex II: Case water-type maps

Maps of non-Case 1 water seasonal and spatial distribution

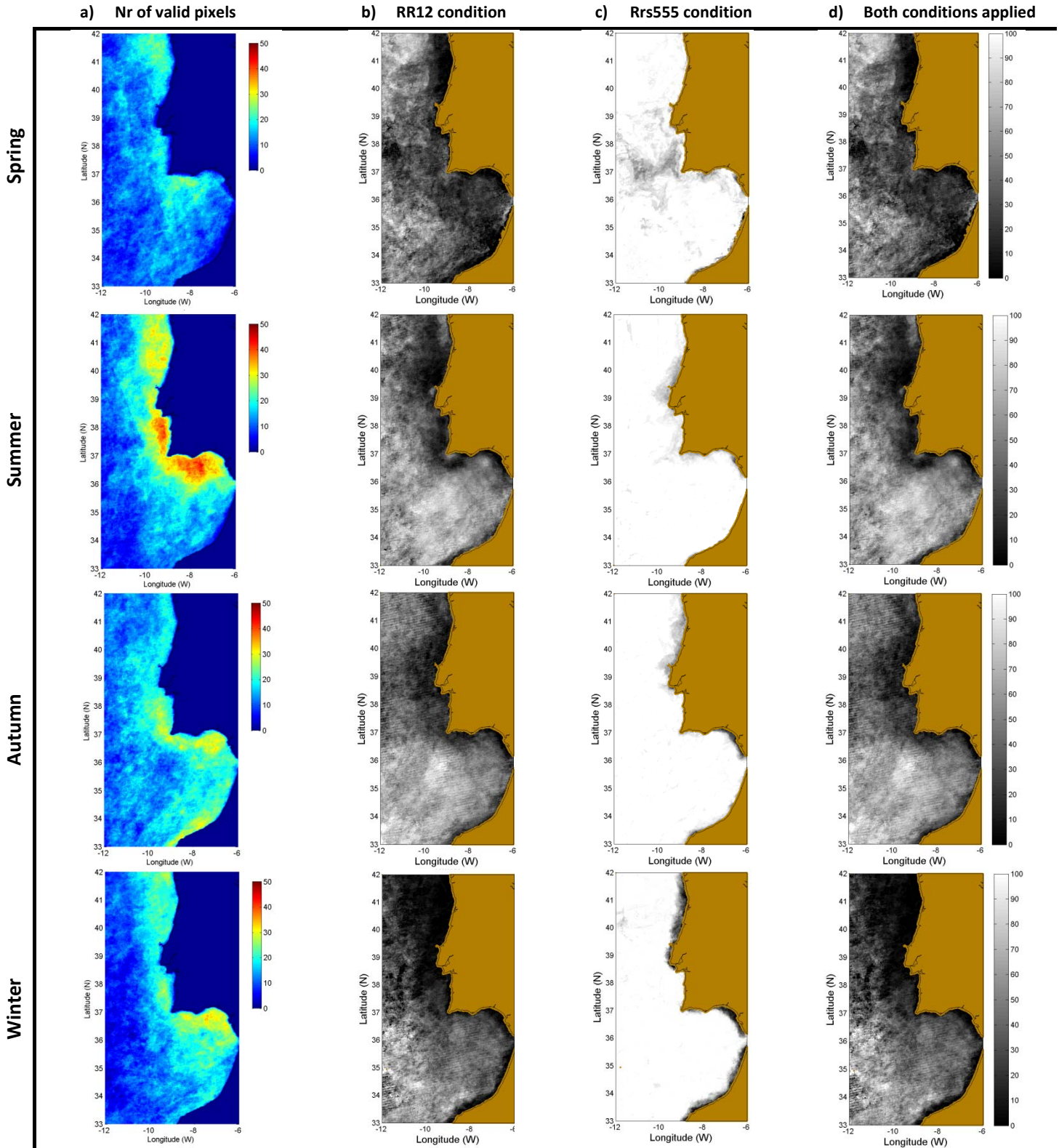


Figure II-1 Maps of percentage of pixel classification as Case 1 waters for 2006, according to Lee and Hu (2006) model using MODIS data. For each season, the number of valid pixels is presented in **a)**. Note that 50 was the maximum assigned value. The percentage of Case 1 pixel classification applying different criteria are presented in **b)** only the RR12_RR53 condition, **c)** only the Rrs555_RR53 condition, and **d)** with both conditions. Note that scale is in percentage and that invalid pixels period are presented in brown.

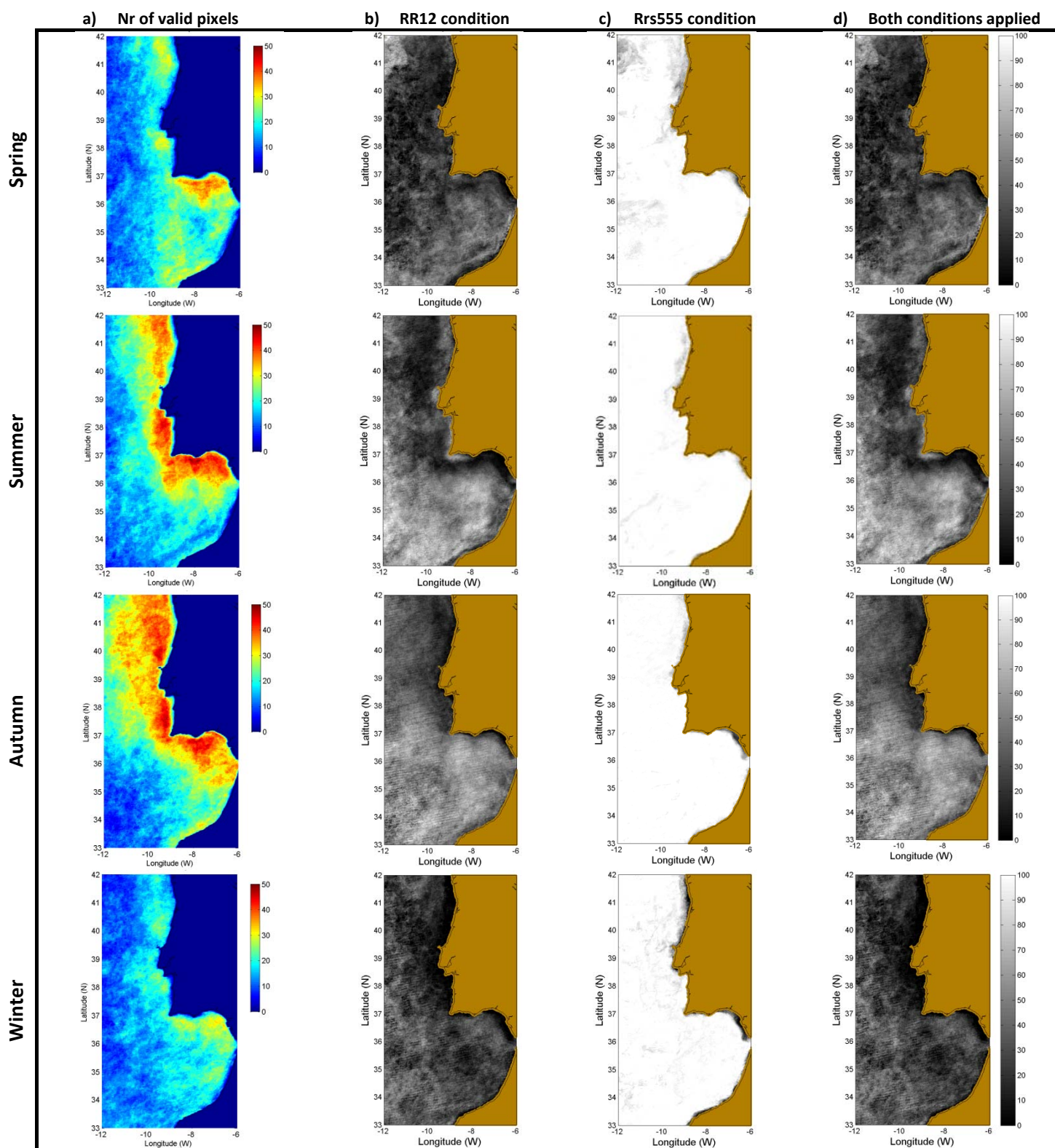


Figure II-2 Maps of percentage of pixel classification as Case 1 waters for 2007, according to Lee and Hu (2006) model using MODIS data. For each season, the number of valid pixels is presented in **a)**. Note that 50 was the maximum assigned value. The percentage of Case 1 pixel classification applying different criteria are presented in **b)** only the RR12_RR53 condition, **c)** only the Rrs555_RR53 condition, and **d)** with both conditions. Note that scale is in percentage and that invalid pixels period are presented in brown.

2008 (MODIS)

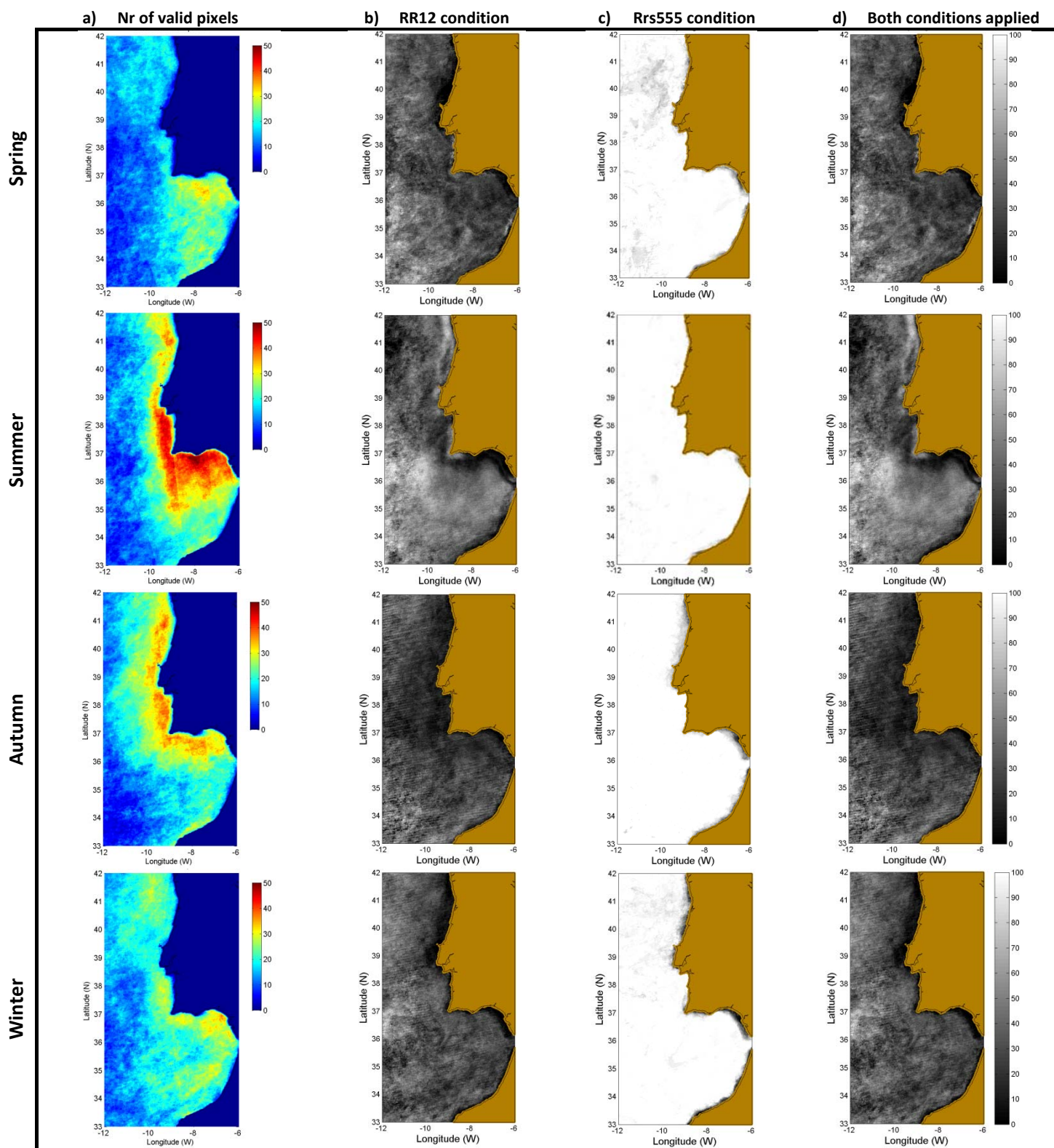


Figure II-3 Maps of percentage of pixel classification as Case 1 waters for 2008, according to Lee and Hu (2006) model using MODIS data. For each season, the number of valid pixels is presented in **a)**. Note that 50 was the maximum assigned value. The percentage of Case 1 pixel classification applying different criteria are presented in **b)** only the RR12_RR53 condition, **c)** only the Rrs555_RR53 condition, and **d)** with both conditions. Note that scale is in percentage and that invalid pixels period are presented in brown.

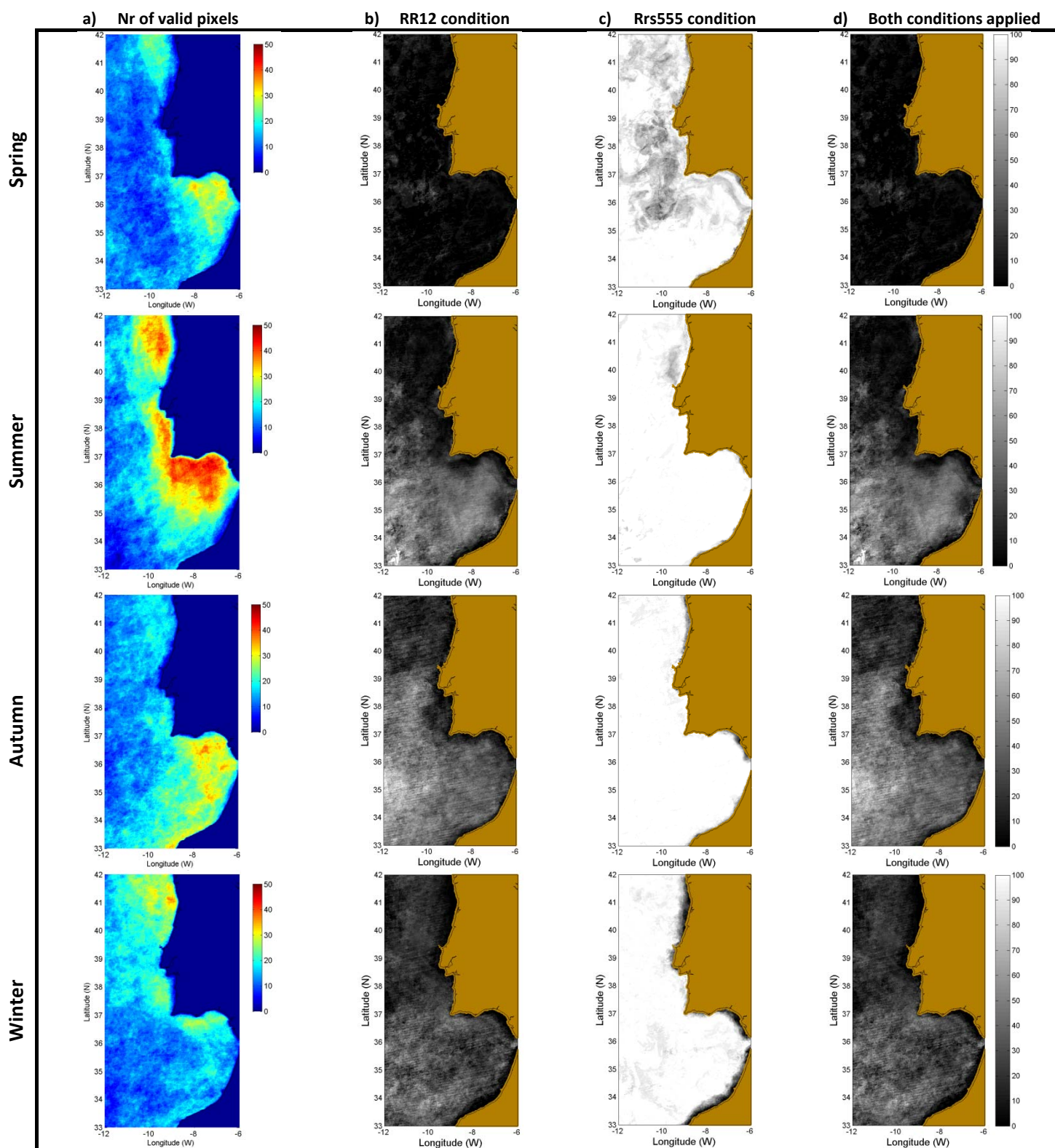


Figure II-4 Maps of percentage of pixel classification as Case 1 waters for 2009, according to Lee and Hu (2006) model using MODIS data. For each season, the number of valid pixels is presented in **a)**. Note that 50 was the maximum assigned value. The percentage of Case 1 pixel classification applying different criteria are presented in **b)** only the RR12_RR53 condition, **c)** only the Rrs555_RR53 condition, and **d)** with both conditions. Note that scale is in percentage and that invalid pixels period are presented in brown.

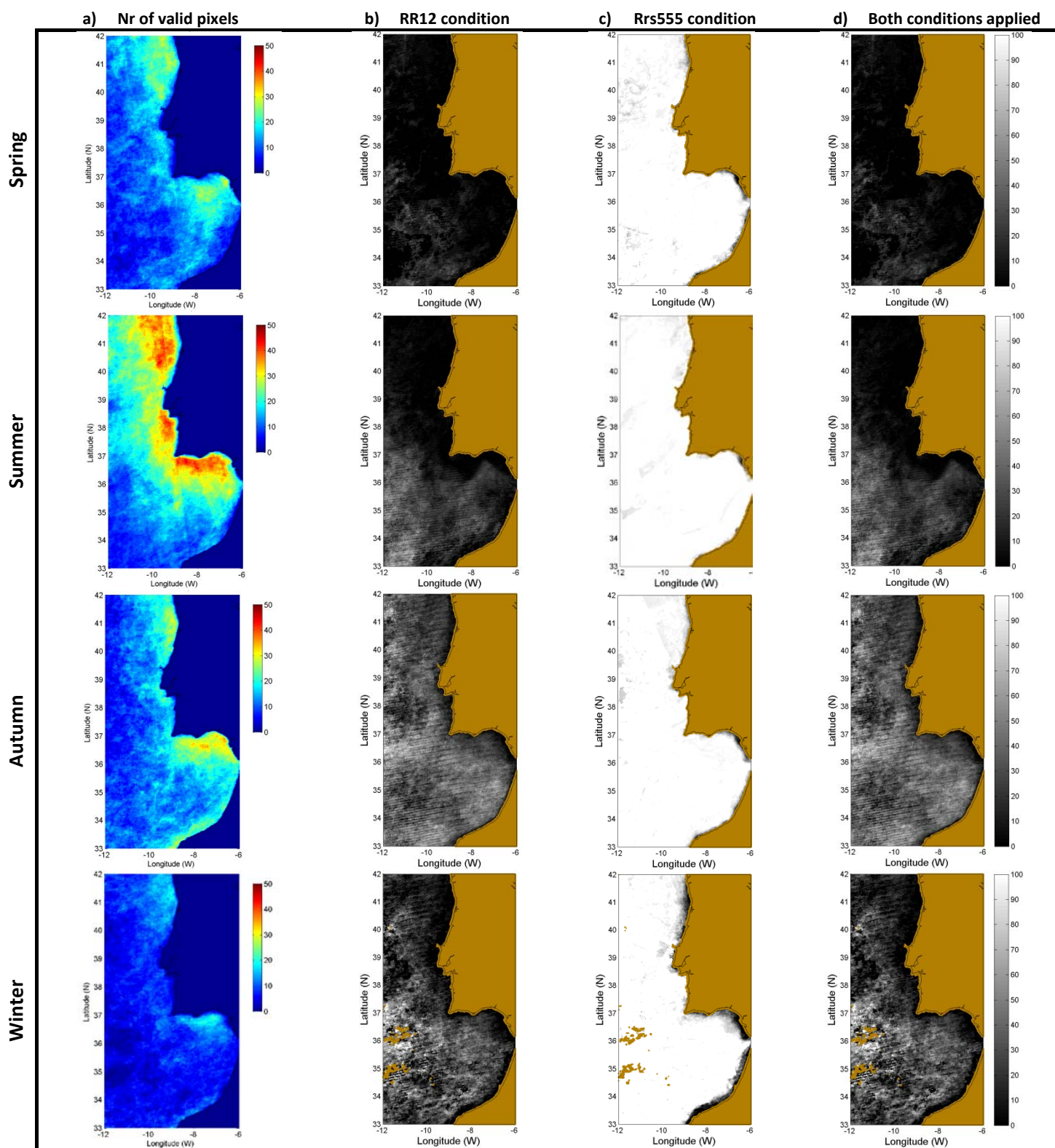


Figure II-5 Maps of percentage of pixel classification as Case 1 waters for 2010, according to Lee and Hu (2006) model using MODIS data. For each season, the number of valid pixels is presented in **a)**. Note that 50 was the maximum assigned value. The percentage of Case 1 pixel classification applying different criteria are presented in **b)** only the RR12_RR53 condition, **c)** only the Rrs555_RR53 condition, and **d)** with both conditions. Note that scale is in percentage and that invalid pixels period are presented in brown.

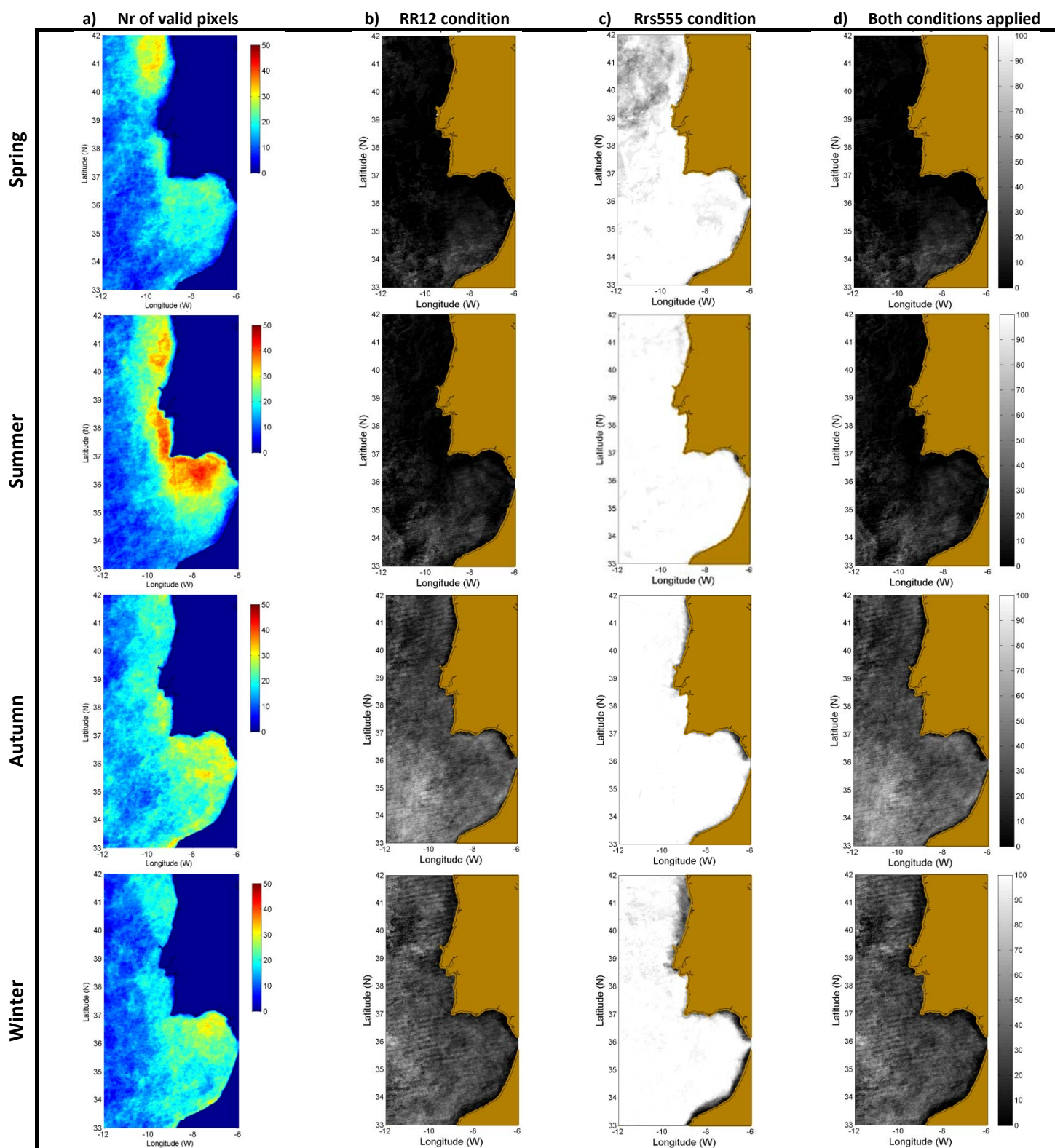


Figure II- 6 Maps of percentage of pixel classification as Case 1 waters for 2011, according to Lee and Hu (2006) model using MODIS data. For each season, the number of valid pixels is presented in **a)**. Note that 50 was the maximum assigned value. The percentage of Case 1 pixel classification applying different criteria are presented in **b)** only the RR12_RR53 condition, **c)** only the Rrs555_RR53 condition, and **d)** with both conditions. Note that scale is in percentage and that invalid pixels period are presented in brown.

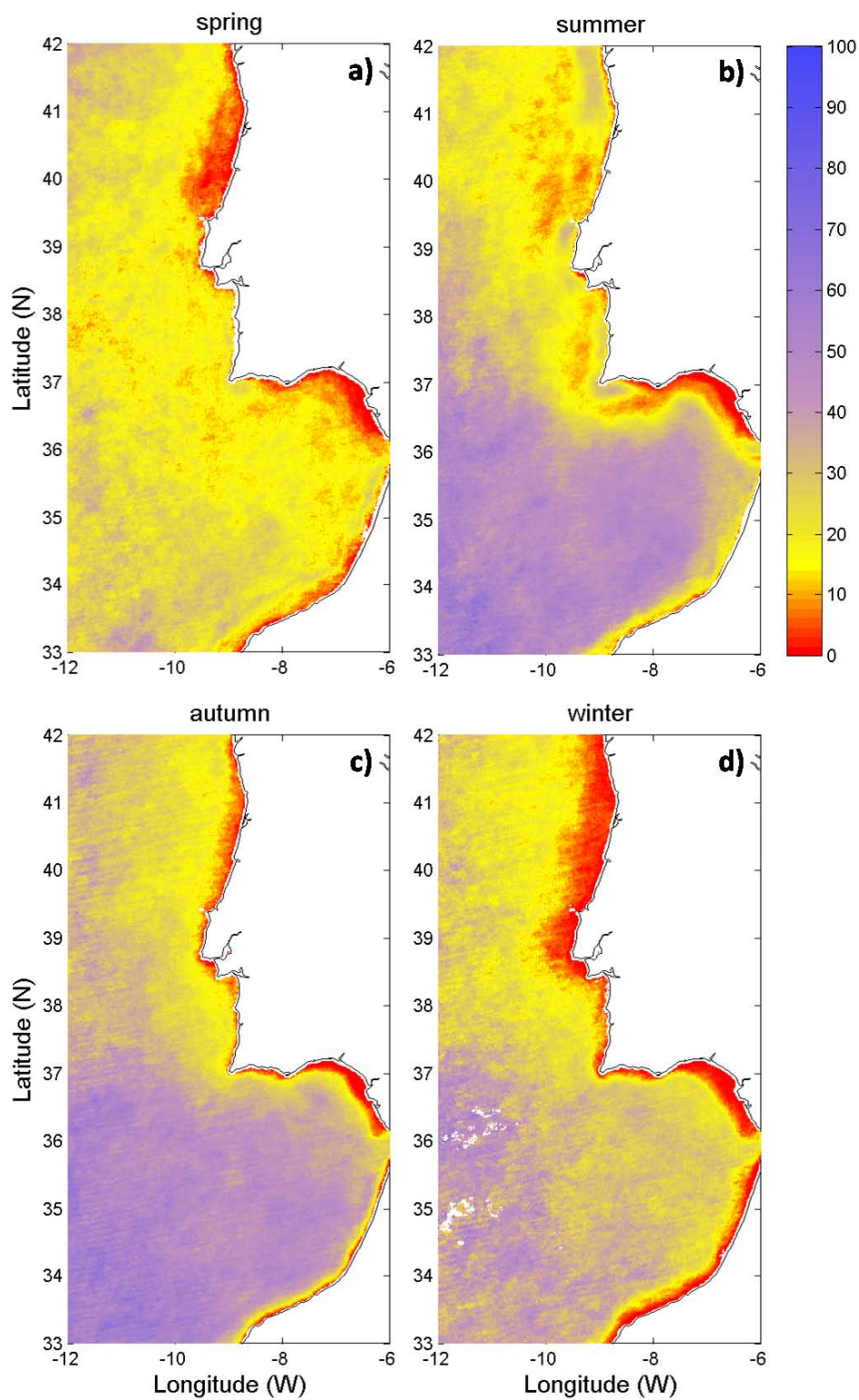


Figure II-7 Seasonal maps of percentage of pixel classification as case1 waters according to Lee & Hu 2006 model conditions for the MODIS data for a 7 years period (2005-2011). The maps of the percentage that each pixel was classified as case 1 for the analysed period applying only the RR12_RR53 condition for **a)** spring, **b)** summer **c)** autumn, and **d)** winter. Scale is in percentage.

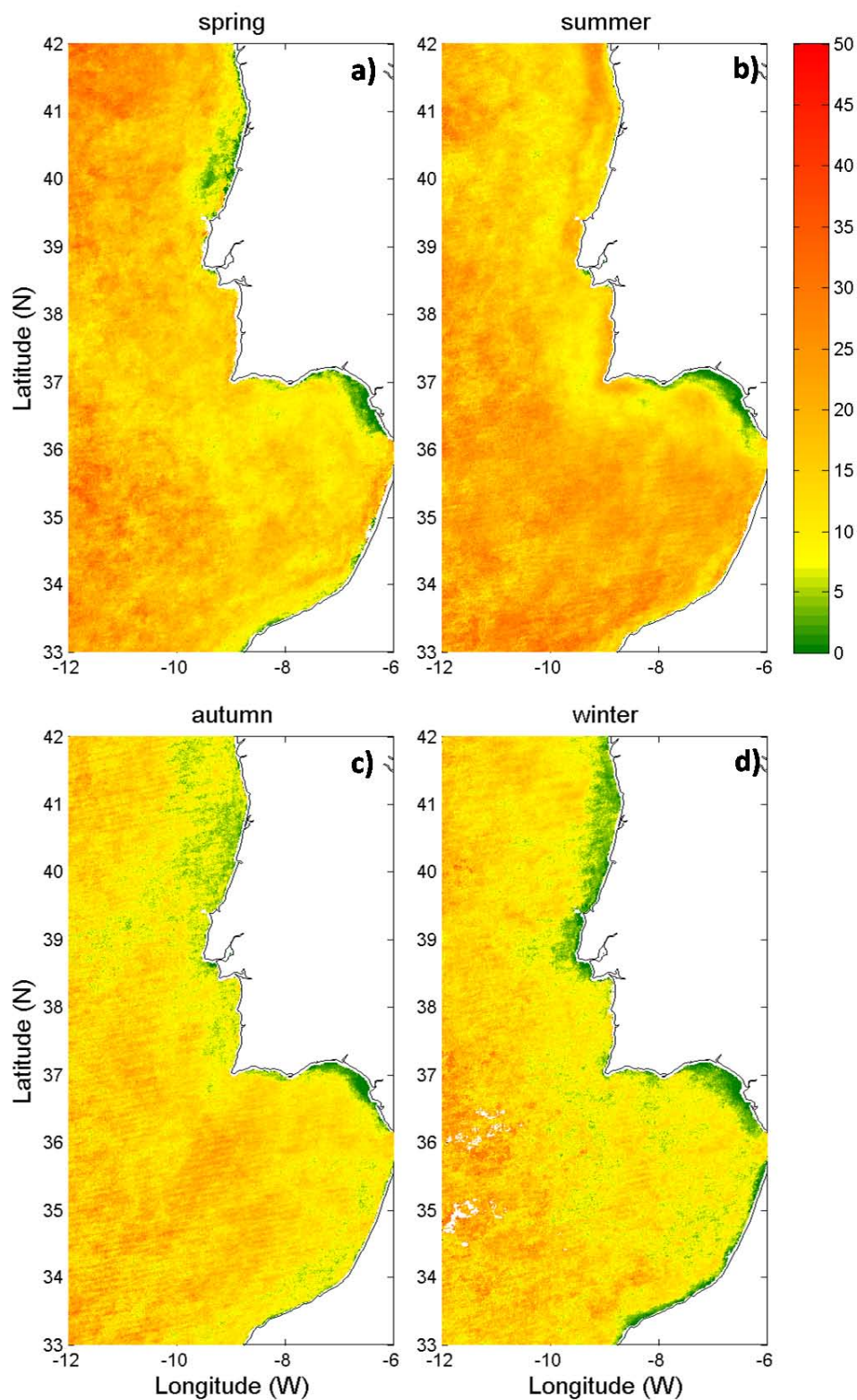


Figure II-8 Maps of standard deviation of seasonal percentage of pixel classification as case1 waters according to Lee & Hu 2006 model (RR12_RR53 condition) conditions for the MODIS data for a 7 years period (2005-2011). That is how variable are the pixels classified for each season of each year compared to the seasonal mean of the seven years for **a)** spring, **b)** summer **c)** autumn, and **d)** winter. Scale is in percentage.

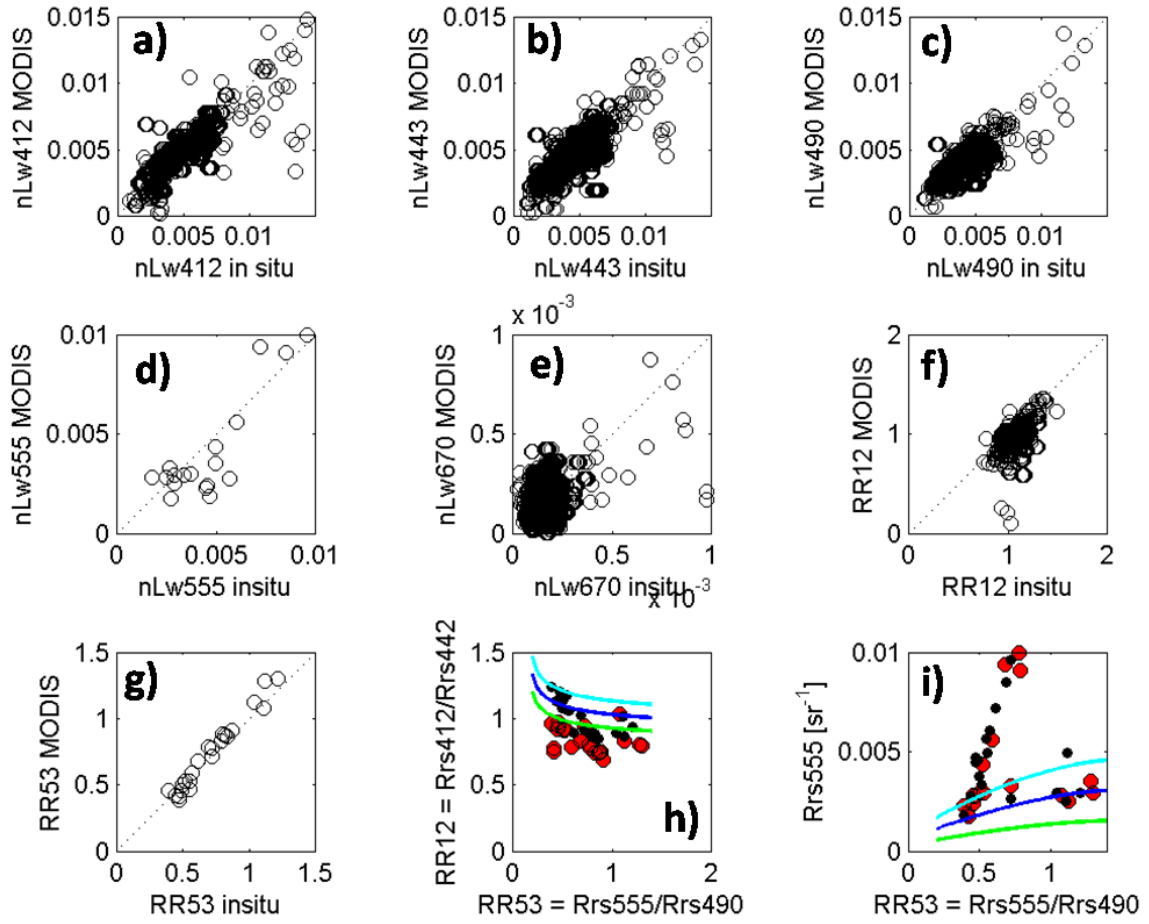


Figure II-9 Validation of radiometric MODIS data with SeaBaSS *in situ* database (samples > 50km from coast): for bands 412nm (a), 443nm (b), 488nm (c), 555nm (d), and 667nm (e). Validation is also performed for RR12 (f) and RR53 (g) ratios. Also presented are the sensor and *in situ* data results superimposed with Lee and Hu (2006) model for the RR12_RR53 condition (h) and the Rrs555_RR53 condition (i): *in situ* data in black, and sensor data in red.

Table I-1 Statistics of MODIS radiometric data comparison with the *in situ* SeaBaSS database (samples > 50km from coast)

MODIS	N	δ	Ψ	Δ	Slope	Offset	r^2	RPD (%)	APD (%)
nLw412	1159	-0.000	0.001	0.001	0.93	-0.000	0.68	-0.09	18.8
nLw443	3164	0.000	0.001	0.001	0.94	0.000	0.63	5.22	16.6
nLw488	3260	-0.000	0.000	0.000	0.88	0.000	0.65	-2.96	12.0
nLw551	23	-0.001	0.002	0.002	0.98	-0.001	0.91	-10.05	22.95
nLw667	2747	-0.000	0.000	0.000	1.09	-0.000	0.47	8.23	41.6
RR12	1099	-0.110	0.154	0.108	1.80	-0.97	0.20	-10.0	10.6
RR53	23	0.024	0.064	0.060	1.16	-0.09	0.97	2.2	7.8

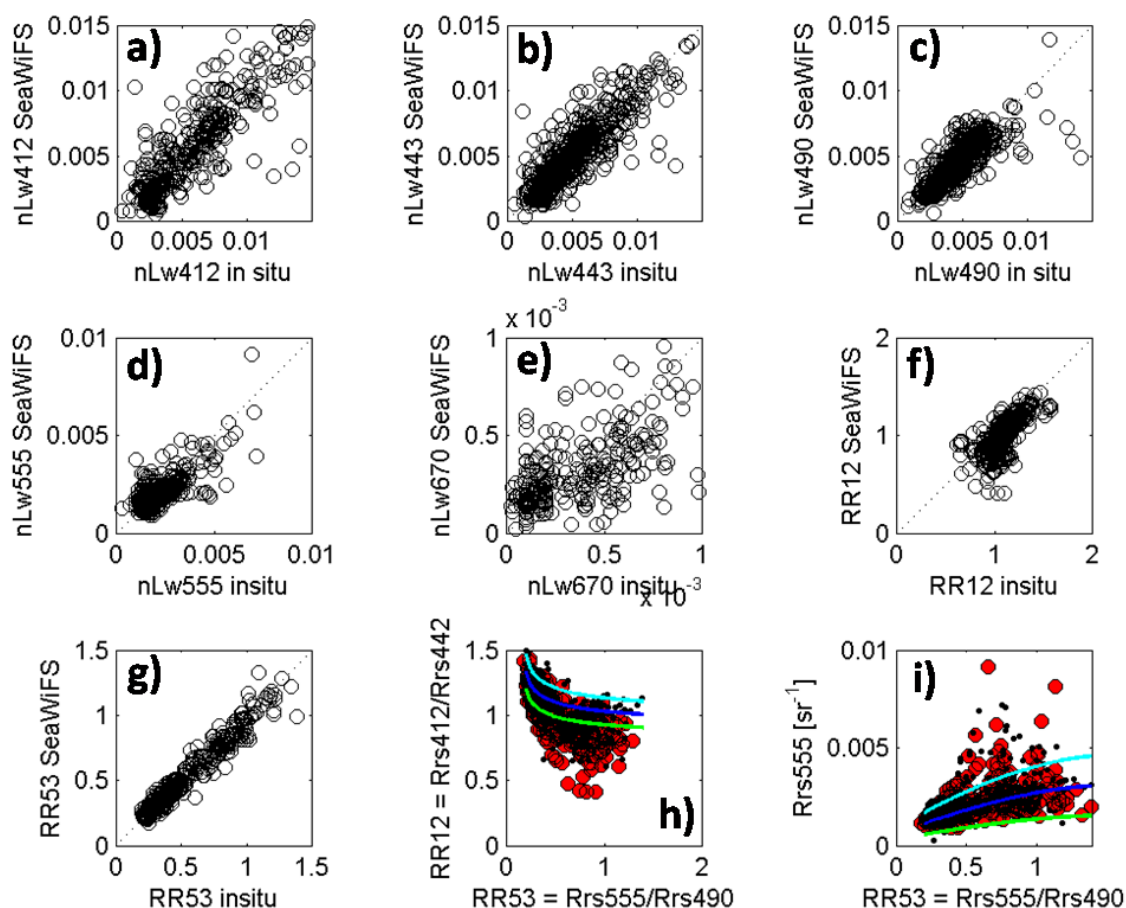


Figure II-10 Validation of radiometric SeaWiFS data with SeaBASS *in situ* database (samples > 50km from coast): for bands 412nm (a), 443nm (b), 488nm (c), 555nm (d), and 667nm (e). Validation is also performed for RR12 (f) and RR53 (g) ratios. Also presented are the sensor and *in situ* data results superimposed with Lee and Hu (2006) model for the RR12_RR53 condition (h) and the Rrs555_RR53 condition (i): *in situ* data in black, and sensor data in red.

Table II-2 Statistics of MODIS radiometric data comparison with the *in situ* SeaBASS database (samples > 50km from coast)

SW	N	δ	Ψ	Δ	Slope	Offset	r^2	RPD (%)	APD (%)
nLw412	392	-0.000	0.002	0.002	1.04	-0.000	0.76	-0.42	29.3
nLw443	592	-0.000	0.001	0.001	0.99	-0.000	0.75	2.47	22.3
nLw488	612	-0.000	0.001	0.001	0.91	0.000	0.69	-2.95	16.8
nLw551	407	-0.000	0.001	0.001	0.63	0.001	0.67	-0.69	22.3
nLw667	274	-0.000	0.000	0.000	0.53	0.000	0.37	22.8	64.7
RR12	392	-0.079	0.222	0.208	2.18	-1.36	0.29	-6.96	12.2
RR53	398	-0.010	0.136	0.135	0.92	0.03	0.80	0.83	10.4

